



Universidad  
del País Vasco

Euskal Herriko  
Unibertsitatea



Ingeniaritza Goi Eskola Teknikoa  
Escuela Técnica Superior de Ingeniería  
Bilbao

# **DEVELOPMENT OF CEMENTITIOUS MATRIX MATERIALS, WITH IMPROVED PERFORMANCE, INCORPORATING BY-PRODUCTS FROM THE STEELMAKING INDUSTRY**



*Author*

**Amaia Santamaría León**

*Supervisor*

José Tomás San José Lombera

Eduardo Rojí Chandro

May 2017, Bilbao





Universidad  
del País Vasco

Euskal Herriko  
Unibertsitatea



Ingeniaritza Goi Eskola Teknikoa  
Escuela Técnica Superior de Ingeniería  
Bilbao

# **DEVELOPMENT OF CEMENTITIOUS MATRIX MATERIALS, WITH IMPROVED PERFORMANCE, INCORPORATING BY-PRODUCTS FROM THE STEELMAKING INDUSTRY**

*Author*

**Amaia Santamaría León**

*Supervisor*

Jose Tomás San José Lombera

Eduardo Rojí Chandro

May 2017, Bilbao



AREA CIENCIA DE MATERIALES  
AREA MECANICA DE FLUIDOS  
AREA CONSTRUCCION



## *Agradecimientos*





## Agradecimientos

Siempre supe que escribir los agradecimientos no iba a ser tarea fácil. Por ello, lo primero quiero pedir disculpas por si me olvido de alguien. Me siento realmente afortunada, por todas las personas que me han ayudado a lo largo de estos 3 años y medio, en los que se ha desarrollado la presente tesis doctoral.

Quiero agradecer al grupo de investigación consolidado IT781-13, por los fondos invertidos en la presente investigación, especialmente por el PIFG005/13. Extender el agradecimiento a todos sus miembros, por sus enseñanzas durante estos años, su apoyo y su trato personal, pero especialmente por haber confiado en mi acogiéndome como un miembro más del grupo.

Agradecer a la Universidad del País Vasco (UPV/EHU), en especial al Vicerrectorado de Investigación, por la financiación aportada a través de la convocatoria de contratación de personal investigador en formación 2013. Tengo que agradecer también al departamento de Ingeniería Minero Metalúrgica y Ciencia de los Materiales por haberme acogido. En especial a mis compañeras que me han apoyado y animado en este camino, y que me han ayudado mucho en mis primeras experiencias en la docencia universitaria.

Agradezco al Ministerio de Economía y Competitividad (MINECO) y a los fondos FEDER la financiación de la presente investigación mediante el Proyecto BIA2014-55576-C2-2-R. No me puedo olvidar de agradecer a todos y cada uno de los miembros del proyecto BLUECONS la gran ayuda que me han proporcionado durante el desarrollo de la tesis, realmente creo que sin vosotros esto no hubiera sido igual. Incluyo en este grupo a Bengo, el mejor alumno de grado que se puede tener.

A los miembros de la división de construcción sostenible de Tecnalia, de LADICIM de la Universidad de Cantabria, de ERAIKER y del laboratorio de Construcción de la Universidad de Burgos agradezco la ayuda prestada, y los conocimientos que me han transmitido.

I gratefully acknowledge the help of Professor Carlo Pellegrino for the chance to work as one of his team members and to all the people that made my stay at Padova such a good experience, especially to Flora Faleschini for helping me so much, and Lesley, Christian and Jaime for all the good experiences we enjoyed there.

A mis directores, Tomás y Eduardo, les agradezco en primer lugar haber apostado por mí, confiar (más que yo) en que era capaz de realizar este trabajo y el apoyo que me han brindado durante el desarrollo de la tesis. No puedo olvidarme de Javier, gracias por tu paciencia y por enseñarme tanto. Espero poder seguir disfrutando de tu conocimiento durante muchos años, tanto el académico (que es mucho), como el personal, creo que consigues que los que te rodeamos seamos un poco mejores personas.

Para finalizar agradezco a mi familia (tanto la nueva, como la de siempre) estar ahí siempre y apoyarme tanto. A mis Tartarugas agradecer que siempre habéis estado conmigo y en esta etapa no ha sido menos. A la cuadri de Algorta gracias por el apoyo que me habéis dado, por todo lo que me habéis escuchado y sobre todo por todos los buenos ratos juntos. Ama aita sin vosotros, sin vuestra educación, enseñanzas, cariño y apoyo nunca habría llegado aquí, gracias por todo. Y a ti, maitia, qué decir, creo que en esta página solo puedo decir gracias por tanto.





## *Summary*





## Summary

One of the most important industries in the north of Spain, especially in the Basque Country, is the steelmaking industry. The production of steel in electric arc furnaces, prevalent in this small region generates huge amounts of industrial steelmaking waste that have to be properly managed. For many years, the Electric Arc Furnace (EAF) slags generated by the steelmaking industry have been dumped as waste material in landfill sites. Nevertheless, many researchers have been investigating ways of standardizing the use of EAF slag in construction and civil engineering, so that it can be used as aggregate in hydraulic and bituminous mixes. In this way, dumping sites will be relieved of this waste and the consumption of natural resources will be decreased.

In this PhD thesis, a step forward has been taken towards standardization of the re-use of waste materials from the steelmaking industry as raw materials in the manufacture of hydraulic mixes for their use in the construction industry. It has been demonstrated that, with the correct mix design, EAF slag concrete of the desired workability may be manufactured and that it can even perform well in real-scale structural elements.

Real-scale Reinforced Concrete (RC) beams with both pumpable and self-compacting concretes have been manufactured to achieve this goal. Following the sustainability approach, it was decided to manufacture the beams, not only with the standard Portland cement type I, but also with cement type IV with the addition of fly ash, in order to manufacture more sustainable concretes.

The decision to work firstly with small samples and to finish the work with real-scale elements was taken to realize this objective. The experimental methods developed to reach the final objective have been divided into three chapters in this PhD thesis. Each chapter has introduced a different level of scale that has broadened the investigation. The introductory chapters have presented the scope of the research and a full description of the materials and methods used in the development of the thesis.

In the first part (Chapter 4), the work performed on mortar mixes has been presented. Firstly, the interaction of the steel slags with cement type IV was analyzed by manufacturing mixes with different dosages and developing mechanical and durability tests. The mechanical properties displayed an excellent behavior.

Subsequently, the manufacture of self-compacting mortar mixes has been presented. It is essential to obtain a good mortar paste, in order to manufacture self-compacting concretes. Several mortar mixes were manufactured and their fresh properties

analyzed. The hardened properties were also evaluated, achieving strengths of up to 100 MPa, and the mixtures manufactured with EAF slag aggregate displayed superior behavior to mixtures manufactured with natural aggregates. This effect is a consequence of a suitable mortar microstructure, as is evident from the MIP and CAT analyses. Accelerated aging tests were also performed on the self-compacting mortar mixes, demonstrating the innocuous effect of EAF slag.

In the second part (Chapter 5), the studies on pumpable and self-compacting concrete mixes with EAF slag added as aggregate have been presented. An in-depth analysis of the workability of self-compacting mixes has shown the essential need for careful control of the fine fraction and selection of a compatible chemical admixture to attain the required flowability. A numerical simulation of the viscous flow of these self-compacting mixes has been proposed, reporting very acceptable results. The mechanical properties of these concretes indicated good performance and the analysis of some SEM observations of the fracture surfaces on the SCC-EAFS concrete revealed significant features, which help us to understand their structure and mechanical behavior.

An extensive testing regime to assess the durability of these concretes has also been described. Some classical tests, such as freezing-thawing and drying-wetting, were conducted until noteworthy deterioration was appreciated in the mixes. Singular tests, such as immersion in sea water in the tidal zone, and a study on reinforcement corrosion in marine environment, were also performed to evaluate the quality and usefulness of this kind of concrete. The results have demonstrated that EAF slag concretes behave in a satisfactory way in these environments.

In the last part (Chapter 6), the manufacture and performance of real-scale EAF slag reinforced beams has been investigated. These beams were manufactured with pumpable and self-compacting concretes and, for each consistency, cement type I and cement type IV were used for manufacturing different mixes. All the mixes displayed good fresh behavior during the casting period, producing beams without any honeycomb. The flexural behavior of the beams was analyzed and yielded results similar to analytical values calculated with the existing formulation. The long-term deflection of the beams was evaluated and all the beams performed well over the full duration of the test.

Analyzing the general conclusions drawn from this research, it can be stated that the main objective of the thesis has been achieved.

# *Table of Contents*





## Table of Contents

Agradecimientos.....	3
Summary.....	7
Chapter 1. Preface .....	15
1.1. Introduction.....	17
1.2. Objectives .....	18
1.3. Structure of the PhD.....	19
Chapter 2. Scope.....	21
2.1. Introduction.....	23
2.2. Steelmaking industry.....	24
2.3. Circular economy .....	34
2.4. The use of steelmaking slag in civil and construction industry.....	36
2.5. Self-Compacting concrete .....	37
2.6. The research team career in relation with steel.....	40
Chapter 3. Materials and Methods .....	49
3.1. Introduction.....	51
3.2. Materials.....	51
3.3. Methods .....	60
Chapter 4. Manufacture and performance of mortar mixes. ....	79
4.1. Introduction.....	81
4.2. The use of steelmaking slags and fly ash in structural mortars.....	83
4.3. The design of self-compacting structural mortar containing heavy steelmaking slags as aggregates .....	115

Chapter 5. Manufacture and performance of concrete mixes .....	143
5.1. Introduction.....	145
5.2. Self-compacting concrete incorporating electric arc furnace slag as aggregate.....	147
5.3. Study of the durability of structural concrete elaborated with electric steelmaking slag as aggregate.....	185
Chapter 6. Manufacture and performance of real scale beams .....	223
6.1. Introduction.....	225
6.2. Performance of real scale beams manufactures with self-compacting and pumpeable electric arc furnace slag concrete .....	227
Chapter 7. Conclusion.....	261
Chapter 8. Future research lines. ....	267
Appendix: Publications and Congresses.....	271



*Chapter 1:*

*Preface*





# 1

## *Preface*

### **1.1. Introduction**

An essential component of moving towards the sustainability of the planet and a circular economy is making use of waste as raw materials, an issue in which many researchers and politicians are engaged. Currently, the construction and civil works industry is one of the heaviest consumers of waste materials. These waste materials may come from their own construction and civil works (demolition and construction wastes), from agricultural industries (palm oil fuel ash, bagasse ash, wood waste ash, bamboo leaf ash, corn cob ash, rice husk ash, etc.) and from industrial processes (silica fume, fly ash, steel slags, etc.).

The iron and steelmaking industry is a very important activity for economies all over the world. It consumes a large amount of raw materials and energy: it is estimated that over 5% of global CO<sub>2</sub> emissions is produced by this industry. There are different types of furnaces in use today in the iron and steelmaking industry and each furnace type generates a different type of waste. There are at least eight different wastes that are produced by this sector:

- Ground granulated blast furnace slag (300 to 400 kg per ton of pig iron)
- Cupola furnace slag (60 to 80 kg per ton of cast iron)
- Ladle furnace slag (60 to 80 kg per ton of steel)
- Electric arc furnace slag (150 to 180 kg per ton of steel)
- Basic oxygen furnace slag (120 to 150 kg per ton of steel)

- AOD-VOD slag (120 kg per ton of stainless steel)
- Milling scales (2 to 10 kg per ton of steel)
- Refractory rubble (8 to 10 kg per ton of iron or steel)

Currently, ground granulated blast furnace slag is the only iron and steelmaking slag with a standardized use as a mineral addition in Portland cement. This PhD thesis is a further example of the many research projects that are underway to standardize the re-use of the other steel slag types, which will otherwise be dumped in landfill sites.

## 1.2. Objectives

The main objective of this PhD thesis is to take a step forward in the standardization of the re-use of waste materials from the steelmaking industry (electric arc furnace slag and ladle furnace slag) as raw materials for manufacturing hydraulic mixes to be used in the construction and civil works industry. This objective is achieved by demonstrating that concretes manufactured with these materials fulfill all the requirements that need to be met for use in construction works.

Some partial objectives have to be established to reach the main objective of the thesis. These partial objectives are:

- To verify that the interaction of the electric arc furnace slag and the ladle furnace slag with different types of EU standardized Portland cements is satisfactory.
- To manufacture self-compacting and pumpable hydraulic mixes, to show that it is possible to manufacture concrete with the desired workability using electric arc furnace slag as aggregate. There are two factors that make this a challenge: the higher density and the rougher shape of electric arc furnace slag compared to the classical aggregates.
- To analyze the fresh rheological properties of the self-compacting mixes in depth which contain steelmaking slags to understand their behavior.
- To obtain EAF slag hydraulic mixes with at least the same mechanical behavior in the hardened state as the mixes manufactured with natural aggregates.

- Likewise, to obtain EAF slag hydraulic mixes with at least the same durability as the mixes manufactured with natural aggregates.
- To show that these EAF slag concretes can be used in typical construction work, functioning as real-scale products (beams for example), and to validate these structural elements in tests by loading them in the standard way, so that they show good mechanical behavior which can be predicted by employing the usual formulations established for ordinary concretes.

### **1.3. Structure of the PhD thesis**

This section will facilitate the reading and understanding of the PhD thesis, outlining the main objectives of each chapter. The thesis is organized into eight different chapters.

#### Chapter 1. Preface

This current chapter is a brief introduction to the research topic. It also includes the main and partial objectives of the PhD thesis and its structure, providing an overview of the whole work.

#### Chapter 2. Scope

The second chapter presents the general context of the thesis to make it easier for the reader to understand the scope of this research field. It presents the problem that provided the motivating reason for undertaking and completing this thesis.

#### Chapter 3. Materials and methods

The third chapter is divided into two parts. The first part is a description of the properties, characteristics and behaviors of the two slags being used, and which are the focus of the research. In the second part the different test methods used during the research are cited; a more detailed description of the methods that are not based on international standards is also included.

#### Chapter 4. Manufacture and performance of mortar mixes

The fourth chapter presents an analysis of the mechanical, physical and chemical properties and the durability of structural mortar mixes manufactured with electric arc furnace slag as aggregate and ladle furnace slag as partial replacement of the fine

fraction of the aggregate and the cement. The manufactured mortars can be divided into two kinds, hence the chapter has two sections: structural mortars with flowable workability manufactured with cement type IV and structural self-compacting mortar mixes.

*Chapter 5. Manufacture and performance of concrete mixes*

In chapter five, the procedure to manufacture self-compacting concrete and pumpable concrete with electric arc furnace slag as aggregate is described. An in-depth analysis of the fresh properties of these concretes has been carried out. Section 2 studies the mechanical, physical and chemical properties of these concretes, and an extensive analysis of the durability of these concretes is included in Section 3.

*Chapter 6. Manufacture and performance of real-scale beams*

The sixth chapter describes the manufacturing process of real-scale beams made from electric arc furnace slag in the production of self-compacting and pumpable concretes. The structural behavior of the manufactured beams is studied, analyzing the data obtained from the tests that are performed: the four-point bending test and the long-term strain bending test.

*Chapter 7. Conclusions*

In chapter 7 a summary of the general conclusions derived from the research is presented. This chapter will help the reader to gain an understanding of the results obtained during the development of the thesis.

*Chapter 8. Future research lines*

Finally, in the last chapter, future research lines are proposed for further work on key aspects related to the standardization of electric arc furnace slags as raw materials in the construction industry which could not be addressed in the course of the research work associated with this PhD thesis.

*Chapter 2:*

*Scope*







# 2

## *Scope*

### **2.1. Introduction**

In this chapter the author wishes to present the reasons that have promoted the development of this PhD thesis. The worldwide situation of the steelmaking industry is analyzed, focusing on electric arc furnace steel production. The industrial history of the Basque Country, the region where this PhD thesis has been carried out, was a determining motivational factor in putting this line of research into practice. Additionally, the belief of the author in the need to work towards a more sustainable economy has also had significant influence.

The research team which developed this thesis has a long history of working with electric arc furnace slag and ladle furnace slag. Its members have published pioneering international and European papers on the uses of these slags in hydraulic mixes. Over the last two decades other research teams around the world have worked on the use of electric arc furnace slag and ladle furnace slag as raw materials in the construction or civil works industries. In Europe, research groups from Italy, Greece and Spain currently stand out for their research work on the standardized use of these materials.

In the following chapters the latest advances by this team on the topic and the main conclusions obtained from this research work are presented. As has been mentioned in the introduction, the aim of this PhD thesis is to make self-compacting concrete using electric steelmaking slags. A brief explanation of the origin of the self compacting concrete and main characteristics is included here, while the latest advances in this

technology and the general procedures for its manufacture are described in next section.

## **2.2. Steelmaking industry**

The steelmaking industry is the world's most important heavy industry, with an annual production of almost 1700 million tones [1]. The main objective of this industry is to produce steel, which will later be manufactured into final products. Nowadays, two different processes are used to obtain the steel.

Iron ore, coking coal and fluxes to produce the steel are the raw materials in the first process. These materials are charged in a blast furnace and are submitted to heat, high pressure and air injection to complete the combustion, transforming the materials from solid to liquid and the iron oxide to metallic iron. Hot pig iron is obtained from this process; this material has an iron content of about 95% and a carbon content of about 3.5–4%. The pig iron has to be transformed in the Basic Oxygen Furnace to obtain steel. A refining process is done in this furnace to remove the excess carbon, phosphorus and sulfur. Then a final adjustment of the chemical composition of the steel is necessary in a third stage [2].

On the other hand, there is the electric arc steelmaking process (shown in Figure 2.1). In this case the main raw material is ferrous scrap, so the main input material is recycled steel and the melting of the steel takes place due to the thermal energy released by the electrodes in the furnace.

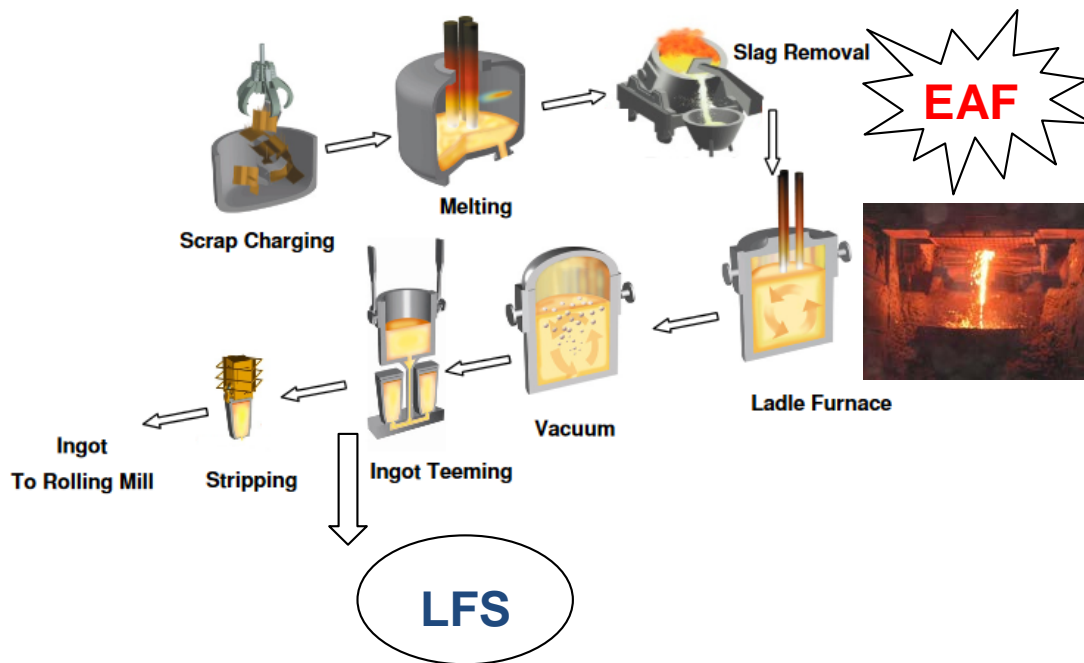


**Figure 2.1:** Electric arc furnace steelmaking process

When this type of furnace started to be introduced a century ago, it was used for manufacturing special steels. However, it is now considered a highly efficient process in which it is possible to produce almost any type of steel. In this case, the process is divided into two stages instead of the three that are at present needed to manufacture steel from iron ore [2].

The first stage, called the primary steelmaking or melting process, is carried out in an electric arc furnace. The scrap, with direct-reduced iron for a chemical balance, is loaded in the furnace in buckets. The heat generated by the electric arc melts the scrap. The arc is an electric current that passes between two electrodes that are lowered into the furnace. After melting, oxygen is blown into the liquid metal to purify the steel, and lime and fluorspar are added that combine with the impurities, forming the slag. Once the required acid or oxidizing refining of the steel is achieved, the furnace is tilted to tip the molten steel into a ladle, which also constitutes a furnace, after the slag, which floats on the surface of the molten steel, has been poured off [3].

The second stage takes place in the ladle furnace: the secondary or basic refining process. After the acid refining, the steel still contains harmful elements that must be removed. It is submitted to a deoxidation process, after which desulfurization takes place, and it then moves into the vacuum chamber for removal of the gases. This process is possible due to the formation on the surface of the molten steel of a basic slag with a high content of lime and magnesia and a lower content of silica and

alumina. Finally the chemical composition is adjusted to obtain steel with specific properties.

### **Worldwide steel market**

The global production of steel is increasing due to the industrialization of emerging countries. In Figure 2.2 it is possible to observe the development of the steel market over the last 15 years. Over this period, the production of steel has almost doubled, while production in Asia has tripled. This means that the growth in the demand for steel has been absorbed by the Asian market, leaving the rest of the markets at the same production levels and even decreasing production.

It is worth mentioning the decrease in production in 2009, when the economic crisis started. It can be seen that the world market has continued growing after this dip, but the European market has not yet recovered to its production level before the crisis. The ongoing economic crisis has led to a marked downturn in manufacturing activity and associated steel demand, which remains 16% below pre-crisis levels, with production remaining at roughly that level for the past 5 years. Even after this decrease, Europe continues to be the second largest producer of steel in the world, with an output of over 177 million tons per year [1].

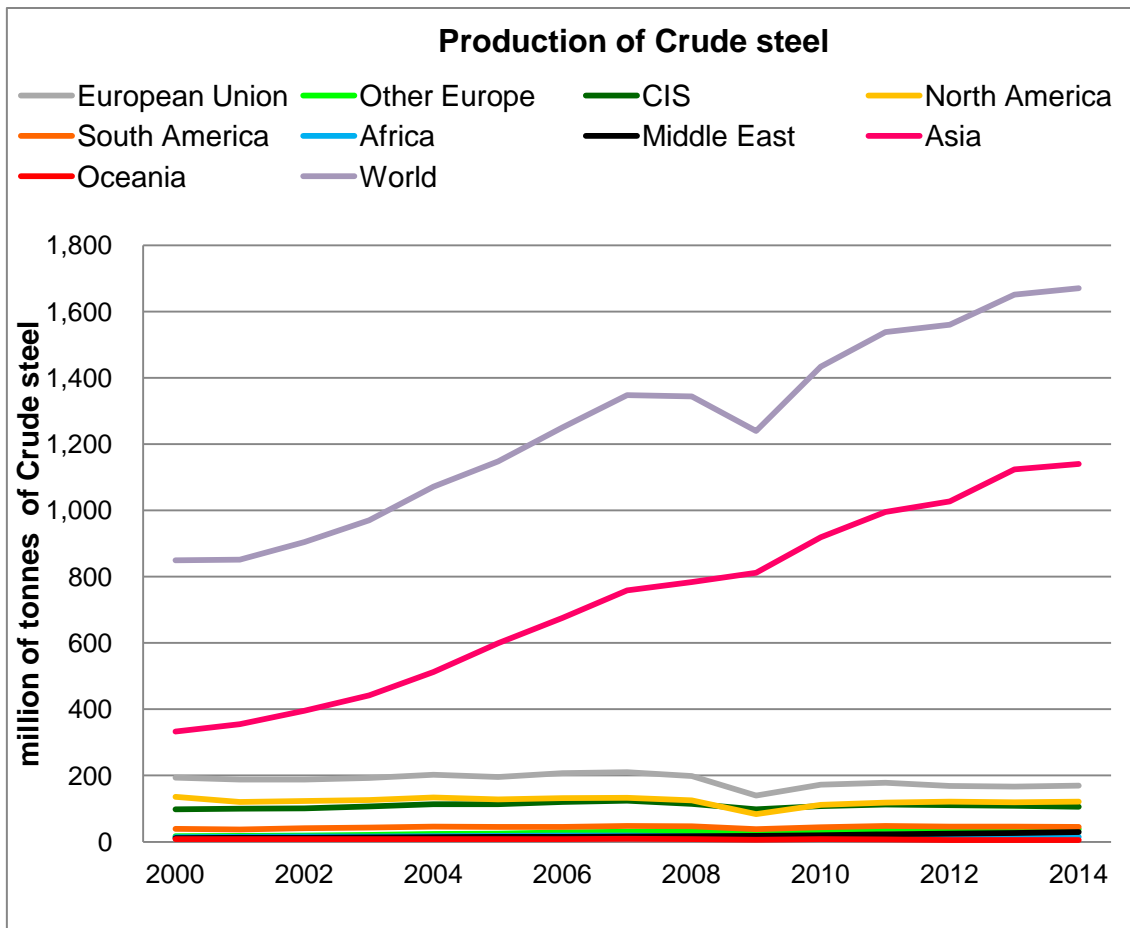


**Figure 2.2:** World crude steel production [4,5]

As is shown in Figure 2.3 in Europe there are six countries where almost 70% of the total crude steel is produced. Germany is the top producer with around 25%, followed by Italy and France, with Spain in fourth position, with almost 8.5%. [4; 5].

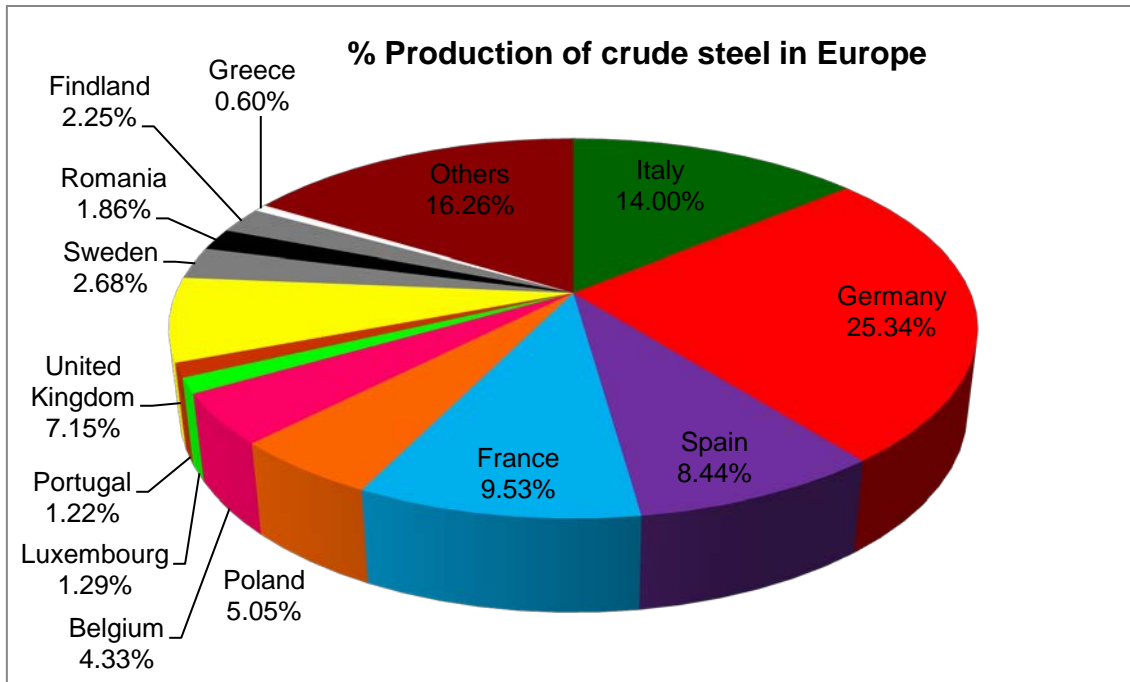


Figure 2.3: Europe crude steel production [4,5]

### Worldwide electric arc steel market

If we look at global production of steel in electric arc furnaces (Figure 2.4)[4; 5], the picture changes somewhat. In Asia, only 15% of the steel is produced in electric arc furnaces. This fact means that, of the total production of crude steel, Asia manufactures 68%, but for steel production in electric arc furnaces this figure falls to 42%.

Likewise, one can see in Figure 2.4 that North America is the second biggest producer of steel in electric arc furnaces, with 17% of the world's total. However, electric steel comprises 61% of the total manufactured steel on that continent

Despite being the second most important region in total steel production, in electric steel the European Union occupies third position, with 15% of world production, while that is 40% of the total steel manufactured in the European Union.

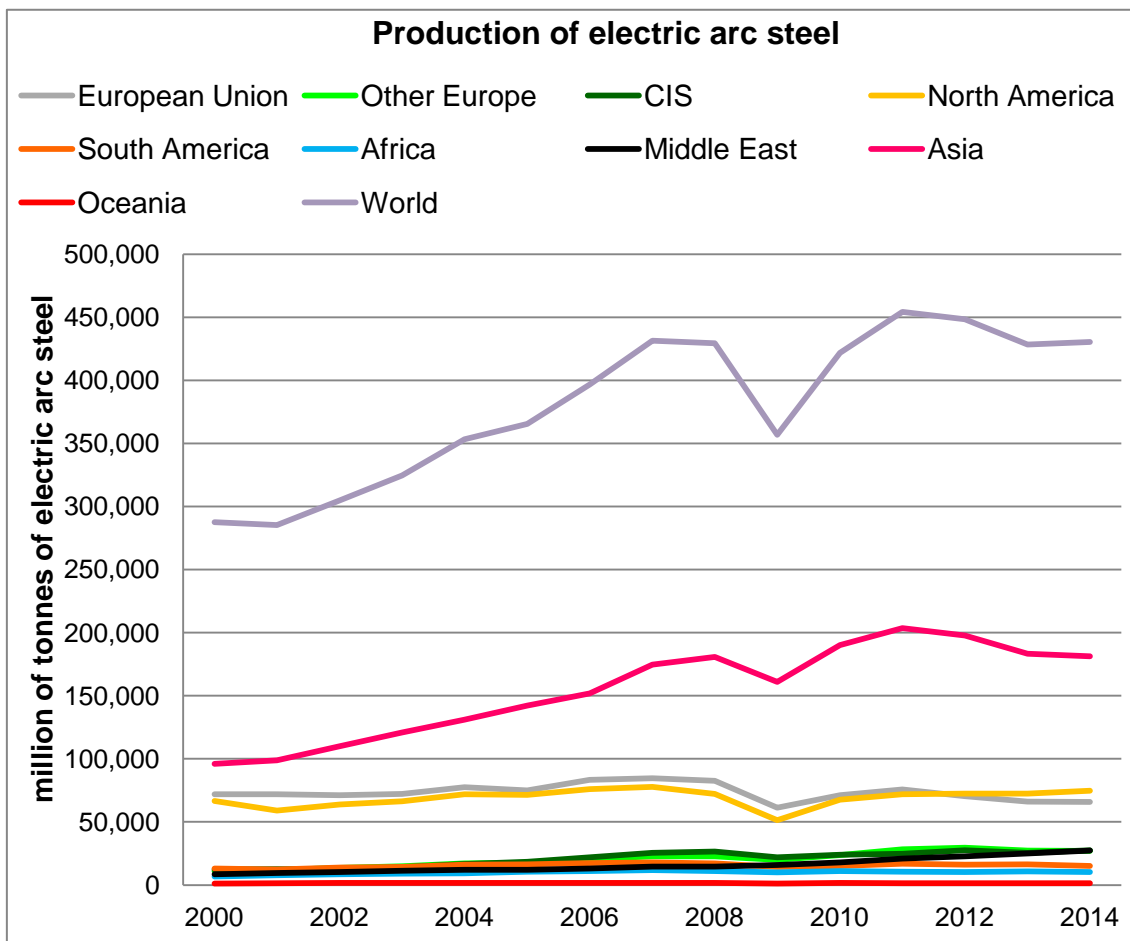


**Figure 2.4:** Global Electric arc steel production [4,5]

In Figure 2.5, the production of electric arc furnace steel is shown in the main European countries where it is manufactured [4; 5]. Italy is where the most EAF steel is produced, then Germany, which is the country that produces the crudest steel but the percentage of EAF steel production is low. In third position, we find Spain with 15% of the total European production.

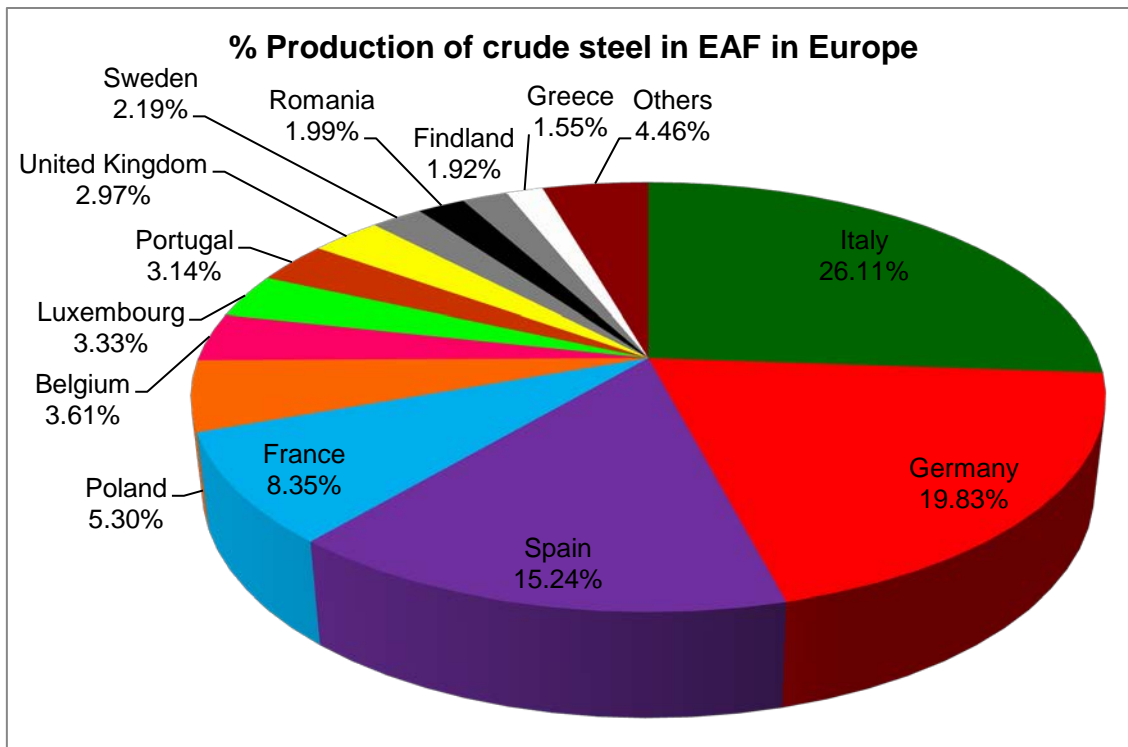


**Figure 2.5:** Europe electric arc steel production [4,5]

### Steelmaking industry in Spain

The Spanish steelmaking industry produced 14.9 million tons of steel in 2015, 4.3% more than in 2014, and 70% of that production was in electric arc furnaces. This increase in production has been assisted by a number of factors [6]:

- The growth of the Spanish economy was 3.2% instead of the expected 2.5%.
- The broad policies of the European Central Bank have caused a decrease in the Euribor rate to 0.06% and an increase in the business credit rate to 10.1%.
- The decrease in the value of the Euro has caused an increase in exports with respect to the USA and other countries that use the dollar.
- The broad fiscal policy in Spain that has reduced taxes.
- The decrease in the price of the raw materials.
























These factors have allowed the sector to start growing again, and hopefully the upward trend will continue in 2016.

The steelmaking plants that are working in Spain today are shown on the map below (Figure 2.6) [7]. This PhD thesis has been developed at the University of the Basque Country, but also a great part of the work has been done at the University of Burgos with the help of the University of Cantabria. On the map it can be seen that there is a concentration of steelmaking plants in these regions.





Figure 2.6: Steel plants at Spain [7]

- |   |  |   |   |
|---|--|---|---|
|    | ACERINOX (steel plant)                                     |    | CAF (steel plant)                               |
|   | Steel plant de Álava (steel plant)                         |   | CELSA Barcelona (steel plant)                   |
|  | Aceros Inoxidables Olarra (steel plant)                    |  | Gerdau Basauri (steel plant)                    |
|  | AG Corrugados Getafe (steel plant)                         |  | Gerdau Reinosa (steel plant)                    |
|  | ArcelorMittal Asturias - Hornos Altos                      |  | Global Steel Wire (GSW) (steel plant)           |
|  | ArcelorMittal Asturias - Planta de Avilés (steel plant LD) |  | MEGASA (steel plant)                            |
|  | ArcelorMittal Asturias - Planta Gijón (steel plant LD)     |  | Megasider Zaragoza (steel plant)                |
|  | ArcelorMittal Madrid (steel plant)                         |  | Nervacero (steel plant)                         |
|  | ArcelorMittal Olaberría (steel plant)                      |  | Productos Tubulares (steel plant)               |
|  | ArcelorMittal Sestao (steel plant)                         |  | Siderúrgica Balboa 2 (steel plant)              |
|  | ArcelorMittal Zumárraga (steel plant)                      |  | Siderúrgica Sevillana (steel plant)             |
|   |  |  | Tubos Reunidos Industrial, S.L.U. (steel plant) |

The steelmaking industries that are located in the three regions where this thesis has been carried out are highlighted in grey.

## Steelmaking industry in the Basque Country

As has been mentioned in the previous section, this PhD thesis has been carried out at the University of the Basque Country, specifically in Bilbao. The Basque Country is an autonomous community in northern Spain. It covers an area of 7234 km<sup>2</sup>, and has a population of 2,162,626 inhabitants [8], with a population density of 300 hab/km<sup>2</sup>. It is divided into three different provinces, as it can be seen in Figure 2.7: Alava, Gipuzkoa and Biscay. The Basque Country borders the provinces of Cantabria and Burgos to the west, the Bay of Biscay to the north, France (the Region of Nouvelle-Aquitaine) and Navarre to the east, and La Rioja to the south.



Figure 2.7: Basque Country map

The steelmaking industry has been one of the most important economic activities in the Basque Country, especially in Biscay and Gipuzkoa. The development of this industry in the Basque region took place because of three important factors [9]:

- The huge iron ore deposits that were in this region.
- The hydrography of the region, providing a readily available source of energy to power the furnaces.
- The presence of extensive areas of forest, where trees were felled for charcoal that the furnaces consumed in large quantities.

The steelmaking industry in the Basque Country dates back to the Roman period, but modern steelmaking started in the 19<sup>th</sup> century with the invention of the blast furnace, which needed coal for steel production and uses Bessemer and Siemens-Martin converters. These innovations, and the capacity to transport the coal, led to this region

becoming the Spanish capital of steel for over two centuries, manufacturing 60% of the Spanish steel production.

The most important plant, now closed, was Altos Hornos de Vizcaya. This mill had, in its best years, a steel production capacity of two million tons and a transformation capacity of three million tons. This was not the only steel manufacturer in Biscay; other important companies were producing steel near the river in Bilbao, such as: Santa Ana de Bolueta, Echevarria, S.A., Babcock & Wilcox and more in Gipuzkoa.

The huge industrial crisis of the 1980s resulted in a big reduction in actual production, and the golden age of the Basque steelmaking industry came to an end, but there are still important steel plants in this region that produce around 4.1 million tons of steel every year, which is 28% of the total production in Spain. Since 1996, when Altos Hornos de Vizcaya closed down, all the steel produced in this region has been in electrical arc furnaces [10; 11].

In Table 2.1, the electric arc furnace steel production in this autonomous region has been compared, using land area and population, with global, European and Spanish production. It has been shown that, per square kilometer, it is 200 times higher when compared with global production, 36 times higher than European production, and 28 times higher than total Spanish production. If we compare it using population density, the results are similar: 30 times higher than the world average, 13 times higher than that of Europe and 9 times that of Spain [4; 5].

Per year	EAF steel (million tons)	Land area ( $\times 10^3 \text{ km}^2$ )	EAF steel/ $\text{km}^2$ land	Population (million)	EAF steel/person
<b>World</b>	430	148,940	2.88	7,376.5	0.058
<b>European Union</b>	66	4,442	14.85	508.45	0.13
<b>Spain</b>	10	506	19.76	46.77	0.21
<b>Basque Country</b>	4	7.23	552.94	2.19	1.83

**Table 2.1:** Comparison of electric arc furnace slag production

The chart shown above underlines the large amount of electric arc steel production in the Basque Country that amounts to 40% of Spanish output. Taking into account that Spain produces 15% of the European Union output and the European Union produces 15% of the world's output, the Basque Country produces 1% of the world's electric arc

steel. This is encouraging data for the economy of this region, but also implies that the sector generates large amounts of steelmaking waste (600,000 tons of EAF slag and almost 120,000 tons of LF slag per year), which has to be stockpiled within this small region.

### **2.3. Circular economy**

Nowadays, the European Union is trying to support the transition toward a more circular economy, also known as a closed loop economy, which will create new jobs, promote global competitiveness and boost sustainable economic growth.

Although the circular economy is a relatively new concept, for a long time many authors have been introducing ideas for working toward a more sustainable planet and a more environmentally friendly economy. Some examples of this are: in 1962 Simmonds published *“Waste products and undeveloped substances: Or, hints for enterprise in neglected fields”* [12]; in 1966, Boulding published *“The Economics of the Coming Spaceship Earth”* [13], and *“Industrial Ecology”* [14] by Ayres and Kneese was published in 1969. The circular economy does not have a clear origin but some names are clearly associated with this concept: Professor John Lyle, William McDonough, Michael Braungart and Walter Stahel [15]. Different schools of thought have presented the principles of the circular economy, such as the Performance Economy [16], Biomimicry [17] and Cradle to Cradle [18].

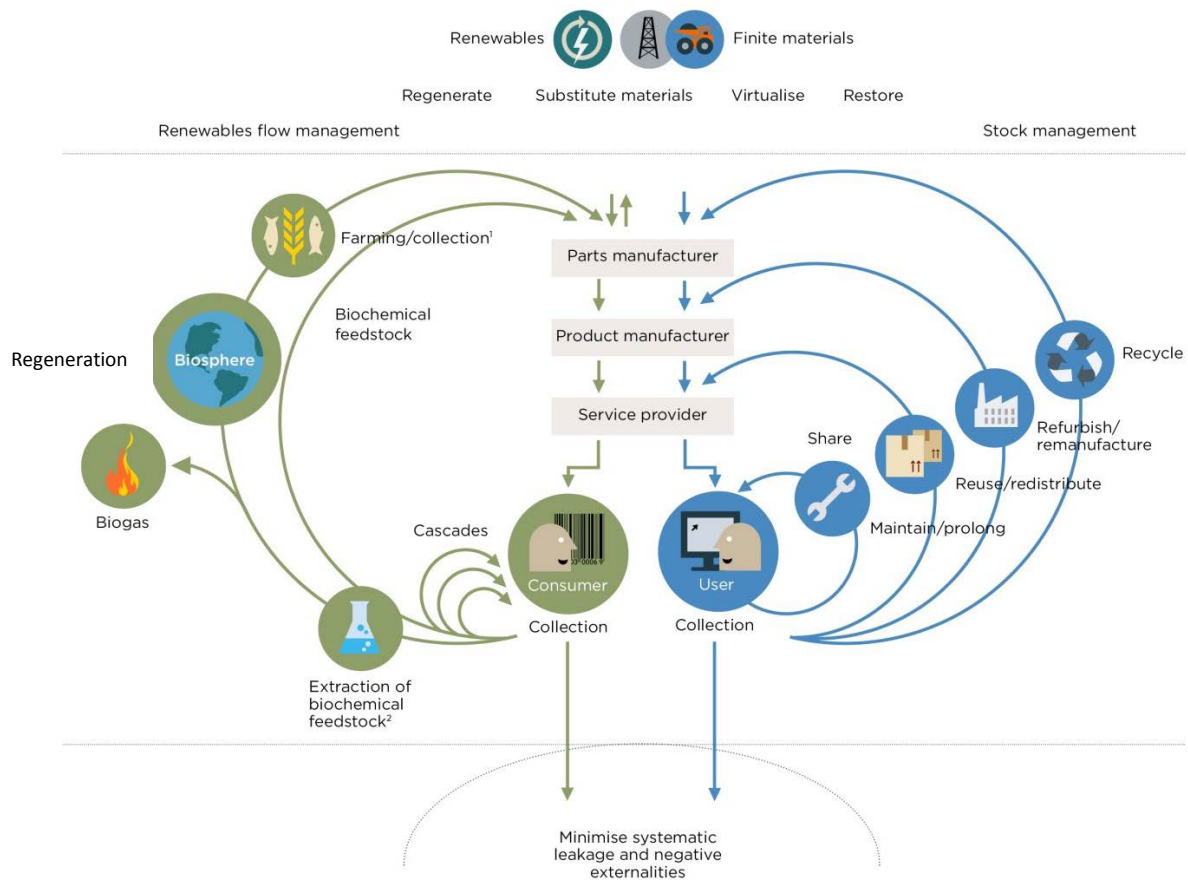


**Figure 2.8:** Circular economy diagram [15]

In fact, the Ellen MacArthur Foundation can be considered one of the driving forces of the circular economy. It describes the circular economy as “a continuous positive development cycle that preserves and enhances natural capital, optimizes resource yields, and minimizes system risks by managing finite stocks and renewable flows” and it presents the system diagram, shown in Figure 2.8, to illustrate the process [15].

Waste management is the main aim in the circular economy, yet, despite the efforts of some governments, only 30% of the total waste material collected globally involves resource recovery (material recovery 11% and energy recovery 19%) [19].

To promote new initiatives in order to work toward a more sustainable planet, and to promote the circular economy, the European Commission decided in December 2014 to withdraw a legislative proposal on waste, and at the same time the commission took on the commitment “to use its new horizontal methods to present a new package by the end of 2015 which would cover the full economic cycle, not just waste reduction targets, drawing on the expertise of all the Commission's services” [20].

The Circular Economy Package adopted by the European Commission consists of an EU Action Plan for the Circular Economy. The idea is to cover the whole cycle: from production and consumption to waste management and the market for secondary raw materials, establishing an ambitious program of actions.

The author of this PhD thesis and the research group in which she participates is convinced that the circular economy is an opportunity to reinvent the economy, making it more sustainable and competitive and bringing benefits for both industries and citizens.

## **2.4. Use of steelmaking slag in the civil works and construction industry**

Since the pioneering papers of Motz, Geiseler and Koros [21-23], there have been many studies that have proposed the reuse of several types of iron and steelmaking slag in construction and civil engineering. Today some of their proposals have become reality, considering that some of these wastes are used as raw materials in the construction industry.

As presented in the previous section, in the Basque Country all the steel is produced in electric arc furnaces, generating huge amounts of electric arc furnace slag and ladle furnace slag. Following the research lines of Motz, Geiseler and Koros, the aim of this thesis is to endeavor to take a step forward in the standardization of these steel slags. This approach will drive their widespread use all over the world, lead to less dumping of steel slags in landfill sites, turn a waste into a high value by-product and promote the circular economy.

A lot of research has been carried out on ladle furnace slag in construction. Using ladle furnace slag for the stabilization of clayey soils [24; 25] and as a replacement of the fine fraction in hydraulic [26-29] and bituminous mixes [30] have been the main research topics for some years, with encouraging results. A lot of research has also been done to develop the use of this material as an active addition to Portland cement to be included in the European standard EN-197 [31-33], which would give this material an added value.

The different uses of electric arc furnace slag in the construction and civil works industry have also been a recurrent research topic over the last 20 years. Research has been developed to analyze its use as bedding material for roads and railways, water

depuration, and energy storage [34-36]. However, the main research topic on the use of electric arc furnace slag has been as aggregate in bituminous mixes [37-43] and in hydraulic mixes [28; 44-51].

Today, the mechanical properties and durability of concretes manufactured with this slag are well known and have been demonstrated to be similar, or even better than concretes manufactured with traditional natural aggregates. The main disadvantages that have usually been found when the slag is reused as aggregate are the higher density and worse workability that the mixes manufactured with this kind of aggregate presented.

In the author's opinion the higher density is not a major problem, due to the higher concrete strength that is usually obtained using this slag as aggregate. However, the workability of the mixes needs to be improved, matching conventional mix design to the properties of the EAF slag. This challenge is the major focus of the PhD thesis: developing and manufacturing self-compacting concretes that meet the highest requirements for their workability.

## **2.5. Self-compacting concrete**

The durability of some unique structures made with concrete has been an issue of interest all over the world for many years. In Japan, during the 1980s, it was a major topic of interest, mainly due to the seismic activity in that country. The need for skilled workers to cast the concrete and to achieve sufficient compaction to create a durable concrete was a real problem, due to a gradual reduction in number of this type of worker in Japan [52].

In 1986, as a solution to making durable concretes without the need for skilled workers, Professor Hajime Okamura proposed manufacturing a concrete that can fill formwork purely by its own weight, with no need for vibration-compaction and with no segregation of the coarse aggregate.

Ozawa and Maekawa developed the study of concrete workability, obtaining the first prototype of self-compacting concrete in 1988 [53]. Initially, this concrete was called "high performance concrete", but soon this term was applied to high strength and durable concretes generally, with no restrictions on their fresh properties. The authors subsequently changed the term to "self-compacting concrete".

The procedure proposed by Professor Okamura [54] to produce these kinds of mixtures can today be considered as “the traditional or conventional way to make self-compacting mixes”. It is a simple mix proportioning system that consists of slightly decreasing the coarse aggregate content to 50% of the solid volume, increasing the fine aggregates paste to 40% of the volume, assuming that the water-cement ratio in volume is 0.9 to 1, and determining the superplasticizer dosage and the final powder-water ratio to ensure self-compactability.

Many authors have shown that it is useful to consider the fresh concrete as a two-phase material, for designing a good self-compacting concrete: as an aggregate skeleton in a “mortar” or “matrix of paste”. By adjusting the superplasticizer dosage and the powder-water ratio it has been observed that it is possible to establish a relationship between the fresh properties of the mortar and the fresh properties and rheology of the final concrete.

A matrix with good viscosity and good flowability is necessary. This matrix phase must have sufficient deformability and flowability to be able to compact under its own weight, but it must also be highly viscous so that the coarse aggregate fraction is efficiently transported without undergoing segregation. Two tests are usually employed, to validate these requirements in the mortar paste: the mini slump flow test and the mini V–funnel test. Different approaches have been taken to relate the results obtained in these tests to the final concrete properties. In the EFNARC [55] specification the recommended values for the mortar paste are 24–26 cm for the mini slump cone test and 7–11 s for the mini V–funnel test, in order to obtain a concrete that fulfills the requirements for it to be considered self-compacting concrete.

Okamura [56] proposed two indices, calculated from the results obtained in the above-mentioned tests: the deformability index ( $\phi_m$ ) and the viscosity index ( $R_m$ ), which are calculated as:

$$\phi_m = (d_1 d_2 - d_0^2) / d_0^2$$

where,  $d_1$  and  $d_2$  represent the after-flow diameter in two orthogonal directions, and  $d_0$  is the 80 mm cone diameter. And:

$$R_m = 10/t$$

where,  $t$  (s) is the measured flow time of the mortar through the funnel.



Assuming a fixed coarse aggregate content, the quality of self-compactability of a certain concrete can be established by correlating its deformability and viscosity indices. Figure 2.9 shows the ranking of self-compactability proposed by Okamura connecting these two indices.

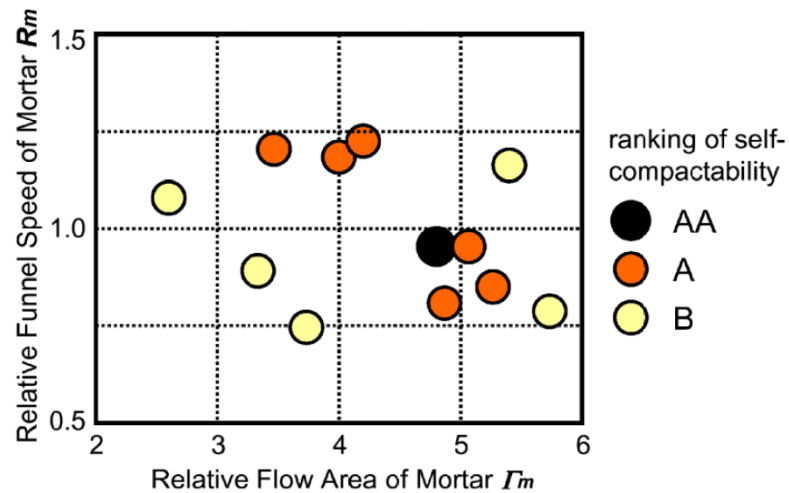


**Figure 2.9:** Ranking of self-compactability [56]

In this thesis, the values proposed by EFNARC and the method proposed by Okamura have been used, as is described in the corresponding chapter.

P. Domone [57] proposed a value of 28–34 cm in the mini slump cone and of 1–7.5 in the mini V–funnel for the mortar paste to result in good self-compacting concrete. He related the properties of the mortars to the fresh concrete properties applying the following formulas:

$$sf_{conc} = 4.8sp_{mor} - 800$$

Where,  $sf_{conc}$  is the concrete slump flow (mm), and  $sp_{mor}$  is the mortar slump (mm)

$$Vf_{conc} = 1.8Vf_{mor} + 1.5$$

Where,  $Vf_{conc}$  is the V-funnel flow time for concrete (s) and  $Vf_{mor}$  in the V-funnel time for the mortars (s).

These two methodologies have been used as the basis for a lot of research into developing self-compacting concretes. Today the technology of self-compacting

concrete is well understood, but plenty of research is still going on regarding this technology. Nowadays, the recurrent topics in the study of self-compacting concrete technology are:

- Fiber-reinforced self-compacting concrete [58-62].
- Self-compacting lightweight concrete.
- The effect of different additions (fly ash, silica fume, GGBS and other natural or artificial pozzolanic materials) on the properties of self-compacting concrete [63;64].
- The use of singular aggregates in self-compacting concrete, i.e. old recycled concrete as coarse aggregate [65-68]. The especially heavy EAF slag can be included with these kinds of materials.

To create a concrete using electric arc furnace slag which has suitable self-compacting properties is a significant challenge, due to the tendency to segregation of this heavy coarse aggregate, and its sharp and rough form which reduces the mix workability. Yeong-Nain Sheen [69-71] has published some articles about the manufacture of a self-compacting concrete using stainless steel slag as aggregate, a rough but not especially heavy slag. In Thessaloniki University, Greece, E. Anastasiou et al [59] has published an article on a self-compacting concrete using ladle furnace slag as an active addition fine aggregate and reinforcement fibers.

## **2.6. Past career experience of the research team in relation to steel slag**

As has been noted, many researchers have investigated the uses of ladle furnace slag and electric arc furnace slag in the construction and civil works industry at a global level. Below are the career details of the research group where this PhD thesis has been developed, concerning this research topic.

In the late 1990s, (96-97) four researchers from Burgos, Santander and Bilbao (Juan Manuel MANSO, José Antonio POLANCO, Javier Jesús GONZÁLEZ and José Tomás SAN JOSÉ), started working together on the uses of steel slags in construction and civil engineering. Today, after a number of advances, they still continue working together for the standardization of steel slags. The evidence for these advances can be seen in the amount of publications they have worked on together, some of them having a significant impact in the field of construction engineering and in the field of materials science [24-27; 30; 31; 45; 48; 72-77].

The first steps taken on this topic are detailed in the PhD thesis of Professor Juan Manuel Manso [78]. In this thesis the use of electric arc furnace slag as aggregate in concrete was analyzed and presented at the University of Burgos in 2001, under the supervision by Professor Javier J. González of the University of the Basque Country. The conclusions of this PhD thesis were as follows:

- Electric arc furnace slag is a heavy stable material suitable for use as aggregate in concrete.
- It is necessary, for the correct behavior of EAF slag as aggregate, that it is not mixed with other wastes or by-products, such as LF slag.
- EAF slag has few fine particles and therefore, to manufacture good concrete, it is necessary to add fine natural aggregates.
- The mortars and concretes manufactured with EAF slag as aggregate show promising mechanical behavior.
- The durability of EAF slag concrete is similar or slightly worse than natural aggregates concrete, but always better than the limits set by the standards.

The second notable work of the team is the PhD thesis of Doctor Milagros Losañez [79]. It was presented in 2005 at the University of the Basque Country. In this case, previous concrete (soil-cement), normal concrete and mortar mixes were manufactured using electric arc furnace slag as aggregate, and using ladle furnace slag for the first time. The conclusions drawn in this case were:

- Concrete mixtures made with EAF slag as an aggregate and LF slag as a fine filler show good mechanical strength.
- With regard to durability, the addition of LF slag to the concrete mixtures should not be considered positive, but the long-term expansive behavior is acceptable.
- Mortar mixtures made with EAF slag as an aggregate (without LF slag) show excellent performance and only slight expansivity.
- Pervious concrete made with EAF slag and LF slag (without cement) constitutes a useful mixture to be used as soil-cement in road-bedding applications.
- Rules for the design of high-quality concrete using steelmaking slags:
  - Appropriate primary crushing and weathering of EAF slag.
  - Appropriate proportioning between the coarse and fine fraction aggregates.
  - Sufficient use of fine inert aggregates, such as siliceous or limestone sands.

- Correct preparatory treatment and limited amounts of LF slag.
- Plasticizer admixtures may subsequently be added to improve workability.

Six years later the PhD thesis of Doctor Idoia Arribas [80] was presented, whose work confirms the good mechanical and durability properties of concretes correctly manufactured with electric arc furnace slag aggregate. During this research, the understanding of mix design was increased, and the procedures to be used were improved. It was verified that the only disadvantages of working with this type of material are the higher density and poorer consistency displayed by the mixtures, requiring more water, in order to manufacture concrete with good workability. This disadvantage was clearly demonstrated during the construction of the foundation slabs and the basement walls of a real building (Kubik) at Tecnalia (formerly Labein), the research center where this PhD thesis was developed in collaboration with the University of the Basque Country.

After the thesis of Doctor Arribas, the main objectives of the present PhD thesis were established. It was stated that higher density is not a great problem because this increased density can be compensated by a gain in strength, making EAF slag concrete a suitable material to function as structural elements. The final step to demonstrate that suitability is to manufacture real scale structural elements and to analyze their structural behavior; which is one of the research objectives described in the present PhD thesis.

It was then necessary to demonstrate that a concrete with the required workability may be manufactured with electric arc furnace slag, by adjusting the mix design and slightly changing the traditional concrete proportions. To achieve this objective, it was decided to manufacture the structural elements with pumpable concrete and with self-compacting concrete, both made with electric arc furnace slag as aggregate.

---

## References

- [1] European Commission. Action Plan for a competitive and sustainable steel industry in Europe. Communication from the commission to the Parliament, the Council, the European Economic and Social Committee and the Committee of Regions. Strasbourg. 2013.
- [2] J.M. Palacios, J.L. Arana, J.I. Larburu, L. Iniesta. Fabricación del acero, Madrid, España: Editorial Spainfo SA. 1998.
- [3] R.J. Fruehan. The Making, Shaping, and Treating of Steel: Ironmaking volume, AISE Steel Foundation. 1999.
- [4] S.S. Yearbook. World steel association. 2005.
- [5] S.S. Yearbook. World steel association. 2015.
- [6] Union de Empresas Siderúrgicas. La industria siderúrgica española. 2015. 2016.
- [7] Union de Empresas Siderúrgicas. Mapa de instalaciones siderúrgicas. 2014.
- [8] Instituto nacional de estadística. Cifras de la población a 1 de enero de 2016. 2016.
- [9] E.J. Hiru. Sector siderometalúrgico. 2013.
- [10] Xabier Barrutia Etxebarria. Altos Hornos de Vizcaya. Análisis crítico del cierre y testimonios vitales. 2015.
- [11] Fernando Capelástegui Herrero. La siderurgia Vizcaína (1876–1996). 1996.
- [12] P.L. Simmonds. Waste products and undeveloped substances: Or, hints for enterprise in neglected fields, R. Hardwicke. 1962.
- [13] K.E. Boulding. The economics of the coming spaceship earth. Environmental Quality Issues in a Growing Economy. 1966.
- [14] R.U. Ayres, A.V. Kneese. Production, consumption, and externalities. The American Economic Review 59 (1969) 282–297.
- [15] E. Macarthur, Towards the Circular Economy: Opportunities for the consumer goods sector. Ellen MacArthur Foundation. 2013.
- [16] W.R. Stahel. The performance economy, Palgrave Macmillan, London. 2010.
- [17] A.B. Lovins, L.H. Lovins, P. Hawken. A road map for natural capitalism. 1999.
- [18] W. McDonough, M. Braungart. Cradle to cradle: Remaking the way we make things. MacMillan. 2010.

- [19] P. Chalmin, C. Gaillochet. From waste to resource: an abstract of the 2006 world waste survey. Paris, Veolia Environmental Services. 2009.
- [20] European Commission. Circular economy strategy. 2016.
- [21] J. Geiseler. Use of steelworks slag in Europe. *Waste Management* 16 (1996) 59–63.
- [22] H. Motz, J. Geiseler. Products of steel slags an opportunity to save natural resources. *Waste Management* 21 (2001) 285–293.
- [23] P.J. Koros. Dusts, scale, slags, sludges... Not wastes, but sources of profits. *Metallurgical and Materials Transactions B* 34 (2003) 769–779.
- [24] J.M. Manso, V. Ortega-Lopez, J.A. Polanco, J. Setien. The use of ladle furnace slag in soil stabilization. *Construction and Building Materials* 40 (2013) 126–134.
- [25] V. Ortega-Lopez, J.M. Manso, I.I. Cuesta, J.J. Gonzalez. The long-term accelerated expansion of various ladle-furnace basic slags and their soil-stabilization applications. *Construction and Building Materials* 68 (2014) 455–464.
- [26] J.M. Manso, M. Losanez, J.A. Polanco, J.J. Gonzalez. Ladle furnace slag in construction 17 (2005) 513–518.
- [27] A. Rodriguez, J.M. Manso, A. Aragon, J.J. Gonzalez. Strength and workability of masonry mortars manufactured with ladle furnace slag. *Resources, Conservation and Recycling* 53 (2009) 645–651.
- [28] I. Papayianni, E. Anastasiou. Production of high-strength concrete using high volume of industrial by-products. *Construction and Building Materials* 24 (2010) 1412–1417.
- [29] V.Z. Serjun, A. Mladenovic, B. Mirtic, A. Meden, J. Scancar, R. Milacic. Recycling of ladle slag in cement composites: Environmental impacts. *Waste Management* 43 (2015) 376–385.
- [30] M. Skaf, V. Ortega-Lopez, J.A. Fuente-Alonso, A. Santamaria, J.M. Manso. Ladle furnace slag in asphalt mixes. *Construction and Building Materials* 122 (2016) 488–495.
- [31] T. Herrero, I.J. Vegas, A. Santamaria, J.T. San-Jose, M. Skaf. Effect of high-alumina ladle furnace slag as cement substitution in masonry mortars. *Construction and Building Materials* 123 (2016) 404–413.
- [32] C. Shi. Characteristics and cementitious properties of ladle slag fines from steel production. *Cement and Concrete Research* 32 (2002) 459–462.

- 
- [33] A. Saez-de-Guinoa Vilaplana, V.J. Ferreira, A.M. Lopez-Sabiron, A. Aranda-Uson, C. Lausin-Gonzalez, C. Berganza-Conde, G. Ferreira. Utilization of Ladle Furnace slag from a steelwork for laboratory scale production of Portland cement. *Construction and Building Materials* 94 (2015) 837–843.
- [34] I. Ortega-Fernandez, J. Rodriguez-Aseguinolaza, A. Gil, A. Faik, B. D’Aguanno. New thermal energy storage materials from industrial wastes: Compatibility of steel slag with the most common heat transfer fluids 137 (2015).
- [35] I. Ortega-Fernandez, A. Gil, A. Faik, J. Rodriguez-Aseguinolaza, B. D’Aguanno. Parametric and thermal management optimization of a steel slag based packed bed heat storage. *ASME 2015 9th International Conference on Energy Sustainability, ES 2015, collocated with the ASME 2015 Power Conference, the ASME 2015 13th International Conference on Fuel Cell Science, Engineering and Technology, and the ASME 2015 Nuclear Forum*. 1. (2015).
- [36] I. Ortega-Fernandez, N. Calvet, A. Gil, J. Rodriguez-Aseguinolaza, A. Faik, B. D’Aguanno. Thermophysical characterization of a by-product from the steel industry to be used as a sustainable and low-cost thermal energy storage material. 89 (2015) 601–609.
- [37] M. Ameri, S. Hesami, H. Goli. Laboratory evaluation of warm mix asphalt mixtures containing electric arc furnace (EAF) steel slag. *Construction and Building Materials* 49 (2013) 611–617.
- [38] M. Skaf, J.M. Manso, A. Aragon, J.A. Fuente-Alonso, V. Ortega-Lopez. EAF slag in asphalt mixes: A brief review of its possible re-use. *Resources, Conservation and Recycling* (2016).
- [39] M. Pasetto, N. Baldo. Mix design and performance analysis of asphalt concretes with electric arc furnace slag. *Construction and Building Materials* 25 (2011) 3458–3468.
- [40] A. Kavussi, M.J. Qazizadeh. Fatigue characterization of asphalt mixes containing electric arc furnace (EAF) steel slag subjected to long term aging. *Construction and Building Materials* 72 (2014) 158–166.
- [41] E.A. Oluwasola, M.R. Hainin, M.M.A. Aziz. Evaluation of asphalt mixtures incorporating electric arc furnace steel slag and copper mine tailings for road construction. *Transportation Geotechnics* 2 (2015) 47–55.
- [42] M. Pasetto, N. Baldo. Fatigue Behavior Characterization of Bituminous Mixtures Made with Reclaimed Asphalt Pavement and Steel Slag. *Procedia - Social and Behavioral Sciences* 53 (2012) 297–306.
- [43] M. Pasetto, N. Baldo. Experimental evaluation of high performance base course and road base asphalt concrete with electric arc furnace steel slags. *Journal of Hazardous Materials* 181 (2010) 938–948.

- [44] C. Baverman, F. Aran Aran. A study of the potential of utilising electric arc furnace slag as filling material in concrete. in: J. J. J. M. Goumans (Ed.), *Studies in Environmental Science. Waste Materials in Construction: Putting Theory into Practice. Proceedings of the International Conference on the Environment and Technical Implications of Construction with Alternative Materials*, Elsevier, (1997), 373–376.
- [45] J.M. Manso, J.J. Gonzalez, J.A. Polanco. Electric arc furnace slag in concrete. 16 (2004) 639–645.
- [46] M. Etxeberria, C. Pacheco, J.M. Meneses, I. Berridi. Properties of concrete using metallurgical industrial by-products as aggregates. *Construction and Building Materials* 24 (2010) 1594–1600.
- [47] S.I. Abu-Eishah, A.S. El-Dieb, M.S. Bedir. Performance of concrete mixtures made with electric arc furnace (EAF) steel slag aggregate produced in the Arabian Gulf region. *Construction and Building Materials* 34 (2012) 249–256.
- [48] J.A. Polanco, J.M. Manso, J. Setien, J.J. Gonzalez. Strength and durability of concrete made with electric steelmaking slag. 108 (2011) 196–203.
- [49] S. Monosi, M.L. Ruello, D. Sani. Electric arc furnace slag as natural aggregate replacement in concrete production. *Cement and Concrete Composites* 66 (2016) 66–72.
- [50] A.S. Brand, J.R. Roesler. Steel furnace slag aggregate expansion and hardened concrete properties. *Cement and Concrete Composites* 60 (2015) 1–9.
- [51] C. Pellegrino, P. Cavagnis, F. Faleschini, K. Brunelli. Properties of concretes with Black/Oxidizing Electric Arc Furnace slag aggregate. *Cement and Concrete Composites* 37 (2013) 232–240.
- [52] H. Okamura, M. Ouchi. Self-compacting high performance concrete. *Progress in structural Engineering and Materials* 1 (1998) 378–383.
- [53] K. Ozawa. High performance concrete based on the durability design of concrete structures. *The Second East Asia-Pacific Conference on Structural Engineering & Construction*. (1989).
- [54] H. Okamura, Self-compacting high performance concrete. *Ferguson lecture for 1996/1997*.
- [55] EFNARC. *Guidelines for self-compacting concrete*. London, UK: Association House (2002) 32–34.
- [56] H. Okamura, M. Ouchi. Self-compacting concrete. *Journal of advanced concrete technology* 1 (2003) 5–15.
- [57] P. Domone. *Mortar Tests for Self-Consolidating Concrete*. *Concrete International* 28 (2006).



- 
- [58] A. Orbe, J. Cuadrado, R. Losada, E. Roji. Framework for the design and analysis of steel fiber reinforced self-compacting concrete structures. *Construction and Building Materials* 35 (2012) 676–686.
- [59] E.K. Anastasiou, I. Papayianni, M. Papachristoforou. Behavior of self-compacting concrete containing ladle furnace slag and steel fiber reinforcement. *Materials & Design* 59 (2014) 454–460.
- [60] A. Orbe, R. Losada, E. Roji, J. Cuadrado, A. Maturana. The prediction of bending strengths in SFRSCC using Computational Fluid Dynamics (CFD). *Construction and Building Materials* 66 (2014) 587–596.
- [61] R. Madandoust, M.M. Ranjbar, R. Ghavidel, S. Fatemeh Shahabi. Assessment of factors influencing mechanical properties of steel fiber reinforced self-compacting concrete. *Materials & Design* 83 (2015) 284–294.
- [62] F. Kolarik, B. Patzak, L.N. Thrane. Modeling of fiber orientation in viscous fluid flow with application to self-compacting concrete. *Computers & Structures* 154 (2015) 91–100.
- [63] M. Jalal, A. Pouladkhan, O.F. Harandi, D. Jafari. Comparative study on effects of Class F fly ash, nano silica and silica fume on properties of high performance self-compacting concrete. *Construction and Building Materials* 94 (2015) 90–104.
- [64] M.H.W. Ibrahim, A.F. Hamzah, N. Jamaluddin, P.J. Ramadhansyah, A.M. Fadzil. Split Tensile Strength on Self-compacting Concrete Containing Coal Bottom Ash. *Procedia - Social and Behavioral Sciences* 195 (2015) 2280–2289.
- [65] D. Carro-Lopez, B. Gonzalez-Fonteboa, J. de Brito, F. Martinez-Abella, I. Gonzalez-Taboada, P. Silva. Study of the rheology of self-compacting concrete with fine recycled concrete aggregates. *Construction and Building Materials* 96 (2015) 491–501.
- [66] K. Kapoor, S.P. Singh, B. Singh. Durability of self-compacting concrete made with Recycled Concrete Aggregates and mineral admixtures. *Construction and Building Materials* 128 (2016) 67–76.
- [67] E. Güneyisi, M. Gesoglu, Z. Algin, H. Yazici. Rheological and fresh properties of self-compacting concretes containing coarse and fine recycled concrete aggregates. *Construction and Building Materials* 113 (2016) 622–630.
- [68] B.M. Vinay Kumar, H. Ananthan, K.V.A. Balaji. Experimental studies on utilization of coarse and finer fractions of recycled concrete aggregates in self compacting concrete mixes. *Journal of Building Engineering* 9 (2017) 100–108.
- [69] Y.N. Sheen, D.H. Le, T.H. Sun. Innovative usages of stainless steel slags in developing self-compacting concrete. *Construction and Building Materials* 101, Part 1 (2015) 268–276.

- [70] Y.N. Sheen, D.H. Le, T.H. Sun. Greener self-compacting concrete using stainless steel reducing slag. *Construction and Building Materials* 82 (2015) 341-350.
- [71] Y.N. Sheen, L.J. Huang, T.H. Sun, D.H. Le. Engineering Properties of Self-compacting Concrete Containing Stainless Steel Slags. *Procedia Engineering* 142 (2016) 79–86.
- [72] J.M. Manso, J.A. Polanco, M. Losanez, J.J. Gonzalez. Durability of concrete made with EAF slag as aggregate. 28 (2006) 528–534.
- [73] J.M. Manso, A. Rodriguez, A. Aragon, J.J. Gonzalez. The durability of masonry mortars made with ladle furnace slag. 25 (2011) 3508–3519.
- [74] J.M. Manso, D. Hernandez, M.M. Losanez, J.J. Gonzalez. Design and elaboration of concrete mixtures using steelmaking slags. 108 (2011) 673–681.
- [75] I. Arribas, I. Vegas, J.T. San-Jose, J.M. Manso. Durability studies on steelmaking slag concretes. *Materials & Design* 63 (2014) 168–176.
- [76] I. Arribas, A. Santamaria, E. Ruiz, V. Ortega-Lopez, J.M. Manso. Electric arc furnace slag and its use in hydraulic concrete. *Construction and Building Materials* 90 (2015) 68–79.
- [77] J.T. San-Jose, I. Vegas, I. Arribas, I. Marcos. The performance of steel-making slag concretes in the hardened state. *Materials & Design* 60 (2014) 612–619.
- [78] J.M. Manso, “Fabricación de hormigón hidráulico con escoria negra de Horno Eléctrico de Arco”. Tesis Doctoral, Universidad de Burgos (2001)
- [79] M.M. Losañez, “Aprovechamiento integral de escorias blancas y negras de acería eléctrica en construcción y obra civil”. Tesis Doctoral, Universidad del País Vasco (UPV/RHU) (2005)
- [80] I. Arribas “Estudio y diseño de hormigones estructurales basados en la incorporación de subproductos siderúrgicos: viabilidad tecnológica” Tesis doctoral, Universidad del País Vasco (UPV/EHU) (2011)

*Chapter 3:*  
*Materials and Methods*

---



# 3

## *Materials and Methods*

### **3.1. Introduction**

The materials used and the methods applied in this thesis are described in the following paragraphs.

This chapter will help the reader to acquire a deeper understanding of electric arc furnace slag and ladle furnace slag. Taking into account that the main objective of the thesis is to take a step forward in the reuse of these wastes, it is important to include a profound analysis of their compositions, properties and characteristics, which is done in the first part of the chapter.

The second part gives the reader an overview of the different methods used for testing the manufactured mortar mixes, concrete mixes and structural elements.

### **3.2. Materials**

The materials used throughout the research that has formed the basis for the development of this PhD thesis are of standard usage in the manufacturing of hydraulic mixes.

Water from the urban supply of the city of Bilbao and different types of cement and crushed limestone of different particle sizes have been used. The amounts, sizes and other properties of these materials will be included in the following chapters.

The originality of this research is the use of electric arc furnace slag and ladle furnace slag in the manufacture of self-compacting mixes. A deep analysis of current

knowledge on the origin, properties and singularities of these materials is set out below.

### **Ladle furnace slag**

Ladle furnace slag comes from the secondary or basic refining of steel, which mainly consists of desulphurization. Almost 80 kg of ladle furnace slag is generated per ton of refined steel.

Basic oxides are predominant in its chemical composition. Calcium and magnesium oxides represent approximately 65% of the weight of the slag, while approximately 30% consists of siliceous and aluminum oxides, which act as fluxes to produce the melting of the former refractory oxides, and the remainder is a small quantity of iron and other oxides which are also present.

The most common appearance of this slag is in a dusty form, because of the spontaneous disintegration of its mass during cooling. This disintegration is mainly due to the allotropic transformation of calcium silicate beta into calcium silicate gamma.

Regarding its physical characteristics, it can be observed in the scanning electron microscope that the dusty particles are polyhedral single crystals, as can be seen in Figure 3.1, or irregular aggregates formed of polyhedral crystals which are porous, hollow and sharp contoured.

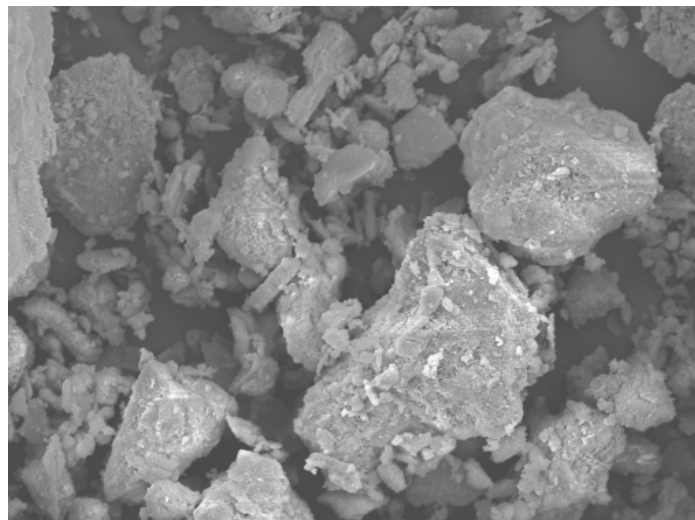


**Figure 3.1:** SEM image of Ladle Furnace slag

Depending on the saturation method of the melting fluxes, ladle furnace slag can be divided into two or three types. There is silica saturated ladle furnace slag, alumina

saturated ladle furnace slag, and the third group is a mix of the first two, a ladle furnace slag with similar quantities of silicon and aluminum oxides.

As confirmed in the literature [1-3], 80% of the mass of ladle furnace slag consists of calcium silicates and calcium aluminates which also contain the presence of magnesium, and other cations. The remainder of the mass is made up of sulfur compounds, small amounts of metallic iron, detachable by magnetic methods, and a little titanium, manganese, sodium and potassium. Free lime and free magnesia can also be found in this type of slag, and this is the main problem regarding its reuse.

As stated in the bibliography [4; 5], these two last compounds are expansive. Free calcium plus water yields calcium hydroxide in a few days, doubling the initial volume of the particles. Free magnesia plus water gives magnesium hydroxide, also doubling the volume, in this case in several weeks or months. If these hydroxides absorb carbon dioxide from the atmosphere they turn into calcium and magnesium carbonates, which can cause even further volumetric expansion.

If this slag is to be reused, it is indispensable to know the quantities of these compounds that are present in it; however, the problem is that there is no satisfactory way for these to be determined. Moreover, the high diversity of reactions that can occur between free lime or free magnesia and environmental agents make it difficult to predict the volumetric expansion of any kind of slag.

It is important to know the origin of the free lime or the free magnesia, if we are to estimate its volumetric expansion. Some authors [4; 6] have previously realized that the free lime in steelmaking slag can be found in two different morphologies, determined as “primary” and “secondary”. The free lime determined as “primary” is a residual free lime that has its origin in the lime added to the flux-slag of the furnace at the start of the heating process, which has not been dissolved and therefore, when in a liquid state at 1640°C, is not combined in silicate or aluminate form. Its particle size varies from 10 to 60 microns. During cooling the slag becomes a dusty material, leaving this unreacted free lime exposed to environmental attack.

The “secondary” free lime, also known as precipitate free lime, is normally found in less quantity than the primary type, or can even be absent in this kind of slag. Its origin is from the decomposition of  $SC_3$  crystals into  $SC_2$  during cooling. It is smaller and not as easy to observe as the “primary” free lime. More time is needed for its reaction with

the environment due to the diffusion process. Normally its size is less than one micron and it is not possible to detect with either EDAX or with SEM.

The origin of free MgO is similar to the “primary” free lime, coming from undissolved particles of burnt periclase in the liquid slag. However, chemical analysis cannot evaluate the quantity of this compound in a reliable way: only X-ray diffraction gives a semi-quantitative estimation of its presence.

One might think that, if some compounds remain unreacted, it is because the stoichiometric balance of the steelmaking is not correct, but the presence of these solid particles in the liquid slag is necessary to protect the refractory wall of the furnace from chemical attack by the slag.

After a detailed evaluation of this kind of slag in a previous work [7], this research team consider that TG, DSC-DTA (or TG-DSC) and XRD analysis are the most useful techniques to determine the amounts of these expansive compounds. Keeping in mind that only approximate results are obtained with these techniques, the actual values can be higher, as has been confirmed [8]. An estimation has to be done of the quantity of these compounds, and a slag can be considered suitable for reuse only if these amounts are kept under reasonable limits.

Besides the expansive compounds having to be kept under certain limits, the presence of sulfur also has to be controlled, due to the possibility of the appearance of undesirable secondary ettringite or thaumasite from the oxidizable sulfurs. In addition, special attention must be paid to the hydration of calcium aluminates and their subsequent conversion to katoite.

Up until now, these undesirable phenomena have been the reason why 400,000 tons of ladle furnace slag are still dumped in landfill sites annually in Spain [9]. However, new research has shown that, if the harmful compounds are kept below certain limits, ladle furnace slag is an excellent raw material for use in different applications in construction and civil engineering.

Finally, some consideration has to be given to the standardization of ladle furnace slag in the construction sector. It should be determined if weathering is necessary before it is used; it seems that, to profit from its hydraulicity, it is better used immediately after cooling, but the presence of expansive compounds has to be taken into account. A deeper analysis of the two different kinds of ladle furnace slag is necessary.



Interaction between the slag and Portland cement with the conventional additions also needs to be analyzed, although no reference to incompatibilities has been found in the literature. Nevertheless, during the development of this thesis special attention has been paid to this issue as well as to the effects of expansive compounds in hydraulic mixes.

### Electric arc furnace slag

Electric arc furnace (EAF) slag comes from the melting process and the primary acid refining of the steel. Between 120 and 180 kg of EAF slag is generated per ton of manufactured steel [10]. After cooling from 1560°C, it becomes a stony, cohesive, slightly porous, heavy, hard and tough material (see Figure 3.2). At first it is almost black, due to iron oxides, but after weathering for some time it becomes a grey color, due to the migration of the free lime to the skin and its reaction with the environment [11].



**Figure 3.2:** Electric arc Furnace slag particle

The presence of iron oxides makes this material heavier than the natural raw materials usually used as aggregates in the construction industry. Sometimes a higher density than ordinary concretes is required (marine coastal blocks, retaining walls, foundations or large basement slabs), but in many cases this property is not wanted. The density ( $\delta$ ) of EAF slag has been recorded to be within the range of 3 to 4 Mg/m<sup>3</sup>. It depends mainly on the content of metallic iron ( $\delta \approx 8$ ), iron and manganese oxides ( $\delta \approx 5$ ) and the internal porosity. The usual content of the element Fe in EAF slag is between 20 and 30%, which implies an iron oxide content of 30 to 45% by weight. For its use in structural concrete, it appears possible to reach a value of between 3.2 to 3.4 Mg/m<sup>3</sup> in the density of EAF slag without affecting the steel or slag quality, reducing the iron

content to 15-20% and the iron oxides to 22-30%. An additional porosity of about 5% in the EAF slag will also contribute to a reduction in its density with no detriment to its properties.

The porosity of the slag can be increased by modifying the cooling method. There are at least two methods used for cooling EAF slag from furnace temperature to room temperature. One method is cooling in continuous mode, dousing a small flow of slag with water. The other method involves pouring the liquid slag into a large pit, depositing a new layer on the previous layer of slag which has solidified, while several water jets cool the upper surface. The cooling rate of the slag in the latter method is slower than in the former case, allowing the gases retained in the slag to escape and reducing its porosity. Therefore, the former method is recommended for obtaining lower densities, because it does not let the gases escape, increasing the porosity of the slag.

The cooling rate of the slag also affects the grading of the particles, due to thermal contraction and spontaneous shrinkage. With the first method, particles, lumps and pieces with a size of less than 40 mm are obtained, which, after metallic iron separation, can be used as gravel. With the second method, pieces of more than 40 mm in size are obtained, which need crushing and metallic iron separation, before their use as aggregate.

The cooling process is not the only process in steelmaking that influences the properties of the slag. The “foaming” of the slag during the last phase in the electric arc furnace and the pouring process can also determine very important criteria for the use of EAF slag. All these operations affect the final quality of the EAF slag and its reuse in the construction and civil engineering sectors.

The steelmaking process, therefore, has a central influence on the quality of the EAF slag that is generated; in the past, steelmakers were not concerned with the quality of their slags as most of it was dumped in landfill sites. Nowadays, collaboration between the producers and consumers of this material is essential, and it would probably be an appropriate time to encourage such collaboration within the EU.

According to the scientific literature, the chemical composition of EAF slag is based on its content of calcium, iron and silicon oxides, which make up over 80%; aluminum, magnesium, manganese and phosphorus oxides are also present. Variations in the proportions of these oxides depend on the kind of steel that is manufactured, the

refractory materials of the furnace and some technological advances. In standard, oxidizing electric arc furnace slag, as can be expected due to its acidic origin, the proportion of acidic oxides (silica, alumina, iron oxide, etc.), is greater than the proportion of basic oxides (lime, magnesia and alkalis) in most cases.

The main compounds of EAF slag are single and complex calcium silicates (containing aluminum, iron or magnesium), and single and complex iron-based oxides (containing calcium, magnesium, chromium and manganese, among others) which are in a liquid state above 1560°C, aided by fluxes such as CaF<sub>2</sub>, which solidify at under 1200°C.

Despite the fact that EAF slag is an “oxidizing” slag, in which the predominant acidic oxides are capable of dissolving all of the basic oxides, it is not uncommon to find some types of EAF slag that contain undissolved particles of free lime. These particles are a consequence of the electric arc furnace procedure; partial addition of lime is sometimes made near the end of the “acid” refining process, without sufficient time for the other acidic slag components to dissolve the lime, and this free CaO remains undissolved in the mass of the slag as it cools.

As has been previously mentioned, free lime in steel slags can be found in two different morphologies, determined as “primary” and “secondary”. The free lime determined as “primary” is a residual free lime that has its origin in the lime added to the flux-slag of the furnace at the start of the heating process, and which has not been dissolved. In fact this primary free lime is in a grainy or spongy solid phase suspended in the liquid slag. In unhydrated slag it is possible to find particle sizes of between 4 and 20 µm in SEM and EDAX analysis.

The “secondary” free lime, also known as precipitate free lime, may be found in the grain boundaries of some iron oxide based compounds (dicalcium ferrite or R-O phase), either dispersed in calcium silicates, in SC<sub>3</sub> crystals or in SC<sub>2</sub> crystals. Normally, it has a size smaller than one micron and may neither be detected with EDAX nor with SEM.

The content of free lime in EAF slag is less than in LD (Linz-Donawitz) converter slag or BOF (Basic Oxygen Furnace) slag. A priori, it could appear that these slags (BOF-LD Converter and EAF) are the same material, due to the presence of the same oxides and their stony gravel presentation, but the lower free lime content in EAF slag makes it superior.

There is a consensus in the literature that the main problem for the use of this slag is its volumetric expansiveness or swelling of pieces, lumps and particles, and free lime is one of the compounds that can generate volumetric changes. Four main reactions have been found to be responsible for the swelling:

- The evolution of silicate  $\beta$  to  $\gamma$  is accompanied by an increase in volume, although this reaction is less likely in EAF slag due to the presence of  $P_2O_5$  and other  $\beta$ -phase stabilizers.
- The long-term oxidation of metallic iron from iron +2 to iron +3, although infrequent, has also been observed in metallurgical slags.
- Low temperature hydroxylation of free CaO and subsequent carbonation in the presence of moisture.
- Free MgO hydroxylation.

By far the most common reaction is the hydroxylation and carbonation of the free lime. This reaction usually occurs within a few weeks or months, yet it has been demonstrated in the literature that the expansiveness of this type of slag is easily reduced [12]. If, after crushing the slag, it is weathered for 90 days with permanent wetting, homogenizing it by periodic turning of the heaps, the original expansion values of between 0.5% and 2.5%, obtained immediately after crushing, can be reduced to values of between 0.15% and 0.4% in tests using the ASTM D 4792 standard.

Nowadays, this is the main reason that the use of EAF slag as a coarse aggregate in hydraulic concrete is widely accepted, while LD slag is mainly used in roadbeds. Maximum levels of volumetric expansion in materials used as concrete aggregates and as road bedding are set at around 1% and 5% respectively, in current standards.

On other hand, the presence of free lime is advantageous for the chemical interaction of the slag with the cement paste. There is evidence of migration (diffusion of ions in aqueous solution) of this oxide from the core to the periphery of the aggregate pieces; periodic visual inspections of a stockpile of EAF slag exposed to weathering recorded changes in color of the external surface material (associated with rainfall and its evaporation) from grey-black to grey-white. The white substance on the external surface was clearly calcium carbonate [11].

When EAF slag is used as aggregate in hydraulic mixes, there is a zone of the material, mortar or concrete, that is directly affected by the slow arrival of CaO, due to this diffusion mechanism in the presence of humidity. This is the interfacial transition zone

(ITZ), between the aggregate particles and the cementitious matrix; it is considered the weakest part of the concrete. In this region, the appearance of microbleeding around the aggregate particles, porosity and some microstructural features depend on several factors, such as aggregate quality and size, the water–cement ratio, the binder and the age of the mix. The morphology and properties of the ITZ evolve at the same time as the hydraulic reactions of the Portland cement take place [13-18].

The ITZ has been described as a zone surrounding the aggregate particles with an average thickness of around 15 to 40  $\mu\text{m}$  [15]. The main characteristics of this zone in the hard concrete that have been identified as important are porosity, a very high content of portlandite, a presence of ettringite, and a lack of hydrated calcium silicates (S-C-H gel). Even the orientation of the portlandite and ettringite crystals and the sizes of the neighboring cement grains before setting have been analyzed. In fact, it is accepted that the conditions of the fresh concrete and its setting and hardening strongly influence the resultant morphology and state of the ITZ. Obviously, the long-term hydration of all cement particles (over weeks or months) and the presence of portlandite will promote slow and progressive changes in the morphology of the ITZ zone.

In the literature [13; 16; 18], it is accepted that the nature of the ITZ morphology plays an important role in the overall permeability and, therefore, the durability of hydraulic mixes, mortars and concretes. However, its influence on mechanical properties such as strength (tensile and compressive), stiffness and toughness have yet to be clearly established.

Therefore, the ITZs created at the end of the setting period in mixes that contain EAF slag (in well manufactured mixes, with low effective water to cement ratios) should differ from those of concretes which contain ordinary aggregates; this “new” ITZ will be smaller and less hollow than when natural aggregates are used. The slow migration of CaO from the core of the EAF slag pieces to the surface, and its subsequent chemical evolution to calcium carbonate, also affects the ITZ morphology. Hence, variations in the morphology and age-evolution of the ITZ around the EAF slag pieces may be expected, accompanied by variations in the global properties of the concrete, such as its permeability, durability, and mechanical properties (tensile and compressive strength and stiffness).

The fracture surfaces of concrete specimens after mechanical tests, in which the larger aggregate pieces have detached themselves from the matrix, are widely accepted as

undesirable. However, when fracturing breaks and divides these coarse aggregate particles in a visible way, showing good adherence and cohesion between matrix and aggregate, the situation is promising. Some authors [13; 16] have observed a generally lower strength of the overall concrete than of its components, the aggregates (calcareous or siliceous) and the cementitious matrix; they have explained this observation by a specific low strength in the ITZ. Hence, it may be stated that the better the quality of the bond in the ITZ, the better the mechanical (tensile and compressive) strength of the concrete. Well manufactured EAF slag concrete, with a compressive strength higher than 45 MPa, shows fracture faces with the coarse aggregate divided. This phenomenon can explain the higher strength that is normally obtained in concretes manufactured with EAF slag aggregate instead of natural aggregate.

### 3.3. Methods

The different methods used will be described in the corresponding chapters. In this section the authors want to give the reader an overview of the methodology used during the development of this PhD thesis.

As has been presented in the structure of this thesis, the methodology used moves from small specimens to bigger ones. Three different scales have been analyzed:

- In the first scale the fresh properties, mechanical behavior, physical properties and durability of mortar mixes has been analyzed.
- The second one covered the analysis of the fresh properties, mechanical behavior, physical properties and durability of self-compacting concretes.
- In the third and last scale, the analysis of the structural behavior of different beams was performed.

Continuing with this methodology, the test methods were divided into three different sections.

#### **Mortar test**

The different test methods used for evaluating the properties of the manufactured mortar are presented in Figure 3.3.

As can be seen in Figure 3.3, most of the methods in use comply with an ASTM or EN standard. In some, however, special methodologies meeting different specifications have been used for their development.

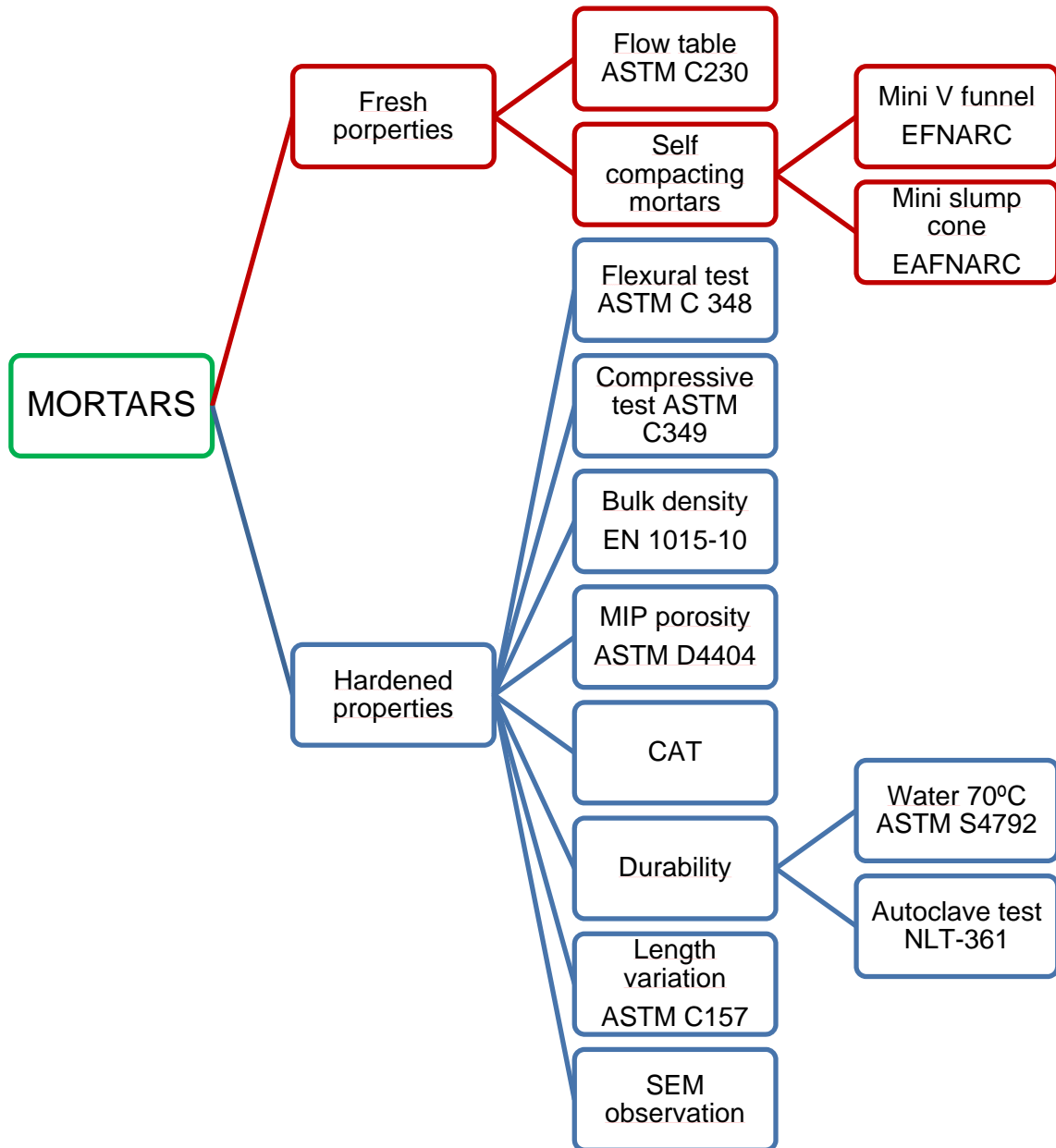


Figure 3.3: Mortar test methods

Mini slump cone

This test is similar to the Abrams cone used to measure the consistency of concrete, but using a cone with smaller dimensions. Its use has been proposed in the European guidelines for SCC [19], and it has been applied by several authors to evaluate mortar and cement paste consistency [20-25]. In addition, different indices have been proposed from the results of this test: relative slump flow, and the index of deformability.

Relative slump flow: 
$$\Gamma_{p/m} = \left[ \frac{(d_1 + d_2)}{2d_0} \right]^2 - 1$$

Index of deformability: 
$$\Gamma_m = \frac{(d_1 d_2 - d_0^2)}{d_0^2}$$

$d_1, d_2$  Measured flow diameters

$d_0$  Flow cone diameter: 80mm



**Figure 3.4:** Measuring of mortar spread

These values enable the comparison of the results of different authors, considering that, in view of the bibliography, different authors have used cones of different dimensions. For example, the cone proposed by EFNARC [19] and used by Okamura [21] and Domone [20] was 60 mm high and had top and base diameters of 70 mm and 100 mm respectively. The cone used by Meborouki [23] was 57 mm high and had top and base diameters of 19 mm and 38 mm respectively.

In this research, the cone used was 40 mm high with top and base diameters of 70 mm and 80 mm respectively. The values obtained in this test (d) were used to compare the consistencies of the different mixes that had been made during the experimental stage. The above-mentioned indices were used to compare the values obtained in this research with the those obtained by other authors.



The test consists of placing the cone at the center of a steel or glass plate and filling it with mortar. The cone is then lifted immediately after the filling is complete and the mortar spreads out over the plate. When it stops spreading, the average diameter ( $d$ ) in two perpendicular directions is measured ( $d_1$ ,  $d_2$ ), as it is shown in Figure 3.4. The mortar spread is visually checked for any segregation or bleeding. The  $d$  value is the one that was used to compare the different mix designs.

### Mini V-funnel

The mini V-funnel test is a reduced scale version of the V-funnel test for concrete. In this case, the funnel has standardized dimensions, and different values are not found in the literature. All the authors have used the same design as that proposed by EFNARC [19], whose shape and dimensions are shown in Figure 3.5.

It is used to evaluate the viscosity of mortar or cement paste. The test consists of measuring the flow time from the opening of the trap door to the first sighting of daylight. For this test, the funnel, in a vertical position, is filled with mortar, and then the gate is opened. The time is recorded ( $t$ ), and this is the value that is used to compare the viscosity of different mixes.

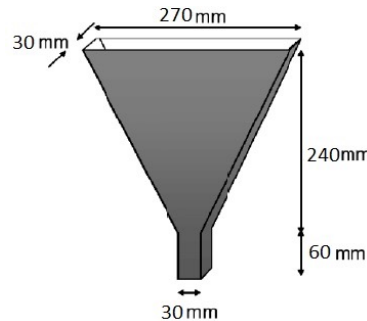


**Figure 3.5:** Mini V funnel dimensions [19].

Okamura (3) defined an index with the results of this test, the viscosity index:

$$R_m = \frac{10}{t}$$

$R_m$ : Viscosity index

$t$ : Measured time (sec) for mortar to flow through the funnel

For self-compacting mortars the use of either test individually will not properly describe the rheology of the mortar mix, but by using both indices it is possible to correlate them, obtaining a more adequate description of its behavior.

### Density

To determine the bulk density of mortars, the steps indicated in standard UNE-EN 1015-10 were followed. The specimens were dried in a stove at 70°C until the mass of the specimens remained constant, when they were removed and weighed on a balance ( $m_d$ ). Then the specimens were kept in water until they acquired a constant mass, when they were weighed again ( $m_{sat}$ ). To obtain the volume of the specimens, they were weighed underwater with a hydrostatic balance, while completely submerged ( $m_i$ ).

The volume of the specimen will be:  $V_s = \frac{m_{sat} - m_i}{\rho_w}$

The bulk density of the mortar was calculated as:  $\rho = \frac{m_d}{V_s}$

### MIP

Mercury intrusion porosimetry has been developed according to the ASTM standard D4404 and is an adsorption technique which uses mercury as the adsorbate. It applies pressure to force the mercury to enter the pores of the mortar. The value of the volume of mercury that has entered the pores allows calculation of the area, the distribution of pore sizes and the percentage of porosity of the slag.

The equipment used was a mercury intrusion-extrusion Micromeritics AutoPore IV 9510. Its resolution of pore size is from 7 nm up to 360  $\mu\text{m}$  ( $3.6 \cdot 10^5$  nm).

### CAT

A CAT (Computerized Axial Tomography) analysis of the cured mixes was also performed, to study their structure in the solid state and to verify the absence of segregation. Images were taken every 0.1 mm to obtain good resolution, including pores sizes of under 0.15 mm.

### Water aqing

Adaptation of Designation: D4792 – 00 (reapproved 2006). Standard Test. Method for Potential Expansion of Aggregates from Hydration Reactions.

The submerged specimens of the mixtures (25x25x285 mm) were held in water at room temperature for 270 days and were then submerged in a 70°C temperature bath in a similar way to that proposed in the ASTM D-4792 standard; they were held for an additional 60-day period under these test conditions.

### Autoclave

The second durability test on mortars was carried out in an autoclave for 48 hours at 0.2 MPa, at a temperature of about 130°C (Spanish standard NLT-361), to evaluate the risk of expansion of certain slag compounds, which can contribute to the deterioration of the hardened material.

### SEM observations

The Scanning Electron Microscopy (SEM) technique is based on low-vacuum observation of backscattered electron (BSE) images, in which the samples were not electrically charged (neither sputtered with gold nor carbon). It was complemented by energy-dispersive X-ray analysis (EDX).

## Concrete test

The different test methods used for evaluating the properties of the manufactured concretes are presented in Figure 3.6.

As can be seen in Figure 3.6, most of the test methods are in accordance with an ASTM or EN standard; other methods have been developed in the same way as with the mortar specimens and are described in the previous paragraphs. However, some of them are unique to concrete, and special methodologies according to different specifications have been used; they are mentioned in the following paragraphs.

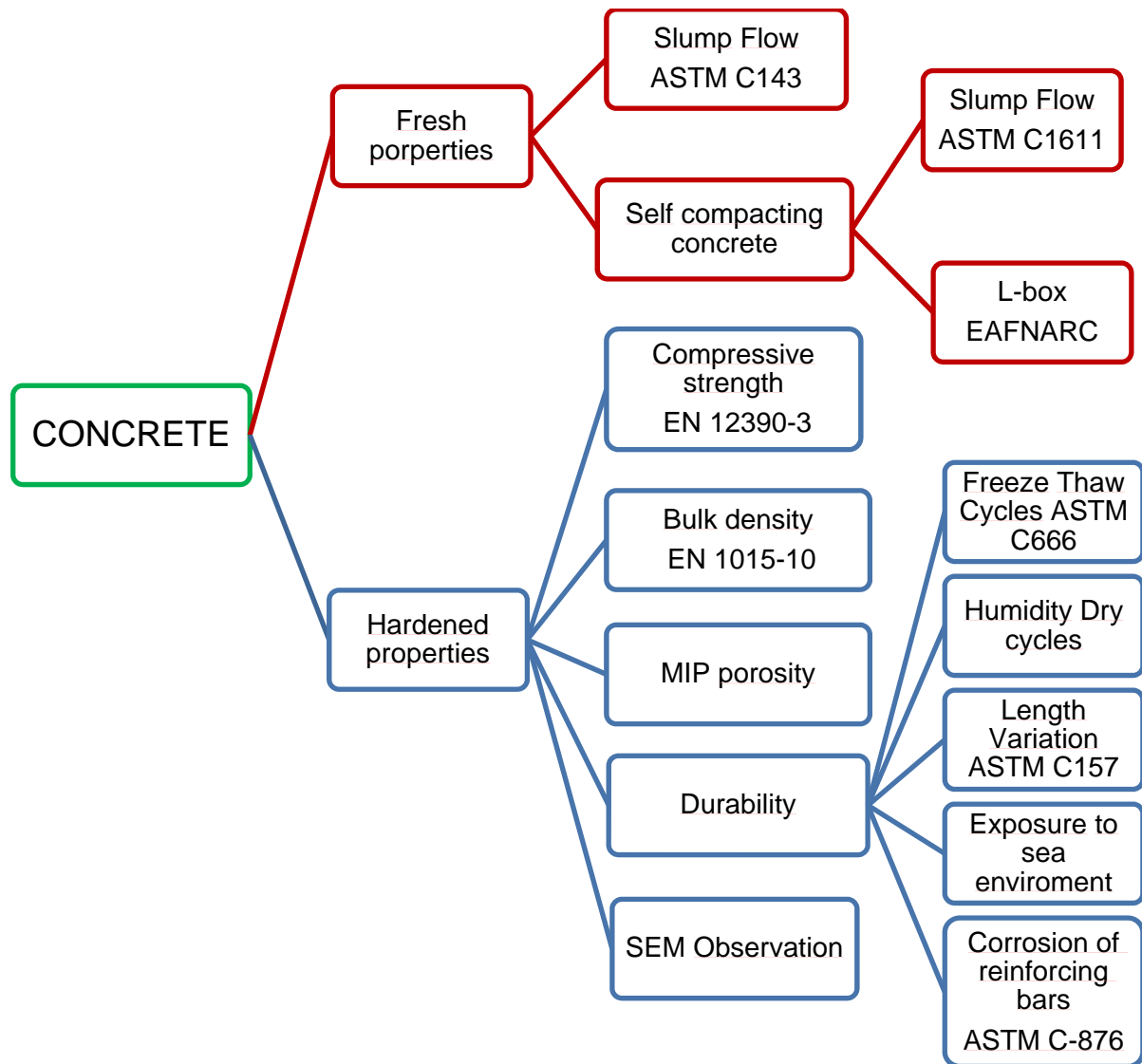
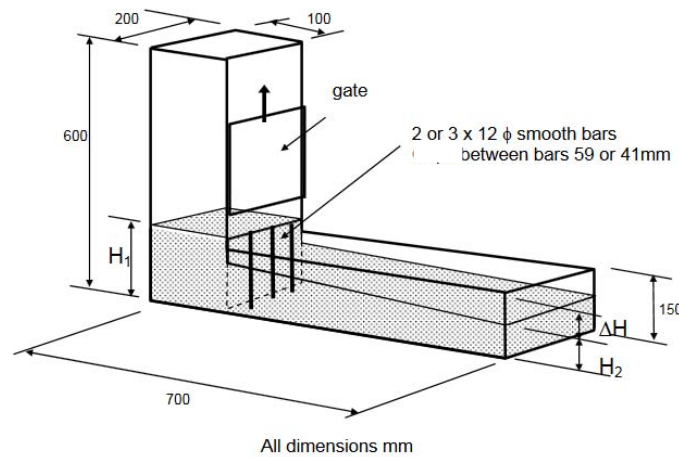


Figure 3.6: Concrete test methods

L-box test

This test was used to measure the passing ability of the concrete and was performed according to the specifications stated in the EFNARC guide [19]. The L-box had the design and dimensions that are shown in Figure 3.7.



**Figure 3.7:** L-box design [19]

To perform the test, the L-box should be placed on a horizontal surface. The concrete is poured into the filling hopper of the L-box and, after allowing it to stand for around 60 seconds, the gate is raised and the concrete flows into the horizontal section of the box. When movement has ceased, the vertical distance is measured immediately behind the gate and at the end of the horizontal section of the L-box, between the top of the concrete and the top of the horizontal section of the box, at three positions equally spaced across the width of the box. The mean value of the three measurements obtained at the beginning and at the end of the box are used to obtain  $H_1$  and  $H_2$  in mm. The passing ability (PA) is calculated with the following equation:

$$PA = \frac{H_2}{H_1}$$

Wetting-Drying cycles

Trials on hardened concrete based on successive alternating cycles of absorption of water (moisture) and forced evaporation of water (drying) in a stove, provide information on the harmful effects of fluctuations in the water content of a material on its integrity and other properties. In particular, in the case of hardened concrete,

two problems come into play, each one of which produces, or can produce, a certain deterioration of properties.

Contractions and linear expansion can be due to thermal variations as well as due to variations in humidity, which is known to directly influence the shrinkage of concrete.

Chemical reactions, primarily the carbonation of portlandite and other sodic or potassic alkalis, that occur at high speed or spontaneously, and whose expansiveness and reactions inhibit hydration, produce deterioration in the strength of the material.

The trial consisted of the following phases:

- Immersion of samples in water for 16 hours.
- Forced desiccation in a stove at 60°C for 8 hours.
- Repetition for the 90 days (90 cycles) of the test.

*Exposure to marine environment*

The specimens were exposed to the marine environment for 16 months. They were located in an intertidal zone. When the tide was in, the specimens were completely submerged, but when the tide was out they were completely in the air. These are the worst conditions that a structure can endure in relation to the marine environment. The cages in which the specimens were held may be seen in Figure 3.8.



**Figure 3.8:** Specimens cages at tidal zone

Two different studies have been done in the specimens ageing in the marine environment. One in specimens that have been exposed during one year and another in specimens exposed over five years.

In short term exposure test 100mm cubic specimens have been used. After the exposition, the specimens were suitably cut into two pieces to evaluate the ions penetration in the mass of concrete. The scanning electron microscopy and the dispersive energy of X-ray micro-analysis techniques were used; the samples were submitted to a low-vacuum pressure in a nitrogen atmosphere, being obtained the image by means of the backscattered electrons.

In the long-term test, cylindrical samples 150x300 mm were used for marine exposition over five years. The analysis were performed using portions of mentioned  $\phi 150$  cylindrical samples of dimension 200 mm large obtained after an initial transversal cut which eliminates 100 mm in length, and a posterior breaking of the longer piece by means of a Brazilian test. The recently broken surfaces of the samples were sprayed with silver nitrate one and plenolphthalein the other one, to evaluate the presence of chloride penetration and carbonation respectively.

#### Corrosion of reinforcement bars.

Samples of 150mm edge, into which a little steel structure formed by bars of 10 mm diameter is embedded (show Figure 3.9), have been submitted to durability tests (wetting-drying with sea water and saline fog chamber submission), controlling periodically its electrochemical corrosion variables.

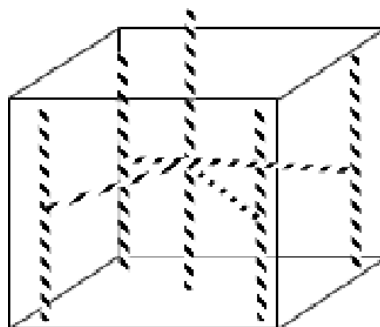


**Figure 3.9:** Internal schema of samples

To evaluate the corrosion risk with the measured of the corrosion potential of steel embedded in a cementitious material the criteria proposed in the ASTM C-879 has been used.

## Real scale beam test

The tests that were performed on the real-scale beams are cited in Figure 3.10.

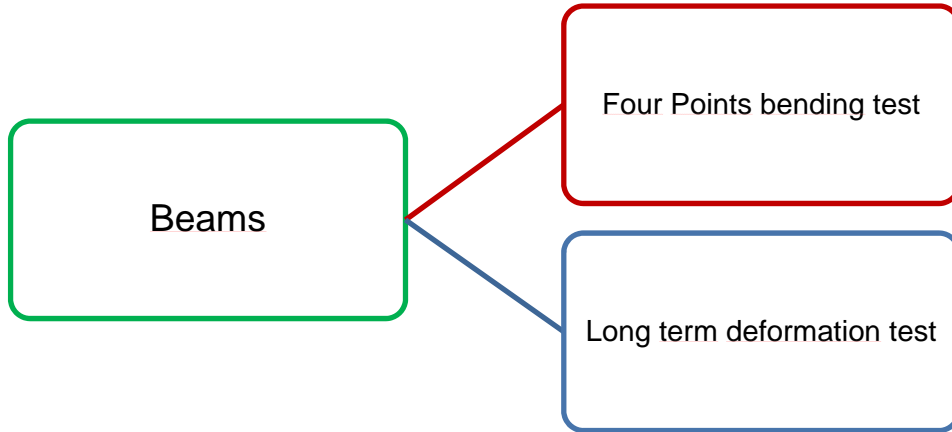


**Figure 3.10:** Real scale beams test methods.

### Four-point bending test

The four-point bending test was performed on the manufactured beams to obtain the values of the failure load, deflection and crack patterns. The load was applied while controlling the stroke displacement. This method makes controlling the increase in the deflection of the beam possible, and it is safer to do the inspection of the cracks in the beams.

Independent electronic equipment linked to transducers measures and stores the values of load, deformations in bands and LVDT displacements that will be used and represented later.

In Figures 3.11, the equipment used and its layout for performing the test are shown in a schematic way, and in Figure 3.12, a real image, taken during the flexural test, shows all the equipment described in the diagrams.



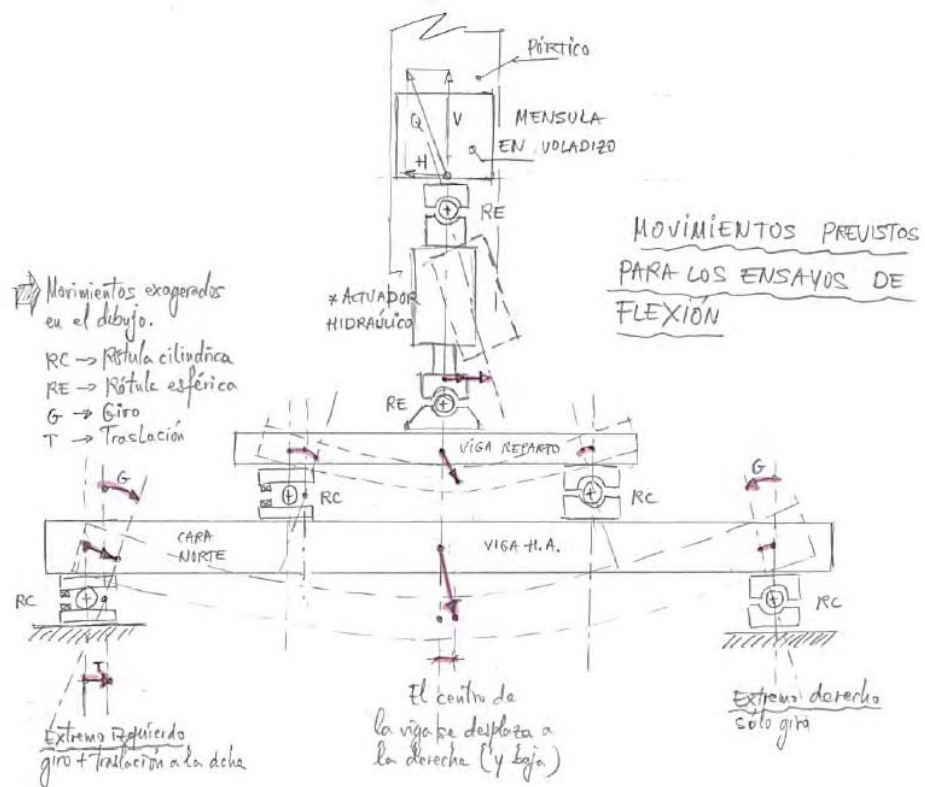
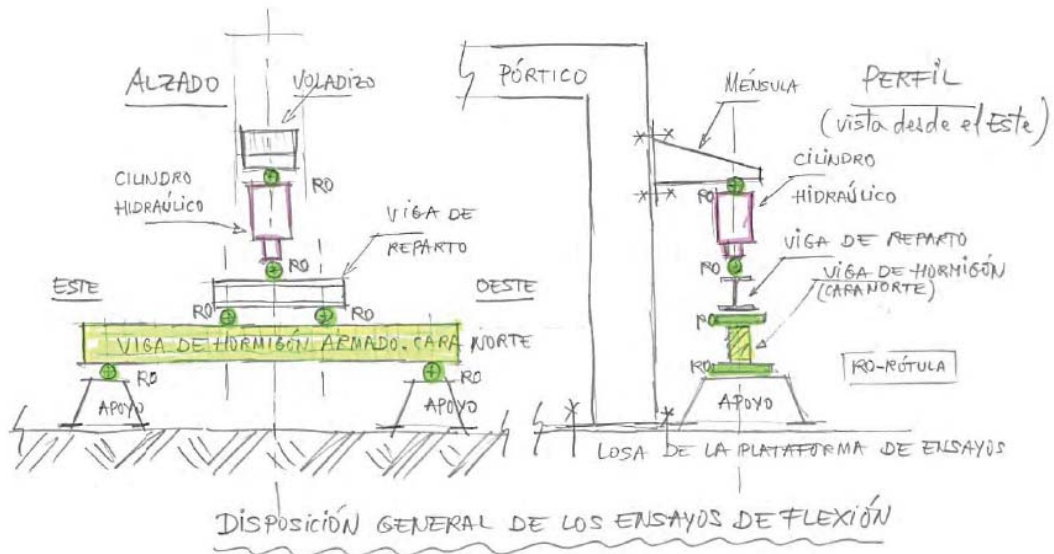
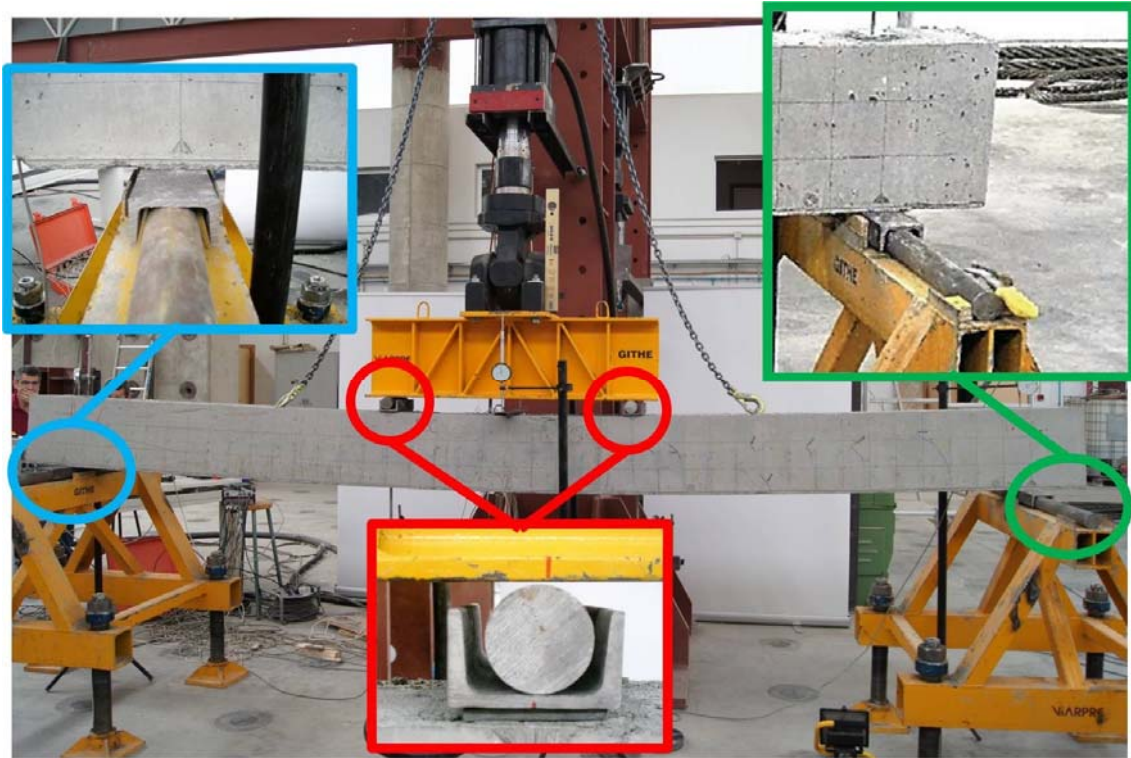


Figure 3.11: Lay out of four point bending test [Bengo courtesy]



**Figure 3.12:** Four point bending test image.

The independent electronic equipment had 20 linked transducers to measure and to record the different deformations, the cracks in the concrete, the strain of the reinforcement, the atmospheric temperature, the load and the displacement of the piston in the hydraulic cylinder. They were used as follows:

- 6 linear variable differential transducers (LVDT).
- 3 strain gauges on the lateral face of the concrete in the middle of the beam.
- 2 strain gauges on the top face of the concrete in the middle of the beam.
- 2 strain gauges on the lower face of the concrete in the middle of the beam.
- 3 strain gauges on the lower reinforcing steel bars in the middle of the beam.
- 1 sensor for measuring the atmospheric temperature.
- 1 sensor for measuring the beam temperature.
- 1 load sensor to measure the force applied by the hydraulic cylinder.
- 1 transducer to measure the displacement of the hydraulic cylinder.

In addition, with the aim of doubling the data on the vertical deformations, four vertical dial gauges were located on the upper face of the beam. In Figure 3.13 the position of the LVDTs and dial gauges are shown and in Figure 3.14 the positions of the strain gauges are shown. The data was recorded using CATMAN software.

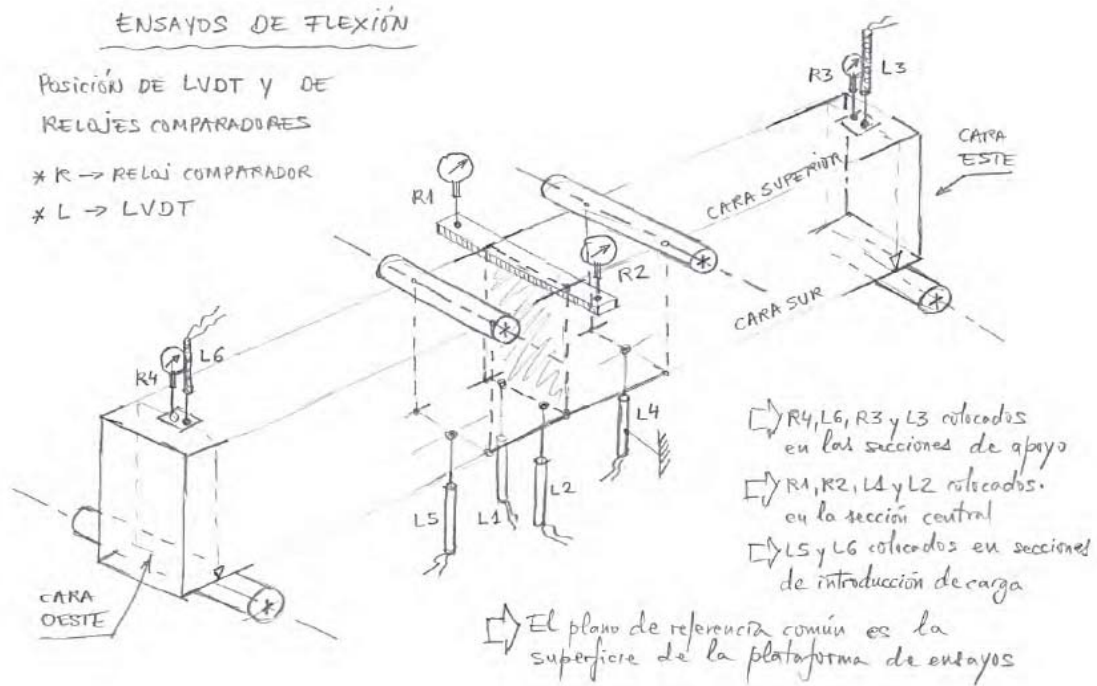


Figure 3.13: Position of LVDTs and Dial gauges[Bengo courtesy]

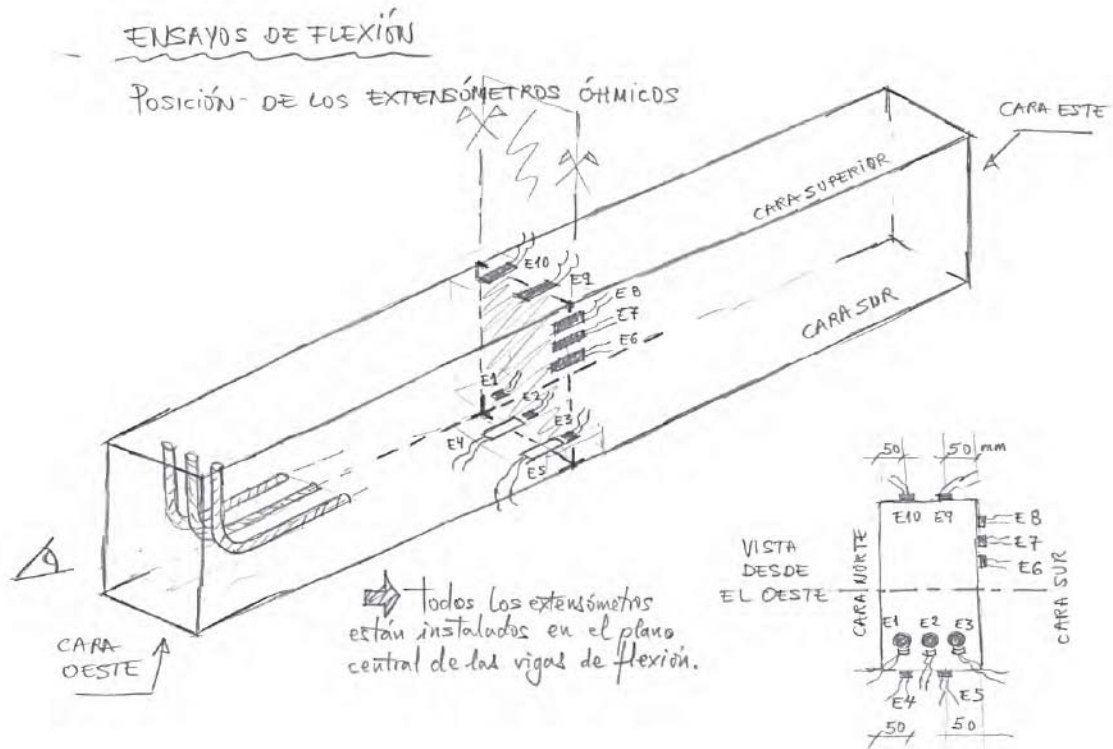


Figure 3.14: Position of strain gauges[Bengo courtesy]

The initial measurements were done while the beam simply supported, with the aim of showing the influence of its own weight on the deformation of the beam. The displacement of the central system of charge was applied at three different speeds. At first, a load rate of 0.5 mm/min was applied; when the first cracks began to appear, the speed was increased to 1 mm/min and, in the final moments of the test, a load rate of 2 mm/min was used.

A 100x100 mm grid was drawn on the beams to better detect the crack formations and at four different times the test was stopped to analyze and draw a crack which had appeared in the beam.

#### Long-term deformation test

Four beams were submitted to a long-term deformation test analyzing the creep of the beams at room temperature. A constant load of 40 kN was applied to each beam for 6 months. The disposition of the beams during that period is shown in Figure 3.15. In Figure 3.16 a diagram of the layout of the test is presented.

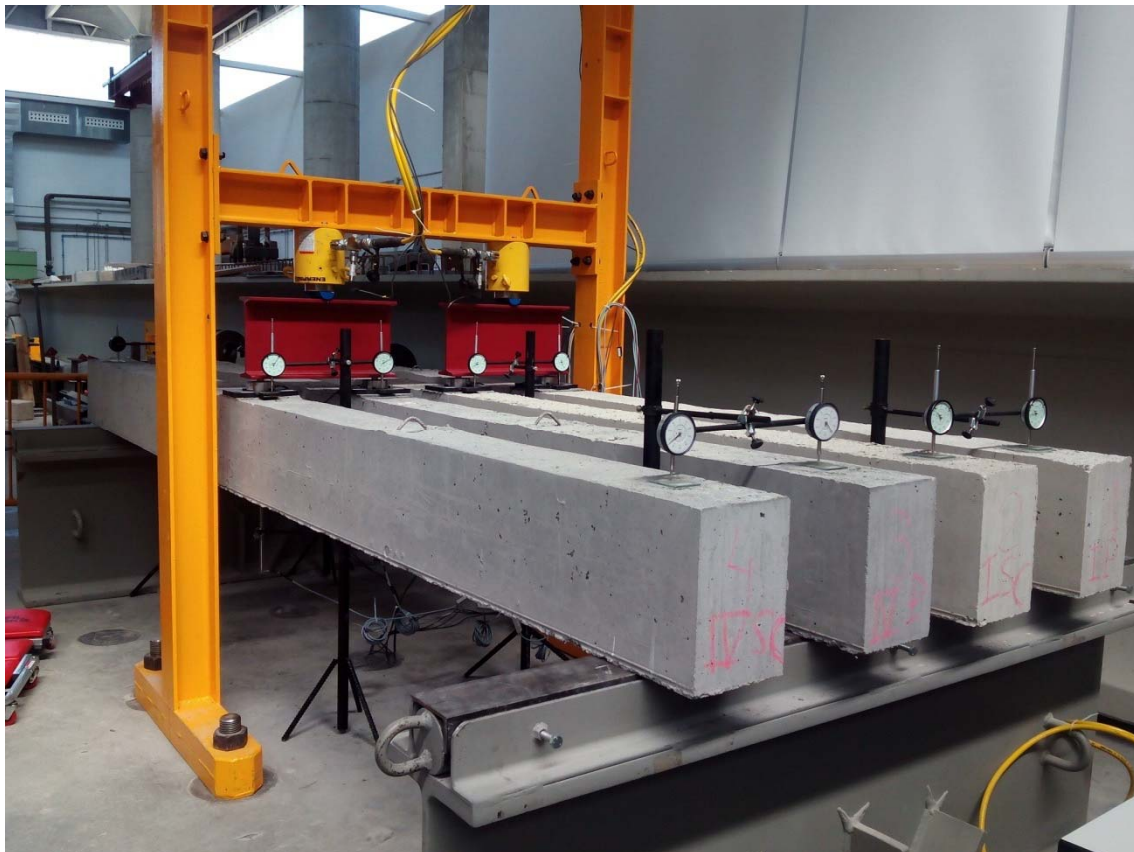


**Figure 3.15:** Disposition of the beams in the long term deformation test

ENSAYO DE FLUENCIA EN FLEXIÓN 3 PUNTOS  
FLECHA DIFERIDA

- Distribución de las 4 vigas. Vista desde ESTE. Cotas en m.

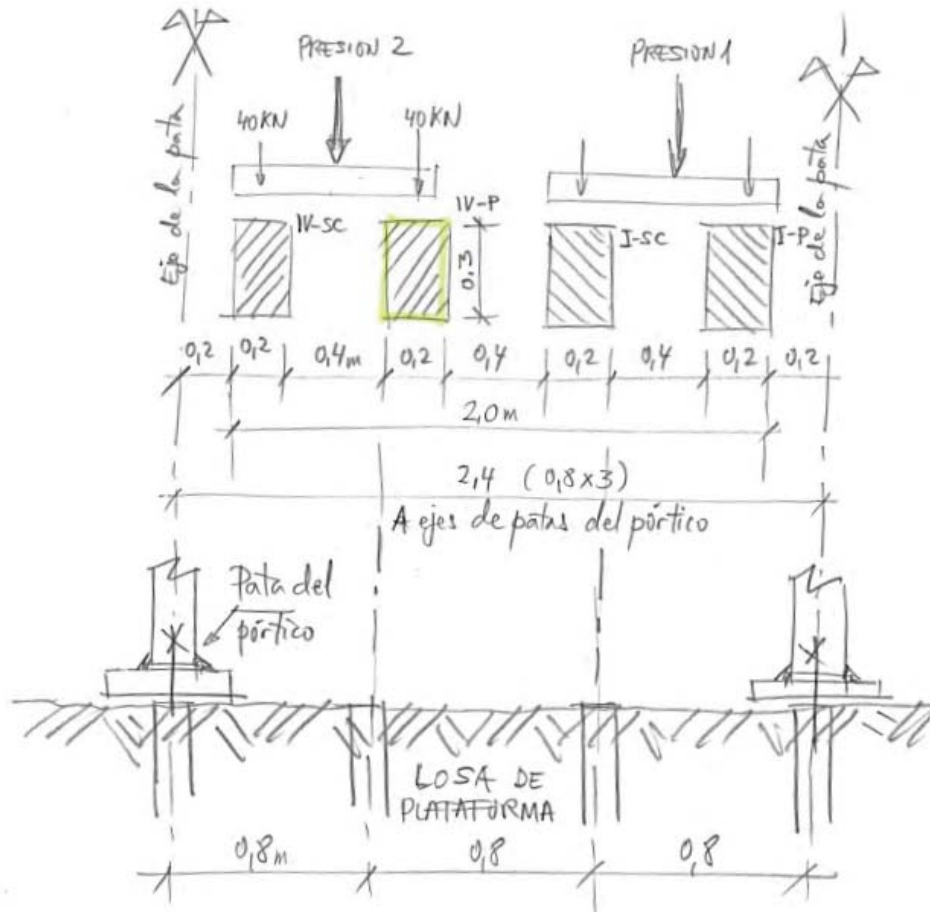


**Figure 3.16:** Lay out of the long term deformation test[Bengo courtesy]

A load transducer was located on the top face of each beam at the point where the force was applied, in order to monitor the load over time. To measure the deformation of the beams, one LVDT was located on the lower face of each beam in the mid span section. At the same point, but on the top face, a dial gauge was located and two other dial gauges were located at the ends of the beams, to measure possible displacements. A strain gauge was also located in the middle of each beam on its lower face to measure the cracks. A diagram of the location of all the transducers is shown in Figure 3.17.

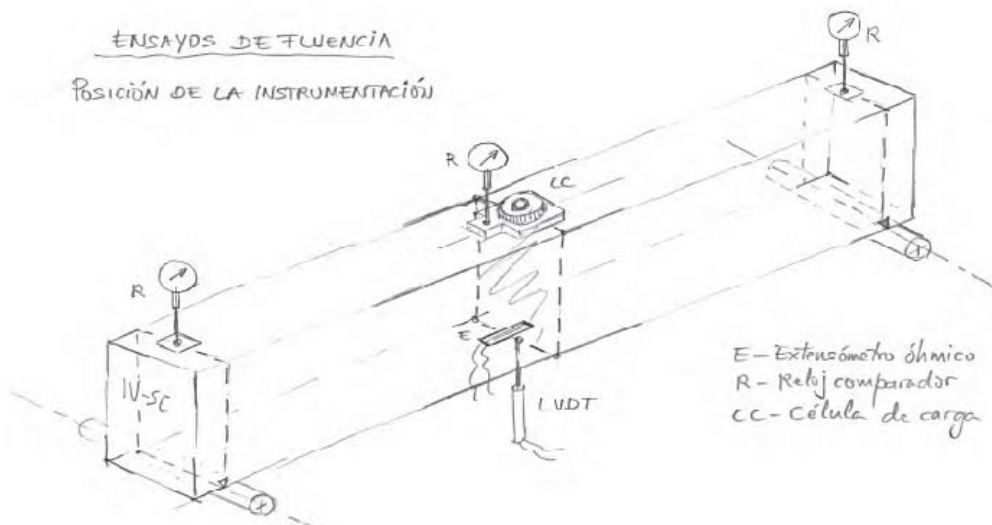


**Figure 3.17:** Transducer position in the long term deformation test[Bengo courtesy]

The data was recorded using CATMAN software which recorded one measurement every second in the first month of the test and after that period it recorded one measurement per minute.

In the same way as in the flexural test, the first measurement was taken when the beam was just supported, to show the influence of its own weight on the beam overall deformation.

Over the time that the test was ongoing, the temperature of the atmosphere was recorded. This parameter should not influence the behavior of the beams very much, but sometimes small deformations can occur due to temperature changes.

## References


- [1] J. Setién, D. Hernández, J.J. González, Characterization of ladle furnace basic slag for use as a construction material. *Construction and Building Materials* 23 (2009) 1788-1794.
- [2] W. Posch, H. Presslinger, H. Hiebler, Mineralogical evaluation of ladle slags at voestalpine Stahl Donawitz GmbH. 29 (2002) 308-312.
- [3] C. Shi, Characteristics and cementitious properties of ladle slag fines from steel production. *Cement and Concrete Research* 32 (2002) 459-462.
- [4] F. Wachsmuth, J. Geiseler, W. Fix, K. Koch, K. Schwerdtfeger, Contribution to the Structure of BOF-Slags and its Influence on Their Volume Stability. *Canadian Metallurgical Quarterly* 20 (1981) 279-284.
- [5] G. Wang, Y. Wang, Z. Gao, Use of steel slag as a granular material: Volume expansion prediction and usability criteria. *Journal of Hazardous Materials* 184 (2010) 555-560.

- [6] J. Waligora, D. Bulteel, P. Degrugilliers, D. Damidot, J.L. Potdevin, M. Measson, Chemical and mineralogical characterizations of LD converter steel slags: A multi-analytical techniques approach. *Materials Characterization* 61 (2010) 39-48.
- [7] V. Ortega-Lopez, J.M. Manso, I.I. Cuesta, J.J. Gonzalez, The long-term accelerated expansion of various ladle-furnace basic slags and their soil-stabilization applications. *Construction and Building Materials* 68 (2014) 455-464.
- [8] T. Herrero, I.J. Vegas, A. Santamaria, J.T. San-Jose, M. Skaf, Effect of high-alumina ladle furnace slag as cement substitution in masonry mortars. *Construction and Building Materials* 123 (2016) 404-413.
- [9] M. Skaf, V. Ortega-Lopez, J.A. Fuente-Alonso, A. Santamaria, J.M. Manso, Ladle furnace slag in asphalt mixes. *Construction and Building Materials* 122 (2016) 488-495.
- [10] S.A. Ihobe, Libro Blanco de minimizacion de residuos y emisiones de escorias de aceria. Sociedad Publica de Gestion Ambiental, Departamento de Ordenación Del Territorio, Vivienda y Medio Ambiente del Gobierno Vasco (1999).
- [11] I. Arribas, A. Santamaria, E. Ruiz, V. Ortega-Lopez, J.M. Manso, Electric arc furnace slag and its use in hydraulic concrete. *Construction and Building Materials* 90 (2015) 68-79.
- [12] J.M. Manso, J.A. Polanco, M. Losanez, J.J. Gonzalez, Durability of concrete made with EAF slag as aggregate 28 (2006) 528-534.
- [13] J.C. Manso, Interfacial transition zone in concrete: state-of-the-art report prepared by RILEM Technical Committee 108-ICC, *Interfaces in Cementitious Composites*/edited by J.C. Maso. RILEM report; 11.
- [14] J.P. Ollivier, J.C. Maso, B. Bourdette, Interfacial transition zone in concrete. *Advanced Cement Based Materials* 2 (1995) 30-38.
- [15] K.L. Scrivener, K.M. Nemati, The percolation of pore space in the cement paste/aggregate interfacial zone of concrete. *Cement and Concrete Research* 26 (1996) 35-40.
- [16] K.L. Scrivener, A.K. Crumbie, P. Laugesen, The Interfacial Transition Zone (ITZ) Between Cement Paste and Aggregate in Concrete. *Interface Science* 12 (2004) 411-421.
- [17] A. Elsharief, M.D. Cohen, J. Olek, Influence of aggregate size, water cement ratio and age on the microstructure of the interfacial transition zone. *Cement and Concrete Research* 33 (2003) 1837-1849.
- [18] P. Monteiro, P.K. Mehta, *Concrete: Microstructure, Properties, and Materials*, McGraw-Hill Publishing, 1996.

- [19] EFNARC, Guidelines for self-compacting concrete. London, UK: Association House (2002) 32-34.
- [20] P. Domone, Mortar Tests for Self-Consolidating Concrete. Concrete International 28 (.
- [21] H. Okamura, M. Ouchi, Self-compacting concrete. Journal of advanced concrete technology 1 (2003) 5-15.
- [22] B. Felekoglu, K. Tosun, B. Baradan, A. Altun, B. Uyulgan, The effect of fly ash and limestone fillers on the viscosity and compressive strength of self-compacting repair mortars. Cement and Concrete Research 36 (2006) 1719-1726.
- [23] A. Mebrouki, N. Belas, J. Vina, A. Arguelles, R. Zenasni, Application of experimental plans method to formulate a self compacting cement paste. Materiales de Construccion; Vol 60, No 298 (2010) DO - 10.3989/mc.2010.483082010.
- [24] B. Benabed, E.H. Kadri, L. Azzouz, S. Kenai, Properties of self-compacting mortar made with various types of sand. Cement and Concrete Composites 34 (2012) 1167-1173.
- [25] M. Mahdikhani, A.A. Ramezani pour, New methods development for evaluation rheological properties of self-consolidating mortars. Construction and Building Materials 75 (2015) 136-143.
- [26] H. Tanyildizi, M. Sahin, Application of Taguchi method for optimization of concrete strengthened with polymer after high temperature. Construction and Building Materials 79 (2015) 97-103.
- [27] H. Tanyildizi, Y. Yonar, Mechanical properties of geopolymer concrete containing polyvinyl alcohol fiber exposed to high temperature. Construction and Building Materials 126 (2016) 381-387.
- [28] G.T.G. Mohamedbhai, Effect of exposure time and rates of heating and cooling on residual strength of heated concrete. Magazine of Concrete Research 38 (1986) 151-158.
- [29] T.Z. Harmathy, Fire safety design and concrete, Longman Scientific & Technical ; Wiley, Harlow, Essex, England; New York, NY, 1993.
- [30] C.S. Poon, S. Azhar, M. Anson, Y.L. Wong, Strength and durability recovery of fire-damaged concrete after post-fire-curing. Cement and Concrete Research 31 (2001) 1307-1318.
- [31] H. Tanyildizi, Post-fire behavior of structural lightweight concrete designed by Taguchi method. Construction and Building Materials 68 (2014) 565-571.



*Chapter 4:*  
*Manufacture and*  
*Performance of Mortar Mixes*





# 4

## *Manufacture and performance of mortar mixes*

### **4.1. Introduction**

Mortar is basically a mixture of sand, water and cement. In this chapter the manufacture of different mortar mixes is described, and their properties in terms of mechanical and physical behavior and durability are analyzed. The chapter is divided into two more sections, each one corresponding to a different experimental project carried out as part of the development of this thesis.

The first project was focused on the interaction of electric arc furnace slag and ladle furnace slag with a Portland cement containing fly ash as a mineral addition. Its main objective is the manufacture of flowable structural mortars, establishing the highest feasible level of replacement of natural materials by waste materials (by products), while producing durable mortars with good mechanical properties.

Then the description of the performance of self-compacting structural mortars mainly manufactured with electric arc furnace slag and some with ladle furnace slag is included. The main objectives are to establish a powder-to-water ratio and to find the optimum superplasticizer dosage for manufacturing good paste; these findings formed the basis for manufacturing self-compacting concretes. High strength mortars were manufactured, some of them attaining a compression value of 100 MPa and showing good durability when subjected to accelerated aging tests.



## **4.2. The use of steelmaking slags and fly ash in structural mortars**

*Construction and Building Materials 90 (2015) 68 -79*



## **Abstract**

The main objective of this work is to produce structural slag mortars of good mechanical strength and workability, while reducing the consumption of Portland clinker, the production of which is a growing source of environmental concern. In this context, the study looks at the preparation of these mortars with steelmaking slags (electric arc furnace slag, ladle furnace slag) in partial substitution of conventional aggregates, and as supplementary cementing materials, and the use of Portland cement that includes a notable proportion of fly-ash. A detailed examination of the characteristics of eight mortar mixes is described. Structural and mechanical analyses are performed on the mixes, to study the role of water-reducer and air-entrainment admixtures; also, shrinkage contraction and other volumetric variations of the mixtures are measured and evaluated. The long-term behavior of these slag mixes appeared acceptable, thereby opening a promising line of work that will eventually establish suitable conditions for their use. The strength-to-weight ratio of these mortars is encouraging although uncertainty persists over the use of air-entrainment admixtures and ladle furnace slag.

## Introduction

The production of steelmaking slags around the world is increasing over time, despite the onset of the economic crisis. It is, therefore, essential to conduct research into applications for this by-product, to reduce its dumping in landfill sites and the production of excessive volumes of waste. By doing so, there would be less extraction of the natural resources that are necessary in those applications, which may otherwise be substituted by slags [1-3].

Several slag types may be listed in this context: blast furnace slag (BFS), basic oxygen-furnace slag (BOS), electric arc-furnace oxidizing slag (EAFS), ladle-furnace basic slag (LFS), argon-oxygen-decarburization slag (AODS), cupola-furnace slag (CFS), open-hearth furnace slag (OHS) and primary desulfurization slag (DS); and even milling scales (MS) [4, 5]. There are at present many research groups studying suitable and reliable applications for each slag type. The construction and building sector will undoubtedly employ most of these by-products [6-17].

Among the aforementioned slag types, BFS and CFS have the highest quality, which after rapid cooling and grinding show good hydraulic properties and excellent durability; the problems arising from their use are almost non-existent [18-21]. Although the performance of EAFS and LFS is less satisfactory [22-40], the objective of this present study is to demonstrate their successful application in several fields [41-60]. The most problematic slag type was obtained from the LD furnace (BOFS), the volumetric expansion of which was far from satisfactory [61-63].

Studies into the application of EAFS and LFS in hydraulic mixes, mortar and concrete, have been conducted by research teams throughout the world. Several groups may be found in the EU [46, 64-82], in Asia and in both South [83, 84] and North America [85, 86]; nevertheless, Asia is the continent with the largest number of such research teams, in both the Middle East [87-91] and the Far East [92-99].

In general, the use of these slags (EAFS and LFS) when applied as aggregates in hydraulic mixes has been relatively successful; the observation of hydraulicity is scarce and requires high particle fineness [100-103]. It is logical, at first, to give little or no consideration to the hydraulic factor in EAFS, the natural presentation of which is in the form of gravel. In contrast, a slight hydraulicity may be analyzed in the LFS, which is presented in the form of dust. The long-term behavior of the mixes obtained with these slags appears acceptable [67, 69, 70, 77, 79], which has opened a promising line



of research that will establish suitable conditions for its use. Several research groups in the EU (from Greece, Italy, Belgium, Germany and Spain) are in contact with the intention of establishing pre-normative rules for the use of these two slag types (EAFS and LFS) in mortar, concrete and bituminous mixes, including particular mixes as self-compacting concrete (EAFS), sprayed concrete (shotcrete) and self-leveling mortar (LFS).

The present work analyses the characteristics of several structural mortars in which these slags are used as aggregates (EAFS and LFS) and SCM (LFS) and it assesses the slight potential hydraulicity of the LFS. The main objective is to obtain good mechanical strength and suitable workability, so as to minimize the use of Portland clinker. Mortar density, due to the high specific weight of EAFS, and its durability are the most important factors to be taken into account; the role of the admixtures (fluidifying, water reducer and air-entrainment) is also thought to be essential. Shrinkage or volumetric contraction is an also relevant characteristic of these mortars, the study of which is necessary to obtain high-quality structural mixtures that contain steelmaking slags.

## **Materials**

### *Water, cement and natural aggregates*

Mains water, containing negligible levels of compounds that can negatively affect the preparation of mortar mixes, was taken from the urban supply of the city of Bilbao.

A Portland cement type IV/B-V 32,5-N, as per UNE-EN 197-1 standard [104] was used in the mixes, the chemical composition of which is shown in Table 1. Its low hydration heat and particle fineness is common in ordinary cements. Only a half of the binder is Portland clinker as its composition by weight of cement comprises 5% of calcium carbonate fines, 40% of fly ash type I, and 50% of Portland clinker, milled with 4% of gypsum.

	Cement IV/B-V	EAFS	LFS
Fe <sub>2</sub> O <sub>3</sub> (%)	3.9	22.3	1.0
CaO (%)	45.5	32.9	59.2
SiO <sub>2</sub> (%)	28.9	20.3	21.3
Al <sub>2</sub> O <sub>3</sub> (%)	12.6	12.2	8.3
MgO (%)	1.8	3.0	7.9
MnO (%)	0.1	5.1	0.26
SO <sub>3</sub> (%)	3	0.42	1.39
Cr <sub>2</sub> O <sub>3</sub> (%)	-	2.0	--
P <sub>2</sub> O <sub>5</sub> (%)	0.45	0.5	--
TiO <sub>2</sub> (%)	0.65	0.8	0.17
Loss on ignition (%)	5.8 (C+CO <sub>2</sub> +H <sub>2</sub> O)	gain	0.5
Porosity (%)		2.6	--
Water absorption (%)		As-sand 3.51 / Fines 1.12	--
Blaine fineness (m <sup>2</sup> /g)	0.385		0.138
Hydration heat (cal/g)	52 (at 7 days)		
Specific gravity (Mg/m <sup>3</sup> )	3.07	As-sand 3.24 / Fines 3.54	3.03
X-Ray diffraction main compounds		Wüstite-Ghelenite- Kirsteinite, Ca-Mn- Oxide	Periclase-Olivine- celite

**Table 1:** Chemical composition (XRF) and other physical properties (EN-12620) of cement and aggregates

A natural siliceous fine aggregate of washed sand (SS) from Arija – Burgos, sized between 0.1 and 0.3 mm and with a fineness modulus of 0.47, was used. The quartz particles were rounded, with a specific gravity of 2.63 Mg/m<sup>3</sup>.

A commercial crushed natural-limestone aggregate (LS), of a size within the range of 0 and 5 mm was used in the mixes. The presence of calcite (95%) was detected as the main mineral. The specific gravity of the LS was 2.67 Mg/m<sup>3</sup>. Its size grading is represented in Figure 1, the fineness modulus of which was 2.9.

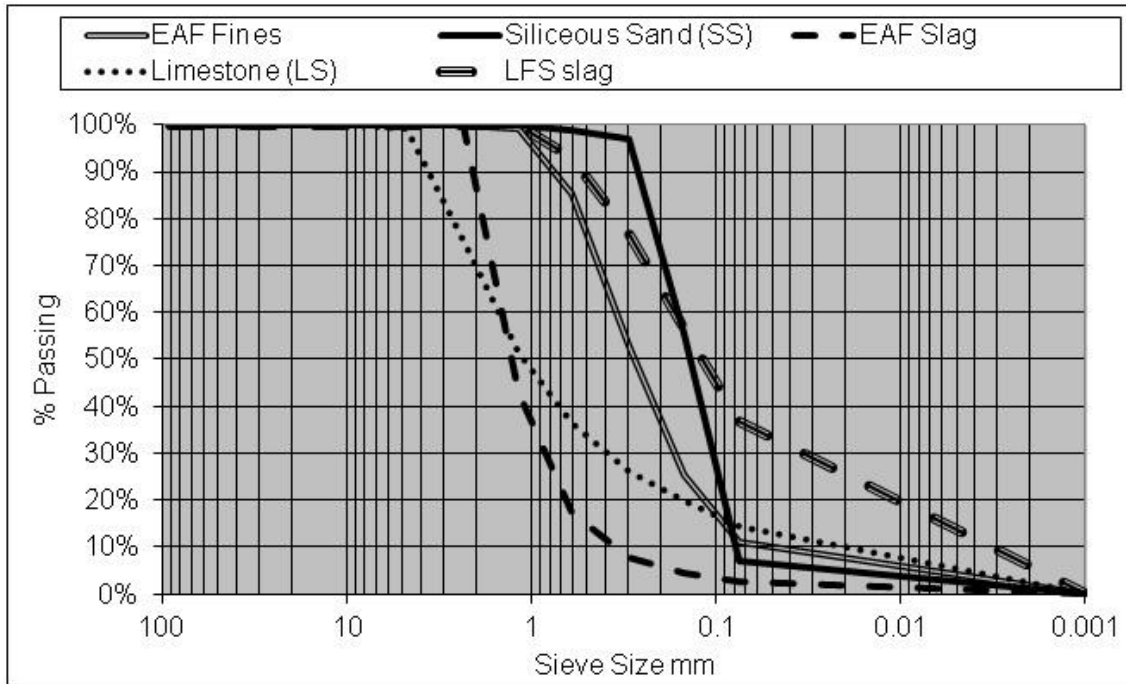


**Figure 1:** Grading curves of limestone sand (LS), EAF slag (two sizes), siliceous sand (SS) and LF slag.

### Electric arc furnace slag

Crushed electric arc furnace slag was supplied by Hormor-Zestoa for use in this research work. Its global chemical composition and physical properties are detailed in Table 1 and its size grading is represented in Figure 1. The fineness modulus of the fine fraction (EAF Fines, EAFF) was 1.4, of a size smaller than 1 mm; the fineness modulus of the as-sand fraction (EAF Slag, EAFS) was 3.3, with sizes of between 0.2 and 2.3 mm.

The factors that influence EAF slag density are its internal porosity (occluded gas), the proportion of iron and manganese oxides (with a density higher than  $5 \text{ Mg/m}^3$ ) and the metallic iron content (lower than one per ten thousand parts); its density was  $3.24 \text{ Mg/m}^3$  in the as-sand fraction, and  $3.54 \text{ Mg/m}^3$  in the fine fraction. X-ray diffraction analyzed the main crystalline components of the slag, also shown in Table 1. There was no noticeable presence of free lime or free magnesia; scarce amounts of uncombined free silica, with gehlenite, kirschsteinite and wüstite as the main compounds of the EAFS.

Ladle furnace slag.

Of the two main types of ladle furnace slag produced in the steelmaking industry (silica-saturated and alumina-saturated), a high-silica low-alumina LFS was used, the chemical composition and X-ray diffraction analysis of which is shown in Table 1. Its main compound is gamma-dicalcium silicate. Following spontaneous disintegration during cooling, it was kept dry and protected from external weathering in individual plastic bags. Its grading with a fineness modulus of 0.75 is shown in Figure 1. The Blaine specific surface was measured at  $0.138 \text{ m}^2/\text{g}$ .

This LFS contained free magnesia (periclase) and dicalcium silicate, as shown by XRD. It also contained an amount of around 15-20% of calcium aluminates (celite, mayenite), both potentially reactive in the presence of water, which produced hydrated-calcium-aluminates that slightly improved the mechanical strength of the mixes. The authors of this article have previously reported in [75] that roughly 30% of the mass of this slag type may be treated as supplementary cementitious material (SCM).

A previous work by the authors on the same LFS [105] established that the contents in potentially expansive compounds were 7% by weight of free-MgO and 6% by weight of free-CaO. The presence of typical sulfide compounds in the basic slag, such as olhamite-jasmondite, susceptible to oxidization, were also observed as well as their conversion to calcium sulfate at high temperature (see Figure 2, peak at  $920^\circ\text{C}$ , oxygen mass gain of 1.5%). This conversion can also happen more slowly at room temperature; subsequently, calcium sulfate is susceptible to produce secondary ettringite in the hardened state, with catastrophic results. Undoubtedly, the use of this kind of slag in hydraulic mixes is a notable risk and should be done in a controlled manner; the high amount of LFS used in some mixes of this work must be qualified as imprudent, as the global content of expansive compounds reached 4.4% (e.g. in M5).

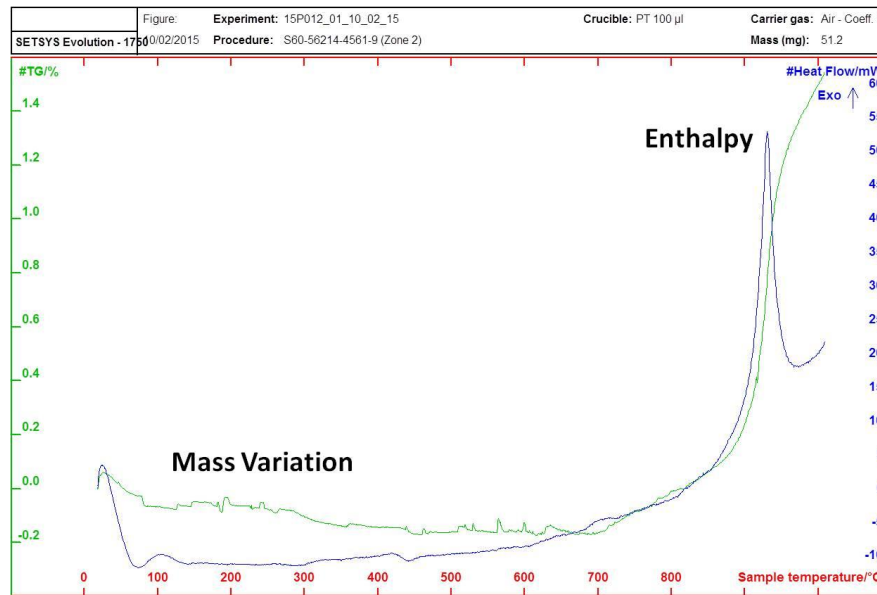


Figure2: Thermo-gravimetric curves of LFS slag.

### Fresh Mixes

A water-cement-aggregate ratio of 1:2:6 (w/c=0.5), the classical in-weight proportions for structural mortars, was fixed for the reference mix (M1). The proportions of Portland clinker plus fly ash were 1:1.1+0.8:6.1. The reference aggregate was quarry-crushed limestone rock sized 0-5 mm (LS); hence, the proportions 1:1.9:6.1 were changed by volume to a ratio of 1:0.6:2.4 or roughly 25:15:60%.

Subsequent volumetric substitutions of the reference aggregate LS by other materials was done in an attempt to conserve (with limited success due to variations in porosity) the volumetric ratio matrix-aggregates in all the mortars; in doing so, seven additional mixes were prepared. The materials for the substitution were: siliceous sand (SS), electric arc furnace slag (EAFS), fine electric arc furnace slag (EAFF) and ladle furnace slag (LFS) in various combinations. It have to be taken into account the hydraulicity of the LFS; it is partially considered as an aggregate (70%), the rest of its amount (30%) have to be considered as SCM and replaced the Portland cement.

Two admixtures, a fluidifying-water-reducer and an air-entrainment agent, were used, the first of which to enhance the workability of all the mixes to obtain fluid mortars, and the second to introduce a controlled amount of air bubbles in the mass, thereby decreasing the density slightly. The workability objective was a runoff-slump on the flow table of over 170 mm; mixes M3, M4, M5 failed to reach this value, showing a typical loss of workability when the two kinds of slag (EAFS and LFS) were used. The shape and the superficial texture of EAFS fine particles (sharp, rough) are not

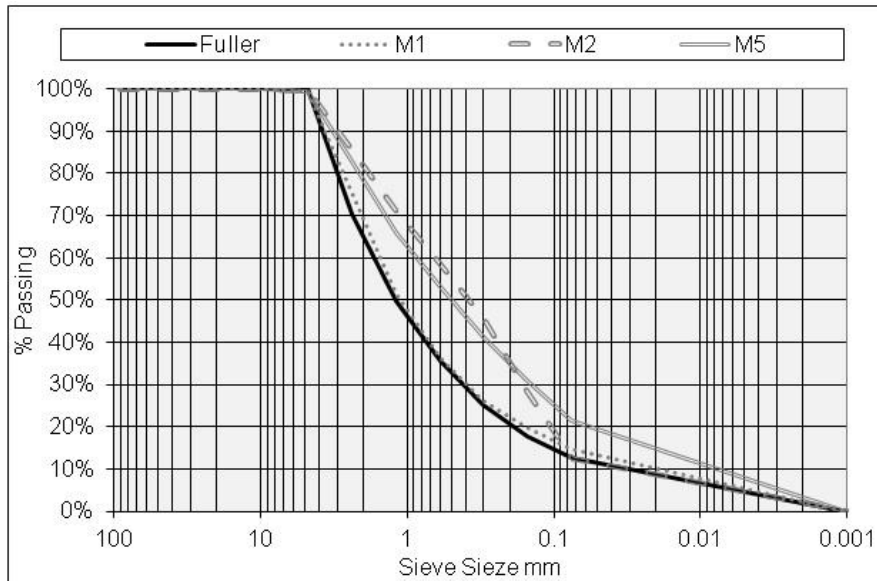
conducive to good workability, and the substitution of this slag in place of the natural aggregate leads to losses in the spreading of mixes, mainly in mix M3. On other hand, the effect of the air-entrainment admixture on entrained air was low in mixes containing LFS[98], as may be observed from the lower than expected values of M4 and M5; the other mixes behaved as expected.

Table 2 and Figures 3a and 3b show the composition and grading of the eight mixes. M1, M2 and M5 (Figure 3a) were mixes without EAFS, the proportioning of which were intended to fit the Fuller's curve; the rest of the mortars contained EAFS and their grading curves were in general well-adjusted to the recommended ASTM C33 [106] interval, as shown in Figure 3b.

The mixtures were cast and kept in prismatic moulds for one day; they were then demolded and submerged in water until their corresponding tests. Two different kinds of prismatic moulds were employed: the standard 40x40x160 mm size for the measurement of both strength and physical properties (18 sample moulds from each mix), and special 25x25x250 mm size specimens (4 from each mix) to monitor dimensional variations (shrinkage-expansion).

Mortar	Components								
	Water	Cement IV/B-V	LS	SS	Aggregates			Admixtures	
					EAFS	EAFF	LFS	WR	AE
<b>M1</b>	257	513	1540	-	-	-	-	4	-
<b>M2</b>	257	513	1078	462	-	-	-	4	5
<b>M5</b>	257	289	1078	-	-	-	749	6	5
<b>M3</b>	257	513			747	1121		4	-
<b>M3air</b>	257	513	-	-	747	1121	-	5	5
<b>M4</b>	257	326	-	-	747	747	500	8	5
<b>M6</b>	257	513	308	-	747	747	-	4	5
<b>M7</b>	257	513	308	308	561	561	-	5	5
<b>M8</b>	257	513	-	616	1121	-	-	5	2.5

**Table 2:** Mix proportioning in kg per cubic meter of reference mortar.



**Figure 3a:** Fuller curve & grading of mixes 1, 2, and 5.

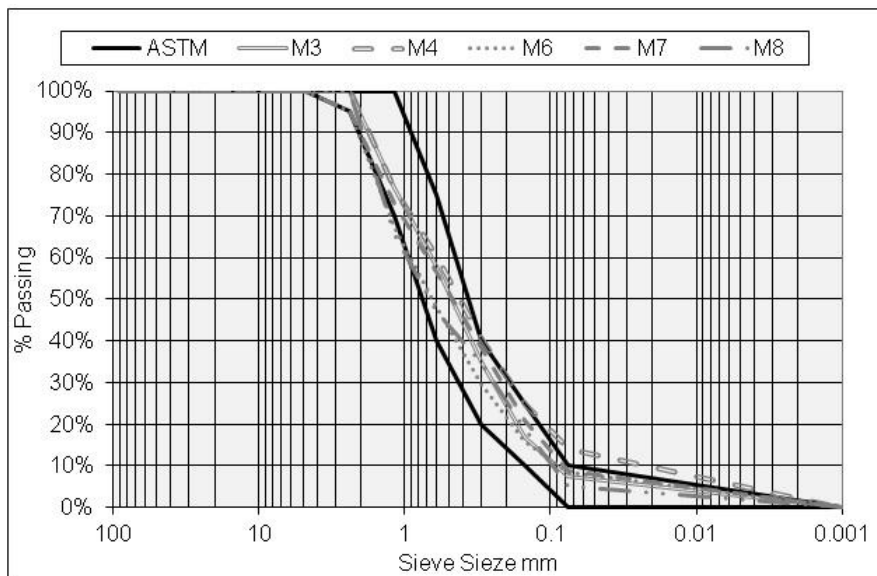


**Figure 3b:** ASTM C33 range and mixes 3,4,6,7,8

**Physical characterization: density and porosity**

The bulk density of the mixes was evaluated by the conventional measurement of in-air and submerged weight; additionally, the porosities and densities were evaluated by Mercury Intrusion Porosimetry (MIP). The results of these measurements and of the entrained air are shown in Table 3.

It should be noted that the MIP porosity in mixtures containing LFS and EAF slag (3-4-5-6-7-8), in which the accessible-to-mercury porosity of both slags is added to the capillary porosity of the cementitious matrix, should be higher than the others (1-2)

*ceteris paribus* (all other variables being similar). Figures 4a and 4b show the MIP-graphs for mixes M2 (usual capillary pore-size distribution in mixes 1-2-3-6-7-8) and M5 (exceptional capillary nano-pore size distribution due to inclusion of LFS, shown by M4 and M5, see also the size range in the third column of Table 3).

MIP porosity increased to values of over 20% in the EAFS mixes with 5% of an air-entrainment admixture (M3air, M6 and M7), except in mixtures M4 and M5. In these last two, it was observed that the presence of LFS “mitigated” the effect of this air-entrainment admixture, and changed the pore-size distribution due to the size of its own porosity, as shown in Figure 4b. The global MIP porosity amount for mixes M4 and M5 was a result of those two circumstances.

The apparent density measured by MIP revealed the presence and amount of heavy EAF slag; in fact, the resultant value of 3.11 Mg/m<sup>3</sup> is fairly accurate in mixture M3 with 70% by occupied volume of EAF slag (average density value 3.4 Mg/m<sup>3</sup>) and 30% by occupied volume of hardened cementitious matrix (average density value 2.4 Mg/m<sup>3</sup>). Similar calculations can be applied to mixes M4-M6 (about 60% in volume of EAF, density value 2.98) and in the set M7-M8 (45% by volume of EAF, values 2.83-2.86). Moreover, the values of bulk density measured by MIP and by the conventional on-air/submerged method to assess the sample specific weight are quite coherent.

Mix	Porosity MIP % vol	Nano-Pores MIP size range	Bulk/Apparent density by MIP Mg/m <sup>3</sup>	Bulk Density classical Mg/m <sup>3</sup>	Fresh Density Mg/m <sup>3</sup>	Air entrained % volume	Workability Spreading in mm
M1	13.1	5-80nm	2.22/2.56	2.22	2.30	2.1	175
M2	17.7	10-70 nm	2.04/2.49	2.03	2.14	8.2	180
M5	19.3	5-500nm	2.05/2.54	2.03	2.17	4.6	140
M3	16.7	5-60nm	2.59/3.11	2.60	2.72	3	115
M3air	27.6	10-60nm	2.25/3.11	2.21	2.36	7.3	130
M4	19.2	10-500 nm	2.41/2.98	2.39	2.52	4.1	160
M6	24.1	6-90nm	2.26/2.98	2.24	2.38	6.8	170
M7	25.7	5-60nm	2.10/2.83	2.06	2.21	7.1	170
M8	16.9	5-90nm	2.38/2.86	2.37	2.47	3.5	175

**Table 3:** Density and porosity of mixtures by MIP, and fresh properties.



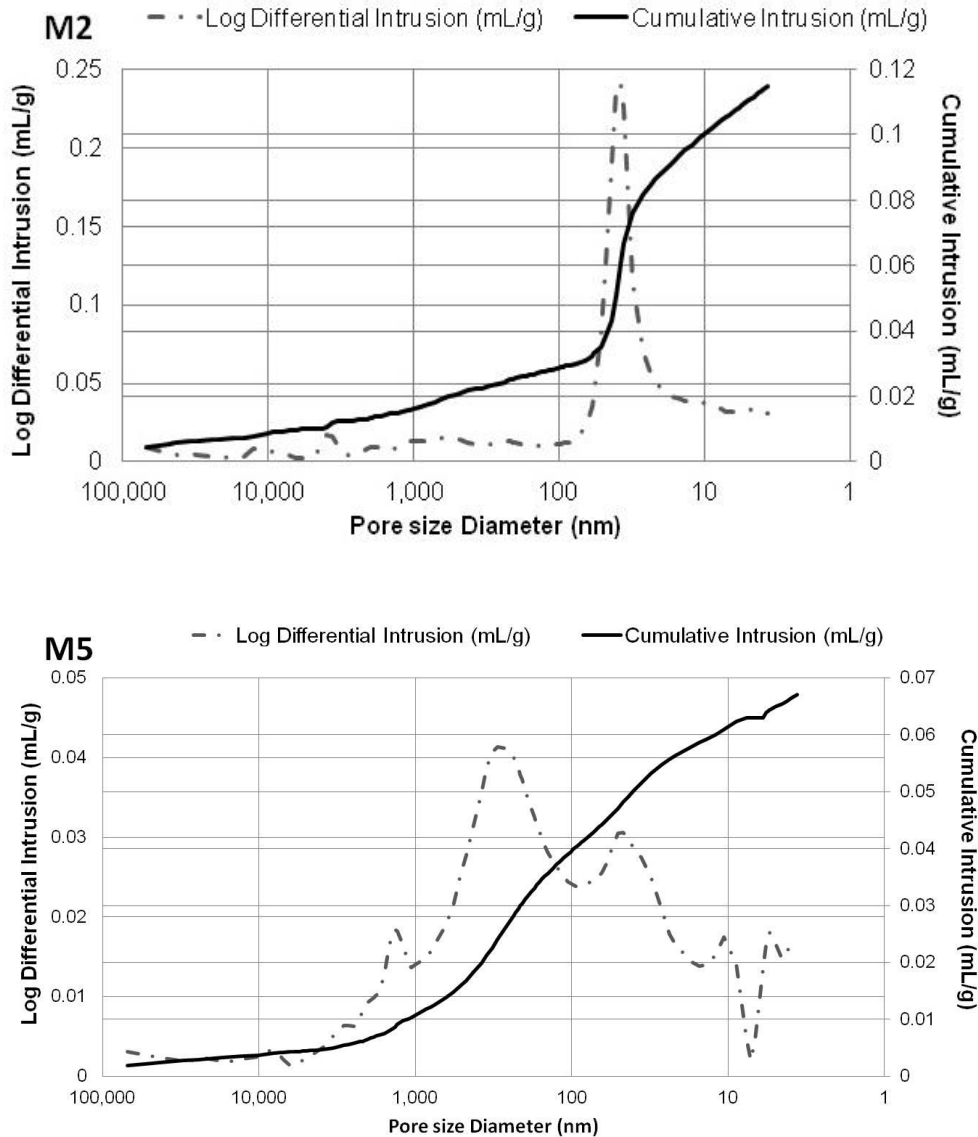


Figure 4: MIP pore size distribution in mixes M2 (4a) and M5 (4b).

### Mechanical properties: compressive and flexural strength, stiffness

The time period of strength measurement for mixes based on type IV/B-V 32.5N cement with a high content (40%) of fly ash, a material of slow pozzolanic reactivity, extends to one year. For most engineering applications, long-term strength is not very relevant, although it is worth noting that when FA was used, long-term strength measurements were more suitable, due to the different evolution of strength over time. Additionally, it should be considered that most of the mixes contained only 280 kg of clinker and gypsum per cubic meter of fresh mass.

Two groups of mixes were prepared in this study: EAF slag and non-EAF slag mortars. The general trend stated in the scientific literature is once again very clear in this

research: mixtures containing EAF slag showed higher mechanical properties than comparable mixes containing natural aggregates. In fact, reference mixture M1 yielded good results in short and long-term tests, but mixture M3 was the strongest. Likewise, we may compare M4 versus M5, and M8 versus M2.

The poorer results of EAFS mixes M3air, M6 and M7 were evident; the porosity values (MIP and entrained air, Table 3) were too high and their mechanical properties decreased. The efficacy of the air-entraining admixture in the presence of EAFS was good in relation to density (15% lower in M3air than in M3) but detrimental in relation to strength (loss of 43%). Hence, its use must be reconsidered or seriously limited in structural mixes.

The good results for the long-term strength of mixes M4 and M5 that contained LFS confirms the role of LFS in enhancing the mechanical properties. We should remember that mix M4 contained EAF slag and 175 kg (53% of 326 kg) of clinker plus gypsum and that mix M5 contained 150 kg of clinker per cubic meter. Their poor short-term results may be noted, see strength at 3 days; the effect of both SCM (fly ash and LFS) was more evident after 28 and 90 days.

Mix M8 yielded good strength; its density (including an outstanding proportion of EAFS, 45% in volume) was only 6% higher than the reference mortar M1, with a 5% lower long-term strength. Finally, the results obtained for the M2 mix were as expected, on account of its characteristics.

The flexural strength of the mixes was varied and, in general, close to the compressive strength, but the value for mixtures M3 M4 and M8, containing EAFS, was remarkable. These better values shown in Table 4 show that EAF aggregate also had a favorable effect on this relevant property of structural concrete. Previous research [79] arrived at the same result, justifying it in terms of slag morphology, rough texture, and the different matrix-aggregate interfaces, which may create stronger links between binder and aggregate.

Ultrasonic pulse velocity,  $V$ , was used to estimate the stiffness in accordance with the formula [107]:

$$E = V^2 \frac{(1 + \nu)(1 - 2\nu)}{1 - \nu} \quad \text{usually } \nu = 0.2 \text{ in concrete}$$

The estimated stiffness values (not valid as Young's modulus) after 360 days are shown in Table 4; as usual for concrete, they correlate with the other mechanical properties. It is worth remarking that the stiffness values in mortars containing EAFS and LFS were lower than those of the reference mixes when the compressive strength was similar or comparable. This result was observed by authors in a previous work [46] and is probably explained by the fact that EAFS gravel stiffness is lower than that of natural aggregate stiffness, due to its internal porosity and the presence of iron oxides which have low rigidity.

	FLEXURAL STRENGTH (MPa)						COMPRESSION (MPa)						Stiffness E (GPa)
	3 Day	7 Day	28 Day	90 Day	180 Day	360 Day	3 Day	7 Day	28 Day	90 Day	180 Day	360 Day	
<b>M1</b>	4.52	7.78	8.17	9.01	9.49	9.84	18.93	28.01	39.71	57.59	63.70	68.2	41.1
<b>M2</b>	4.60	6.59	9.13	9.29	9.28	10.5	18.86	26.05	40.79	45.69	49.1	49.3	31.3
<b>M5</b>	1.64	3.37	6	6.53	8.09	9.59	6.13	18.23	35.39	42.2	48	49.2	28.6
<b>M3</b>	5.50	7.07	9.56	11.3	11.7	12.2	25.51	33.56	49.10	64.70	74.41	78.3	41.8
<b>M3air</b>	3.95	5.34	5.46	8.42	9.04	9.28	13.58	18.66	26.83	36.68	42.65	46.9	25.6
<b>M4</b>	1.34	3.62	5.16	9.34	10.2	11.3	3.66	13.33	29.98	52.26	58.1	61.7	32
<b>M6</b>	4.0	5.04	6.48	7.87	9.05	9.68	13.39	17.93	28.82	37.22	45.02	50.7	28.4
<b>M7</b>	4.98	5.12	6.43	7.35	7.97	8.16	17.25	19.97	27.00	32.74	37.8	41.7	25.2
<b>M8</b>	4.52	5.73	7.65	10.4	10.8	11.2	17.15	24.32	36.29	53.59	62.58	64.9	37.4

**Table 4:** Mechanical tests results

### Analysis of physical and mechanical results

Reference mixture M1 is an excellent model for a comparison of aggregate packaging, because its grading adjusts quite well to Fuller's curve (see Figure 3a) for a maximum aggregate size of 4.75 mm; hence, the MIP capillary porosity was low (13.1%). Air represents only 2.1% in volume due to the high fluidity of the mixture as seen in Tables 3 and 4.

In Figure 3a, mixture M2, in partial substitution of the limestone in M1 by siliceous sand showed a worse fit with Fuller's curve. The use of an air-entraining admixture increased the air content and the MIP porosity and slightly decreased the density and, more remarkably, the mechanical strength; the benefit of the air-entrainment admixture is uncertain. Mixture M5 included LFS and limestone sand (LS), so as to observe the influence of the ladle furnace slag, considered a partial binder (SCM). Its aggregate grading adjusted poorly to the Fuller curve in the fines zone (sieve #200) and both its air content and its MIP porosity were low. As a result, its mechanical strength was similar to M2, despite the lower clinker content, so the long-term hydraulicity of

the LFS and its interaction with the fly ash in the cement should be considered positive. The role of LFS fines in relation to workability was considered negative.

Mixture M3 included EAFS in two sizes, as-sand (EAFS) 0.2-3 mm, and fines (EAFS) <1mm; this mixture of aggregate sizes meets the ASTM C33, as shown in Figure 3b. Despite the use of admixtures it showed poorer workability (the lowest slump) than the reference mix M1 and excellent mechanical properties. The entrained air in M3 was expected, due to low fluidity during its mixing. The fresh density of the M3 mortar decreased from 2.72 to 2.36 (13%) and its workability was improved by air-entraining admixture in the M3air mixture; the efficiency of the air-entraining admixture was good in the presence of the EAF slags, although the mechanical performance of M3air was poor compared to other results of this work. Comparing the main mixes of this batch, the fresh density of M3 was 18% higher and its strength was 15% higher than the reference mortar (M1).

Mixture M4 included EAFS and EAFS and the ladle furnace slag (LFS) used as the finer fraction had an excess of fines, as shown in Figure 3b; these amounts of aggregates had a negative effect on workability, because of the lack of fluidity produced by both slags. The results in terms of density were high despite the air-entraining admixture and the mechanical behavior of the mix with a low content of cement was good, as in M5.

Mixtures M6, M7 and M8 used heavy EAFS combined with natural aggregates; the adjustment to the ASTM C33 was good, and the densities were close to the reference M1 with the use of air-entrainment; however, the capillary porosity and entrained air increased due to the use of that admixture, decreasing their mechanical properties. Mixture M8 had the best performance from among these three mixes, low air-entrainment, good workability and mechanical strength, with a higher density than the reference mix.

### **Dimensional stability - Shrinkage**

Two specimens (25x25x250 mm) of each eight mixtures (except M3, including M3air) were kept submerged in water following demolding, and a further two were kept in air, all of them in the same chamber at room temperature, 20°C±2. Their length was measured in a rigid frame equipped with a 0.01 mm precision apparatus. Figure 5 shows the evolution of the shrinkage length for all mixes, each point is the average of the measurements on two samples; the upper set of values corresponds to submerged

specimens and the lower set of values to in-air specimens. The measured values were almost-constant from an age of 250 days, as seen in Figure 5, although the in-air specimens were controlled throughout the year.

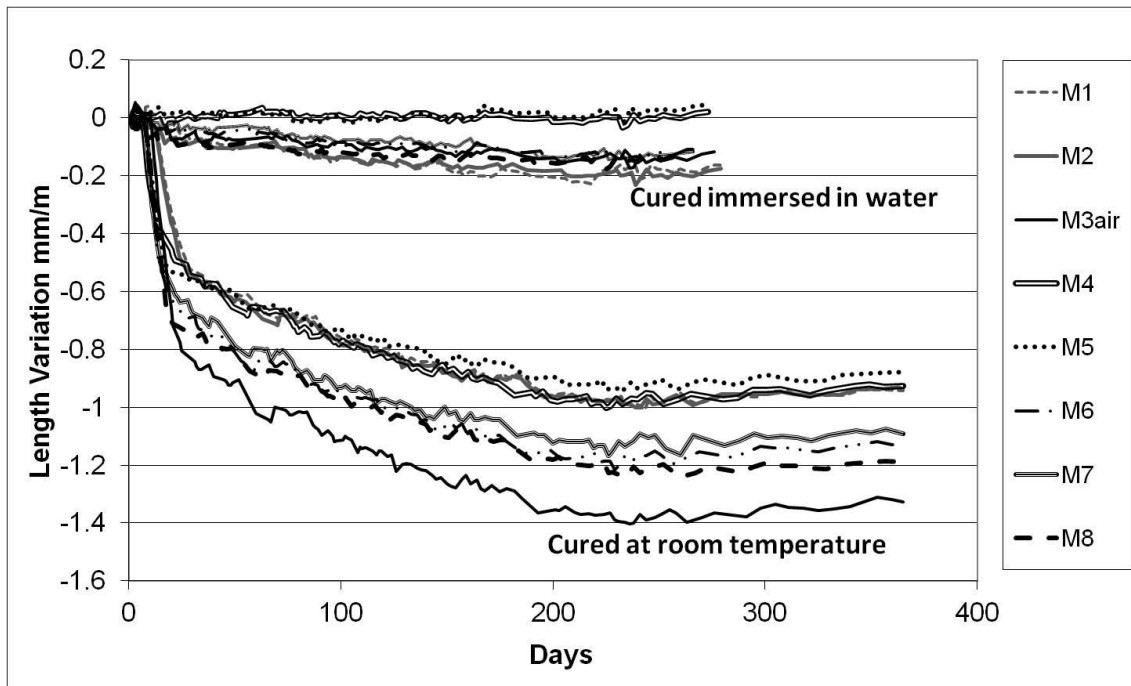


**Figure 5:** Evolution of specimen length over time: the upper curves refer to the submerged specimens and the lower curves to the in-air specimens.

In the submerged specimens, a contraction of about 0.2 mm/meter was noticeable in six mixtures, except those (M4-M5) containing LFS. The reaction of expansive components free-CaO and free-MgO in these specimens compensated the general trend towards slight contraction and their average value was almost zero. Contraction values of 0.2 mm/m were reported in the mixtures containing EAF slag and also in the reference mixtures M1-M2. This behavior is associated with the presence of large amounts of fly ash as pozzolanic material, the slow hydration of which produces this effect; the same effect occurs in the on-air specimens, giving rise to high global-shrinkage values.

The asymptotic values of the in-air specimens after 250 days differed widely, as may be seen in Figure 5. The asymptotic value of the shrinkage in the reference mix M1, and in the other almost-reference mix M2, was close to 1 mm/m, a value in this kind of mortars that usually represents an “acceptable maximum” in the world of structural mortars for construction.

Mixture M5, containing LFS but no EAFS, showed a value of 0.9 mm/m, a logical value owing to the superposition of the slight internal expansivity of some LFS compounds and the shrinkage shown by the reference mixes. In the same way, mixture M4 containing EAFS and LFS showed a value about 1 mm/m. It should be remarked that this expansion could be deleterious even though it may compensate shrinkage contraction. Mixture M3 (maximum content in EAFS) had 1.4 mm/m, and M6, M7 and M8 (lower content in EAFS) had values of between 1.2 and 1.1 mm/m. For instance, it appears evident that the growing presence of EAFS as aggregate in the mixtures increased their shrinkage contraction, associated with a lower elastic modulus [107] and it is even possible that a high amount of entrained air in mixtures containing EAF slag also favors this contraction.

### **Durability tests**

The submerged specimens of mixtures (25x25x250 mm), cited in the former section, were held at room temperature water over 270 days and were then submerged in a 70°C temperature bath in a similar way to that proposed in the ASTM D-4792 standard; they were held for an additional 60-day period under these test conditions.

M3 and the other mixes without LF slag (M1-2-6-7-8) had no problems and there was a moderate expansion of their length over time in 70°C water, with values of between 0.1 and 0.2 mm/meter. The aforementioned expansion has to be deducted from the contraction value of 0.2 mm/m obtained in the shrinkage test of the former section. The final result in the global length variations of the relevant mixes was virtually zero.

However, the mixtures containing LFS, M4 and M5, showed an evident and detrimental expansion, as may be seen in Figure 6b, in which these specimens are curved and, especially in the case of M5, are even broken as well. The M3 specimens remained straight, as expected. The amount of LFS in these mixes was excessive with regard to durability and the effect of the expansive compounds was evident.

An additional durability test in which the specimens were submerged for 180 days in water and oven dried was performed in an autoclave test on cubic pieces of a size of roughly 25 mm obtained from other specimens. This test followed the norms detailed in Spanish NLT-361 standard "Determination of aging degree in steelmaking slag"; slightly different from the conventional autoclave test for Portland cement in that they were performed at a pressure 0.2 MPa over 48 hours. The result was mainly observed on the lateral plate faces of the pieces and in the presence of small particles that

disintegrated from the sample in each container; the results were graded as “integrity maintained”, “superficial scaling”, “general cracking” and “total destruction”.

The results for the behavior of the mixes was generally good (integrity maintained in almost all mixes M1-2-3-6-7-8) except in mixtures M4 and M5; once again, the mixes containing ladle-furnace slag, in which the expansive compounds played a fundamental role. The photo in Figure 6a shows the final state of mixture M4 specimen, resulting in “general cracking”; the result of mixture M5 was “total destruction”, in which the mass of the M5 specimen were reduced to as-sand particles.



**Figure 6a and 6b:** Samples after durability tests

### **Relevant SEM observations**

A SEM analysis was performed on the fracture surface of the samples that were broken in the above-mentioned autoclave test. The technique is based on low-vacuum observation of backscattered electron (BSE) images, in which the samples were not electrically charged (neither sputtered with gold nor carbon). It was complemented by energy-dispersive X-ray analysis (EDX),

As is well-known, the internal expansion of some compounds included in the LFS produces long-term detrimental effects in the hardened mixes. Figures 7a and b show two expansive particles of different chemical composition found in the specimen of the M5 mix. As stated in the previous section on ladle furnace slag, the kind of LFS used in these experiments contained free-MgO, 7% by weight, and free-CaO in 6% by weight. It is expected that the expansive hydration or hydro-carbonation of these species [107] and their remarkable amounts will produce expansion and subsequent deleterious effects in the hardened mixes.

The particles of expanded compounds embedded in a stony hardened mass can be identified because of the notable cracking produced in their vicinity. Mapping of magnesium, calcium, silicon, oxygen and carbon in a large region of the fracture surface also identified these kinds of particles.

Indeed, Figure 7a shows a particle based on magnesium and oxygen and the presence of carbon, the elemental composition of which was obtained after micro-analysis EDX, shown in the lower-right-hand-side of the image. This particle was initially free-MgO, and the proportions obtained between Mg and O indicated that its current composition must be magnesium hydroxide (brucite), which is probably partially carbonated.

In a similar way, Figure 7b shows a particle of calcium carbonate, from an initial particle of free-CaO, firstly hydrated and subsequently carbonated throughout the accelerated aging durability test. Both particles were 20-30 microns large after their volumetric expansion and were partially or totally cracked by the mechanical stresses generated during the rupture of the specimen. They are surrounded by a cracked region of the cementitious matrix, in which the “granular” C-S-H detached particles may also be seen.

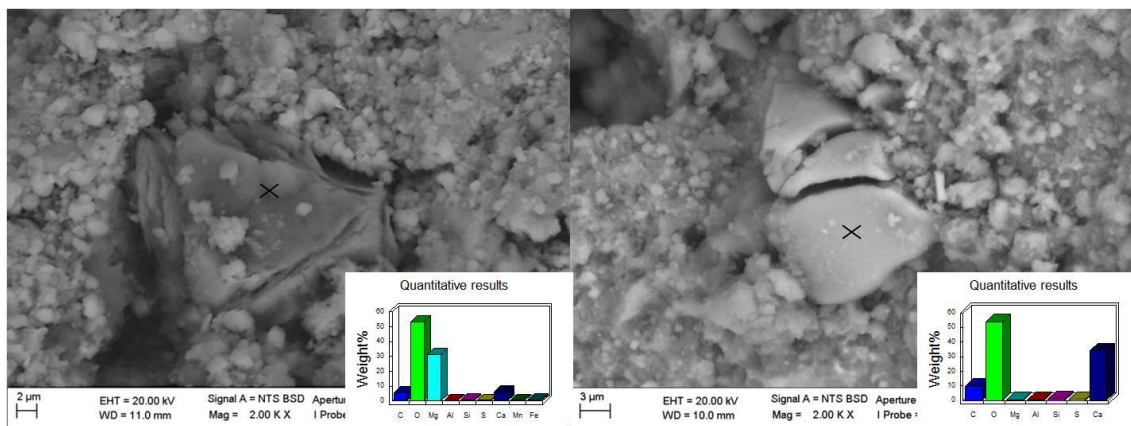


**Figure 7:** Brucite-magnesium carbonate (left) and Calcium carbonate (right)

## Conclusions

The use of a Portland cement containing a notable amount of fly ash has proved positive in these structural mortar mixes: their workability was acceptable and the mechanical properties showed an excellent mechanical strength to clinker content ratio.



The compressive strength of 78 MPa was reached after one year with a mix employing EAF slag as aggregate; this compressive strength is promising in relation to the following step of performing similar concrete mixes. The stiffnesses of the mixes containing slag were, in general, lower than the stiffnesses of the natural aggregate mixes of similar strength.

The density of M3 was 18% higher and its strength was 15% higher than the reference mortar M1. The efficiency of the use of EAF slag in terms of structural use was (neither favorable nor unfavorable) intermediate. From this point of view, the feasibility of the use of these kinds of mortars in structural applications was positive.

From an engineering standpoint, the use of air-entraining admixtures in the EAF slag mortars is of no relevance, because the loss of strength (78.3 to 46.9 in M3) was not compensated by the gain in density (2.36 versus 2.72 in M3), and the eventual increase of workability due to its presence can be obtained using other admixtures that are not detrimental for the strength.

The long-term shrinkage of the mixes containing EAF slag as aggregate was significantly higher than the shrinkage of the reference mixes. The presence of ladle furnace slag hardly mitigated this outcome in an effective way despite its well-known expansivity.

Only mixtures M4 and M5, with a high content of LFS, were problematic in relation to durability. The others had few or no durability problems at all. However, any final decision on the maximum content of LFS in hydraulic engineering mixes will depend on the results of future in-depth studies performed on several kinds of LFS of variable composition and with varying contents of expansive compounds.

## **References**

- [1] Motz H., Geiseler J., Products of steel slags an opportunity to save natural resources, *Waste management*, 21 (2001) 285-93.
- [2] Shelburne W., Degroot D., The use of waste and recycled materials in highway construction, *Civil engineering practice*, 13 (1998).
- [3] Tomellini R., Summary report on RTD in iron and steel slags: development and perspectives, Technical Steel Research, Report Prepared for the European Commission EUR 19066, Brussels, Belgium, 1999.

- [4] Al-Otaibi S., Recycling steel mill scale as fine aggregate in cement mortars, *European Journal of Scientific Research*, 24 (3) (2008) 332-8.
- [5] Qasrawi H., Shalabi F., Asi I., Use of low CaO unprocessed steel slag in concrete as fine aggregate, *Construction and Building Materials*, 23 (2009) 1118-25.
- [6] Akinmusuru J.O., Potential beneficial uses of steel slag wastes for civil engineering purposes, *Resources, Conservation and Recycling*, 5 (1991) 73-80.
- [7] Koros P.J., Dusts, Scale, Slags, Sludges... Not wastes but sources of profits, *Metallurgical and Materials Transactions B*, 34 (2003) 769-79.
- [8] Kumar Metha P., Global Concrete Industry Sustainability, *Concrete International*, 31 (2009) 45-8.
- [9] Geiseler J., Use of Steelworks slag in Europe, *Waste Management Research*, 16 (1996) 1-3.
- [10] Jähren P., Do not forget the other Chapters!, *Concrete International*, 24 (7) (2002) 41-4.
- [11] Garcia C., San José J.T., Urreta J.I., Reuse and valorization in civil works of electric arc-furnace (EAF) slag produced in C.A.P.V., in: Gaballah I., Hager J., Solozabal R. (Eds.), *Global Symposium on Recycling, Waste Treatment and clean Technology (REWAS)*, San Sebastian, 1999, pp. 417-24.
- [12] Naik T.R., Greener concrete using recycled materials, *Concrete international*, 24 (2002) 45-9.
- [13] Papayianni I., Anastasiou E., Concrete Incorporating High Volumes of Industrial By-Products, *Role of Concrete in Sustainable Development—Proceedings of International Symposium Dedicated to Professor Surendra Shah*, Aristotle University Greece, Sept, 2003, pp. 595-604.
- [14] Papayianni I., Anastasiou E., Production of high-strength concrete using high volumes of industrial by-products, *Construction and Building Materials*, 24 (2010) 1412-7.
- [15] Tüfekçi M., Demirbaş A., Genç H., Evaluation of steel furnace slags as cement additives, *Cement and Concrete Research*, 27 (1997) 1713-7.

- [16] Wang G., Wang Y., Gao Z., Use of steel slag as a granular material: Volume expansion prediction and usability criteria, *Journal of Hazardous Materials*, 184 (2010) 555-60.
- [17] Anastasiou E., Georgiadis Filiakas K., Stefanidou M., Utilization of fine recycled aggregates in concrete with fly ash and steel slag, *Construction and Building Materials*, 50 (2014) 154-61.
- [18] Kuo W.T., Hou T.C., Engineering properties of alkali-activated binders by use of desulfurization slag and GGBS, *Construction and Building materials*, 66 (2014) 229-34.
- [19] Kuo W.T., Wang H.Y., Shu C.Y., Engineering properties of cementless concrete produced from GGBFS and recycled desulfurization slag, *Construction and Building Materials*, 63 (2014) 189-96.
- [20] Guo X., Shi H., Effect of steel slag admixture with GGBS on performances of cement paste and mortar, *Advances in cement Research*, 26 (2) (2014) 93-100.
- [21] Shojaei M., Behfarnia K., Mohebi R., Application of alkali-activated slag concrete in railway sleepers, *Materials & Design*, 69 (2015) 89-95.
- [22] Bignozzi M.C., Sandrolini F., Andreola F., Barbieri L., Lacellotti I., Recycling electric arc furnace slag as unconventional component for building materials, in: Ganjian Z.C.N. (Ed.), 2nd International Conference on sustainable construction materials and technologies, Ancona Italy, 2010.
- [23] Anastasiou E., Papayianni I., Standards for the use of steel industry by-products as aggregates for the production of concrete, 1st Hellenic Conference of EVIPAR on Utilization of industrial by-products in Construction, Thessaloniki, 2005, pp. 347-56.
- [24] Brand A.S., Roesler J.R., Steel furnace slag aggregate expansion and hardened concrete properties, *Cement and Concrete Composites*, 60 (2015) 1-9.
- [25] Liapis I., Papayianni I., Advances in chemical and physical properties of electric arc furnace carbon steel slag by hot stage processing and mineral mixing, *Journal of Hazardous Materials*, 283 (2015) 89-97.

- [26] López F.A., López-Delgado A., Balcázar N., Physico-chemical and mineralogical properties of EAF and AOD slags, *Afinidad LIII*, 53 (1996) 39-46.
- [27] Muhmood L., Vitta S., Venkateswaran D., Cementitious and pozzolanic behavior of electric arc furnace steel slags, *Cement and Concrete Research*, 39 (2009) 102-9.
- [28] Murphy J.N., Meadowcroft T.R., Barr P.V., Enhancement of the cementitious properties of steelmaking slag, *Canadian Metallurgical Quarterly*, 36 (1997) 315-31.
- [29] DePree P.J., Ferry C.T., Mitigation of expansive electric arc furnace slag Brownfield redevelopment, *GeoCongress, Geosustainability and Geohazard Mitigation*, New Orleans, 2008, pp. 271-8.
- [30] Petkova V., Samichkov V., Some rheological properties of composite slag-cement mortars with secondary industrial waste, *Construction and Building Materials*, 21 (2007) 1177-81.
- [31] Qasrawi H., The use of steel slag aggregate to enhance the mechanical properties of recycled aggregate concrete and retain the environment, *Construction and Building Materials*, 54 (2014) 298-304.
- [32] Rađenović A., Malina J., Sofilić T., Characterization of ladle furnace slag from carbon steel production as a potential adsorbent, *Advances in Materials Science and Engineering*, 2013 (2013).
- [33] San José J., Reutilización y valorización en obra civil de escorias de horno de arco eléctrico producidas en la CAPV, *Arte y Cemento*, (2000) 124-6.
- [34] Sawaddee A., A study of properties of Portland cement containing electric arc furnace slag microsilica and superplasticizer, Thailand, 1997.
- [35] Serjun V.Z., Mirtič B., Mladenović A., Evaluation of ladle slag as a potential material for building and civil engineering, *Materiali in Tehnologije*, 47 (2013) 543-50.
- [36] Setién J., Hernández D., González J.J., Characterization of ladle furnace basic slag for use as a construction material, *Construction and Building Materials*, 23 (2009) 1788-94.

- [37] Tavakolli H., Azari A., Ashrafi K., Pour M.S., Cementitious properties of steelmaking slag, *Technical Journal of engineering and applied sciences TJEAS journal*, (2013) 1071-3.
- [38] Wang Q., Yang J., Yan P., Cementitious properties of super-fine steel slag, *Powder Technology*, 245 (2013) 35-9.
- [39] Yildirim I.Z., Prezzi M., Chemical, mineralogical, and morphological properties of steel slag, *Advances in Civil Engineering*, 2011 (2011).
- [40] Yildirim I.Z., Prezzi M., Steel Slag: Chemistry, Mineralogy, and Morphology, in: Iskander M., Suleiman M.T., Anderson J.B., Debra F. Laefer (Eds.), *IFCEE 2015*, San Antonio, Texas, 2015.
- [41] Biradar K.B., Chakravarthi V.K., Arun Kumar U., Efficacy of industrial waste admixture in improving engineering performance of clayey soil - A quantitative study, *American journal of engineering research*, 3 (9) (2014) 251-63.
- [42] Bosela P., Delatte N., Obratil R., Patel A., Fresh and hardened properties of paving concrete with steel slag aggregate. Propiedades para firmes de hormigón fabricados con áridos siderúrgicos, *Revista técnica de la asociación española de carreteras*, 4 (166) (2009) 55-66.
- [43] Chan C.M., Jalil A., Some insights to the reuse of dredged marine soils by admixing with activated steel slag, *Advances in Civil Engineering*, (2014).
- [44] Fronek B.A., Feasibility of expanding the use of steel slag as a concrete pavement aggregate, *Cleveland State University*, 2012.
- [45] Mäkikyro M., *Converting Raw Materials into the Products - Road Base Materials Stabilized with slag-based binders*, Department Process and Environmental Engineering, University of Oulu, 2004.
- [46] Arribas I., Santamaría A., Ruiz E., Ortega-Lopez V., Manso J.M., Electric arc furnace and its use in hydraulic concrete, *Construction and Building Materials*, 90 (2015) 68-79.
- [47] Manso J., Ortega-Lopez V., Polanco J., Setién J., The use of ladle furnace slag in soil stabilization, *Construction and Building materials*, 40 (2013) 126-34.

- [48] Montenegro J., Celemín-Matachana M., Cañizal J., Setién- Marquínez J., Ladle furnace slag in the construction of embankments: expansive behavior, *Journal of Materials in Civil Engineering*, 25 (2013) 972-9.
- [49] Natali Murri A., Rickard W.D.A., Bignozzi M.C., van Riessen A., High temperature behaviour of ambient cured alkali-activated materials based on ladle slag, *Cement and Concrete Research*, 43 (2013) 51-61.
- [50] Nistor L., Ene A., Drasovean R., On the possibility of using the slags from iron and steel industry in road construction from the point of view of their physical-mechanical properties, *Analele Universitatii Dunarea de Jos din Galati. Fascicula II - A anul XXIV*, (2006) 92-7.
- [51] Oluwasola E.A., Hainin M.R., Aziz M.M.A., Characteristics and Utilization of Steel Slag in Road Construction, *Jurnal Teknologi*, 70 (2014).
- [52] Papayianni I., Anastasiou E., Optimization of ladle furnace slag for use as a supplementary cementing material, *Measuring, monitoring and modeling concrete properties*, Springer, 2006, pp. 411-7.
- [53] Papayianni I., Anastasiou E., Effect of granulometry on cementitious properties of ladle furnace slag, *Cement and Concrete Composites*, 34 (2012) 400-7.
- [54] Pasetto M., Baldo N., Mix design and performance analysis of asphalt concrete with electric arc furnace slag, *Construction and Building Materials*, 25 (2011) 3458-68.
- [55] Pasetto M., Baldo N., Cement bound mixtures with metallurgical slags for road constructions: mix design and mechanical characterization, *IM Inżynieria Mineralna*, 14 (2013) 15--20.
- [56] Petry T.M., Little D.N., Review of stabilization of clays and expansive soils in pavements and lightly loaded structures—history, practice, and future, *Journal of Materials in Civil Engineering*, (2002).
- [57] Rubio A., Carretero J., La aplicación de las escorias de acería en carreteras, *Ingeniería Civil*, 80 (1991) 5-9.
- [58] San José J., Uría A., Escorias de horno de arco eléctrico en mezclas bituminosas, *Arte y Cemento*, (2001) 122-5.

- [59] Sofilić T., Sofilić U., Brnardić I., The significance of iron and steel slag as by-product for utilization in road construction, 12th International Foundrymen conference Sustainable Development in Foundry Materials and Technologies, 2012.
- [60] Yildirim I.Z., Prezzi M., Use of steel slag in subgrade applications, Joint Transportation Research Program, Indiana Department of Transportation and Purdue University, West Lafayette, Indiana, 2009.
- [61] Wachsmuth F., Geiseler J., Fix W., Koch K., Schwerdtfeger K., Contribution to the structure of BOF-slugs and its influence on their volume stability, *Canadian Metallurgical Quarterly*, 20 (1981) 279-84.
- [62] Frias M., San-José J.T., Vegas i., Steel slag aggregates in concrete: The effect of ageing on potentially expansive compounds, *Materiales de Construcción*, 60 (2010).
- [63] Erlin B., Jana D., Forces of hydration that can cause havoc in concrete, *Concrete International*, 25 (11) (2003) 51-7.
- [64] Adegoloye G., Beaucour A.-L., Ortola S., Noumowé A., Bétons de granulats de laitier d'aciérie de four électrique inox: propriétés mécaniques et facteurs de durabilité., 31 émes Rencontres de l'AUGC, Ens, Cachan, 2013.
- [65] Adegoloye G., Beaucour A.-L., Ortola S., Noumowé A., Concrete made of EAF slag and AOD slag aggregates from stainless steel process: mechanical properties and durability, *Construction and Building Materials*, 76 (2015) 313-21.
- [66] Arribas I., San-José J.T., Vegas I., Hurtado J., Chica J., Application of steel slag concrete in the foundation slab and basement wall of the Tecnalia Kubik building, in: Euroslag (Ed.), 6th European slag conference, Madrid, 2010, pp. 251-64.
- [67] Arribas I., Vegas I., San-José J.T., Manso J.M., Durability studies on steelmaking slag concretes, *Materials and Design*, 63 (2014) 168-76.
- [68] Baverman C., Aran F., A study of potential of utilizing electric arc furnace slag as filling material in concrete, *Waste Materials in Construction: Putting theory into Practice*, (1997) 373-6.

- [69] Chinnaraju K., Ramkumar R., Lineesh K., Nithya S., Sathish V., Study on concrete using steel slag as coarse aggregate replacement and ecosand as fine aggregate replacement, *International Journal of Research in Engineering & Advanced Technology*, 1 (2013) 1-6.
- [70] Etxeberria M., Pacheco C., Meneses J.M., Berridi I., Properties of concrete using metallurgical industrial by-products as aggregate, *Construction and Building Materials*, 24 (2010) 1594-600.
- [71] Faleschini F., De Marzi P., Pellegrino C., Recycled concrete containing EAF slag: Environmental assessment through LCA, *European Journal of Environmental and Civil Engineering*, 18 (9) (2014) 1009-24.
- [72] Faraone N., Tonello G., Furlani E., Maschio S., Steelmaking slag as aggregate for mortars: effects of particle dimension on compression strength, *Chemosphere*, 77 (2009) 1152-6.
- [73] Manso J.M., Polanco J.A., Losañez M.M., Gonzalez J.J., Ladle furnace slag in construction, *Journal of Materials in Civil Engineering*, 17 (2005) 513-8.
- [74] Manso J.M., Setién J., Investigación de nuevos usos de las escorias de hornos eléctrico de arco (EAF): la oportunidad de los hormigones, *Hormigón y Acero*, 241 (2006) 51-7.
- [75] Manso J.M., Hernández D., Losañez M., Gonzálz J., Design and elaboration of concrete mixtures using steelmaking slag, *ACI Materials Journal*, (2011) 673-81.
- [76] Manso J.M., González J.J., Polanco J.A., Electric arc furnace slag in concrete, *Journal of Materials in Civil Engineering*, 16 (2004) 639-45.
- [77] Papayianni I., Anastasiou E., Utilization of Electric Arc Furnace Steel Slags in Concrete Products, 6th European Slag Conference, EUROSLAG pub, 2010, pp. 319-34.
- [78] Papayianni I., Anastasiou E., Concrete incorporating high-calcium fly ash and EAF slag aggregates, *Magazine of Concrete Research*, 63 (2011) 597-604.
- [79] Pellegrino C., Cavagnis P., Faleschini F., Brunelli K., Properties of concrete with black/oxidizing electric arc furnace slag aggregate, *Cement and Concrete Composites*, 37 (2013) 232-40.



- [80] Polanco J., Manso J., Setien J., González J., Strength and durability of concrete made with electric steelmaking slag, *ACI Materials Journal*, 108 (2011) 196-203.
- [81] Rodriguez A., Manso J., Aragón A., González J., Strength and workability of masonry mortars manufactures with ladle furnace slag, *Resources, Conservation and Recycling*, 53 (2009) 645-51.
- [82] San José J.T., Vegas I., Arribas I., Marcos I., The performance of steel-making slag concrete in the hardened state, *Materials and Design*, 60 (2014) 612-9.
- [83] Geyer R.T., Dal Molin D., Vilella A.C.F., Evaluation of durability of the reinforced concrete with electric arc furnace addition, *Congresso Annual Associação Brasileira de Metalurgia e Materiais*, 2001.
- [84] González-Ortega M., Segura I., Cavalaro S., Toralles-Carbonari B., Aguado A., Andrello A., Radiological protection and mechanical properties of concretes with EAF steel slags, *Construction and Building Materials*, 51 (2014) 432-8.
- [85] Fronck B., Bosela P., Delatte N., Steel slag aggregate used in Portland cement concrete, *Transportation Research Record*, (2012) 37-42.
- [86] Patel J.P., Broader use of steel slag aggregates in concrete, Ph D Thesis, Cleveland State University, 2008.
- [87] Abu-Eishah S., El-Dieb A., Bedir M., Performance of concrete mixtures made with electric arc furnace (EAF) steel slag aggregate produced in the Arabian Gulf region, *Construction and Building Materials*, 34 (2012) 249-56.
- [88] Al-Negheimish A.I., Al-Zaid R.Z., Utilization of local steel making slag in concrete, *Journal of King Saud University*, 9 (1997) 39-55.
- [89] Alizadeh R., Chini M., Ghods P., Hoseini M., Montazer S., Shekarchi M., Utilization of Electric Arc Furnace Slag as Aggregates in Concrete--Environmental Issue, *Proceedings of the 6th CANMET/ACI international conference on recent advances in concrete technology*. Bucharest, Romania, 2003, pp. 451-64.
- [90] Mohammed N., Arun D P., Utilization of Industrial Waste Slag as Aggregate in Concrete Applications by Adopting Taguchi's Approach for Optimization, *Open Journal of Civil Engineering*, 2012 (2012).

- [91] Tarawneh S.A., Gharaibeh E.S., Saraireh F.M., Effect of using steel slag aggregate on mechanical properties of concrete, *American Journal of Applied Sciences*, 11 (2014) 700.
- [92] Chen M., Zhou M., Wu S., Optimization of blended mortars using steel slag sand, *Journal of Wuham University of Technology - Materials*, (2007) 741-4.
- [93] Kim S.W., Lee Y.J., Kim K.H., Bond behavior of RC beams with electric arc furnace oxidizing slag aggregates, *Journal of Asian Architecture and Building Engineering*, 11(2) (2012) 359-66.
- [94] Morino K., Iwatsuki E., Utilization of electric arc furnace oxidizing slag as concrete aggregate, *Minerals, Metals and Materials Society/AIME, REWAS'99: Global Symposium on Recycling, Waste Treatment and Clean Technology.*, 1999, pp. 521-30.
- [95] Morino K., Iwatsuki E., Durability of concrete using electric arc furnace oxidizing slag aggregates, in: Press S.A. (Ed.), *Infrastructure regeneration and rehabilitation improving the quality of life through better construction : a vision for the next millennium*, Sheffield, 1999.
- [96] Morino K., Iwatsuki E., Properties of concrete using electric arc furnace oxidizing slag aggregates, *JSCCE second international conference on engineering materials*, California, USA, 2001, pp. 269-80.
- [97] Kim S.-W., Kim Y.-S., Lee J.-M., Kim K.-H., Structural performance of spirally confined concrete with EAF oxidising slag aggregate, *European Journal of Environmental and Civil Engineering*, 17 (2013) 654-74.
- [98] Fujii T., Ayano T., Sakata K., Freezing and thawing resistance of steel-making slag concrete, *Journal of Environmental Science for Sustainable Society*, 1 (2007) 1-10.
- [99] Wang W.C., Feasibility of stabilizing expanding property of furnace slag by autoclave method, *Construction and Building Materials*, 68 (2014) 552-7.
- [100] Berordier E., Scrivener K., Understanding the filler effect on the nucleation and growth of C-S-H, *Journal of American Ceramic Society*, 97 (12) (2014) 3764-73.

- [101] Lun Y., Zhou M., Cai X., Xu F., Methods for improving volume stability of steel slags as fine aggregate, *Journal of Wuhan University of Technology - Materials Science Edition*, October (2008) 737-42.
- [102] Mäkelä M., Heikinheimo E., Välimäki I., Dahl O., Characterization of industrial secondary desulphurization slag by chemical fractionation with supportive X-ray diffraction and scanning electron microscopy, *International Journal of Mineral Processing*, 134 (2015) 29-35.
- [103] Hekal E., Abo-El-Enein S., El-Korashy S., Megahed G., Hydration characteristics of Portland cement - Electric arc furnace slag blends, *HBRC Journal*, 9 (2013) 118-24.
- [104] CEN European Committee for standardization, Rue de Stassart, 36. Brussels B-1050.
- [105] Ortega-López V., Manso J.M., Cuesta I.I., González J.J., The long-term accelerated expansion of various ladle-furnace basic slags and their soil-stabilization applications, *Construction and Building Materials*, 68 (2014) 455-64.
- [106] Annual Book of ASTM Standards, ASTM International, West Conshohocken, 19429-2959. PA, USA, 2008.
- [107] Mehta P.K., Monteiro P.J., *Concrete: microstructure, properties, and materials*, McGraw-Hill New York, 2006.



### **4.3. The design of self-compacting structural mortar containing heavy steelmaking slags as aggregates**

*Sent to Cement and Concrete Composites (February 2016)*



## **Abstract**

Several types of self-compacting structural mortars are designed and manufactured, at a preliminary experimental stage leading to the preparation of more complex self-compacting mixes. These mixes incorporate slags from electric steelmaking (acid slag and basic slag) as aggregates, which even act as secondary cementitious materials with slight pozzolanic activity. Some mortars include addition of fly ash to reduce consumption of Portland clinker. The design of these mortar types implies precise dosages to obtain suitable mixes that resist segregation, and their preparation requires special characteristics of deformability and viscosity. The internal structure of the resultant mixes was characterized by Mercury Intrusion Porosimetry (MIP) and Computerized Axial Tomography (CAT). The performance of mortars was good in terms of acceptable mechanical, compressive and tensile strengths and suitable stiffness values. Dimensional-shrinkage tests were also performed to evaluate the main engineering characteristics of these structural mortars. The results for durability and other characteristics were satisfactory, encouraging future research in this field.

## Introduction

The recycling of waste into useful resources is one of the priorities in the EU program HORIZON 2020. Continuously produced both globally and in Europe in large amounts, these by-products of the steelmaking process (Electric Arc Furnace Slag – EAFS and/or Ladle Furnace Slag – LFS) are all too-often dumped in landfill sites. Nevertheless, they could be reused in efficient ways in several applications. The construction and the civil-engineering sectors have the most potential to consume a high volume of these materials [1-14]. Their reuse would also mean less dumping at landfill sites and would finally contribute to an increase in global sustainability. The Spanish steelmaking industry, mainly but not exclusively based in northern regions, produces around one million tons of EAF slag and 0.3 million tons of LFS [15] annually. Logically, interest in its application is more pressing in these regions.

Various properties of steelmaking slags make them appropriate raw materials in a number of applications [16-21]. Over recent years, their introduction in hydraulic [22-26] and bituminous mixes [27-29] has been extensively studied, as well as for soil stabilization in roads and embankments [30-33], among other applications.

Several research groups in all five continents are currently investigating the conditioning and the re-use of steelmaking slags [34-41]. Studies on both blast furnace slag and basic oxygen furnace slag (BOF-LD slag) may be considered classic; some dating back to over a century. More recent studies on electric arc furnace slag and ladle furnace slag started after the global increase in the production of “electric steel”, based on the smelting and refining of ferric scrap in primary (acid) and secondary (basic) metallurgical processes. A development in research that has extended around the world since the mid-1970s; the resultant slags have constituted a relevant global environmental problem since the early 1990s. Our research group in Spain began work on this subject towards the end of that decade [42-49].

The use of these slags as aggregates and even secondary or supplementary cementitious materials (SCM) in hydraulic mortars is proposed in this investigation. Many scientific studies in the literature have demonstrated that the hardened properties of mortar and concrete made with EAF slag aggregates are similar or even better than hydraulic mixes made with natural aggregates; their mechanical strength and other relevant characteristics are sometimes improved. The disadvantage of using these aggregates is the poorer workability of hydraulic mixes in the fresh state and their higher density in the fresh and the hardened state [50-64]. A recent work by



these authors has developed research on structural mortars made with EAFS and LFS [65].

Self-compacting mortar and concrete is a relatively new technology. Its performance has been enhanced over recent decades and its advantages are increasingly appreciated in the construction sector. The main objective of the present research is to fabricate this type of mortar with EAFS and LFS aggregates in partial substitution of natural aggregates, to produce self-compacting mixes for use under the same situations/conditions as conventional concrete and with the same technologies.

The design of these sorts of mixes is complex, because they have to fulfill specific flowability and viscosity requirements in the course of pouring and casting, to prevent aggregate separation from the paste, and to prevent segregation during setting time, due to heavy aggregate decantation [66-74]. When EAF slag is used as aggregate in self-compacting mixes, potential segregation of the coarse aggregate is more likely, because of its higher density (values of 3 to 4 Mg/m<sup>3</sup> versus 2.4 to 2.8 in natural aggregates). Especially as coarse aggregates remain suspended in a cementitious matrix (sometimes flowing-moving and sometimes motionless), the density of which has values in the interval of 2-2.4 Mg/m<sup>3</sup>. If research teams with experience in the use of EAF slag are to obtain satisfactory hydraulic mixes, they have to balance the above-mentioned contradictory requirements in its design. Chemical admixtures used to control mix fluidity and viscosity are of capital importance for the success of this endeavor.

The first step will consist in the design and preparation of self-compacting mortars using EAFS aggregates (less than 4 mm in size), and LFS fine fractions or mineral powder; the second step will be to prepare a self-compacting concrete using EAF slag as both coarse and fine aggregate. In the present study, different mortar mixes were designed to establish appropriate self-compacting mixtures designed for the introduction of EAFS aggregate, and consisting of SCM (LF slag, fly ash) and fine aggregate content at graded sizes, and proportionate amounts of water and chemical admixtures. This research group is convinced that the use of EAF slag concrete constitutes a feasible option in the near future. At present, this research team is working in association with several European research groups (Spain, Italy, Greece, Belgium, Germany...), with the purpose of establishing pre-normative rules in this field.

## Materials and mixes

### Cement, water and natural aggregates

Two types of cement were used in the present research. A Portland cement type I 42.5 R complying with standard UNE-EN 197-1 was used in most of the mixtures; in a few mixes, a Portland cement type IV/B-V 32.5-N was used. Type I cement consists of 90% Portland clinker, 5% calcium carbonate powder fines, and 5% gypsum. The composition by weight of type IV cement is 5% calcium carbonate powder fines, 40% fly ash type I, and 50% Portland clinker, milled with 4% gypsum. Cement with fly-ash addition is promising when aggregates are susceptible to give out free CaO; the quality of the interfacial transition zone could be enhanced by the presence of pozzolanic material, as has been suggested by authors in a recent work [42].

Water from the urban mains supply of the city of Bilbao was used in the hydraulic mixes that contained no harmful compounds for their quality.

A commercial crushed natural limestone, sized between 0 and 5 mm, was used as fine aggregate in the reference mixes. Its main mineral was calcite (95%), with a specific gravity of  $2.67 \text{ Mg/m}^3$  and a fineness modulus of 2.9, the gradation of which is shown in Figure 1. A fine fraction, obtained by sieving the aggregate, to promote a viscous cementitious matrix in the fresh state, was necessary to achieve the self-compacting characteristics in the mixes containing EAFS as aggregate. These “limestone fines”, of a size smaller than 0.6 mm (sieve N<sup>o</sup> 30 ASTM), had a fineness modulus of 1.03, the gradation of which also appears in Figure 1.

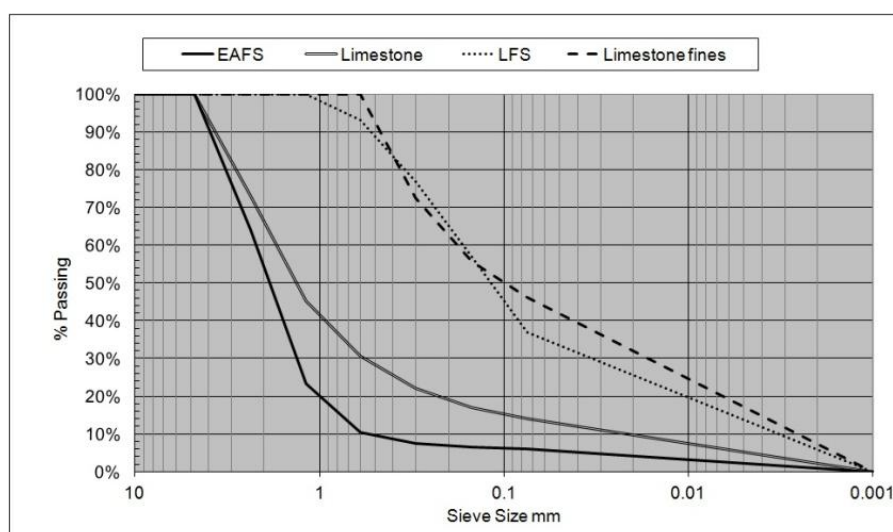


**Figure 1:** Grading of the raw materials

Slag

Crushed Electric Arc Furnace slag (EAFS) supplied by the company Hormor-Zestoa was used in this research. Its global chemical composition, physical properties and its main crystalline components (obtained by XRD) are detailed in Table 1; its grading is included in Figure 1.

Compounds	EAFS (0-5 mm)	LFS
Fe <sub>2</sub> O <sub>3</sub> (%)	22.3	1.0
CaO (%)	32.9	59.2
SiO <sub>2</sub> (%)	20.3	21.3
Al <sub>2</sub> O <sub>3</sub> (%)	12.2	8.3
MgO (%)	3.0	7.9
MnO (%)	5.1	0.26
SO <sub>3</sub> (%)	0.42	1.39
Cr <sub>2</sub> O <sub>3</sub> (%)	2.0	--
P <sub>2</sub> O <sub>5</sub> (%)	0.5	--
TiO <sub>2</sub> (%)	0.8	0.17
Loss on ignition (%)	gain	0.5
Water absorption (%)	1.12	--
Specific gravity (Mg/m <sup>3</sup> )	3.42	3.03
X-Diffraction main compounds	Wüstite-Ghelenite Kirsteinite	Periclase-Olivine- mayerite

**Table 1:** Chemical composition and physical characteristics of slags

An additional high-silica low-alumina ladle furnace slag (LFS) was used in this work. It has a density of 3.03 Mg/m<sup>3</sup> and a fineness modulus of 0.75. Its chemical composition and X-ray diffraction analysis in Table 1 shows that its main compound was dicalcium silicate (olivine); its grading also appears in Figure 1. It should be said that a fraction (30%) as suggested in [22, 45] of the total amount of LFS added to the hydraulic mixes could show SCM binder properties; the remainder of the LFS should be considered additional fine fraction.

Design of mixes

Okamura [67] proposed a methodology to design an efficient self-compacting mix, which may now be considered the conventional solution. His methodology for the preparation of self-compacting mixtures using natural aggregates with densities of below 3 units such as limestone, sandstone among others, is in general very useful. If the coarse aggregate is denser quartzite, granite or basalt, Okamura's proportions should be slightly corrected; if the aggregate is artificial, heavier, rougher and sharper

as in the case of the EAF slag, the new solutions described in this work are needed. A high number of mixes were tested in this study, the most relevant and outstanding of which are reported below.

Seven different mixes were designed to study the performance of self-compacting structural mortar fabricated with steelmaking slags; Table 2 shows their compositions and Figure 2 shows their grading. Mixes S-1 and S-2, in which EAF slag was not used, may be considered reference mixes; however, ladle furnace slag was used in S-2. Mixes S-3, S-4, S-5, S-6 and S-7 included EAFS and some of them included LFS. The LFS content represented 33% of the total binder (PC+LFS partial) in mixes S-2 and S-4, while this percentage was 20% in S-5 and S-7. Furthermore, the cement used in the S-6 and the S-7 mixes was type IV, instead of type I cement used in the rest of the mixes .

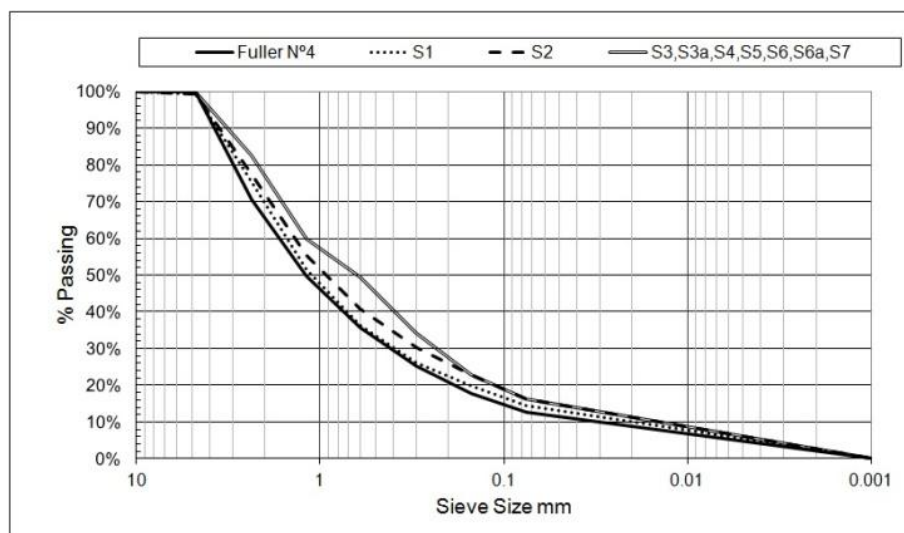


**Figure 2:** Grading of the mixes

EAF slag aggregate sized 0-5 mm was used in mixes S-3, S-4, S-5, S-6 and S-7, in a volume proportion in fresh mortar close to 35%, with the addition of a noticeable amount of small-sized limestone fines (0-0.6 mm). The substitution of crushed limestone by EAFS in the above-mentioned mixes was in equal volumes to the reference mixes only for particle sizes of over 0.6 mm. The water-to-fines ratio was kept close to 0.2 in all mixes.

In all cases, a plasticizer and viscosity conditioner admixture supplied by CHRYSO modified the self-compacting mixes to achieve a suitable flowability and consistency. Additionally, an air entrainment admixture was used in S-3 and S-6 (giving rise to mixes S-3a/S-6a), to decrease the density of the mix, compensating the heavier EAFS aggregate.

(\*) The numerical value is the equivalence of cement type IV to cement type I.

Mix Design (kg/m <sup>3</sup> )		S-1	S-2	S-3/3a	S-4	S-5	S-6/6a	S-7
Type-I cement		551	496	551	496	518	330(*)	310(*)
Fly ash							220	205
LFS			183		183	106		106
Limestone	Small-size aggr <5 mm	1584	1470					
	Fine fraction <0.6 mm			632	504	558	632	558
EAFS <5 mm				1259	1259	1259	1259	1259
Water		220	220	220	220	220	220	220
Plasticizer		1.2%	1.2%	1.6%	1.5%	1.5%	1.5%	1.5%
Air-entraining admix				0/0.2%			0/0.1%	
Fresh density		2.45	2.42	2.74/2.33	2.71	2.71	2.72/2.39	2.61

**Table 2:** Mix designs

## Test Methods

The mortars were mixed in a conventional standardized mortar-mixer and poured into twelve 40x40x160 mm moulds; four 25x25x287.5 mm specimens per mix were cast, to evaluate shrinkage and potential expansion. These were demoulded after 24 h and submerged in water, except for the ones used to evaluate dry shrinkage contraction. The tests were divided into two stages, fresh properties and hardened properties.

### Fresh properties

Workability is probably the most important of all the fresh characteristics of a self-compacting mixture. The flowability-viscosity values needed for a self-compacting mix are: spreading 180 mm in the mini-slump cone, and a V-funnel passing time between 7 and 11 seconds. Additionally, density was also estimated.

A mini-slump flow conic mould with base diameters of 70 by 80 mm and a height of 40 mm was filled with the mixture. Having positioned and then removed the cone from the mortar mass, the final diameter of the spread mixture across the steel plate was measured; the absence of segregation or bleeding in the mixture was verified by a visual inspection. A mini V-funnel test was also used; this test measures flow time from the opening of a bottom trap door until the first sighting of daylight. The flow time was recorded in each case. The dimensions of the apparatus are specified in EFNARC [75], which has demonstrated its suitability to evaluate the self-compacting properties of mortars made with a maximum aggregate size of 5-6 mm.

Using the results from the above-mentioned tests, Okamura [70] defined two indices to evaluate the deformability ( $\Gamma_m$ ) and the viscosity ( $R_m$ ) of the mix:

$\Gamma_m = (d_1 d_2 - d_0^2) / d_0^2$ : where,  $d_1$ ,  $d_2$  represent the after-flow diameter in two orthogonal directions; and  $d_0$  is the 80 mm cone diameter.

$R_m = 10/t$  : where,  $t$ (sec) is the measured flow time of the mortar through the funnel.

These indices are used to evaluate the suitability of the proposed dosage for the manufacture of self-compacting concretes with good fresh properties.

### Hardened properties

The mix specimens were held underwater at room temperature during curing and hardening over a period of 180 days; after which their dry density was evaluated. The strength evolution of the mixes was measured in flexural tests performed on 40x40x160 mm specimens and then two pieces from each specimen were tested under compression in a 40x40 mm base. An estimation of the elasticity modulus (stiffness modulus, not valid as the Young's modulus of the material) was obtained from ultrasonic pulse propagation velocity measurements.

MIP (Mercury Intrusion Porosimetry) tests were performed and the results are shown in Table 5. A CAT (Computerized Axial Tomography) analysis of the cured mixes was also performed, to study their structure in the solid state and to verify the absence of segregation; the results are also shown in Table 5.

Shrinkage length variations of in-air specimens were measured to study the contraction of mixtures over time due the drying effect. Durability tests were performed by placing the samples in an autoclave, for 48 hours at 0.2 MPa, at a temperature of around 130°C (Spanish standard NLT-361) [76], and also a test submerging the specimens used in length variation test in water at 70°C (ASTM D-4792 standard) [77], to evaluate the risk of expansion of certain slag compounds, which could contribute to the deterioration of the hardened mortar.

## **Results**

### Fresh properties

The results of the mini-slump cone test and mini V-funnel tests on the mortars are given in Table 3. As expected, the results showed that the EAFS mortar had slightly less

workability than the conventional aggregate mortar. However, the role of the plasticizer and viscosity controller admixture was decisive and positive. It enhanced the spreading of EAFS mixes and gave them a suitable visual appearance, as shown in Figure 3.



**Figure 3:** Spreading of the mixture S4 in the mini slump cone

Mixes S6 and S7 prepared with Portland cement type IV (containing fly ashes) showed good short-term flowability. As expected, the inclusion of air-entrainment admixtures decreased the flowability of mixtures 3a and 6a (Table 3), decreasing their fresh density (Table 2) and increasing their volume of occluded air.

	Mini-slump flow (mm)	V-funnel (s)
S-1	195	9.4
S-2	190	8.2
S-3	190	9.5
S-3a	180	8.7
S-4	185	9.6
S-5	188	9.4
S-6	205	8.7
S-6a	195	8.0
S-7	200	8.8

**Table 3:** Flowability of mixes

The relationship between the indices of deformability and viscosity proposed by Okamura [70] for self-compaction are shown in Figure 4. These results were compared with other values that Okamura categorized as excellent (AA), good (A) and acceptable (B), as shown in Figure 4.

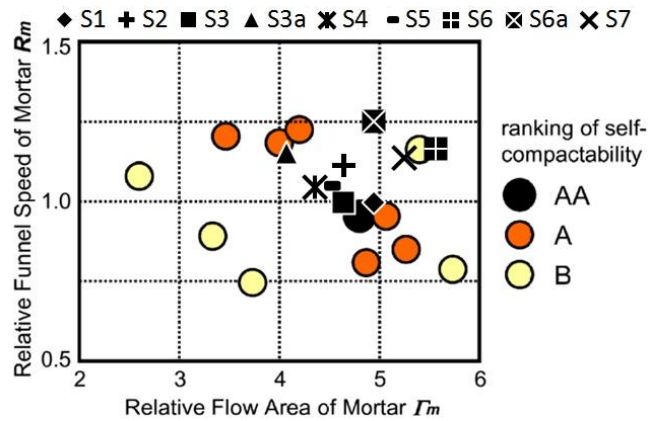


**Figure 4:** Okamura's map

The reference mix incorporating natural aggregate (S-1) and the slag aggregate (S-3) mix showed the best relationship between deformability and viscosity and the mix obtained with these materials is expected to have excellent (AA) self-compacting properties.

Mixes S-2, S-4, and S-5, with ladle furnace slag showed a good relationship, though slightly worse behavior, than mixes S-1 and S-3. In this case, their viscosity was higher and their deformability lower, but the expected self-compaction should be good, so it could be said that the proportions used in these mixtures were promising. The effect of the air-entrainment admixture in the fresh properties of the mortar may be seen in S-3a. The values of this mix showed lower viscosity and lower deformability than the above-mentioned mixes; the self-compacting behavior of concretes made with this mortar phase dosage (A) is expected to be good.

The effect of using cement IV instead of cement I is shown in the results for mixes S-6, S-6a and S-7. In these cases, their viscosity was low and their deformability was high in the short term; the self-compacting mortars manufactured in this way were acceptable in Okamura's map. In future works, lower admixtures dosages may be recommended in the mixes containing cement IV, to obtain a better relationship. Additionally, these data were seen to vary after several minutes; the rheology of these cement mixes (thixotropy-rheopexy) should be more extensively analyzed.

With regard to the fresh density, special attention should be given to those mixes prepared with air entrainment admixture (S-3a and S-6a) The decrease in the fresh density value, due to air entrainment, was around 13% (2.72 to 2.33 or 2.39 Mg/m<sup>3</sup>) and a similar decrease in strength could be considered admissible. Entrained air



increased by more than 10% (see MIP and CAT porosity results) in both cases, an amount that might endanger the mechanical properties.

### *Hardened properties*

#### *Density*

The dry densities of the hardened mortars are given in Table 5. It may be seen that the average density of the limestone mortars increased by 11% in the specimens with EAFS aggregate (values close to 2.7 versus 2.4 Mg/m<sup>3</sup>). As mentioned, the density of the specimens with an air entrainment admixture decreased to 13%, with final values similar to those of limestone mortars.

According to the dosages stated in Table 2, the theoretical proportion of EAFS in the dry mortars is about 50% in weight (40% in volume), a value lower than the 60% reached in mortar mixes (not self-compacting) described in a recent article [65], and much lower than the 70% or so of the contents of EAFS coarse aggregate in low-workability concrete [8]. The characteristics of self-compacting mixes (deformability and viscosity) are incompatible with EAFS contents greater than 55% in weight of dry-mix, according to our extensive research.

#### *Strength*

The results of compressive and flexural strength after 3, 7, 28, 90 and 180 days of underwater curing are given in Table 4 and in Figure 5; the stiffness modulus was also measured at 180 days of curing. These results (mainly after 180 days) showed strength and stiffness improvements with the use of EAFS aggregate (see S-3 versus S-1 and S-4-S-5 versus S-2). At short term (3 days) it can be observed two set of mixes, those showing higher values (S-1, S-3 and S-5), and the rest of mixes showing lower values by different reasons.

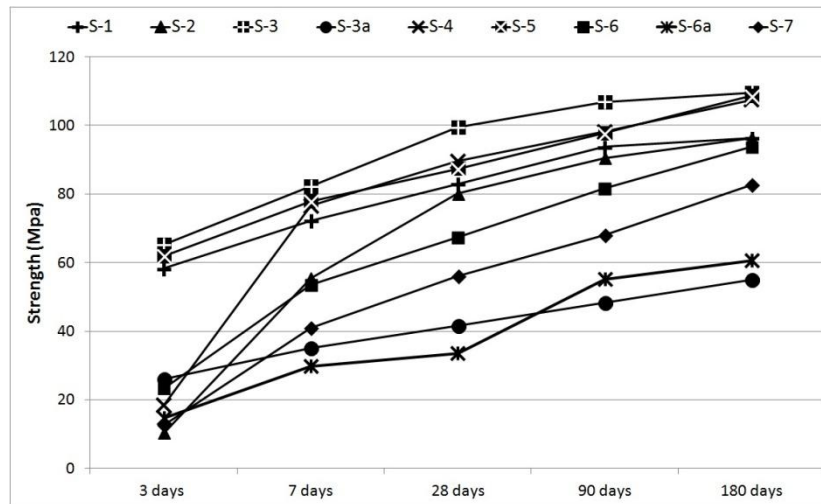


**Figure 5:** Compressive strength of mixes

The use of LFS decreased the mix strengths at early ages in some cases (see S-2 versus S-1 and S-4 versus S-3), although the mixes reached almost the same strength as those without LFS in the long term. The mix S-5 shows a lower content of LFS (20% of total binder) than S-4 (30%) and its strength at 3 days is really good; it seems that the amount of LFS must be carefully controlled to avoid short term weakness. The development in the strength of the specimens with LFS might indicate that the hydraulic activity of this slag is activated at medium term, and its effect is visible in the long term more than in the short term.

The fly ash effect is good, as expected, in the long-term results. After 180 days, mix S-6 presented a slightly lower compressive and flexural strength, but close to that shown by S-1, after the simultaneous expected effects of the presence of EAFS (enhancement) and fly ash (diminution). The comparison between S-7 versus S-2 (or S-6) shows interesting results; the simultaneous use of both SCM (LFS and FA) gave rise in S-7 to a lower strength at medium and long term, but the reached values are notable.

The effect of the air entrainment admixture is detrimental at anyone age, Figure 5, causing a severe loss of strength that in no way compensates the gain in weight; the value in S-3a is half of what was reached by S-3, and the value in S-6a is the 64% of the S-6 value. The use of these sorts of admixtures is therefore not recommended.

The results in terms of flexural strength confirm the results obtained in compression tests, with a notable enhancement in mixtures S3, S4 and S5 containing EAFS aggregate. The use of this kind of aggregate is advantageous with regard the tensile strength of mortars.

Ultrasonic pulse velocity measured the stiffness modulus, yielding results that are on the whole comparative values, but with little absolute meaning as a Young's modulus. These results were also coherent with the results in compression and the use of EAFS aggregate had no influence on this variable.

	Compressive strength (MPa)					Flexural strength (MPa)					Stiffness modulus (GPa)
	3 days	7 days	28 days	90 days	180 days	3 days	7 days	28 days	90 days	180 days	180 days
S-1	58.3	72.3	82.9	93.7	96.3	8.46	10.75	12.68	13.28	14.58	55.8
S-2	10.4	55.5	80.1	90.5	96.4	2.15	9.94	10.73	11.43	13.73	53.7
S-3	65.3	82.3	99.5	106.9	109.6	9.35	12.50	12.41	14.11	15.36	61.3
S-3a	26.1	35.0	41.5	48.2	55.0	1.98	7.22	8.57	9.79	10.27	37.7
S-4	18.5	76.6	89.5	92.2	107.5	3.63	10.56	11.92	13.39	15.42	59.3
S-5	61.9	77.9	87.4	97.7	108.6	7.53	12.82	12.85	14.87	15.23	61.5
S-6	23.4	53.5	67.3	81.6	93.7	4.95	8.75	10.76	11.48	14.12	56.1
S-6a	14.6	29.7	33.5	55.1	60.6	4.83	6.21	7.86	9.56	10.64	44.4
S-7	12.6	40.9	56.1	68.1	82.7	2.71	6.82	11.3	12.68	13.34	52.4

**Table 4:** Hardened properties of different mixes

*MIP analysis*

The results of Mercury Intrusion Porosimetry (MIP) analysis of the different mixes showed that they were on the whole well-performed. Only mix S-7 revealed a higher than expected capillary porosity value; the interaction between LFS and FA is not completely satisfactory, as previously mentioned. Recall that the “leitmotiv” in this experimental work is self-compacting mortars with suitable characteristics; hence, the results in these other proprieties of mortars were, at the start, secondary.

Propriety	S-1	S-2	S-3/3a	S-4	S-5	S-6/6a	S-7
Dry density (Mg/m <sup>3</sup> )	2.37	2.35	2.68/2.24	2.67	2.66	2.65/2.34	2.56
MIP Bulk density (Mg/m <sup>3</sup> )	2.38	2.38	2.70/2.37	2.69	2.67	2.69/2.44	2.53
MIP App density (Mg/m <sup>3</sup> )	2.52	2.51	2.91/2.90	2.90	2.94	2.91/2.92	2.94
MIP porosity (% vol)	5.3	5.4	6.9/18.3	7.5	9.4	7.2/16.6	13.2
CAT porosity (% vol)	0.5	1.5	1.6/6.2	2.4	3.2	2/3.7	1.6
CAT matrix (% vol)	99.5	98.5	54.4/53.2	57.2	54.1	57.6/56	52.9
CAT EAFS (% vol)	-	-	43.4/40.2	40	42.2	40.1/40	44.9
CAT metallic iron (% vol)	-	-	0.5/0.3	0.3	0.4	0.3/0.3	0.5

**Table 5:** MIP and CAT results on mixes

As shown in Table 5, the capillary porosity readings of reference mixes S-1 and S-2 is in the order of 5-6%; this is an excellent value, but it must be understood as an average between the capillary porosity of the cementitious matrix (higher than 5-6%) and the porosity of aggregates included in the tested sample (about 1-2% as geological characteristic of limestone), which constitutes an amount of around 40% in volume. So, the real value of the capillary porosity of the cementitious matrix could be estimated at 10%, consistent with their mechanical characteristics.

With added EAFS (mixes S-3, S-4 and S-5), this value is increased to 7-9%, probably due to the porosity of the new slag aggregates, estimated to be in the interval 4 to 10%. Finally, the presence of LFS in the mixes has no clear affect on their capillary porosity.

The use of air-entrainment admixture in S-3a and S-6a produced a logical increase in MIP, also changing pore-distribution size, revealing a greater quantity of pore sizes within the interval of 0.1 to 150 microns (Figure 6b, mix S-3a) in a comparison between a typical distribution of mixes (Figure 6a, mix S-3) and the distribution of a mix with this admixture. In the curve representing cumulative intrusion, the interval of 0.1 to 3 microns shows a sharp increase in the slope of the curve for mix S-3a, the figures have been illustrated to show similar slopes in both the intervals 8-50 nm and 50-80 nm, so that they may be easily compared.

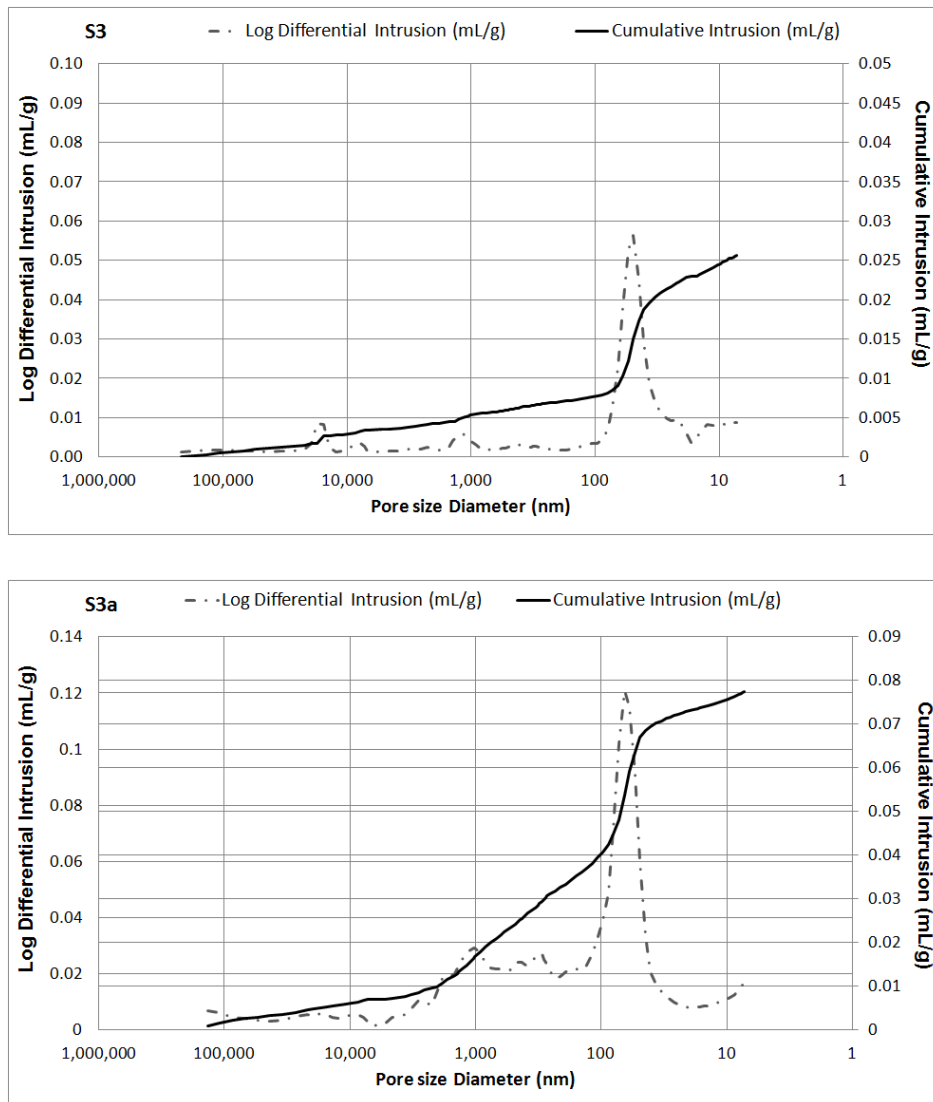


**Figure 6:** Pore distribution in mixes S3 and S3a

The bulk density MIP values are in general quite coherent with the dry-density values measured by the classical methods of weight in air and submerged weight of oven-dry prismatic specimens (40x40x160 mm), as prescribed in basic standards. Only the discrepancy is more pronounced in mixes S-3a and S-6a, due to their high spherical (air entrained) porosity and to the way that the MIP test was performed, employing a little piece (10x10x20 mm) of a broken prismatic sample; in this piece the “skin effect” is not there, and broken spherical pores appear on the surface, having a slightly lower measured bulk volume than in the unbroken prismatic samples. Finally, the results for the apparent density for all of the EAFS mixes were similar and coherent between each other; the same way may be said of the reference mixes.

### CAT analysis

Computerized Axial Tomography (CAT) observations completed the study of this research work. This technique is based on a tri-dimensional mapping built from a set of X-ray plate sections of the sample [78]. In our case, 40x40x15 mm samples from all mixes were analyzed and the results are presented in graph form, following removal of the superficial region (external superficial layer) of the pieces so as not to quantify regions with anomalous aggregate distribution.

The pixel resolution in this analysis means we may appreciate microstructural features of a larger size than 150 microns or so. In a previous work by ours [49], it was stated that the addition of MIP porosity (lower than 170 microns) and CAT porosity (higher than 150 microns) in the mixes may be approximated with the total value of holes in the mass, including capillary and spherical air-void porosity.

The use of X-ray mapping distinguishes between the different kinds of materials and particles that compose the sample according to their density; dark grey in the regions of lower density and light grey in the regions of higher density. In the case of our mixes, following image analysis and treatment, it was possible to observe the metallic iron (almost white, with a density close to  $8 \text{ Mg/m}^3$ ), the EAFS (clear, density 3.5 units), the cementitious matrix (dark, density about 2.4 units), the air (black, density 0.0012 units) and even the water (density 1), where present. Unfortunately, the cement hydration products, fine limestone, LFS and even unreacted cement grains and unreacted fly ash may only be distinguished with great difficulty, if there at all, in the cementitious matrix. Hence, the results of this analysis are shown in Table 5 and Figure 7, in terms of metallic iron, pores, and the ensemble of EAFS-cementitious matrix.

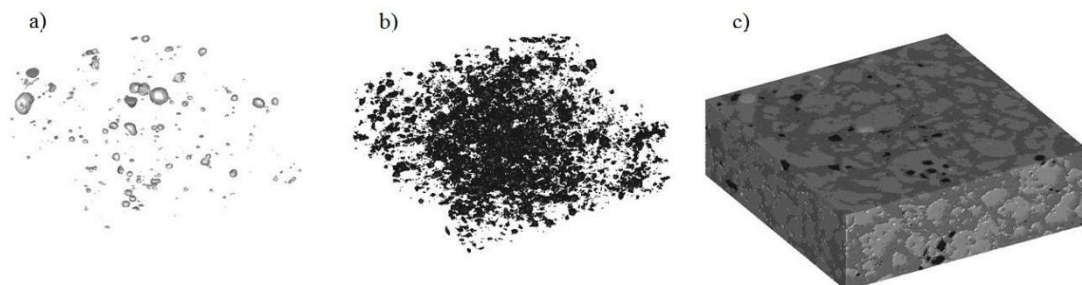


**Figure 7:** Results of CAT observations on S-6 mix: a) metallic iron; b) pores; c) EAF slag (clearer) and cementitious matrix (darker).

The CAT results in Table 5 showed a higher air-entrained porosity in the mixes with air-entrainment admixture (S-3a and S-6a), and a metallic iron content in the range 3 to 5 per thousand in volume; slightly high than a prudent value for the structural application of one per thousand in volume, equivalent to 3 per thousand in weight as it has been stated by the professional experience of authors in civil works.

The volumetric amount of EAFS is about 40% (as expected) in all the mixes, a measured value that is influenced by the degree of EAFS segregation in the sample part extracted for observation. Segregation of this heavy aggregate, suspended in the interior of fluid cementitious matrices of a lower density, occurs very easily. Other images trying to separate the limestone fines from the cementitious matrix were confusing and less useful under visual analysis.

The values of cementitious matrix volume in Table 5 for the dry EAFS mixes include the hydrated binders, the very fine (lesser than 0.6 mm) aggregates, the capillary porosity and spherical porosity with sizes under 150 microns. Their amount is within the interval of 53 to 57%.

In mixes S-1 and S-2, the cementitious matrix volume proportion, including the above-mentioned components added to the limestone aggregate, reached total values close to 99%. Hence, in mixes made with natural aggregates with densities of under 2.7 Mg/m<sup>3</sup>, the CAT technique is less useful, and porosity values after its use are never larger than 0.15 mm; the rest are the ensemble of cementitious matrices and aggregates. This CAT porosity value could be replaced by the classical standardized measurement of air-entrained in fresh mortars.

#### *Length Variation*

In Figure 8, the length evolution results for 287.5 mm long sample specimens are shown for mixes S-1, S-2, S-3, S-4, and S-5. The specimens were kept in-air (Dry) at room temperature for 9 months and submerged (Wet) at room temperature for 120 days; subsequently, the wet specimens were submerged in water at 70°C, a long-term hot-water test described in the following section. This batch of tests was only performed on the mixes containing type-I cement; the influence of fly ash has previously been detailed in a former article of authors [65].

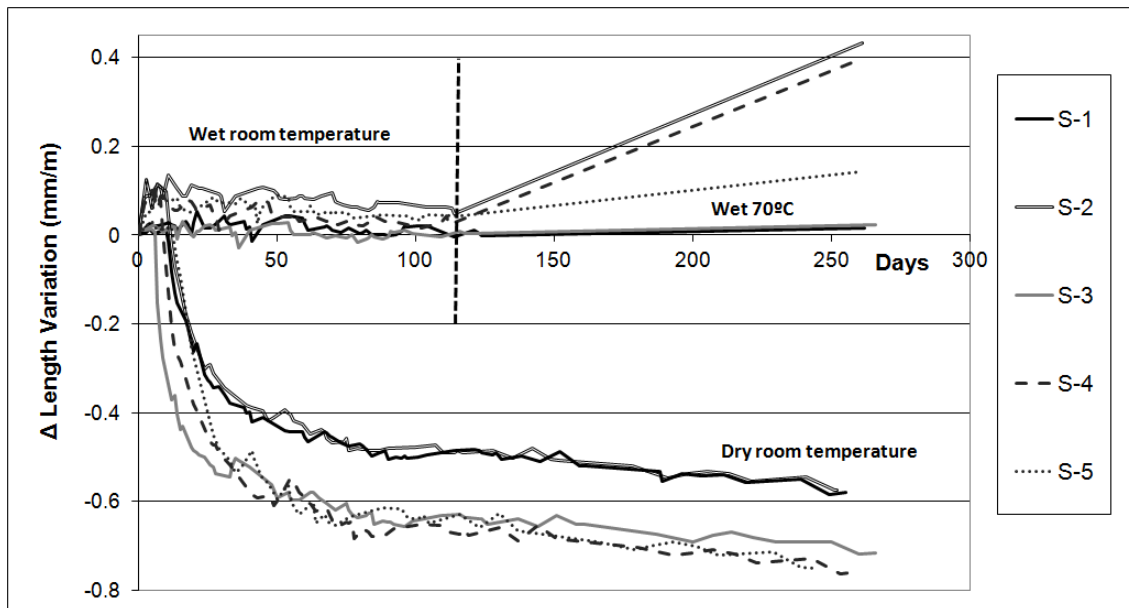


**Figure 8:** Length variation in shrinkage tests

The length variation of the submerged samples, as may be expected in the well-performed hydraulic mixes, was almost null after four months at room temperature, showing that the presence of any kind of slag is innocuous in the proportions that were used. However, even though a slight expansion (0.05-0.07 mm/m) is appreciated in mixes S-2, S-4, and S-5, which contain binder in proportions of 20-30% of LFS, that effect is negligible in mixes S-1 and S-3.

Dry shrinkage in our mixes was more noticeable and agreed with the results of other authors [16]. The maximum contraction values reached by several mixes was close to 0.8%; a value lower than the classical 1 mm/m in mortar, probably due to the high amount of limestone fines used in all the mixtures which mitigate the shrinkage. In a recent work [65], the authors found shrinkage values up to 1.2 mm/m in mixtures containing similar slag types, but their fine fraction content of limestone aggregates was smaller and the presence of fly ash also enhanced the final value.

Mixtures S-1 and S-2 (reference mixtures, without EAF slag) showed the smallest long-term values, about 0.6 mm/m, and the mixtures containing either EAF or LFS showed the highest values. In the aforementioned work [65], the authors affirmed that the presence of EAFS enhanced shrinkage contraction, due to its lower elasticity modulus, a finding confirmed in these experimental results. Moreover, the presence of LFS (a more expansive slag in theory, but in this case present in moderate proportions) produced no visible effects after nine months.



### Durability

The first durability test was performed in an autoclave, over 48 hours at 0.2 Mpa, in the presence of water vapor and at a temperature close to 130°C, according the Spanish standard NLT-361 [76], on pieces of the initial prismatic samples which remained integral after the mechanical tests. The weight of the samples was evaluated before and after the test, and the disintegrated material was also collected and weighed.

This test, with satisfactory results, was performed only on mixes S-2, S-3, S-4 and S-5, containing LFS and/or EAFS; specimen integrity (no cracks generated) was the result, and only very slight superficial scaling with negligible amounts of detached material was observed in mixes S-2 and S-4.

Additionally, as mentioned in the former section, mixes S-1, S-2, S-3, S-4 and S-5 were submerged in 70°C water (inspired in the ASTM D-4792 standard) [77] after their immersion over 120 days at room temperature. They remained in hot water for a similar period of time until 270 days, as shown in Figure 8. This test is intended to evaluate the long-term risk of slag compound expansion, which can contribute to the deterioration of the hardened mortar.

The results of this last test gave satisfactory results. In fact, the higher LFS content of mixes S-2 and S-4, correspond to the more expansive mixes that reached values of 0.4 mm/m; mix S-5 reached 0.15 mm per meter, while the S-1 and S-3 samples (without LFS) were not expansive. Despite the fact that this expansive behavior (0.4 mm/m) could be considered as slightly dangerous, it should be emphasized that these samples were kept submerged under water and the effect of dry shrinkage was not present. The superposition of both wet expansion and dry contraction is globally understood to have a slight contractive effect, taking their respective magnitudes into account. Hence, the final results of the durability tests were positive for all the mixes prepared in this work.

In Figure 9, the superficial appearance of the samples submerged at 70°C over 5 months may be observed. A slight scaling on the external surface could be appreciated in specimens S2, S4 and S5 with LFS, in a similar way as appreciated following the autoclave test; the surface in specimens S1 and S3 is fairly smooth. The authors experience is that this surface effect is unavoidable when LFS is used in hydraulic mixes.



**Figure 9:** Samples after immersion in water at 70°C.

## Conclusions

The conclusions from this work can be summarized as follows:

- Self-compacting structural mortar mixes have been successfully designed and fabricated using EAFS as heavy aggregate; careful control of the fine fraction is strongly recommended.
- The use of LFS as an SCM binder: a value of 20% of total binder can be recommended; it could even be admissible in proportions of 30%. Its presence slightly postpones the increase in mechanical strength of mixes, with no notable detriment in the final value.
- The global results in terms of mechanical strength are promising in all the mixes. This effect is a consequence of a suitable mortar microstructure, as revealed in the MIP and CAT analyses.
- The simultaneous use of fly ash, as an addition with the LFS, and EAFS aggregate yield acceptable results in general, showing good compatibility, and economizing on total consumption of Portland clinker.
- The results of potential expansion tests performed on the mixes showed the innocuous effect of EAFS, and even using appropriate proportions of LFS they were within safe margins.
- The use of EAF slag aggregate contributes to a slight increase in drying shrinkage against the use of conventional aggregates.
- Air-entrainment admixtures should not be employed, because of the high strength loss produced after their use.

## References

- [1] Akinmusuru JO. Potential beneficial uses of steel slag wastes for civil engineering purposes. *Resour Conserv Recy.* 1991;5(1):73-80.
- [2] Faleschini F, De Marzi P, Pellegrino C. Recycled concrete containing EAF slag: Environmental assessment through LCA. *Eur J Environ Civ Eng.* 2014;18(9):1009-24.
- [3] Fronek BA. Feasibility of Expanding the use of Steel Slag as a Concrete Pavement Aggregate, PhDT Cleveland State University; 2012.[http://rave.ohiolink.edu/etdc/view?acc\\_num=csu1344208168](http://rave.ohiolink.edu/etdc/view?acc_num=csu1344208168)
- [4] Serjun VZ, Mladenovic A, Mirtic B, Meden A, Scancar J, Milacic R. Recycling of ladle slag in cement composites: Environmental impacts. *Waste Manage.* 2015;43:376-85.
- [5] García C, San José JT, Urreta JI. Reuse and valorization in civil works of electric arc furnace (EAF) slag produced in C.A.P.V. In: Gaballah I, Hager J, Solozabal R, editors. *Waste Treatment and clean Technology (REWAS)*. San Sebastian 1999. p. 417-24.
- [6] Motz H, Geiseler J. Products of steel slags an opportunity to save natural resources. *Waste Manage.* 2001;21(3):285-93.
- [7] Jähren P. Do not forget the other chapters!. *Concrete int.* 2002; 24(7):41-4.
- [8] Koros PJ. Dusts, Scale, Slags, Sludges. . . Not Wastes, but Sources of Profits. *Metall Mater Trans B.* 2003;34(6):769-79.
- [9] Mehta PK. Global concrete industry sustainability. *Concrete inter.* 2009;31(2):45-8.
- [10] Papayianni I, Anastasiou E. Concrete Incorporating High Volumes of Industrial By-Products. *Role of Concrete in Sustainable Development—Proceedings of International Symposium Dedicated to Professor Surendra Shah.* Aristotle University Greece,sept 2003. p. 595-604.
- [11] Rubio AR, Carretero JG. La aplicación de las corias de acería en Carreteras. *Ing Civ.* 1991;80:5-9.
- [12] Serjun VZ, Mirtič B, Mladenovič A. Evaluation of ladle slag as a potential material for building and civil engineering. *Mater Tehnologije.* 2013;47(5):543-50.
- [13] Shelburne WM, Degroot DJ. The use of waste & recycled materials in highway construction. *Civ Eng Pract.* 1998;13(1):5-16.

- [14] Tomellini R. Summary report on RTD in iron and steel slags: development and perspectives Technical Steel Research, Report Prepared for the European Commission EUR 19066. Brussels, Belgium,1999. p. 351-2.
- [15] San José JT. Reutilización y valoración en obra civil de escorias de horno eléctrico de arco producidas en la CAPV. *Arte y Cemento*. 2000;124(6).
- [16] Brand AS, Roesler JR. Steel furnace slag aggregate expansion and hardened concrete properties. *Cem Concr Compos*. 2015;60:1-9.
- [17] López FA, López-Delgado A, Balcázar N. Physico-chemical and mineralogical properties of EAF and AOD Slags. *Afinidad*. 1996;53(461):39-46.
- [18] Setién J, Hernández D, González JJ. Characterization of ladle furnace basic slag for use as a construction material. *Constr Build Mater*. 2009;23(5):1788-94.
- [19] Yildirim IZ, Prezzi M. Chemical, mineralogical, and morphological properties of steel slag. *Adv Civ Eng*. 2011;2011.
- [20] Yildirim IZ, Prezzi M. Steel slag: Chemistry, mineralogy, and morphology. *IFCEE Geotechnical Special Publication* 2015. p. 2816-25.
- [21] Faleschini F, Brunelli K, Zanini MA, Dabalà M, Pellegrino C. Electric Arc Furnace Slag as Coarse Recycled Aggregate for Concrete Production. *J Sustain Met*. 2015:1-7.
- [22] Al-Negheimish AI, Al-Zaid RZ. Utilization of local steel making slag in concrete. *J King Saud University*. 1997;9(1):39-55.
- [23] Anastasiou E, Georgiadis Filikas K, Stefanidou M. Utilization of fine recycled aggregates in concrete with fly ash and steel slag. *Constr Build Mater*. 2014;50:154-61.
- [24] Arribas I, San-José J, Vegas I, Hurtado J, Chica J. Application of steel slag concrete in the foundation slab and basement wall of the Tecnalia kubik building. 6th European Slag Conference Proceedings. Madrid, Euroslag2010. p. 251-64.
- [25] Bosela P, Delatte N, Obratil R, Patel A. Fresh and hardened properties of paving concrete with steel slag aggregate. *Propiedades para firmes del hormigón fabricado con áridos siderúrgicos*. *Revista técnica de la Asociación Española de la Carretera*. 2009;4(166):55-66.
- [26] San-José JT, Vegas I, Arribas I, Marcos I. The performance of steel-making slag concretes in the hardened state. *Mater Des*. 2014;60:612-9.
- [27] Pasetto M, Baldo N. Mix design and performance analysis of asphalt concretes with electric arc furnace slag. *Constr Build Mater*. 2011;25(8):3458-68.

- [28] Pasetto M, Baldo N. Cement bound mixtures with metallurgical slags for road constructions: Mix design and mechanical characterization. *Inzynieria Mineralna*. 2013;14(2):15-20.
- [29] San José JT, Uría A. Escorias de horno de arco eléctrico en mezclas bituminosas. *Arte y Cemento*. 2001;1905:122-5.
- [30] Manso JM, Ortega-López V, Polanco JA, Setién J. The use of ladle furnace slag in soil stabilization. *Constr Build Mater*. 2013;40:126-34.
- [31] Montenegro JM, Celemín-Matachana M, Cañizal J, Setién J. Ladle furnace slag in the construction of embankments: Expansive behavior. *J Mater Civ Eng*. 2013;25(8):972-9.
- [32] Yildirim IZ, Prezzi M. Use of Steel Slag in Subgrade Applications. Publication FWA/IN/JTRP-2009/32 Joint Transportation Research Program. West Lafayette, Indiana . Indiana Department of Transportation and Purdue University; 2009.
- [33] Ortega-López V, Manso JM, Cuesta II, González JJ. The long-term accelerated expansion of various ladle-furnace basic slags and their soil-stabilization applications. *Constr Build Mater*. 2014;68:455-64.
- [34] DePree PJ, Ferry CT. Mitigation of expansive electric Arc furnace slag in Brownfield redevelopment. *GeoCongress 2008: Geosustainability and Geohazard Mitigation*. 178 ed. New Orleans, LA 2008. p. 271-8.
- [35] Frías Rojas M, San-José JT, Vegas I. Árido siderúrgico en hormigones: proceso de envejecimiento y su efecto en compuestos potencialmente expansivos. *Materiales de Construcción*. 2010;60(297):33-46.
- [36] Murphy JN, Meadowcroft TR, Barr PV. Enhancement of the cementitious properties of steelmaking slag. *Can Metall Quart*. 1997;36(5):315-31.
- [37] Papayianni I, Anastasiou E. Optimization of ladle furnace slag for use as a supplementary cementing material. In: editor M, editor. *Measuring, Monitoring and Modeling Concrete Properties*. Konsta-gdoutos Springer; 2006. p. 411-7.
- [38] Patel JP. Broader use of steel slag aggregates in concrete. PhD Thesis Cleveland State University, 2008
- [39] Qasrawi H, Shalabi F, Asi I. Use of low CaO unprocessed steel slag in concrete as fine aggregate. *Constr Build Mater*. 2009;23(2):1118-25.
- [40] Jin R, Chen Q, Soboyejo A. Survey of the current status of sustainable concrete production in the US. *Resour Conserv Recy*. 2015;105:148-59.
- [41] Yildirim IZ, Prezzi M. Geotechnical Properties of Fresh and Aged Basic Oxygen Furnace Steel Slag. *J Mater Civ Eng*. 2015;27 (12): 04015046.


- [42] Arribas I, Santamaría A, Ruiz E, Ortega-López V, Manso JM. Electric arc furnace slag and its use in hydraulic concrete. *Constr Build Mater.* 2015;90:68-79.
- [43] Arribas I, Vegas I, San-José JT, Manso JM. Durability studies on steelmaking slag concretes. *Mater Des.* 2014;63:168-76.
- [44] Manso JM, Gonzalez JJ, Polanco JA. Electric arc furnace slag in concrete. *J Mater Civil Eng.* 2004;16(6):639-45.
- [45] Manso JM, Hernández D, Losañez MM, González JJ. Design and elaboration of concrete mixtures using steelmaking slags. *ACI Mater J.* 2011;108(6):673-81.
- [46] Manso JM, Losañez M, Polanco JA, Gonzalez JJ. Ladle furnace slag in construction. *J Mater Civ Eng.* 2005;17(5):513-8.
- [47] Manso JM, Setién J. Investigación de nuevos usos de las escorias de horno eléctrico de arco (EAF): la oportunidad de los hormigones. *Hormigón y acero.* 2006;241:51-7.
- [48] Polanco JA, Manso JM, Setién J, González JJ. Strength and durability of concrete made with electric steelmaking slag. *ACI Mater J.* 2011;108(2):196-203.
- [49] Rodríguez A, Manso JM, Aragón A, González JJ. Strength and workability of masonry mortars manufactured with ladle furnace slag. *Resour Conserv Recycl.* 2009;53(11):645-51.
- [50] Abu-Eishah SI, El-Dieb AS, Bedir MS. Performance of concrete mixtures made with electric arc furnace (EAF) steel slag aggregate produced in the Arabian Gulf region. *Constr Build Mater.* 2012;34:249-56.
- [51] Pellegrino C, Cavagnis P, Faleschini F, Brunelli K. Properties of concretes with black/oxidizing electric arc furnace slag aggregate. *Cem Concr Compos.* 2013;37(1):232-40.
- [52] Etxeberria M, Pacheco C, Meneses JM, Berridi I. Properties of concrete using metallurgical industrial by-products as aggregates. *Constr Build Mater.* 2010;24(9):1594-600.
- [53] Froněk B, Bosela P, Delatte N. Steel slag aggregate used in portland cement concrete. *Transp Res Rec* 2012. p. 37-42.
- [54] González-Ortega MA, Segura I, Cavalaro SHP, Toralles-Carbonari B, Aguado A, Andrello AC. Radiological protection and mechanical properties of concretes with EAF steel slags. *Constr Build Mater.* 2014;51:432-8.
- [55] Morino K, Iwatsuki E. Utilization of electric arc furnace oxidizing slag. In: Gaballah I, Hager J, Solozabal R, editors. *Minerals, Metals and materials Society/AIME, REWAS'99: Global Symposium on Recycling, Waste Treatment and Clean Technology.* San Sebastian,1999. p. 521-30.

- [56] Morino K, Iwatsuki E. Properties of concrete using electric arc furnace oxidizing slag aggregates. JSCE second international conference on engineering materials. California, USA 2001. p. 269-80.
- [57] Papayianni I, Anastasiou E. Production of high-strength concrete using high volume of industrial by-products. 2010;24(8):1412-7.
- [58] Papayianni I, Anastasiou E. Utilization of Electric Arc Furnace Steel Slags in Concrete Products. 6th European Slag Conference, EUROSLAG pub, 2010. p. 319-34.
- [59] Papayianni I, Anastasiou E. Concrete incorporating highcalcium fly ash and EAF slag aggregates. Mag Concr Res. 2011;63(8):597-604.
- [60] Pellegrino C, Faleschini F. Experimental behavior of reinforced concrete beams with electric arc furnace slag as recycled aggregate. ACI Mater J. 2013;110(2):197-205.
- [61] Pellegrino C, Gaddo V. Mechanical and durability characteristics of concrete containing EAF slag as aggregate. Cement Concrete Comp. 2009;31(9):663-71.
- [62] Qasrawi H. The use of steel slag aggregate to enhance the mechanical properties of recycled aggregate concrete and retain the environment. Constr Build Mater. 2014;54:298-304.
- [63] Tarawneh SA, Gharaibeh ES, Saraireh FM. Effect of using steel slag aggregate on mechanical properties of concrete. Am J Appl Sci. 2014;11(5):700-6.
- [64] Khafaga MA, Fahmy WS, Sherif MA, Hamid AMNA. Properties of high strength concrete containing electric arc furnace steel slag aggregate. J Eng Sci. 2014;42(3):582-608.
- [65] Santamaría A, Rojí E, Skaf M, Marcos I, González JJ. The use of steelmaking slags and fly ash in structural mortars. Constr Build Mater. 2016;106:364-73.
- [66] Anastasiou EK, Papayianni I, Papachristoforou M. Behavior of self compacting concrete containing ladle furnace slag and steel fiber reinforcement. Mater Des. 2014;59:454-60.
- [67] Okamura H. Self-compacting high-performance concrete. Concrete int. 1997;19(7):50-4.
- [68] Celik K, Meral C, Gursel AP, Mehta PK, Horvath A, Monteiro PJ. Mechanical properties, durability, and life-cycle assessment of self-consolidating concrete mixtures made with blended portland cements containing fly ash and limestone powder. Cement Concrete Comp. 2015;56:59-72.
- [69] Nepomuceno MC, Pereira-de-Oliveira L, Lopes S. Methodology for the mix design of self-compacting concrete using different mineral additions in binary blends of powders. Constr Build Mater. 2014;64:82-94.

- [70] Okamura H, Ouchi M. Self-compacting concrete. *J Adv Concr Technol.* 2003;1(1):5-15.
- [71] Jin J, Domone P. Relationships between the fresh properties of SCC and its mortar component. In: Shah SP, Daczko JA, Lingscheit JN, editors. *First North American Conference on the Design and use of Self-Consolidating Concrete*, Center for Advanced Cement-Based materials, 2002. p. 37-8.
- [72] Bonen D, Shah SP. Fresh and hardened properties of self-consolidating concrete. *Prog Struct Eng Mat.* 2005;7(1):14-26.
- [73] Tomasiello S, Felitti M. EAF slag in self-compacting concretes. *Facta universitatis - series: Architecture and Civil Engineering.* 2010;8(1):13-21.
- [74] Sheen Y-N, Le D-H, Sun T-H. Innovative usages of stainless steel slags in developing self-compacting concrete. *Constr Build Mater.* 2015;101:268-76.
- [75] The Self-Compacting European Project Group. *The European guidelines for self-compacting concrete: specification, production and use.* 2002.
- [76] NLT standars. Transport Laboratory. Ministerio de Fomento, Spain.
- [77] *Annual Book of ASTM Standars*, ASTM International, West Conshohocken, 19429-2959. PA, USA, 2008.
- [78] Suzuki T, Ogata H, Takada R, Aoki M, Ohtsu M. Use of acoustic emission and X-ray computed tomography for damage evaluation of freeze-thawed concrete. *Constr Build Mater.* 2010;24(12):2347-52.



Chapter 5:  
*Manufacture and  
Performance of Concrete Mixes*





# 5

## *Manufacture and performance of concrete mixes*

### **5.1. Introduction**

Concrete is basically a mixture of coarse aggregates, sand, water and cement. In this chapter the manufacture and the performance of different pumpable and self-compacting concrete mixes are described. The chapter is divided into two more main sections.

The second section of this chapter consists of a discussion on the most suitable mix design for the manufacture of self-compacting concretes. Meeting the requirements for self-compactability has not been an easy challenge. The normal considerations are not useful when mixing self-compacting concrete with electric arc furnace slag as aggregate, due to the higher density and rougher shape of this aggregate, which have to be accounted for. An in-depth analysis of the fresh properties of the mixes that were obtained is included, followed by the analysis of their mechanical and physical properties.

In the third section of the chapter, the extensive testing for durability which was carried out on the concretes described in the previous section is presented. The behavior of the mixes manufactured in the former section was studied after they were subjected to freezing-thawing cycles, wetting-drying cycles, exposure to a marine environment and corrosion of reinforcement bar at marine environment. The results obtained are really promising.



## **5.2. Self-compacting concrete incorporating electric arc-furnace steelmaking slag as aggregate**

*Materials and Design 115 (2017) 179–193*



## **Abstract**

Electric arc-furnace slag (EAFS) is an industrial by-product that can be employed in hydraulic mixes used in the field of construction and civil engineering. The design and preparation of self-compacting mixes with this aggregate is a challenge, due to the loss of workability that always accompanies its use in concrete. Only through careful design of the characteristics and proportions of the components in each mixture will an acceptable workability be achieved. Thus, criteria and methods are proposed in this paper for successful preparation of these types of mixtures. Several concrete mixes are manufactured to obtain self-compaction characteristics and their main properties are analyzed with regard to their use as structural concrete. Electron microscopy observations and dispersive energy analysis are used to study the microstructural features of these mixes. Finally, a numerical simulation is proposed as a useful method that estimates the viscous properties of the mixes and their workability, based on the dosage and the characteristics of their components.

## Introduction

Over some decades, sustainability has evidently come to form part of the main objectives in scientific research. Attention has focused on the sustainable aspects of employing steelmaking slags [1-8]. The re-use of ironmaking and steelmaking slags as promising and good quality materials has been studied in copious technical and scientific publications from research groups around the world. [9-15].

Ironmaking and steelmaking slags have demonstrable and direct results in sectors such as construction and agriculture. Both sectors are large-scale consumers of raw materials, so substitution of their raw materials for waste products from any other industrial sector, including steelmaking, could represent an important advance in relation to the issue of sustainability that is a high priority in the EU [16-28].

The steelmaking industry produces several types of slags. Interest is predominantly focused on the slags that are produced in large volumes. The most abundant in the EU are blast furnace slags, followed by oxygen-converter slag and then Electric Arc-Furnace slag (EAFS). The last-mentioned slag is preponderant in the northern region of Spain, where this research was conducted, and it forms the object of this work. More than a century ago, ground granulated blast furnace slag was found to demonstrate advantageous qualities when added to concrete exposed to maritime conditions. Hence, the hydraulic mixes used in construction and building can be considered suitable candidates to incorporate large amounts of steelmaking slags. In this way, a deep knowledge of the types, characteristics and proprieties of these materials is an indispensable objective that researchers diligently continue to pursue.

The most common hazard associated with the use of steelmaking slags in any application is that some of them are expansive materials [29-34], containing non-stable compounds, that represent unpredictable risks over the medium term (months, years) in the design and performance of engineering constructions. This problem of expansive behavior is widely studied and discussed in the scientific field and present-day knowledge of the problem means that, in most cases, it can be controlled.

Good quality mortars and concretes have been prepared by several research teams around the world using EAFS aggregates. The feasibility of these mixes has been demonstrated as having suitable performance levels and durability, resulting in competitive materials. The main drawbacks have been their poorer workability and their higher density than conventional mixes, made using natural aggregates. The



solution to the high-density problem is resolvable by affordable increases in material strength, while keeping the strength-to-density ratio at the same values as conventional concrete [35-42]. The second problem, poor workability, can be analyzed, approached and almost solved by focusing investigative work on suitable chemical admixtures for the preparation of high-workability mixes [43-54].

Self-compacting mortar and concrete (described as self-consolidating mixtures by Mehta and Monteiro book) [4] are undoubtedly the most challenging. Largely under their own weight, these mixes can be adequately poured into moulds and formwork in which the reinforcing steel (ribbed bars or rebars) are distributed. Their viscosity and their internal cohesion have to meet particular conditions, even though, at the outset, their properties might appear contradictory [55-59].

The preparation of SCC (Self-Compacting Concrete) mixes with conventional natural aggregates must keep to well-established rules. The use of heavy and sharp aggregates (natural or artificial) complicate the task, due to the appearance of excessive cohesiveness and the risk of segregation and decantation of the coarse aggregate particles suspended in the cementitious matrix [60, 61]. Hence, the subject of this investigation is self-compacting structural concrete mixes, which our research team has successfully prepared.

### *Self-Compacting Concrete*

Three decades ago, Okamura [55, 56] showed how to design a self-compacting concrete, which we may now consider the “classical” solution. This methodology is, in general, useful for the preparation of self-compacting mixtures using natural aggregates, limestone, and sandstone, with densities of below  $2.7 \text{ Mg/m}^3$ . The fundamentals are simple: water (density 1.0) transports fine particles sizes of under 0.15 mm (cement, natural rocks) of higher density (i.e. density 3.0 and 2.6) due to their small size; the resulting paste combines with fine aggregate particles (density 2.6, maximum size of 5 mm) and the resulting “mortar” then incorporates larger-sized aggregate particles (same density, with a maximum size of 20 mm) constituting the self-consolidating concrete.

EFNARC recommendations [62] provide guidance (concerning slump flow, viscosity, passing ability, and segregation resistance) to prepare several types and classes of Self-Compacting Concrete, according to the properties required in each particular case, using conventional aggregates. In this guide the typical proportions used for

manufacturing self-compacting concrete with natural aggregates (Table 1) are also specified. These proportions will be useful for comparison with the final amounts used in this research to perform SCC mixes with EAFS as aggregates.

Constituent	Typical range by weight [kg/m <sup>3</sup> ]	Typical range by volume [l/m <sup>3</sup> ]
<b>Powder</b>	380 – 600	
<b>Paste</b>		300 – 380
<b>Water</b>	150 – 210	150 – 210
<b>Coarse aggregate</b>	750 – 1000	270 – 360
<b>Fine aggregate (sand)</b>	Content balances the volume of the other constituents, typically 48-55% of total aggregate weight	
<b>Water/Powder ratio (by volume)</b>		0.85 – 1.10

**Table 1:** EFNARC SCC [62] recommendations specifying guideline values for SCC.

According to the EFNARC document on viscosity modifying admixtures (VMA) for concrete [63], the rheology of fresh concrete can be characterized by its yield point and plastic viscosity in a Bingham viscous model:

- The yield point (cohesion) describes the shear stress needed to start the concrete moving. It may be assessed by practices such as the slump test.
- Plastic viscosity describes concrete resistance to flow under external stress. The speed of flow is related to the plastic viscosity of the mix.

The balance between the yield point and plastic viscosity is key to obtaining an appropriate concrete rheology. Viscosity modifier admixtures change the rheological properties of concrete, by increasing plastic viscosity, but usually only cause a small increase in the yield point. Admixtures known as plasticizers decrease the yield point and are often used in conjunction with a VMA for their optimization.

The characteristics and requirements of the EFNARC SCC guidelines [62] are shown in Table 2. Clearly, the initial requirements for concretes manufactured in this work are minimal, i.e. slump-flow SF1, viscosity class VF2, L-box PA1, and segregation resistance class SR1.

Characteristic	Preferred test metho(s)	Specification	Classes	Values
Flowability	Slump-flow test	Slump-flow in mm	SF1	550 to 650 mm
			SF2	660 to 750 mm
			SF3	760 to 850 mm
Viscosity (rate of flow)	T <sub>500</sub> slump-flow test, or V-funnel test	T <sub>500</sub> , in s, or V-funnel time in s	VS1/ VF1	≤ 2 / ≤ 8 s
			VS2/ VF2	> 2 / 9 to 25 s
Passing ability	L-box test	Passing ability	PA1	≥ 0,80 with 2 rebars
			PA2	≥ 0,80 with 3 rebars
Segregation	Segregation resistance (sieve) test	Segregation resistance in %	SR1	≤ 20 %
			SR2	≤ 15 %

**Table 2:** EFNARC prescriptions [62]

According to this EFNARC document, there are three classifications of self-compacting concrete:

- The powder type of SCC is characterized by large amounts of powder (all material < 0.15 mm), usually within the range of 550 to 650 kg/m<sup>3</sup>. This provides the plastic viscosity and hence the segregation resistance. The yield point is determined by the addition of superplasticizer.
- In the viscosity type of SCC the powder content is lower (350 to 450 kg/m<sup>3</sup>). The segregation resistance is mainly controlled by a VMA and the yield point by the addition of superplasticizer.
- In the combination type of SCC the powder content is between 450 to 550 kg/m<sup>3</sup>, but the rheology is also controlled by a VMA and an appropriate dose of superplasticizer.

In these recommendations, an ASTM N° 100 (0.15 mm) sieve [64] is stipulated as the limit size of “powder” in self-compacting mixes, and its amounts are specified within some limits. The aforementioned value is left aside in our investigation that uses EAFS as aggregate and substituted by the concept “bearing paste”; the upper limit particle size for “bearing paste” in self-compacting mortar has proved to be 0.6 mm (sieve N° 30). In the present work that describes EAFS self-compacting concrete, this “bearing paste maximum value of particle size” was increased to 1.18 mm (N° 16 sieve); additionally, appropriate admixtures (viscosity modifier, plasticizer...) must also be used to obtain suitable characteristics for self-consolidating mixes.

In the present article, the EAFS concrete with characteristics close to those of a self-compacting mix could be classified as “the powder type” or “the combination type” in the EFNARC classification [62], because the intention in this research is to prepare a mixture that is suitable in terms of plastic viscosity and segregation resistance.

## Research background

Taking the above considerations into account, the challenge is to prepare a hydraulic mix with a suitable in-fresh rheology that may be considered a self-compacting concrete. Additionally, this goal should be attained using materials currently available in the field of construction and building: commercial cement and natural aggregates from the region, added to electric arc furnace slags aggregates from nearby steelmaking factories.

When the aggregates (fine, coarse) are denser than usual ( $>2.8 \text{ Mg/m}^3$ ), i.e. quartzite, granite or basalt, the recommended proportions in the guidelines for SCC mixes should be slightly corrected; finally, if the aggregate is especially heavier, rougher and sharper as in the case of the EAF slag, the innovative solutions that we describe in this paper are needed.

It is well-known that liquids have the capacity to keep in suspension for a long time and to transport solid particles of greater density dispersed within them, thereby preventing their decantation-deposition at lower layers. Stokes' Law,  $R = 6\pi\mu r v$ , allows us to calculate the decantation velocity,  $v$ , (or relative velocity) of spherical solid particles in a static liquid mass in a laminar flow regime, regardless of the interaction at the liquid-solid interface (surface tension, hydrophilia-hydrophobia). This drag force,  $R$ , will be in equilibrium with the resulting gravitational force, i.e. the submerged weight (based on the difference in densities between the solid pieces and the liquid mass) of the particles. The variables for consideration are the viscosity of the liquid mass  $\mu$  and the radius  $r$  (size) of the coarse particles.

As with Stokes's Law, it also appears evident that the ratio between external surface extension and the weight of rounded particles is the main variable to consider: the lower this value, the stronger the drag. In the case of spheres, this quotient is  $3/\rho \cdot r$ , inversely proportional to the radius,  $r$ , of the particle and to its specific density,  $\rho$ . According to the evidence from these empirical observations, we can state that it is easier to transport solid particles of both a moderate density (compared to the density of the liquid mass) and of a lower size in a moving viscous liquid.

There are experimental hydrodynamic laws in the literature, for example see Graf Walter Hans[65], which estimate the transport capacity of liquid masses in movement. Those laws clearly state that the transport capacity of liquid masses is enhanced when the velocity of their movement is increasing. The problem is not trivial in terms of empirical calculations, if we take into account that the velocity of movement of spreading concrete is always moderate, due to its high viscosity and low acting forces (its own weight), and if we consider the other characteristics of the particles to be transported (heavy, rough, sharp).

The quantity of coarse particles to be transported (volumetric amount) is also a key variable, because of the interaction between these particles during transport; if the amount is excessive their transport is increasingly difficult and, finally blocked, due to coarse particle migration and the associated “bridging” effect. Additionally, when we have a liquid (originally water in our case), in which we have a wide range of particle sizes in suspension, their influence on the viscosity and on the apparent density of the fluid mass is evident. In this case, an analysis of the drag and the transport of the coarser particles should consider the presence of suspended finer (smaller) particles and even their hydrophilic-hydrophobic character. Thus, a precise grading should be established for the smaller suspended particles, so that they work together in an active way in the transport of the coarser particles, as a “bearing paste”.

According to the recommendations of EFNARC contained in Table 1 of the former section, a well-prepared SCC of conventional (density  $2.6 \text{ Mg/m}^3$ ) aggregates, with a maximum aggregate size of  $\frac{3}{4}$ " (19 mm), could be formulated per cubic meter in the following way: paste 360 l (water 180 l plus powder smaller than N<sup>o</sup> 100-0.15 mm 180 l), cement 300 kg, coarse aggregate 340 l, fine aggregate 380 l; density of aggregates  $2.6 \text{ Mg/m}^3$ , and fractions smaller than 0.15 mm, amounting to 12% of the total aggregate. According to those data, we have a well-prepared SCC containing 340 l (885 kg) of coarse aggregate transported by 360 l of paste, which has a density of  $180+300+(80 \times 2.6) \text{ kg}$  in 360 l, resulting in  $1.9 \text{ Mg/m}^3$ . In other words, a certain volume of paste (bearing paste) transports a slightly lower volume of coarse aggregate of a size no larger than 19 mm, with densities that differs in the order of 0.7 units. The rest of the fine aggregate, 300 l of conventional aggregate sized under 4.75 mm (380 l minus 80 l included in the paste), is less significant because of its small size, which facilitates its easy transport. These volumetric proportions are very significant in the preparation of self-compacting mixes, and we will use them in our calculations as our “reference mixes”.

Thixotropy is a property defined in the EFNARC SCC guidelines [63] as: “The tendency of a material to progressive loss of fluidity when allowed to rest undisturbed but to regain its fluidity when energy is applied”. Usually, this definition refers to a pure fluid-liquid material, but it can also be applied to a composite material such as a concrete with a fluid paste-matrix composed of water and finer particles in suspension. This property is really useful in engineering practice, because it helps to avoid the segregation of heavy-coarse aggregates in concrete when the mass is in a static situation (after pouring into molds, until its initial setting), but it obviously compels us to evaluate the spread characteristics of the mix and to pour the concrete after the shortest possible time following the dynamic mixing of the raw materials. In real terms, the pouring of SCC concrete into a big mold is slow, and the initial characteristics of mass fluidity will differ from its ultimate fluidity during the final phases of pouring.

## **Materials and methods**

### *Cement, water and natural aggregates*

Two types of cement were used in the present research: first, a Portland cement type I 52.5 R; second, a Portland cement type IV/B-V 32.5-N; both in accordance with UNE-EN 197-1 standard. The type I cement includes 90% Portland clinker, 5% calcium carbonate powder fines and 5% gypsum. The composition by weight of the type IV cement includes 5% calcium carbonate powder fines, 40% fly ash type I, 50% Portland clinker, and 4% gypsum. Water was taken from the urban mains supply of the city of Bilbao, containing no compounds that could affect the hydraulic mixes.

A commercial crushed natural limestone qualified as fine aggregate (maximum size 4.75 mm, fineness modulus 2.9 units, bulk density 2.6 Mg/m<sup>3</sup>) and medium-size aggregate (sized 5-12 mm, fineness modulus 6 units) was used partially or totally in the mixes; the main mineral component of these aggregates was calcite (95%) and can be considered a classical or conventional component of concrete. The same material was also used in the mixes after sieving through 0-0.6 mm and 0-1.18 mm sieve ranges (passing through ASTM [64] sieves N<sup>o</sup> 30 and N<sup>o</sup> 16), the fineness moduli of which were 0.7 and 1.5 units, respectively. The grading of all the above-mentioned fractions is shown in Figure 1.

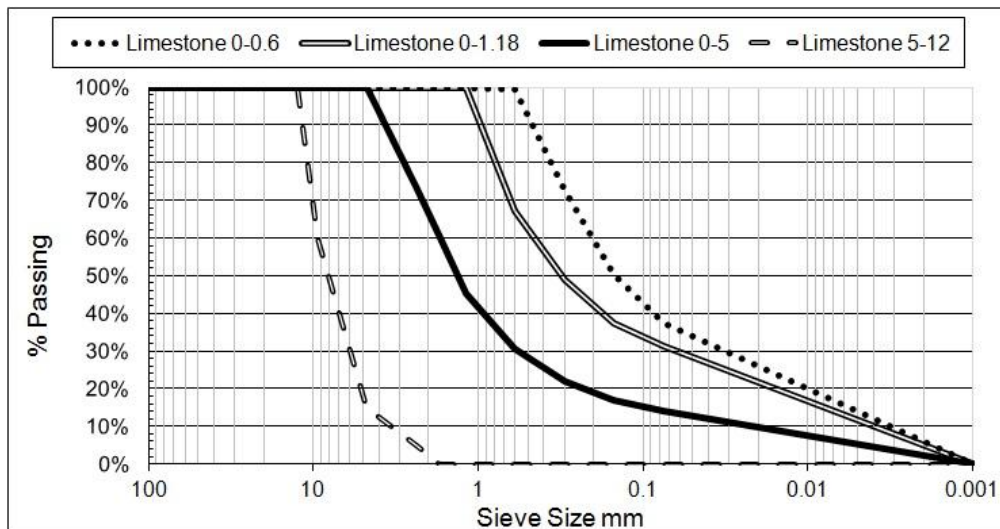


**Figure 1:** Grading of natural aggregates.

### Slags

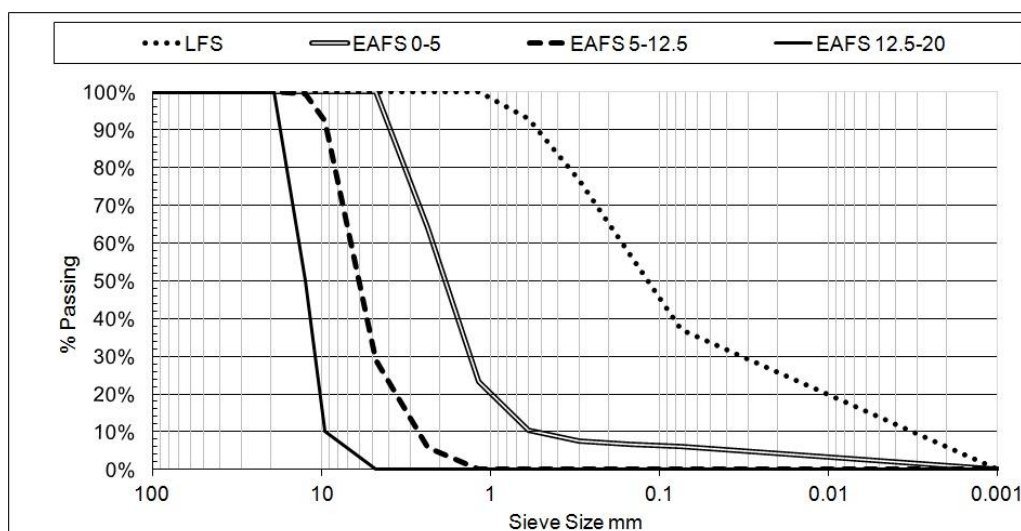
Crushed Electric Arc-Furnace slag (EAFS) in three size fractions (fine <4.75 mm, medium <12.5 mm, and coarse <20 mm with specific gravity  $3.42 \text{ Mg/m}^3$ ), supplied by the company Hormor-Zestoa, was used in this research. The chemical composition and some physical properties are detailed in Table 3. Their grading is shown in Figure 2.

An additional high-silica low-alumina ladle furnace slag (LFS) was used in this work. It has a density of  $3.03 \text{ Mg/m}^3$  and a fineness modulus of 0.75 units. Its chemical composition and X-ray diffraction analysis in Table 3 shows that its main compound was dicalcium silicate (olivine); see also its grading in Figure 2. A fraction of the total amount of LFS added to the hydraulic mixes could show binder properties such as supplementary cementing material (SCM), as suggested in [39, 66]; the rest of the LFS can be considered as an additional fine aggregate fraction.

Some earlier works by the authors [35, 66] contain more detailed descriptions of these kinds of slag; their main characteristics are considered indispensable for a full understanding of the mixes that are presented in the present article.

Compounds [%-wt]	EAFS (0-5 mm)	LFS
Fe <sub>2</sub> O <sub>3</sub>	22.3	1.0
CaO	32.9	59.2
SiO <sub>2</sub>	20.3	21.3
Al <sub>2</sub> O <sub>3</sub>	12.2	8.3
MgO	3.0	7.9
MnO	5.1	0.26
SO <sub>3</sub>	0.42	1.39
Cr <sub>2</sub> O <sub>3</sub>	2.0	--
P <sub>2</sub> O <sub>5</sub>	0.5	--
TiO <sub>2</sub>	0.8	0.17
Loss on ignition	gain	0.5
Water absorption	1.12	--
Specific gravity [Mg/m <sup>3</sup> ]	3.42	3.03
X-ray diffraction main compounds	Wustite-Ghelenite Kirsteinite	Periclase-Olivine Mayenite

**Table 3:** Chemical composition and physical characteristics of slags





compaction conditions. The performance of some of them is not considered a self-compacting mix according to the specifications of the EFNARC [62], so they were considered as “pumpable” concretes that are also very useful in structural engineering. The high workability mixes obtained in this work were qualified as self-consolidating mixes or self-compacting concrete.

The most important objective in this study is to establish a global dosage in the aggregates mixture to reach the conditions of self-compacting mixes, including the additional condition of including the highest amount of EAF slag. It is evident that the inclusion of very small amounts of EAFS obtains an SCC in a relatively easy way; conversely, an excessive amount of EAFS makes that objective impossible. The global proportion of EAFS (of any size) by volume described for self-compacting mortars in a recent work by the authors of this study was around 35%; this value is an initial reference for the new concretes, but it could eventually be modified in accordance with the optimization of mixes.

The cement content was fixed in the range 300-350 kg per cubic meter of concrete; it is evident that the strength of these mixtures is not High-Strength-Concrete (HSC), which is unnecessary for most structural elements. Also, the contents of water and admixtures were considered consequences of the proposed targets, to obtain pumpable or self-compacting mixes; the water content had to be kept to amounts slightly lower than 200 kg per cubic meter. The recommendations from the manufacturers of the admixtures were observed, although the proportions were close to or slightly higher than the recommended maximum amounts.

At this point in the design of these mixes, the authors stated that a new “bearing paste” can be defined as the combination of water, cement and aggregate fine fractions, the sizes of which range from zero to a fixed value. This value was fixed at 0.6 mm in the structural mortars that have previously been analyzed by authors; while it was 1.18 mm in concrete mixes with a maximum aggregate size of 12 and 20 mm. The fixed value is easily recognizable as the “shoulder” of the mix grading curve as is shown below.

The simplest approach to obtaining a “bearing paste”, capable of transporting medium and coarse EAFS aggregates with a density of  $3.4 \text{ Mg/m}^3$ , could be to increase paste density to values close to  $2.7 \text{ Mg/m}^3$  ( $3.4$  minus  $0.7$  units), as was cited in the former section for SCC made with normal aggregates. But this idea is in practice unfeasible, because the components are always the same in this cementitious matrix (water,

cement and mineral particles) and their proportions always similar (ratio water-cement-fines), accepting low variations. So, this bearing paste density will be considered an almost constant value close to  $1.9 \text{ Mg/m}^3$ , which cannot be efficiently increased. It is therefore compulsory to modify (enhance) the rheological characteristics of this bearing paste. The choice of increasing the amount of fine particles in the mix design of EAF concretes has been explored in some research works reported in the literature, as a resource to improve workability. In our mixes, the most affordable solution was to increase the amount and the size range of mineral particles from 0-0.15 mm (the original size limit for the paste in the EFNARC recommendations [62]) to 0-0.6 in mortars, or even to 0-1.2 mm for concrete, and to consider these amounts of particles as a part of the new “bearing paste”; its resultant rheology has changed with respect to a “conventional paste” of a standardized self-compacting concrete, and showed an acceptable drag coefficient of 1.2-1.3 units, a coefficient that represents the difference in densities between the bearing paste and the transported coarse pieces, bring our value suitable to transport pieces of heavier EAFS aggregate.

The internal composition of this bearing paste, in terms of its size grading and proportion of components, its proportion in relation to total concrete volume, and the global proportion of EAFS aggregate particles that form part of the SCC concrete, are the variables that have to be fixed through detailed experiments and the corresponding testing of the resultant properties. In this task, the collaboration of the “super-plasticizer” admixture is decisive, and a good choice is essential; however, it would be erroneous to see this component as the principle key to SCC manufacture. At this point, it should be said that not all super-plasticizers on the market are compatible with all types of aggregates; finding a suitable admixture for our purposes in the case of the EAFS aggregate was no easy task. Over thirty mixtures were prepared and tested in this investigation, although only the most significant are presented in the following section.

#### *Preparation of mixes*

EAF slag sized 0-5 mm was used as part of the fine aggregate in mixes, but its presence in the bearing paste was less significant, due to its low proportion of fines smaller than 1.18 mm in its grading (about 20%, see figure 2). The fine fraction of the mixture was increased with the addition of a significant amount of crushed limestone sized 0-1.18 mm, as mentioned in the former section. The coarse aggregate was EAF slag medium-gravel sized 5-12 mm; EAF gravel sized 12-20 mm was also used in one mixture. The EAFS aggregates were added in an almost-saturated “sprinkled” state, taking into

account their outstanding capacity to absorb water. It is very difficult to fix a relevant value for this characteristic, which largely depends on the foundry parameters for heat at each stage of the steelmaking process. From an engineering point of view (during the construction of real structures), it is almost impossible to control the actual porosity and the water absorption properties of each EAF slag batch in a “practical” and consistent way, and its use in a saturated state gives a simple solution to this problem.

The water-cement ratio was kept close to 0.6 in the mixes. The cement was mainly type I 52,5R, and in one case a type IV cement was also used; the amount used was in the range of 300 to 350 kg per cubic meter, seeking to obtain a compressive strength of 40 MPa after 28 days, and 50 MPa after 90 days. Plasticizer and viscosity conditioner admixtures were used in these mixtures in the recommended proportions by the manufacturer.

Another important condition in the design of mixes was the proportion of fines (smaller than 0.15 mm, sieve N<sup>o</sup> 100), which was kept slightly below 20% by volume in these SCC mixes. A very large amount is indispensable in a self-compacting mix, but their excessive presence could lead to an increase in water demand and eventual bleeding. The Spanish standard EHE-08 specifies a maximum content of these fines in 100 liter per cubic meter for general purpose concrete; in the case of SSC, this amount is unspecified in the standard and, in our experience, may be raised by 20%.

In Table 4, nine of these research mixes are detailed in their composition, and some fresh properties (density, workability) are also shown in the last rows. These nine mixes were chosen from previously manufactured lots, on account of their relevance. They reveal the successive steps followed in this study to find a suitable SCC containing EAFS as coarse aggregate. The first set of columns, P 1-5, corresponds to pumpable concretes, and the second set, SC 1-4, are self-compacting concretes. From an engineering standpoint, it would be helpful to remember that a maximum aggregate size of 12.5 mm ( $\frac{1}{2}$ " ) is suitable for use in concrete elements reinforced with steel bars, such as beams and floor framing; in other structural elements with fewer rebar reinforcements, such as columns and ground slabs, a maximum aggregate size of 20 mm ( $\frac{3}{4}$ " ) is recommended. Both maximum sizes are analyzed in this study, so as not to overlook practical engineering aspects.

Mix Design [kg/m <sup>3</sup> ]		P1	P2	P3	P4	P5	SC1	SC2	SC3	SC4
CEM I 52.5 R		300	300	350	350	350	350	350	210(*)	350
Fly ash									140	
Limestone	Sieved fraction <0.6 mm		760	760						
	Sieved fraction <1.2 mm				450	680	680	900	900	900
	Fine aggregate <5 mm	1050					550			
	Medium aggregate 5-12 mm						720			
LFS			80							
EAFS	<5 mm		550	735	800	700		550	550	450
	5-12 mm	1050	750	735	1050	900		670	670	420
	12-20 mm									420
w/b		0.53	0.66	0.5	0.51	0.51	0.51	0.55	0.55	0.5
Superplastizicer [%]		2	2	1.47	2.5	1.82	2.5	2	2	2
Fresh density [Mg/m <sup>3</sup> ]		2.6	2.65	2.78	2.84	2.75	2.46	2.62	2.75	2.87
Slump/Spread in Abrams cone [mm]		160/	180/	190/	180/	220/450	/580	/680	/560	/520

**Table 4:** Mix designs

Referring to pumpable concretes, P1 to P5, they all contain coarse aggregate EAFS sized between 5 and 12 mm; the first shows a fine aggregate formed only of limestone. Compared to the Fuller's curve, Figure 3, a slightly low proportion of particles sized between 0.075 mm and 1mm is evident in this P1 mix, but it is useful as a reference mix for pumpable concretes. Perhaps an increase in the limestone fine aggregate produces a better global grading size, but our objective is to use the highest possible amount of EAFS, for which there are better options, as will be shown.

Mixtures described in column 2 to 5 of Table 4 show fine aggregate fraction (smaller than 5 mm) mixed between limestone (of several maximum sizes) and EAFS, in a progressive search for the ideal proportions. In Figure 3, the grading of these mixes by volume is shown to be close to Fuller's curve; the amount of aggregate fines smaller than 0.15 mm is visible in each curve, and a reference value could be 14%. Mixture P2 includes ladle furnace slag LFS, the influence of which is not positive for the workability, due to its high absorption. The fifth mixture of this set, P5, is the best-performing mixture face to workability, having 50% by volume of EAFS (density 3.4

units) and about 55% of “bearing paste” (cement, water and mineral fraction smaller than 1.2 mm), which contains 20% fines, mainly limestone and cement.

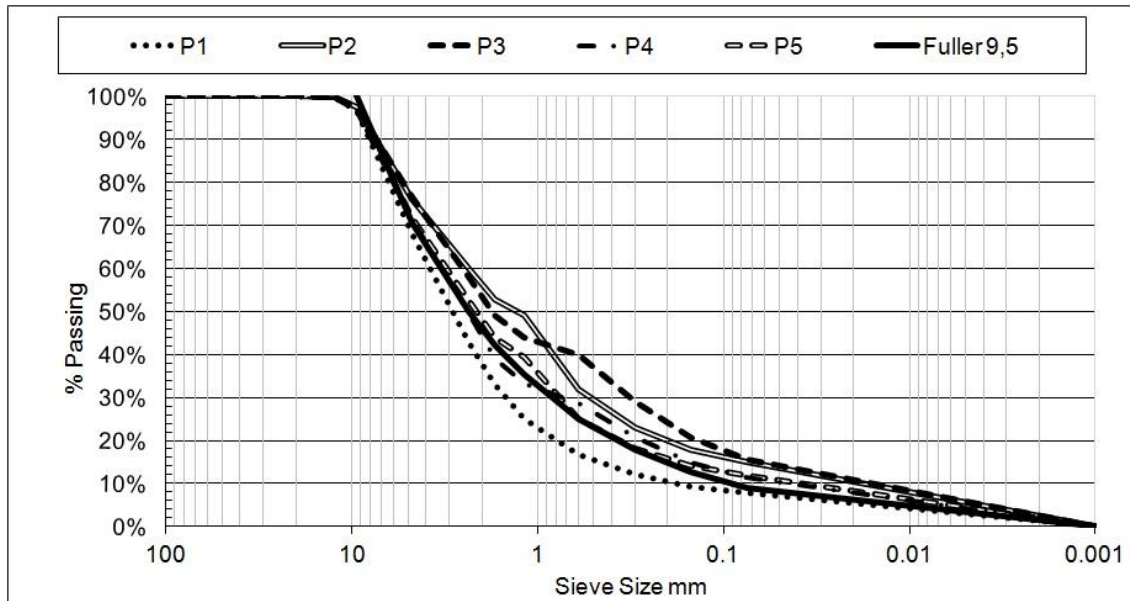


**Figure 3:** Grading of pumpable mixes in volume.

As regards the SCC mixes, the first reference concrete SC1 only contained limestone aggregates, and it easily reached the in-fresh conditions for SCC; it had a content of almost 20% in fine fraction aggregate particles under 0.15 mm. The water-to-paste ratio (<0.15 mm) in the fresh state yielded a result of around 0.46 (195 divided by  $195+(300/3.1)+(40\% \cdot 680/2.6)+(16\% \cdot 500/2.6)$ ). Fuller’s curve with a maximum size of 12.5 mm with this dosage is shown in Figure 4.

SC2 is certainly an excellent and probably an exemplary self-compacting mix, and SC3 was manufactured in a similar way to SC2, using cement type IV containing fly ash; the visible effect was a loss of workability (due to a poor interaction between the admixture used and the fly ash) with respect to SC2. The self-compaction characteristics of the SC4 mix were not very good although it can be also considered a self-compacting mixture (slump over 500 mm). Considering the amount of aggregate particle sizes smaller than 0.15 mm, mainly limestone and cement, mixes SC2, SC3 and SC4 all showed a value close to 20%. Their in-fresh water to paste ratio was around 0.44 units.

Figure 4 shows the size grading in volume of these mixtures, and two versions of Fuller’s curve are included, so as to compare all the SC mixtures, corresponding to maximum aggregate sizes  $\frac{3}{8}$ ” (9.5 mm) and  $\frac{3}{4}$ ” (19 mm). The aforementioned “shoulder” (referring to Fuller’s curve) is easily appreciated in the abscissa 1.18 mm.

The amount by volume of EAFS aggregate at 34% was similar in the SC mixes; in these cases the “bearing paste” content is close to 66% (two-thirds) in fresh volume.

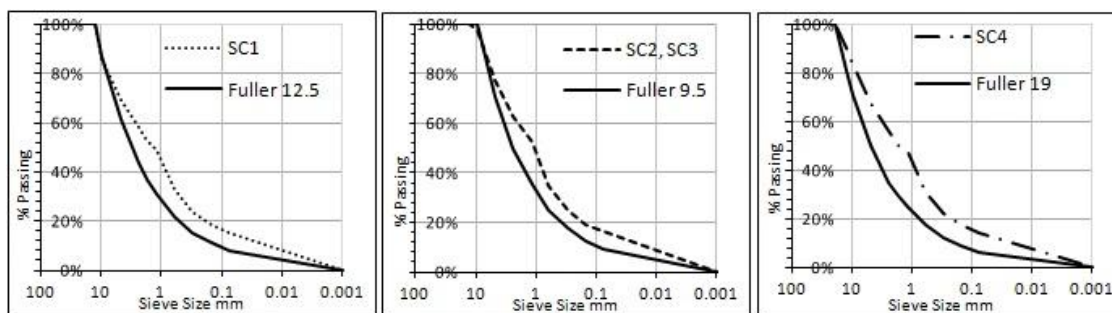
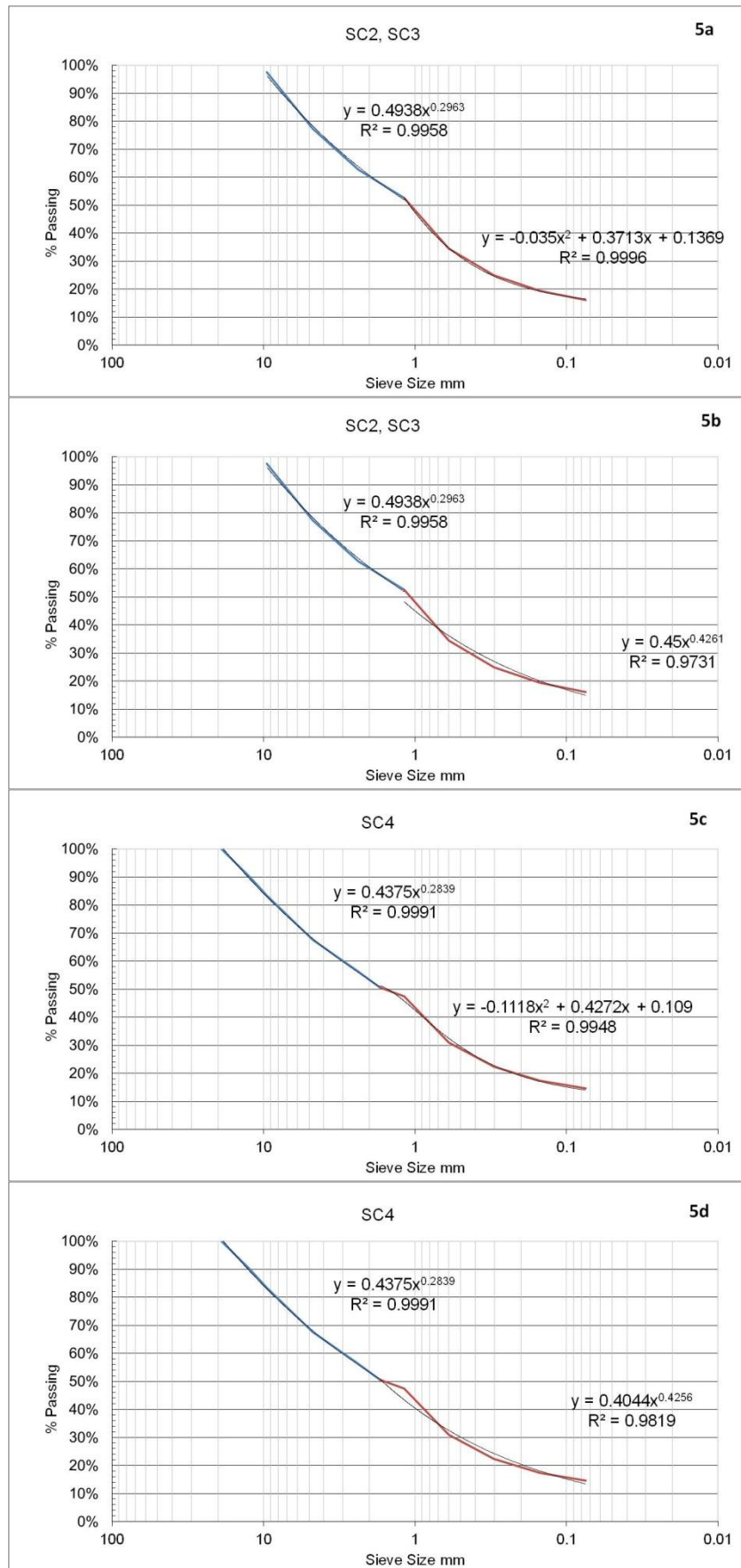


**Figure 4:** Grading of self-compacting mixes by volume.

Some equations could be proposed for the volumetric grading curve of the EAFS self-compacting mixes, shown in Figures 5a, 5b, 5c and 5d. The whole curve is composed of two monotonic regions separated by a shoulder. The first (the larger sizes) approximately corresponds to a variation in the exponent of Fuller’s equation; the original Fuller exponent for round particles is  $n=0.5$  (square root) and, in this special case of SCC, the adjusted exponent is close to  $n=0.3$  (SC2 and SC3 almost cube root).

The second monotonic curve (from the shoulder to smaller sizes) could be adjusted by a potential function (Figures 5b 5d) similar to Fuller’s equation, or by a polynomial function (Figure 5a 5c). The polynomial adjustment is very precise (almost a straight line in a linear scale), but may not be extended to sizes under the ASTM N° 250 [64] sieve (0.063 mm). The potential adjustment is less precise, but it is useful down to very low sizes. It should be remembered that we are using a commercial limestone fine aggregate (subsequently passed through a N° 16 ASTM [64] sieve), the grading (see Figure 1) of which is acceptable and is adjusted to Fuller’s curve. However, it is evident that other commercial products of this kind could give slightly different grading characteristics and, in consequence, could generate different coefficients when employed, requiring similar adjustments.



Figures 5a 5b 5c 5d: coefficient adjustments.

## In-fresh characterization and rheological behavior

The in-fresh rheological characteristics of the self-compacting mixes are shown in Table 5. Among the three EAFS mixes (SC2 SC3, and SC4), the first shows very good properties of self-compaction (show Figure 6). The second, SC3, includes fly-ash in partial substitution of clinker; the loss of workability is evident, though it meets the minimal characteristics to be considered as SCC. The third, SC4, includes EAFS sized until 20 mm; its self-compaction performance is poor. The EAFS mixes neither showed evidence of segregation nor of blocking.

Mixture	Slump-flow in mm	Passing ability L-box
SC1	580 (SF1 class)	0.85 (PA2 class)
SC2	680 (SF2 class)	0.9 (PA2 class)
SC3	560 (SF1 class)	0.8 (PA2 class)
SC4	520 (SF1 class)	0.35 (2 rebar)

**Table 5:** Flowability characteristics of mixes



**Figure 6:** SC2 Slump cone

Computational Fluid Dynamics (CFD) techniques were applied, in order to establish a relation between the performance of the different concrete batches and their rheological parameters. In this case, an Eulerian multiphase simulation was performed. Among the several available methods, the Volume of Fluid (VOF) approach has been adopted. This method has proven suitable to simulate concrete flow [67, 68].



The constitutive stress-deformation equation of the selected viscoplastic material corresponded to the Bingham plastic model. Its equation,  $\tau = \tau_0 + \mu \cdot \dot{\gamma}$ , will predict the behavior of the concrete mass when the shear stress,  $|\tau|$ , is higher than the yield stress,  $\tau_0$ . If the threshold value is not exceeded, the shear rate,  $|\dot{\gamma}|$ , is null, and the mass behaves as a solid with little or no flow. The dynamic viscosity is denoted by  $\mu$ . Although other authors [69, 70] state that concrete flow is governed by a non-Newtonian generalized power law, such as the Herschel-Bulkley fluid with three unknown variables (consistency, flow index, yield shear stress), the consistency factor (K) and the power-law index (n) of that model are not easily determined. The Bingham model can lead to negative yield stresses, which are physically impossible, but since the aim of the study was to design a SCC with the highest amount of EAF slag, a not excessively flowable SCC was expected, avoiding the mentioned drawback. Moreover, in contrast, the Herschel-Bulkley model tends to overestimate the yield stress. It can be assumed that for standard quality control tests to be performed, where the flow time and flow distance are moderate and also the shear rate, the proposed Bingham model [71] is sufficiently accurate. The main difference between both models arise for high shear rates, i.e.: concrete pumping, etc, while the simulated tests depend only on the concrete mass weight. Once the mix with the best performance is selected, further studies will fine-tune the mix design according to the Herschel-Bulkley model, if necessary, to promote its commercial use on the market.

As shown in Figures 7a, 7b and 7c, the Abrams cone slump-spread flow test [72], the V-funnel test [72] and the L-Box test [72] were simulated for the four concrete mixes. The estimated rheological parameters, as a result of the computational modeling, were set to fulfill the requirements of the real tests that were performed (see Table 5).

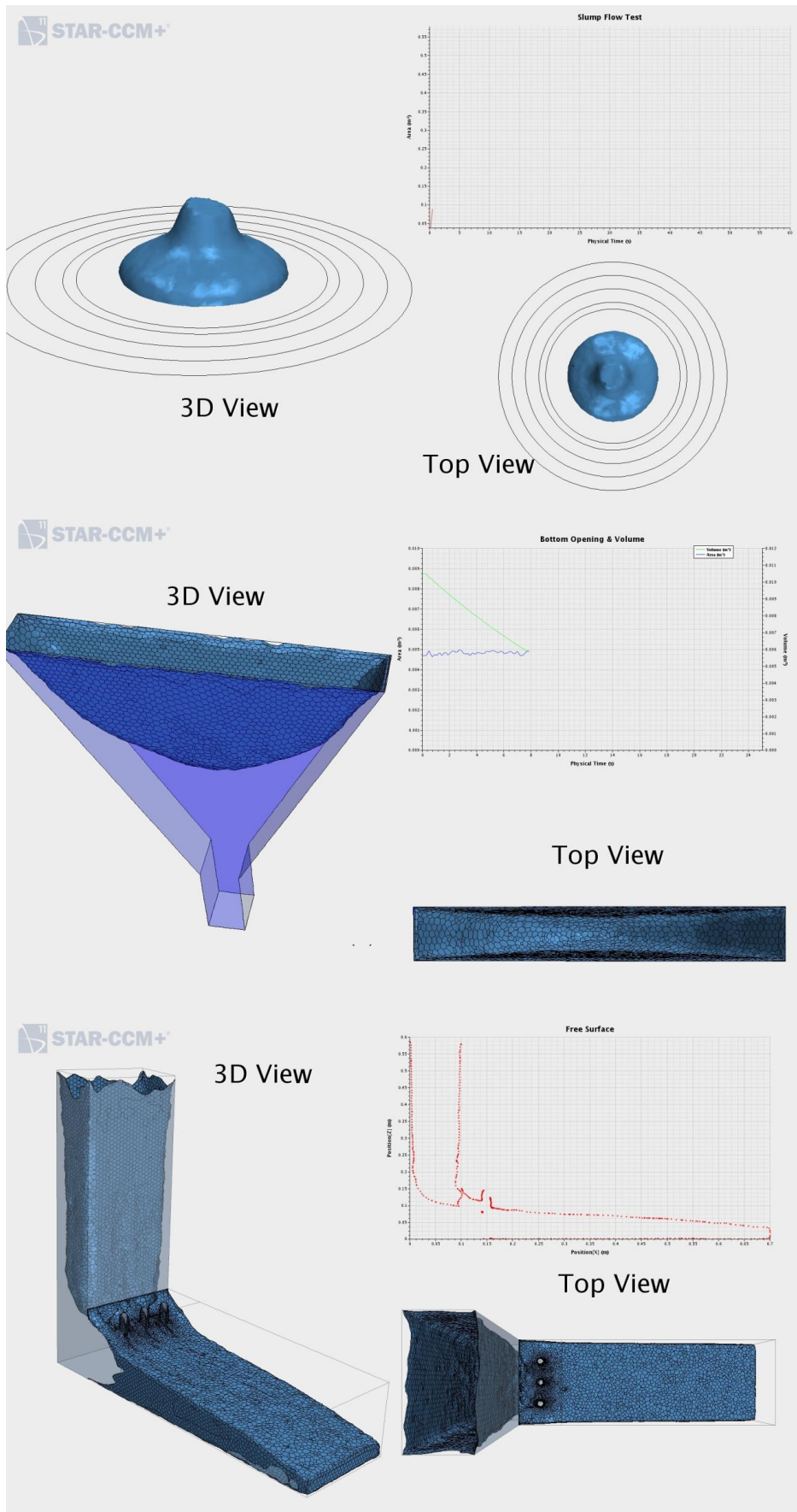


Figure 7a 7b and 7c: Slump flow, V-funnel and L-Box tests simulation

Table 6 summarizes the yield stress,  $\tau_0$ , and dynamic viscosity,  $\mu$ , parameters determined for each of the four concrete mixes. The discrepancies in the passing ability correspond to the low accuracy of the manual measurements compared to the result of the simulated fine mesh, but a relatively similar range of differences prevails. As expected, two of the mixes, SC1 and SC3, presented similar characteristics. On the contrary the most viscous mix, SC2, showed a reduced yield stress to achieve a higher spread during the slump flow test and a better passing ability in the L-box test. The SC4 mix showed low viscosity (segregation risk) and high yield stress (low passing ability), despite the difference in the number of rebars (two rebars) used in the trials and those used in the simulation (3 rebars).

Mixture	Yield stress [Pa]	Dynamic viscosity [Pa·s]	Slump-flow [mm]	V-funnel time [s]	Passing ability L-box 3 rebar
SC1	125	65	580	23	0,7
SC2	60	80	680	19	0,8
SC3	170	55	560	21	0,65
SC4	220	35	520	15	0,1

**Table 6:** Results of computational simulations

A direct comparison with the corresponding mix designs (see Table 4) can be deduced from the results obtained in the computational simulations. The raw materials are similar in the self-compacting mixes, although SC1 includes only fine and coarse limestone aggregates, and the rest of mixes substitute the gravel for EAFS aggregates. Comparing the reference mix, SC1, with SC2, the increase of the fine fraction, by over 32%, clearly appeared to enhance flowability, due to the lubrication provided by the limestone fines; also the yield stress decreased, although a slight increment of the viscosity was noted due to the enlarged amount of bearing paste. This increase provided an improved stability to the mass and counteracted the loss of workability that may arise from the use of EAFS aggregates instead of conventional limestone aggregates.

Although mix SC3 was based on the design used for SC2, the change of cement type entailed a negative effect on flowability. The substitution of CEM I for CEM IV had a negative effect on the excellent behavior of SC2, probably due to the dispersive action of the admixtures which were only effective on the clinker particles, without exerting repulsive forces between the fly ash particles. Therefore, the lubrication between the EAFS aggregates was not so effective and as a result, the yield stress increased.

The last mix, SC4, included a coarser fraction of EAFS, which comprised particle sizes of between 12 and 20 mm up to the 30% of the EAFS aggregates. Obviously, a remarkable decrease in flowability was expected; this dosage adjustment is not sufficient to achieve similar self-compaction properties in the concrete than in the previous batches and will be followed up in future work.

## **Hardened properties**

### Density

The dry densities of the hardened concretes are shown in Table 7; these densities and the fresh densities in Table 4 are in good correlation, as may be expected. The samples were dried in a stove at 60°C for one week, after an immersion-curing period of 28 days from their manufacturing.

It may be seen that the average density of the slag concretes increased by about 15% with respect to those of concrete made using classical aggregates (values close to 2.7 in almost all mixes versus 2.3 Mg/m<sup>3</sup> showed by the SC1 mix). This drawback is usually compensated by the increase in the strength and stiffness of EAFS concretes, as confirmed in recent articles by the authors [35, 39]. The “pumpable concrete” mixes include lower amounts of limestone fines and higher amounts of EAFS than the “self-compacting concrete” mixes, hence, the density of the former was, in general, higher than the density of SC2 and SC3.

### Strength

The results of compressive strength on cubical 100x100x100 mm samples after 7, 28, 90 and 180 days of underwater curing appear in Table 7; the initial goal of preparing structural concrete with a strength of over 40 MPa at 28 days and a cement content of under 360 kg per cubic meter was in general achieved. The SC3 mix prepared with the type IV cement only reached these strengths at 180 days.

Property	P-1	P-2	P-3	P-4	P-5	SC-1	SC-2	SC-3	SC-4
Comp. str 7 days [MPa]	61	46	53	61	39	44	47	19	47
Comp. str 28 days[MPa]	67	54	61	69	46	51	53	31	58
Comp. str 90 days[MPa]	68	56	67	71	54	56	55	36	64
Comp. str 180 days[MPa]	73	60	71	74	62	64	61	41.5	67
Stiffness mod 28 day [GPa]	57.5	45.6	55	55.3	38	46.4	46.5	29	48
Dry density [Mg/m <sup>3</sup> ]	2.51	2.5	2.7	2.63	2.59	2.35	2.53	2.67	2.79
MIP Bulk density [Mg/m <sup>3</sup> ]	2.53	2.50	2.68	2.62	2.57	2.34	2.53	2.63	2.80
MIP App density [Mg/m <sup>3</sup> ]	2.89	2.97	3.05	3.09	2.96	2.59	3.03	3.19	3.21
MIP porosity [% vol]	12.3	15.5	12.2	15.2	13.5	9.9	16.6	17.5	12.8

**Table 7:** Strength and MIP of the mixes

In the pumpable concrete, the compressive strength results were rather similar in the P1, P3 and P4 mixes. The P2 mix containing ladle furnace slag showed a lower short- and medium-term strength, with a slightly enhanced long-term strength, probably due to the hydraulic reaction of ladle slag. Mixture P5 also showed a lower strength, perhaps associated with an excess of fine fraction among its components; however, this additional amount of fine fraction favored its workability, which is essential in this work, obtaining slumps as high as 220 mm in the Abrams cone without any segregation of heavy EAF slag. The P5 mixture was the last step in the work to obtain self-compacting mixes with this slag.

The self-compacting concretes showed, as expected, lower strength levels than the “good” pumpable concretes P1, P3 and P4; the results at 28 days were in the interval 50-60 MPa versus 60-70 MPa in pumpable concrete. The high amount of fine fraction materials and water (indispensable to obtain the appropriate workability) harmed the strength of self-compacting mixes, which reached strengths of 60-65 MPa after 180 days; at that point, the good P mixes exceeded 70 MPa in strength. The presence of fly ash was detrimental to short and medium term strength in SC3; the interaction of the admixture with this by-product produced no advantages, unlike other hydraulic mixes (performed with other sorts of admixtures) in which this active addition was of benefit [66].

The global results obtained in the SC2 mix can be qualified as excellent, showing better rheological characteristics than those of classical self-compacting concrete SC1 and

similar mechanical characteristics. In this case, we cannot state that the increase in the mechanical performance of electric arc-furnace slag concrete compensates the increase in own weight, with a fresh or dry density, but it is well-known in structural engineering that this factor is of minor relevance in most cases (ordinary buildings); only in singular constructions such as large bridges or big roof-covers is it a factor decisive. In these cases, the use of self-compacting concrete made with EAF slag as aggregate is neither advisable nor recommendable.

The stiffness modulus, measured by ultrasonic pulse velocity after 28 days of curing, yielded results that were quite consistent with those of the compression test, but the use of the EAFS aggregate instead of the natural aggregate, produced a slightly lower stiffness, in general, in the hardened hydraulic mixes. Additionally, it should be said that these largely comparative results have no rigorous significance as a Young's modulus of these materials. They must be tested under different conditions to obtain the true values of this magnitude.

MIP analysis

In the present research, the MIP (Mercury Intrusion Porosimetry) technique was employed, using an Autopore IV 9500 apparatus (Micromeritics) at a pressure of 33,000 psi to study the evolution of the pore structure. The results of the MIP analysis of the different concrete types showed that they were on the whole well-performed mixes. The obtained values were, in general, within the range of 12-16%, with the exception of mix SC1 containing classical limestone aggregates. It should be taken into account that the total porosity was the addition of porosity from the capillary water of the cementitious matrix and from the presence of porous EAF slag. In fact, the value of the only mix that contained no slag, SC1, was five units smaller than the average of the rest of mixes.

In Figure 8a, the cumulative intrusion curved for samples of mixes P1 and SC2 are shown and, in Figure 8b, the graphics of MIP pore size frequency in terms of differential intrusion, taken from the Figure for cumulative intrusion, is also shown. In all cases, a significant peak (maximum frequency) in the vicinity of 100 nm may be appreciated in our mixes (true for all the mixes, though only two are included in the figures) between the pore sizes of 20-200 nm, due to capillary porosity. The porosity amount of a size between 20 to 200 nm was close to the interval of 8 to 10%.

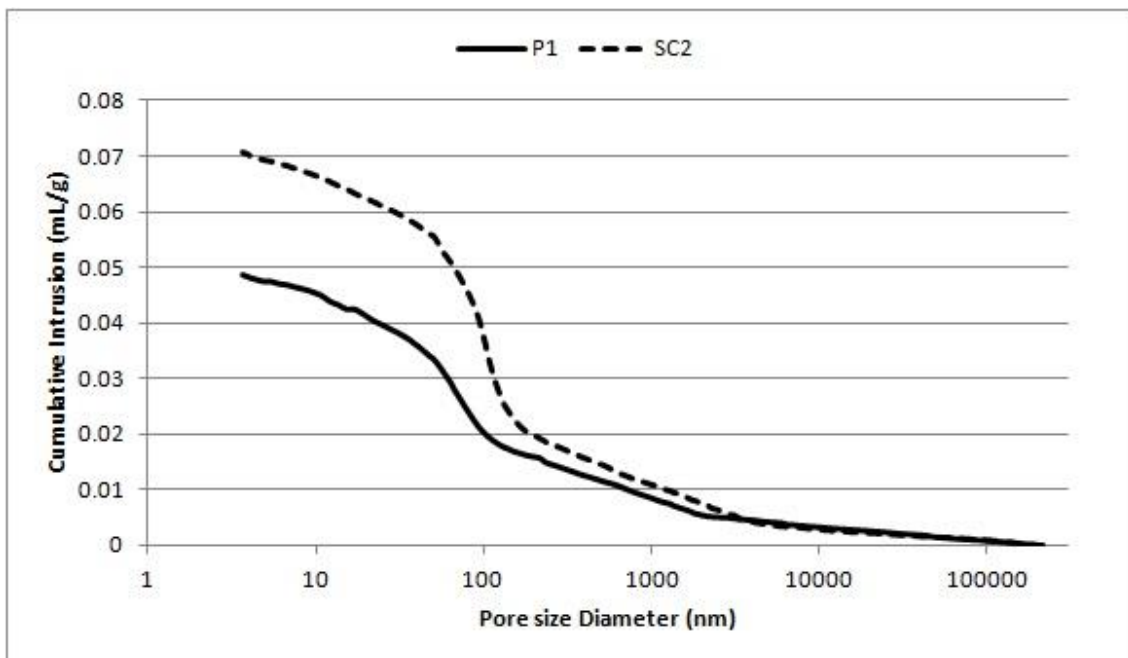


**Figure 8a:** MIP cumulative intrusion in mixes P1 and SC2.

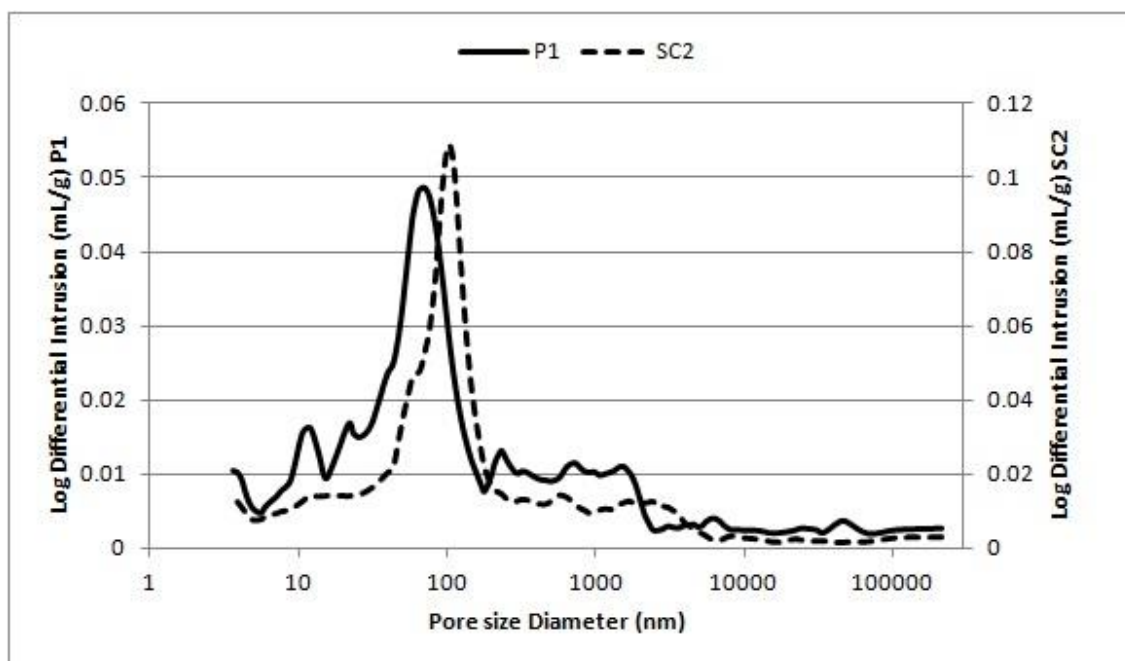


**Figure 8b:** MIP differential intrusion in mixes P1 and SC2

The additional pore size between 200 to 200000 nm depended on the porosity of the matrix added to that of the EAF slag. In the case of SC1, this last porosity (>200nm) was only 1.8% of a total 9.9%; in other mixes, this value varied in the interval of 4 to 8%. In general, it can be stated that the porosity value was slightly higher in the SCC (as SC-2 and SC-3) than in the pumpable mixes, due to the greater volume of water used in the preparation of the SCC mixes.

The bulk density and apparent density values provided by the MIP technique were, in general, coherent with the macroscopic density values measured using the conventional method of air weight and submerged weight. The bulk density MIP value of each mix was in general quite coherent with its dry density value measured by the conventional method; however, it was less coherent in the hydraulic mixes that included electric arc furnace slag. In general, the samples in the MIP tests were small-sized pieces (i.e. one cubic centimeter), without the addition of coarse aggregate (size > 5 mm). In the macroscopic measures of density, a whole cubic or prismatic sample was used and some discrepancy might therefore be expected.

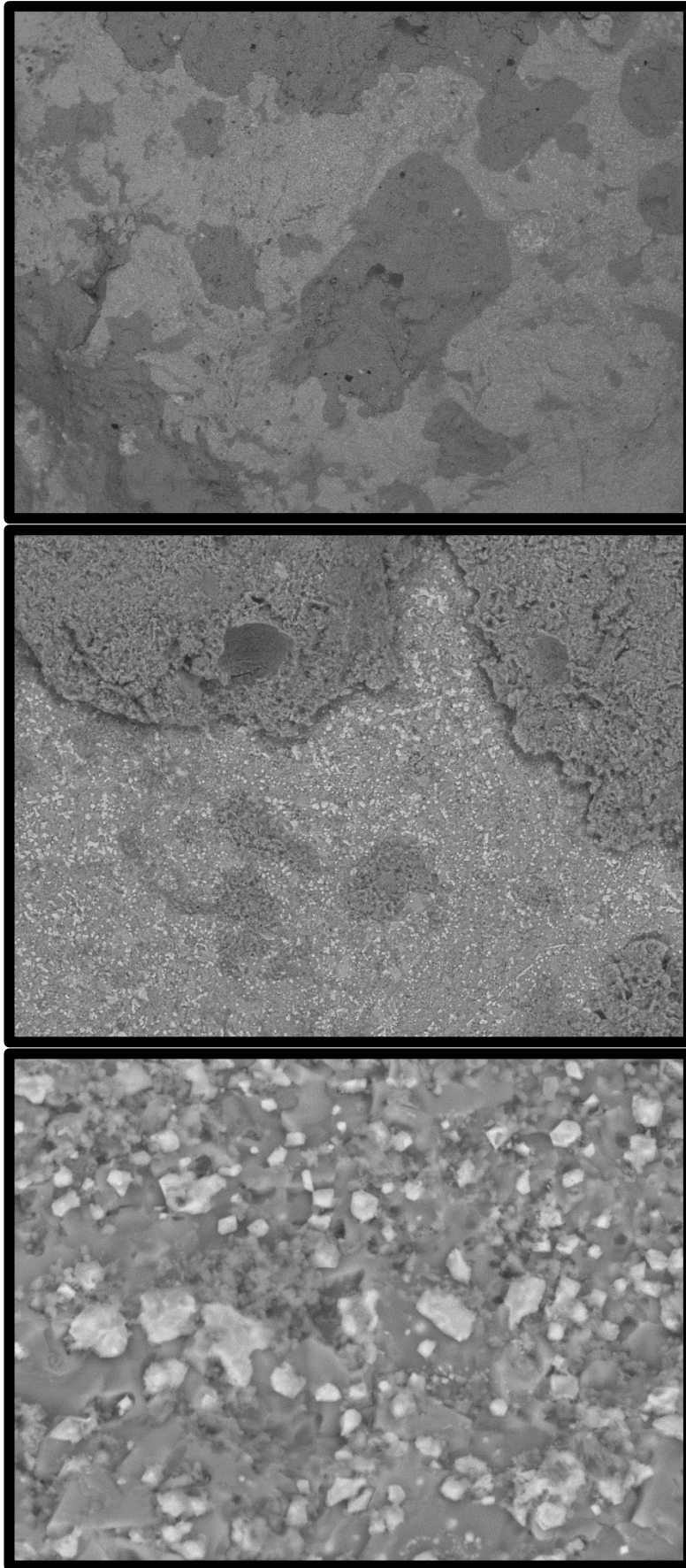
Finally, the results for the apparent density for all of the EAFS mixes were similar and coherent between each other; and the same may be said of the SC1 reference mix.



*SEM observations on concrete fracture surfaces*

Fractographic observation of the SCC specimens revealed some interesting details that are illustrated and commented in this section. Pieces of mixtures P2 (“pumpable” concrete) and SC2 (self-compacting concrete), obtained after compression tests to failure, were observed using low-vacuum scanning electron microscopy (SEM) with the backscattered electrons technique, with no carbon or gold coating. No essential differences were observed between the characteristics of the above-mentioned mixtures and they all had similar features that could be analyzed and evaluated.

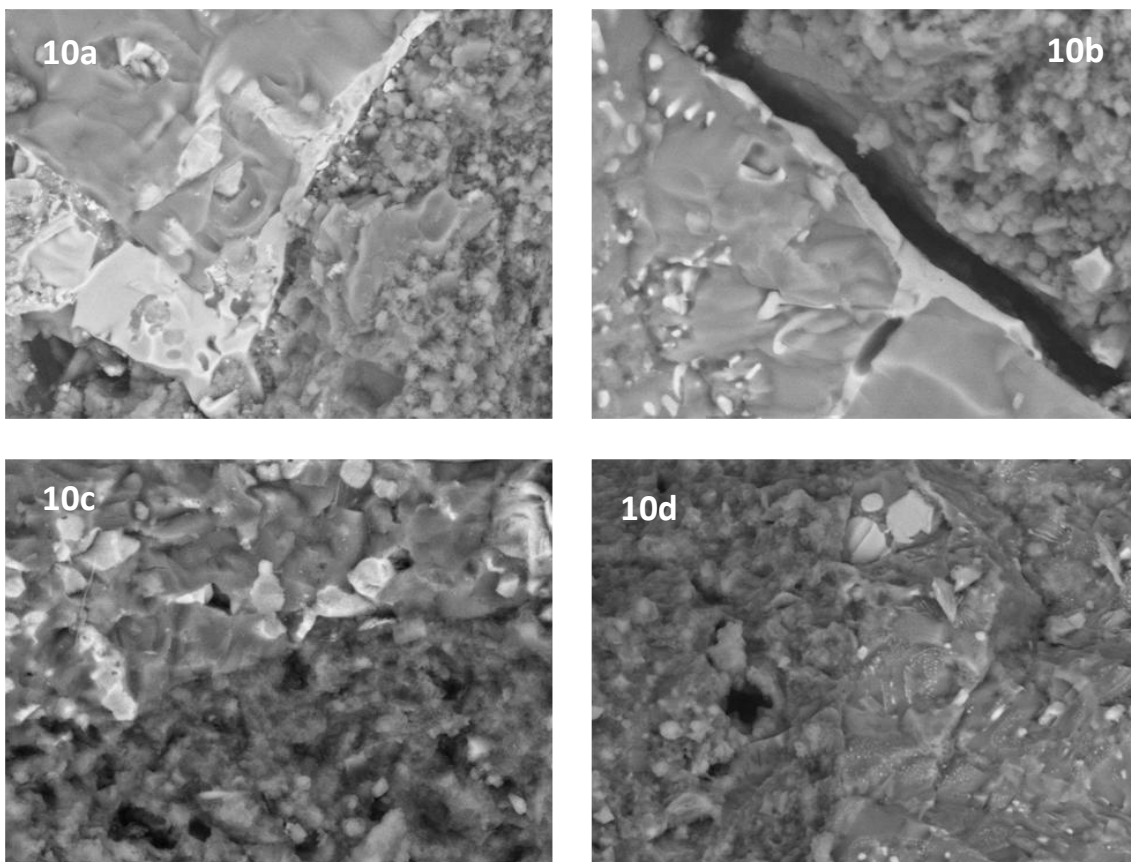
Figure 9a shows the contour (the “skin”) of an EAFS aggregate particle as part of the general fracture surface of an SC2 specimen. The existence of regions with good adherence of cementitious paste (dark, wrinkled) and regions of weaker adherence are visible, where the cementitious paste has separated from the EAFS pebble due to shear cracking. Figure 9b shows the naked surface of the EAFS sample (smoother, mottled by clearer small particles).



**Figures 9a, 9b 9c: SEM images SC2**

A higher magnification of this region, Figure 9c, reveals an outstanding presence of “white” particles of iron oxide (wüstite) in a grey matrix of silicates; in this grey region it is possible to distinguish some small “creased” zones of adhered cementitious paste on plate zones of silicates. It is reasonable to affirm that the adherence between paste and EAFS aggregate was good on the hydrophilic compounds of the slag (ghelenite, olivine, calcite, kirsteinite...), but the role of the hydrophobic iron oxides (wüstite and others) emerging on the surface contours was negative.

In Figure 10, the surface of P2 shows broken EAFS aggregate particles and broken cementitious paste in the vicinity of its contour, including the Interfacial Transition Zone (ITZ). Hence, examples of good as well as cracked and weakened adherence can be observed [35]. Figure 10a shows a poorly densified ITZ region (hole, rift) alongside an iron oxide coating of a piece of aggregate; in Figure 10b, the ITZ can be seen to have split open due to the shear stress effects of the test. In figures 10c and 10d, an “almost-perfect” ITZ is shown, the aggregate having a small proportion of “white” iron oxide particles on the surface contours; the apparent white particles correspond to the inside of the broken EAFS aggregate particles. In Figures 10a and 10b, the “clean” cleavage of the silicates on the inside of the EAFS particles may be seen.



**Figures 10a, 10b, 10c, and 10d: SEM images P2**

Dispersive energy X-ray micro-analysis (EDX) was performed on one of last samples, the images of which show the “almost white” coating of the EAFS aggregate particles in Figure 11. The results prove that this substance mainly consists of iron oxide (wüstite in solid solution with other metals as calcium, manganese...); Table 8 shows the results of this analysis.

Element	Weight%	Atomic%
O K	31.47	58.76
Al K	2.80	3.10
Si K	2.31	2.45
Ca K	6.04	4.50
Ti K	4.85	3.02
Mn K	5.82	3.17
Fe K	46.72	24.99

**Table 8:** EDX analysis

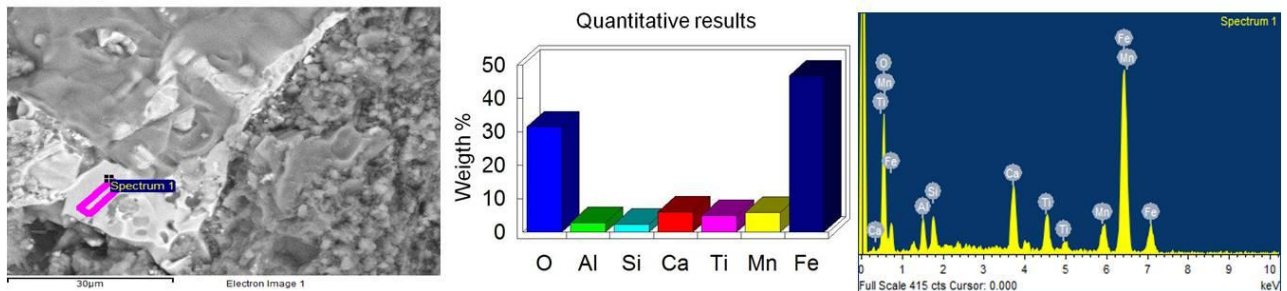


**Figure 11:** EDX analysis

## Conclusions

The conclusions of this study are as follows:

- The reuse of electric arc-furnace slag in the manufacturing of pumpable structural concrete is a useful, affordable, and viable solution.
- It is possible to prepare self-compacting mixes using electric arc-furnace slag as coarse and fine aggregate, using appropriate doses and compatible chemical admixtures.
- The numerical simulation of the viscous flux of these self-compacting mixes using a suitable model leads to very acceptable results.
- The analysis of these self-compacting concretes in the hardened state points to a cohesive internal structure with reasonably good mechanical properties.

- SEM observation of the fracture surfaces in the SCC-EAFS concrete showed significant features to understand their structure and their mechanical behavior

## References

- [1] P. Bosela, N. Delatte, R. Obratil, A. Patel, Fresh and hardened properties of paving concrete with steel slag aggregate, 9th International Conference on Concrete Pavements, (2008) 836-853.
- [2] P. Jahren, Do not forget the other chapters!, Concrete international 24(7) (2002) 41-44.
- [3] P.J. Koros, Dusts, scale, slags, sludges... Not wastes, but sources of profits, Metallurgical and Materials Transactions B 34(6) (2003) 769-779.
- [4] P.K. Mehta, Global concrete industry sustainability, Concrete international 31(02) (2009) 45-48.
- [5] T.R. Naik, Greener concrete using recycled materials, Concrete international 24(7) (2002) 45-49.
- [6] W. Shelburne, D. Degroot, The use of waste and recycled materials in highway construction, Civil engineering practice 13(1) (1998) 5-16.
- [7] R. Tomellini, Summary report on RTD in iron and steel slags: development and perspectives, Technical Steel Research, Report Prepared for the European Commission EUR 19066, Brussels, Belgium, 1999.
- [8] İ. Yüksel, A review of steel slag usage in construction industry for sustainable development, Environment, Development and Sustainability (2016) 1-16.
- [9] J.O. Akinmusuru, Potential beneficial uses of steel slag wastes for civil engineering purposes, Resources, Conservation and Recycling 5(1) (1991) 73-80.
- [10] E. Anastasiou, K. Georgiadis Filikas, M. Stefanidou, Utilization of fine recycled Materials 50 (2014) 154-161.
- [11] M.C. Bignozzi, F. Sandrolini, F. Andreola, L. Barbieri, I. Lancellotti, Recycling Electric Arc Furnace Slag as Unconventional Component for Building Materials, Proceeding of 2nd International Conference on Sustainable Construction Materials and Technologies, 2010, pp. 28-30.
- [12] F. Autelitano, F. Giuliani, Electric arc furnace slags in cement-treated materials for road construction: Mechanical and durability properties, Construction and Building Materials 113 (2016) 280-289.

- [13] B.A. Fronek, Feasibility of Expanding the Use of Steel Slag as a Concrete Pavement Aggregate, (2012). ETD Archive. Paper 372.
- [14] J. Geiseler, Use of steelworks slag in Europe, *Waste Management* 16(1–3) (1996) 59-63.
- [15] H. Motz, J. Geiseler, Products of steel slags an opportunity to save natural resources, *Waste Management* 21(3) (2001) 285-293.
- [16] J.N. Murphy, T.R. Meadowcroft, P.V. Barr, Enhancement of the cementitious properties of steelmaking slag, *Canadian Metallurgical Quarterly* 36(5) (1997) 315-331.
- [17] M. Pasetto, N. Baldo, Mix design and performance analysis of asphalt concretes with electric arc furnace slag, *Construction and Building Materials* 25(8) (2011) 3458-3468.
- [18] M. Pasetto, N. Baldo, Cement bound mixtures with metallurgical slags for road constructions: Mix design and mechanical characterization, *Inżynieria Mineralna* 14 (2) (2013) 15-20.
- [19] T.M. Petry, D.N. Little, Review of stabilization of clays and expansive soils in pavements and lightly loaded structures—history, practice, and future, *Journal of Materials in Civil Engineering* (2002) 14 (6) 447-460.
- [20] H. Qasrawi, F. Shalabi, I. Asi, Use of low CaO unprocessed steel slag in concrete as fine aggregate, *Construction and Building Materials* 23(2) (2009) 1118-1125.
- [21] A. Rubio, J. Carretero, La aplicación de las escorias de acería en carreteras, *Ingeniería Civil* 80 (1991) 5-9.
- [22] J. San José, Reutilización y valorización en obra civil de escorias de horno de arco eléctrico producidas en la CAPV, *Arte y Cemento* (1891) (2000) 124-126.
- [23] J. San José, A. Uría, Escorias de horno de arco eléctrico en mezclas bituminosas, *Arte y Cemento* (1905) (2001) 122-125.
- [24] T. Sofilić, U. Sofilić, I. Brnardić, The significance of iron and steel slag as by-product for utilization in road construction, 12th International Foundrymen conference Sustainable Development in Foundry Materials and Technologies, 2012 419-436.
- [25] M. Tüfekçi, A. Demirbaş, H. Genç, Evaluation of steel furnace slags as cement additives, *Cement and Concrete Research* 27(11) (1997) 1713-1717.
- [26] I.Z. Yildirim, M. Prezzi, Chemical, mineralogical, and morphological properties of steel slag, *Advances in Civil engineering* (2011) 1-13.
- [27] R. Jin, Q. Chen, A. Soboyejo, Survey of the current status of sustainable concrete production in the US, *Resources, Conservation and Recycling* 105 (2015) 148-159.

- [28] H.A. Colorado, E. Garcia, M.F. Buchely, White Ordinary Portland Cement blended with superfine steel dust with high zinc oxide contents, *Construction and Building Materials* 112 (2016) 816-824.
- [29] A.S. Brand, J.R. Roesler, Steel furnace slag aggregate expansion and hardened concrete properties, *Cement and Concrete Composites* 60 (2015) 1-9.
- [30] P.J. DePree, C.T. Ferry, Mitigation of Expansive Electric Arc Furnace Slag in Brownfield Redevelopment, *GeoCongress 2008*, pp. 271-278.
- [31] M. Frías, J. San-José, I. Vegas, Steel slag aggregate in concrete: the effect of ageing on potentially expansive compounds, *Materiales de Construcción* 60(297) (2010) 33-46.
- [32] I. Liapis, I. Papayianni, Advances in chemical and physical properties of electric arc furnace carbon steel slag by hot stage processing and mineral mixing, *Journal of Hazardous Materials* 283 (2015) 89-97.
- [33] F. Lopez, Physico-chemical and mineralogical properties of EAF and AOD slags, *EOSC'97: 2 nd European Oxygen Steelmaking Congress, 1997*, pp. 417-426.
- [34] G. Adegoloye, A.L. Beaucour, S. Ortola, A. Noumowe, Mineralogical composition of EAF slag and stabilised AOD slag aggregates and dimensional stability of slag aggregate concretes, *Construction and Building Materials* 115 (2016) 171-178.
- [35] I. Arribas, A. Santamaría, E. Ruiz, V. Ortega-López, J.M. Manso, Electric arc furnace slag and its use in hydraulic concrete, *Construction and Building Materials* 90 (2015) 68-79.
- [36] I. Arribas, I. Vegas, J.T. San-José, J.M. Manso, Durability studies on steelmaking slag concretes, *Materials & Design* 63 (2014) 168-176.
- [37] F. Faleschini, M. A. Fernández-Ruíz, M.A. Zanini, K. Brunelli, C. Pellegrino, E. Hernández-Montes, High performance concrete with electric arc furnace slag as aggregate: Mechanical and durability properties, *Construction and Building Materials* 101 (2015) 113-121.
- [38] J.M. Manso, J.J. Gonzalez, J.A. Polanco, Electric arc furnace slag in concrete, *Journal of materials in civil engineering* 16(6) (2004) 639-645.
- [39] J.M. Manso, D. Hernández, M.M. Losanez, J.J. González, Design and Elaboration of Concrete Mixtures Using Steelmaking Slags, *ACI materials journal* 108(6) (2011) 673-681.
- [40] C. Pellegrino, F. Faleschini, Experimental behavior of reinforced concrete beams with electric arc furnace slag as recycled aggregate, *ACI Materials Journal* 110(2) (2013) 197-205.

- [41] C. Pellegrino, V. Gaddo, Mechanical and durability characteristics of concrete containing EAF slag as aggregate, *Cement and Concrete Composites* 31(9) (2009) 663-671.
- [42] J.T. San-José, I. Vegas, I. Arribas, I. Marcos, The performance of steel-making slag concretes in the hardened state, *Materials & Design* 60 (2014) 612-619.
- [43] S.I. Abu-Eishah, A.S. El-Dieb, M.S. Bedir, Performance of concrete mixtures made with electric arc furnace (EAF) steel slag aggregate produced in the Arabian Gulf region, *Construction and Building Materials* 34 (2012) 249-256.
- [44] A.I. Al-Negheimish, R.Z. Al-Zaid, Utilization of local steel making slag in concrete, *Journal of King Saud University* 9 (1) (1997) 39-51.
- [45] E.K. Anastasiou, I. Papayianni, M. Papachristoforou, Behavior of self compacting concrete containing ladle furnace slag and steel fiber reinforcement, *Materials & Design* 59 (2014) 454-460.
- [46] N. Faraone, G. Tonello, E. Furlani, S. Maschio, Steelmaking slag as aggregate for mortars: Effects of particle dimension on compression strength, *Chemosphere* 77(8) (2009) 1152-1156.
- [47] B. Fronek, P. Bosela, N. Delatte, Steel slag aggregate Used in Portland cement concrete: US and international perspectives, *Transportation Research Record: Journal of the Transportation Research Board* (2267) (2012) 37-42.
- [48] K. Morino, E. Iwatsuki, Utilization of electric arc furnace oxidizing slag as concrete aggregate, *Minerals, Metals and Materials Society/AIME, REWAS'99: Global Symposium on Recycling, Waste Treatment and Clean Technology.*, 1999, pp. 521-530.
- [49] I. Papayianni, E. Anastasiou, Concrete incorporating high-calcium fly ash and EAF slag aggregates, *Magazine of Concrete Research* 63(8) (2011) 597-604.
- [50] L. Coppola, S. Lorenzi, A. Buoso, Electric arc furnace granulated slag as a partial replacement of natural aggregates for concrete production, *Proceedings of the Second International Conference on Sustainable Construction Materials and Technologies*, 2010.
- [51] A. Sekaran, M. Palaniswamy, S. Balaraju, A Study on Suitability of EAF Oxidizing Slag in Concrete: An Eco-Friendly and Sustainable Replacement for Natural Coarse Aggregate, *The Scientific World Journal* (2015) 1-8.
- [52] S. Monosi, M.L. Ruello, D. Sani, Electric arc furnace slag as natural aggregate replacement in concrete production, *Cement and Concrete Composites* 66 (2016) 66-72.



- [53] L. Rondi, G. Bregoli, S. Sorlini, L. Cominoli, C. Collivignarelli, G. Plizzari, Concrete with EAF steel slag as aggregate: A comprehensive technical and environmental characterisation, *Composites Part B: Engineering* 90 (2016) 195-202.
- [54] I. Netinger Grubeša, M. Jelčić Rukavina, A. Mladenović, Impact of High Temperature on Residual Properties of Concrete with Steel Slag Aggregate, *Journal of Materials in Civil Engineering* 28(6) (2016) 10.1061/(ASCE)MT.1943-5533.0001515, 04016013.
- [55] H. Okamura, Self-compacting high performance concrete, *Concrete International* 19(7) (1997) 50-54.
- [56] H. Okamura, M. Ouchi, Self-compacting concrete, *Journal of advanced concrete technology* 1(1) (2003) 5-15.
- [57] B. Benabed, E.-H. Kadri, L. Azzouz, S. Kenai, Properties of self-compacting mortar made with various types of sand, *Cement and Concrete Composites* 34(10) (2012) 1167-1173.
- [58] J. Jin, P.L. Domone, Relationship between the fresh properties of SCC and its mortar component, in: S.P. Shah, J.A.Daczko, J.N. Lingscheit (Eds.) *First North American Conference on the Design and use of Self- Consolidating Concrete*, Center for Advanced Cement-Based Materials, 2003, pp. 37-42.
- [59] D. Bonen, S.P. Shah, Fresh and hardened properties of self-consolidating concrete, *Progress in Structural Engineering and Materials* 7(1) (2005) 14-26.
- [60] S. Tomasiello, M. Felitti, EAF slag in self-compacting concretes, *Facta universitatis-series: Architecture and Civil Engineering* 8(1) (2010) 13-21.
- [61] Y.-N. Sheen, D.-H. Le, T.-H. Sun, Innovative usages of stainless steel slags in developing self-compacting concrete, *Construction and Building Materials* 101 (2015) 268-276.
- [62] EFNARC, *Specification, Guidelines for Self-Compacting Concrete*, European Federation of Producers and Applicators of Specialist Products for Structures (2002).
- [63] EFNARC, *Guidelines for Viscosity Modifying Admixtures For Concrete*, September, 2006.
- [64] A. International, *Annual Book of ASTM Standards*, West Conshohocken, 19429-2959. PA, USA, 2008.
- [65] W.H. Graf, *Hydraulics of Sediment Transport*, Water Resources Publications 1984.
- [66] A. Santamaría, E. Rojí, M. Skaf, I. Marcos, J.J. González, The use of steelmaking slags and fly ash in structural mortars, *Construction and Building Materials* 106 (2016) 364-373.

- [67] N. Roussel, A. Gram, M. Cremonesi, L. Ferrara, K. Krenzer, V. Mechtcherine, S. Shyshko, J. Skocec, J. Spangenberg, O. Svec, L.N. Thrane, K. Vasilic, Numerical simulations of concrete flow: A benchmark comparison, *Cement and Concrete Research* 79 (2016) 265-271.
- [68] A. Orbe, R. Losada, E. Rojí, J. Cuadrado, A. Maturana, The prediction of bending strengths in SFRSCC using Computational Fluid Dynamics (CFD), *Construction and Building Materials* 66 (2014) 587-596.
- [69] D. Feys, R. Verhoeven, G. De Schutter, Why is fresh self-compacting concrete shear thickening?, *Cement and Concrete Research* 39(6) (2009) 510-523.
- [70] C.F. Ferraris, L.E. Brower, Comparison of Concrete Rheometers: International Test at LCPC (Nantes, France) in October, 2000, National Institute of Standards and Technology Gaithersburg, MD, USA2001.
- [71] F. Kolařík, B. Patzák, L.N. Thrane, Modeling of fiber orientation in viscous fluid flow with application to self-compacting concrete, *Computers & Structures* 154 (2015) 91-100.
- [72] CEN European Committee for standardization, Rue de Stassart, 36. Brussels B-1050.

**5.3. A study on the durability of structural concrete incorporating electric steelmaking slag as aggregate.**



## **Abstract**

The durability of structural concrete mixes prepared with Electric Arc Furnace (EAF) slag aggregates is tested for use in normal and aggressive environments. The mixes are shown to have good physical characteristics, mechanical properties and dimensional stability. Samples of “pumpable” and “self-compacting” concrete mixes are subjected to severe testing, to assess their resistance to marine environments. The mixes are subjected to freezing-thawing and drying-wetting tests up until deterioration. Real immersion in marine water in the tidal zone and tests on reinforcement bar corrosion are also performed to evaluate the quality and utility of this sort of concrete. The behavior of the proposed mixes in these expositions was satisfactory, confirming their suitability for use in structural applications exposed to aggressive environments.

## Introduction

Some decades ago, the pioneering proposals [1-5] to use electric steelmaking slags as aggregates in concrete were welcomed as a potential means of reusing steelmaking slag waste. In these initial studies, several areas of use were proposed for the application of these products; among which efficient applications for construction and civil engineering sectors that currently consume vast amounts of natural resources. The target is clearly to substitute these high levels of consumption for reasonable amounts of re-usable by-products avoiding their disposal in dumping sites.

Important measures from the European Union such as environmental regulations, Council decisions and directives [6,7] concern the re-use of steelmaking slag and the reduction of its dumping in landfill sites. EU member states are actively encouraged through various projects to respond to this challenge to recycle electric-arc furnace slag, in so far as their domestic levels of slag production may permit them to do so. Electric arc furnaces are responsible for most steel manufacturing in southern Europe [8] where the by-products from steelmaking industrial processes are now a topical research area aiming to produce viable concrete products for use in construction and engineering projects.

Over the last decade, several international research groups have been engaged in research into hydraulic and bituminous concrete including electric arc furnace slag (oxidizing, from the acid refining of liquid steel) for use as aggregates [9-16]. In particular, research groups in Greece (University of Thessalonika), Italy (University of Padua) and Spain (Universities of the Basque Country, University of Burgos and University of Cantabria) [17-37] are currently working to achieve significant advances in this field. Their aim is to conduct pre-standardization studies that will eventually incorporate steelmaking slag in relevant building codes throughout the E.U.

After investigating efficient manufacturing methods of non-reinforced (massive) concrete containing EAF slag as aggregate over the past decade, this research group in Spain is now investigating efficient manufacturing methods for structural concrete that contains these slag aggregates. Recent publications of these authors have shown advances in this field, in which there is still a significant way to go [38,39].

The three main obstacles to this objective are as follows: the reduced workability of in-fresh concrete, the increase in the density of hardened concrete, and the risk of losing its good properties after a long service life, taking into account the singular

characteristics of this aggregate. Each of the above-mentioned disadvantages, and others that further studies might unearth, have to be successfully negotiated, to produce a manufacturing standard for the construction sector concerning the use of EAF slag in structural concrete.

The proposal in this paper concerns the application of EAF slag concrete to structural elements. It consists of the preparation of two different types of concrete in terms of their in-fresh workability: the manufacture of “pumpable” concrete of high workability, class S3 and S4, and the manufacture of self-compacting concrete with good flowability, with a spread of over 500 mm from the Abrams cone. The challenge is significant, considering the inherent and well known loss of workability associated with the use of these aggregates; careful dosing and the use of appropriate admixtures is indispensable.

The present article contains the results of several tests on the durability and the long-term behavior of various structural concretes (pumpable and self-compacting mixes), the preparation and characteristics of which have been described in a recently published paper by these authors. Therefore some previously published details on the main features of these manufactured [38] will only be very briefly described in this paper. So it reports the results of certain physical properties, strength and stability, and emphasizes the results of the durability tests on these concretes, comparing their characteristics in relation to conventional concrete.

### **Scope of the research**

The specificity of concrete made with electric arc furnace (EAF) slag as an aggregate that performs as a self-compacting concrete is a singular challenge. At present, little research in the scientific literature [40-42] has been reported on this question, and there is a gap in the literature relating to the durability studies of these concretes. These EAF slag concretes will, undoubtedly, still require considerable analysis before their global behavior is comparable to conventional concrete mixes.

Firstly, the evidence suggests that concrete manufactured with EAF slag is not of similar durability to those of conventional concrete when exposed to aggressive marine environments. Rather, many researchers [21,29,43] with significant experience in this field share the view that an initial assessment would suggest the poor durability of these concretes. In this paper, the durability issues are studied and the results

reveal that, where possible, the aforementioned disadvantages may to some extent be mitigated.

Molds of cubic and prismatic specimens were prepared, using the same mixes proposed by authors of a recent article on this subject [38]. Many were subsequently used in the durability tests that will be described in the following sections. The main properties of the hardened concrete are discussed, i.e. mechanical strength, porosity, capillary absorption and water penetration under pressure, as well as the results of measuring long-term concrete shrinkage in the atmosphere, anticipating an eventual expansion of the aggregates. Autoclave test on mixes completes this study.

A series of conventional freezing-thawing and wetting-drying cycles were then performed as part of the durability tests, throughout which damage to the material was controlled by means of an indirect evaluation of its stiffness, measuring the propagation speed of ultrasonic waves through its mass and a final evaluation of compressive strength.

The aim of this work is to analyze the structural behavior of this material as “reinforced concrete” for use in highly saline marine environments. For that purpose, several concrete samples were exposed to seawater in intertidal zones over varied periods of time. The penetration of chloride and sulfate ions inside the specimens, and the eventual carbonation of Portlandite were monitored. Likewise, electrochemical tests to evaluate corrosion in steel reinforcement bars were also performed, to estimate the durability of EAF slag concrete and steel rebars that are standard in structural concretes.

Finally some conclusions are advanced to facilitate the practical use of this sort of reinforced concrete mix in the construction and the reliability of structural engineering elements in marine environments.

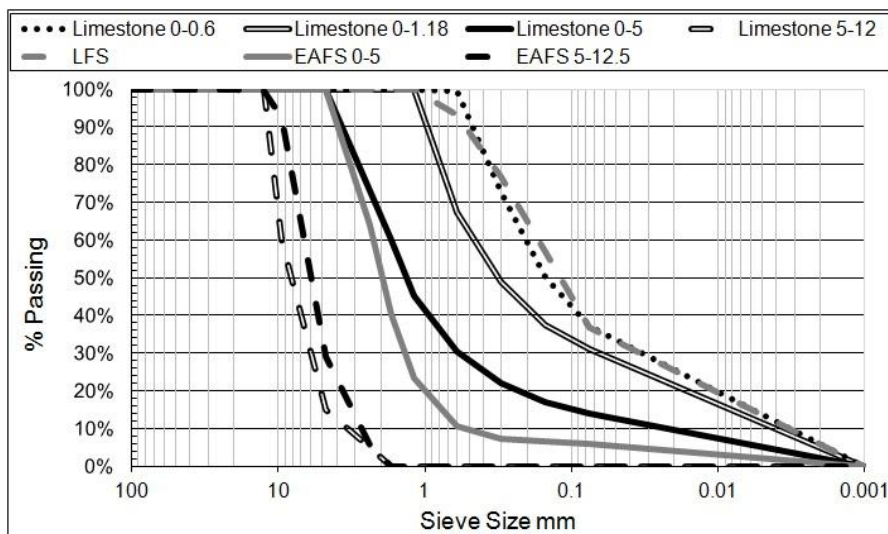
## **Materials and mixes**

### *Cement, water and natural aggregates*

A Portland cement type I 52.5 R was used in this research, except in one sample prepared with a Portland cement type IV/B-V 32.5-N that included a pozzolanic (fly ash) material in the mix; both in accordance with UNE-EN 197-1 standard [44]. Water with no compounds that might adversely affect the hydraulic cement mixes was taken from the urban mains supply of the city of Bilbao (Spain).



A commercial crushed natural limestone with a fineness modulus of 2.9 units, a maximum size of 5 mm, and a bulk density of 2.6 Mg/m<sup>3</sup> was used as a fine aggregate in some mixes. The same material was also used to increase the workability of other mixes (see Table 1) after screening through 0-0.6 mm and 0-1.18 mm sieve ranges, with fineness moduli of 0.7 and 1.5 units, respectively. A coarse crushed limestone aggregate (5-12 mm) of the same density was also used in one case, see Table 1. The main mineral component of all these aggregates was calcite (95%). The gradation of all of the above-mentioned fractions is shown in Figure 1.



Some earlier works by the authors [31,38,39] contain more detailed descriptions of this type of LFS slag. Those properties provide complementary information to the analysis presented in this study.

(\* ) Equivalence to the type IV cement used (EN 197-1).

Mix Design (kg/m <sup>3</sup> )		P1	P2	P4	P5	SC1	SC2	SC3
CEM I 52.5 R		300	300	350	350	350	350	210(*)
Fly ash								140
Limestone	Sieved fraction <0.6 mm		760					
	Sieved fraction <1.2 mm			450	680	680	900	900
	Fine aggregate <5 mm	1050				550		
	Medium aggregate 5-12 mm					720		
LFS			80					
EAFS	<5 mm		550	800	700		550	550
	5-12.5 mm	1050	750	1050	900		670	670
Water		160	200	180	180	180	195	195
Plasticizer (% weight of cement)		2	2	2.5	2	2.5	2	2
Fresh density (Mg/m <sup>3</sup> )		2.6	2.65	2.84	2.75	2.46	2.62	2.65
Occluded air (% vol)		1.9	2.5	2.1	2.4	1.6	2.2	6.3
Slump/Spread in Abrams cone (mm)		160/	180/	180/	220/450	/580	/680	/560

**Table 1:** Mix composition

Compounds (% weighth)	EAFS (0-5mm)	LFS
Fe <sub>2</sub> O <sub>3</sub> (%)	22.3	1.0
CaO (%)	32.9	59.2
SiO <sub>2</sub> (%)	20.3	21.3
Al <sub>2</sub> O <sub>3</sub> (%)	12.2	8.3
MgO (%)	3.0	7.9
MnO (%)	5.1	0.26
SO <sub>3</sub> (%)	0.42	1.39
Cr <sub>2</sub> O <sub>3</sub> (%)	2.0	--
P <sub>2</sub> O <sub>5</sub> (%)	0.5	--
TiO <sub>2</sub> (%)	0.8	0.17
Loss on ignition (%)	gain	0.5
MIP porosity average (%)	8	--
Specific gravity (Mg/m <sup>3</sup> )	3.42	3.03
X-ray diffraction main compounds	Wüstite- Ghelenite Kirsteinite	Periclase -Olivine Mayenite

**Table 2:** Chemical composition and physical characteristics of the slags

### Mixes: Proportioning and fresh properties

Seven different concrete mixes were prepared to study relevant aspects of their durability. Table 1 lists the details of their dosing. Mixes labeled Px can be considered as “pumpable mixes”, while those labeled SCx can be considered as “self-compacting mixes”, due to the evident differences in their workability, as reported in previous works by the authors [38]. The selection of mixes in the present article coincides with those used in the recent paper cited above, with the exception of mix P3 [38].

Mix P1 can be considered as a sort of “reference specimen”, due to its configuration as a mix that contains electric arc furnace slag as a coarse aggregate, and crushed limestone as fine aggregate. Mix SC1 could also be considered a “reference specimen” among the self-compacting mixes, due to the exclusive use of limestone aggregates in its composition. Mix P2 has a configuration close to self-compacting mix, but including

a small proportion of ladle furnace slag. The grading curves of all the mixes are shown in Figure 2.

The components of these different mixes were prepared in conventional mixers and cast in place in the fresh state in cubic molds of 100x100x100 mm and prismatic molds of 70x70x280 mm. Additional samples of some mixes were cast for other tests. Several tests were performed on the fresh mixes to verify their physical properties and their workability; some of these results are included in the last rows of Table 1. Details on these in-fresh tests have been extensively described in [38], as previously mentioned.

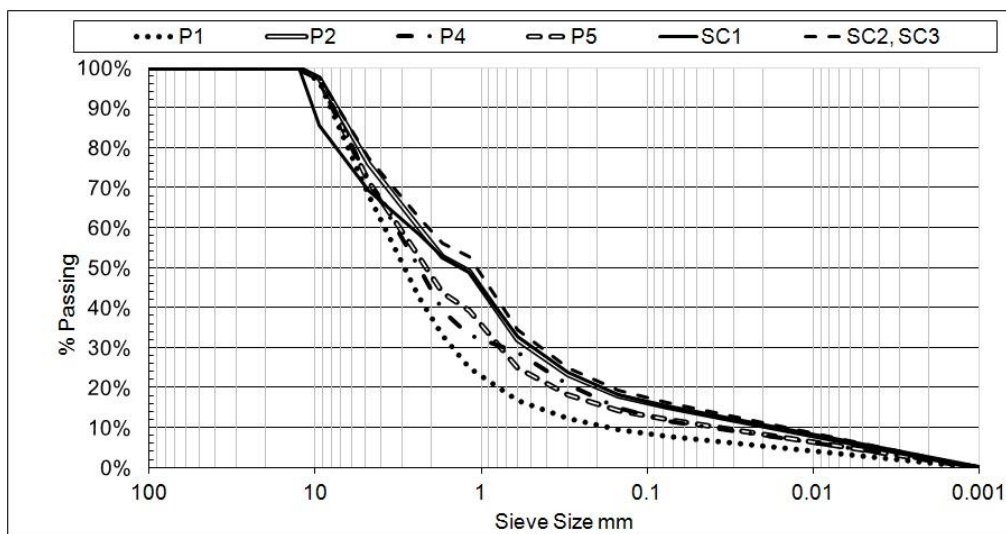


Figure 2: Proportioning of mixes.

## Mixes: Hardened properties

### Density and mechanical strength

The dry densities of the hardened concretes are shown in Table 3, which correlate well with the fresh densities shown in Table 1. The average density of the slag concretes increased from 12 to 15% with respect to those of concrete made using coarse and fine limestone aggregates, i.e. values in the interval of 2.5 to 2.6 in almost all mixes versus 2.35 Mg/m<sup>3</sup> shown by the SC1 mix.

The results of compressive strength after 7, 28, 90, 180 and up to 360 days of curing appear in Table 3. The mixes prepared with cement I 52.5R showed strength of over 45 MPa at 28 days. Mix SC3 prepared with the cement type IV only reached a similar strength after 180 days; the use of this sort of cement is not advantageous in terms of structural efficiency (strength/density ratio), and it has the highest index of occluded air from among all the mixes, due to the singular interaction between the plasticizer

and viscosity conditioner admixture and the pozzolanic addition (fly ash) [first article of mortars].

The results of the compressive strength of the “pumpable” mixes were similar in the P1 and P4 mixes. Mix P2 contains a significant proportion of ladle furnace slag, and mix P5 showed a lower strength associated with higher fine fraction content; however, this additional amount of fine fraction favored workability, essential in this work to obtain slumps as high as 220 mm in the Abrams cone test. Mix P5 was the last pumpable mix prepared to obtain self-compacting mixes in this work. The results after the Brazilian test in terms of tensile strength, close to the level of 5 MPa, are coherent with the compressive strength of the concrete and showed a good quality material.

(\*) mix SC-3 showed 50 MPa after one year

Property	P-1	P-2	P-4	P-5	SC-1	SC-2	SC-3
<b>Compressive strength 7 days(MPa)</b>	61	46	61	39	44	47	19
<b>Compressive strength 28 days(MPa)</b>	67	54	69	46	51	53	31
<b>Compressive strength 90 days(MPa)</b>	68	56	71	54	56	55	36
<b>Compressive strength 180 days(MPa)</b>	73	60	74	62	64	61	41.5 (*)
<b>Brazilian test at 360 days (MPa)</b>	5.02	5.22	5.96	5.5	4.45	4.62	5.43
<b>Dry density (Mg/m3)</b>	2.51	2.5	2.63	2.59	2.35	2.53	2.5
<b>MIP porosity (% vol)</b>	12.3	15.5	15.2	13.5	9.9	16.6	17.5

**Table 3:** Strength and MIP of the mixes

The self-compacting mixes SC1 and SC2 showed lower compressive strength levels than the higher quality pumpable concretes P1 and P4 but similar to those P2 and P5; the results of SC1 and SC2 at 28 days were in the interval 50-55 MPa versus 65-70 MPa in good pumpable concrete. The high amount of fine fraction materials and the higher water-cement ratio (indispensable to obtain the appropriate workability) weakened the short-term strength of the self-compacting mixes; in the long term, SC1 and SC2 reached fairly good values of 60-65 MPa. The global results (in both the fresh and the

hardened state) obtained in the SC2 mix can be qualified as excellent and represent the best performing self-compacting concrete to emerge from this work. Mix SC3, made with type IV cement, reached 50 MPa after one year.

### MIP analysis

Mercury Intrusion Porosimetry (MIP) was employed, using an Autopore IV 9500 apparatus (Micromeritics) at a pressure of 33,000 psi, to study the pore structure on samples held for 180 days in a moist chamber. The specific results of the pore structure of a concrete that the MIP analysis provides are indispensable to any evaluation of the resistance of concrete mixes to deterioration. Remembering the general rule, the porosity of these cementitious matrixes is in proportion with the water used in the mix, minus the water fraction absorbed by EAF slag.

The values obtained in terms of global porosity were, in general, within the range of 12-16%, with the exception of mix SC1 containing conventional limestone aggregates. It should be noted that the total measured porosity is the addition of porosity from the capillary water of the matrix, added to that coming from the present EAF slag which represents between 40 and 60% of the total volume. The MIP porosity of the EAF slag was within an interval of 4-10% (in our case close to 8% as it has been included in Table 2), and the most frequent pore sizes were between 0.2 and 50 microns, as in Figure 3, but the structure of this porosity differs from that of the cementitious matrix: it arises from the cooling of the slag and the associated phenomenon (slag foaming, gas vacuoles, phase transformations, and thermal contractions...). In fact, the water absorption of EAF slag is, in general, higher than that showed by natural aggregates (in the order of 4-8%). Hence, the MIP porosity of SC-1, made with natural aggregates, is low in comparison with the MIP porosity of the other mixes containing EAF slag aggregate. In the P4 mix, an excellent compressive result was apparently associated with a higher MIP porosity value, but it has the highest content in EAF slag.

The graphics of pore size frequency distribution in the mixes are shown in Figures 4a, 4b, and 4c. In Figure 4a the differential intrusion curve of mixes P1 and SC1 are shown; in Figure 4b mixes P4 and P5 show the capillary porosity of the cementitious matrix added to that coming from the EAF slag (peaks between 200 and 50,000 nm) and, finally, in Figure 4c the pore distribution of the P2, SC2 and SC3 is showed. In all cases, a significant peak (maximum frequency) exists in the vicinity of 100 nm (between the pore sizes of 40-150 nm), mainly due to matrix capillary porosity. If we exclude the contribution of the EAF slag MIP porosity, it can be stated that the MIP porosity of

these mixes is quite similar; as a consequence, the properties derived from this porosity will also be similar.

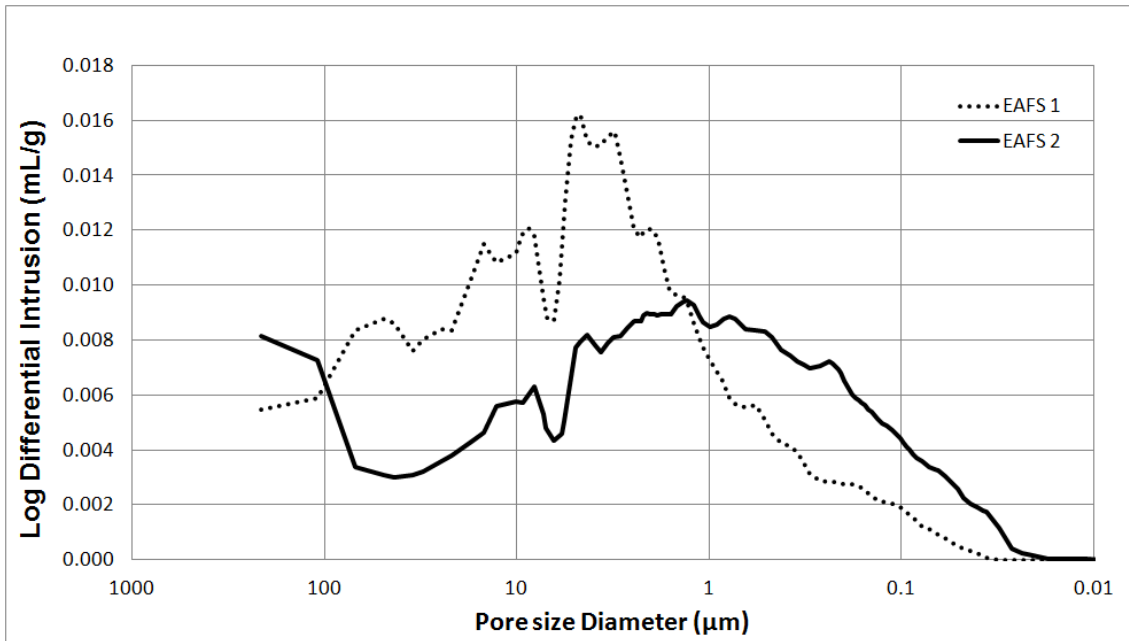


**Figure 3:** MIP results on two samples of the electric arc furnace slag used in this work.

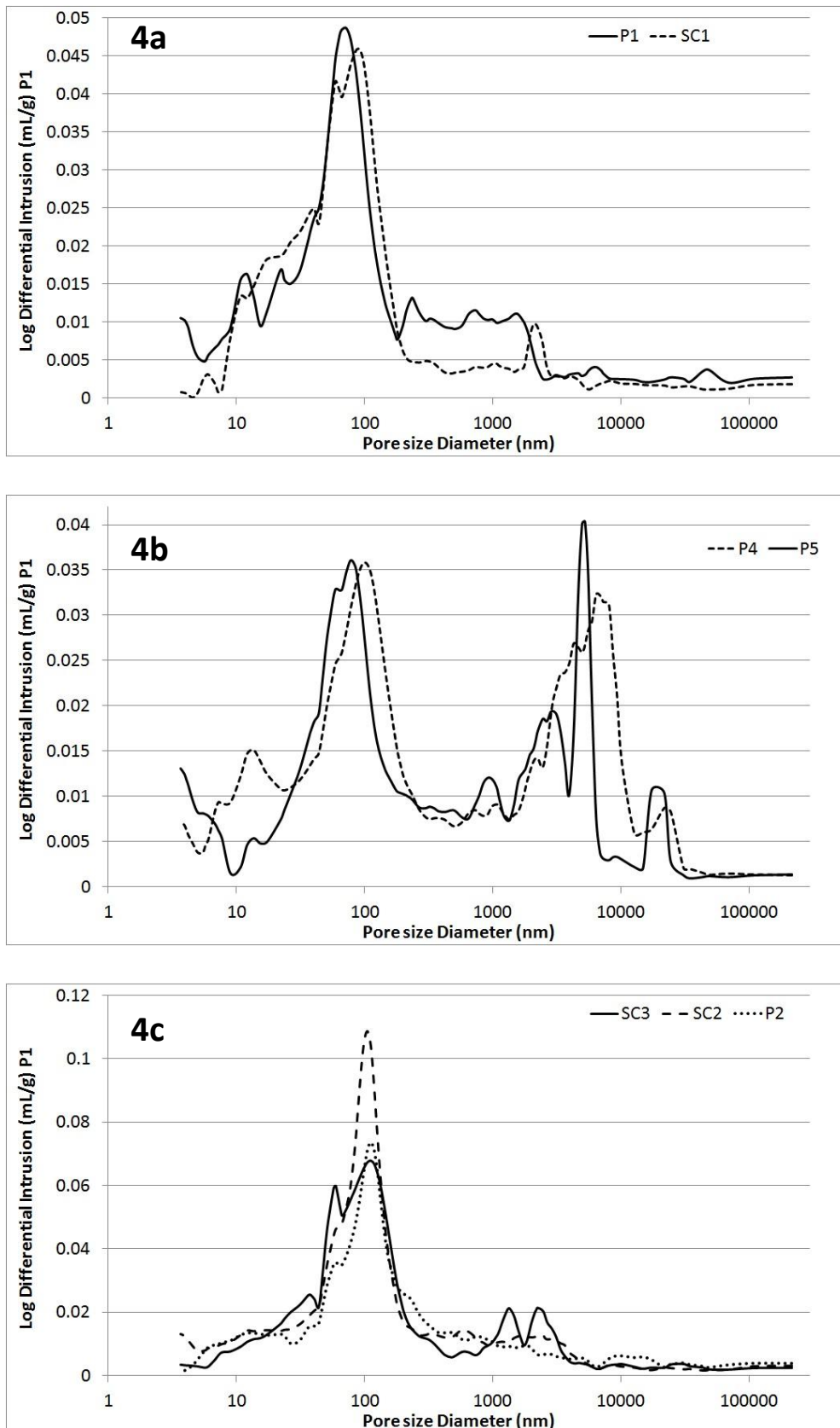


Figure 4a, 4b and 4c: MIP differential intrusion in mixes.



*Dimensional stability - Shrinkage.*

Prismatic specimens sized 70x70x280mm were used to evaluate the dimensional changes due to long-term dry shrinkage of the concrete mixes. These sample dimensions are acceptable for testing the mixes with a maximum aggregate size of 12 mm. Two samples of each mix were kept in air at room temperature over several months after their removal from the molds and their elongation was controlled in a rigid frame equipped with a suitable apparatus for length measurement.

Figure 5 represents the evolution of the shrinkage length for all mixes, where each point is the average of the measurements on two samples; the measured values were almost-constant from an age of 90 days. As Figure 5 shows, shrinkage values are globally smaller than in the pumpable mixes in the self-compacting mixes. As stated in recent works [39,46], the mixes with EAF slag as aggregate in general showed a slightly higher dry shrinkage than the mixes containing natural aggregates, due to the lower elastic modulus of EAF slag and the higher stiffness of the natural aggregates; the higher the proportion of EAF slag, the greater their contraction. If we take into account the higher volumes of EAF slag in several pumpable mixes (except P-1), the long-term results are coherent with these statements. Mix SC-1 contained no EAF slag and had the smallest shrinkage value; on the contrary, mix P-4 that contained EAF slag had the highest shrinkage values and showed the highest contraction from among the pumpable mixes.

As stated in previous [39], the influence of a pozzolanic addition as fly ash can slightly increase the shrinkage values, and the presence of ladle furnace slag can, due to its expansion, slightly mitigate these values. However, these effects are not visible in the concrete mixes tested in this study, due to the decisive influence of coarser aggregate stiffness; hence the final shrinkage rate of mix SC-3 is close to that of mix SC-2.

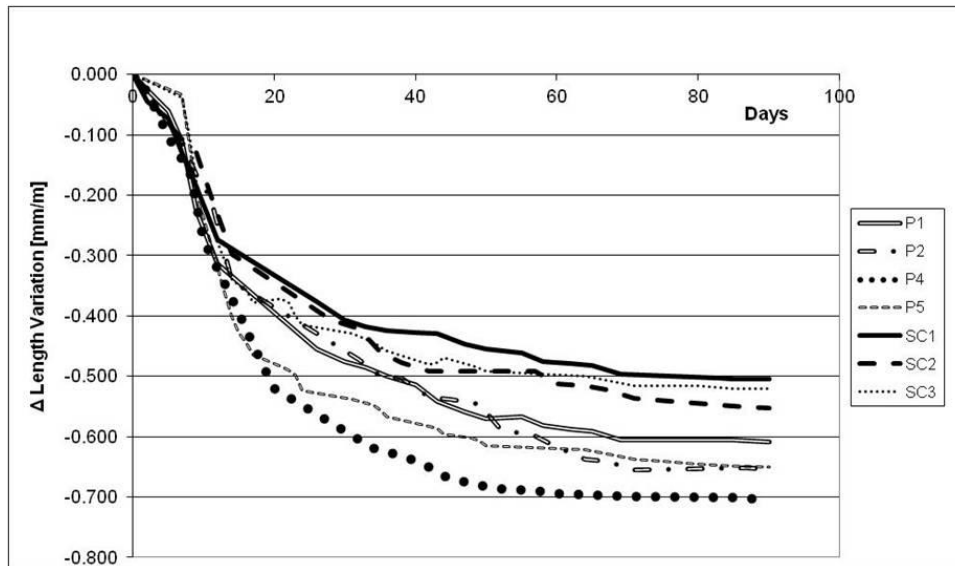


**Figure 5:** Shrinkage contraction of mixes

### Water penetration under pressure

Conventional tests on the penetration depth of water under pressure were performed on the concrete mixes in accordance with the EN 12390-8 standard [44]. The results provide an idea of concrete permeability and, therefore, an idea of the durability of these mixes in the face of tests in which interaction with water plays a decisive role. The samples had previously been immersed in liquid water until saturation (until constant weight). Table 4 shows the results in terms of the evaluation of the water penetration area (maximum and average depth of penetration), measured on the region of the sample in which the liquid water is visible after breakage in a Brazilian test. The indirect tensile strength of the samples was also evaluated in this final rupture test.

In general, the mixes containing EAF slag showed better resistance to water penetration (impermeability) than concrete made with natural aggregates. As shown in Table 4, the maximum of all the EAF slag mixes was below 20 mm in the water penetration test, which is a very good result in terms of mix quality. Good durability results may be expected in tests exposing the concrete to water.

Mix	P-1	P-2	P-4	P-5	SC-1	SC-2	SC-3
<b>Maximum (mm)</b>	16	18	14	10	25	19	15
<b>Average (mm)</b>	10	8	9	7	16	8	7

**Table 4:** Test results of water penetration under pressure.

Capillary absorption of water

Capillarity tests were performed on samples according to the UNE 83982 standard [44], “Determination of the capillary suction in hardened concrete. Fagerlund method”. The Darcy laws of water permeation in porous media are always behind these considerations.

In this test, the lower faces of 100 mm x 100 mm cubic samples were exposed to water by placing them in a tray. The 5 mm thin layer of water in the tray rises by capillary action from the bottom to the top of the sample. In this case, half of a 100 mm cubic samples (50 mm high) of mixes are placed on some coarse sand particles that assist the penetration of the water through the lower cut face (both aggregate and matrix visible, with no skin effect) of the sample and to ascend by capillarity to the upper face. The mass gain of the sample is periodically evaluated. Curves representing this mass gain against the square root of time are drawn, as shown in Figure 6. The test ends when the absorption of water terminates and the mass of the saturated sample stabilizes and remains constant over time.

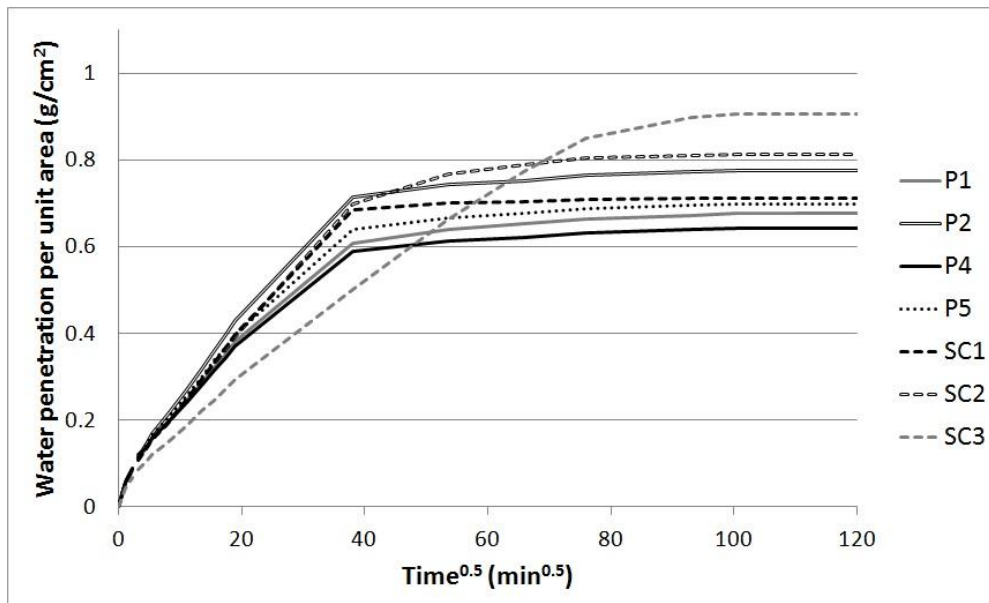


**Figure 6:** Capillary absorption of mixtures.



**Figure 7:** Mix SC3 showing high spherical porosity.

The Fagerlund method requires the calculation of three magnitudes; first, the resistance to water penetration  $m$ ; second, the effective porosity  $\varepsilon$ ; and third, the capillary absorption coefficient  $K$ . The first is a value representative of the resistance (inverse of speed) to the permeation process in square root units of time divided by height of penetration, the second represents the porosity of the available concrete that can be filled by water, and the third is a global characteristic of the capillary process, in terms of its unitary mass of absorbed water divided by the exposed surface and square root of the time unit. This magnitude is really a combination of the two former variables. The usual units in these calculations are grams, minutes and centimeters, following the traditions of Darcy's law.

The influence of these characteristics on the durability of concrete, in situations where the water (rain, sea or river immersion) is present, is decisive, i.e. freezing-thawing, wetting-drying and exposure to sea environments. Concrete permeability and resistance to the penetration of liquids is also assessed in this test.

The results obtained for all of the mixes are compiled in Table 5; the differences between them are small except for mix SC3, made with cement type-IV, which included a high content of fly ash. This mix showed a lower slope than the other mixes under consideration (higher value of “ $m$ ”) in the rising zone of the curves. In Figure 7, the large amount of spherical pores can be appreciated, due to the occluded air of this mix (Table 1, value 6.3%). It is well-known that the presence of these spherical pores leads to concrete mixes of low-permeability. Additionally, the higher effective porosity “ $\varepsilon$ ” is shown in this test, in coherence with the results of its MIP porosity.

Among the other mixes, the differences are of minor magnitude; the presence of ladle furnace slag in mix P2 led to a slightly higher capillary coefficient. The difference between mixes SC1 and SC2 deserves comment; in the first state of the Fagerlund curve (before the sharp point in the abscissa “ $t_n$ ”) the curves coincide almost perfectly; in the second part of the curve, there is a gentle-slope in the last zone in which other kinds of porosities (other than capillary porosity) are prevalent, the almost null porosity of the limestone aggregate and the high porosity of the EAF slag can be easily appreciated constituting total effective porosity.

	$\Delta$ Weighth (g)	sqrt $t_n$ (min <sup>0.5</sup> )	m (min/cm <sup>2</sup> )	$\epsilon_e$ (cm <sup>3</sup> /cm <sup>3</sup> )	K (g/(m <sup>2</sup> * $\sqrt{\text{min}}$ ))
<b>P1</b>	67.7	35	49	0.1354	1.93
<b>P2</b>	77.7	34	46	0.1554	2.29
<b>P4</b>	64.3	33	43	0.1286	1.96
<b>P5</b>	69.8	34	46	0.1396	2.06
<b>SC1</b>	71.2	35	49	0.1424	2.03
<b>SC2</b>	81.4	42	70.5	0.1628	1.94
<b>SC3</b>	90.6	66	172.8	0.1812	1.38

**Table 5:** Capillary results

## Durability tests

### Freezing-thawing tests

Two 100x100x100 mm cubic samples from each of the mixes were tested in freezing-thawing tests after a curing time of 90 days immersed in water. The whole freezing-thawing test comprised 122 cycles, each lasting for one day, at which point the test ended with the appearance of large-scale cracking on the sample surface (the cracking became apparent from cycle 105). A full 48-hour cycle involved 24 hours of storage in a freezer at  $-15\text{ }^{\circ}\text{C}$  followed by 24 hours of immersion in water at room temperature. The structural state of the samples was periodically controlled by verifying their external appearance and by measuring the ultrasonic pulse velocity, as an estimation of the stiffness of the concrete. Finally, a compressive test of the samples was performed when their deterioration was evident, and their final mass was measured; the results are compiled in Table 6.

(\*) this strength results after 180 days of curing; the hydration of pozzolan does not stop during the tests.

Mixture	Strength 90 days (MPa)	Stiffness before (GPa)	Strength frozen (MPa)	Stiffness frozen (GPa)	Mass loss frozen (g)/2500	Strength moist (MPa)	Stiffness moist (GPa)	Mass loss moist (g)/2500
P1	68	57.5	45.7 (-33%)	36.1 (-37%)	39.5	40.2 (-41%)	31 (-46%)	127
P2	56	45.6	37.8 (-32%)	29.8 (-35%)	23.8	53.5 (-4.5%)	38.8 (-15%)	140.5
P4	71	59.5	41.6 (-41%)	31.6 (-47%)	60	68.9 (-3%)	50.7 (-15%)	162.6
P5	54	50.6	48.3 (-11%)	42.8 (-15%)	54.4	52.9 (-2%)	47.2 (-6.7%)	116
SC1	56	46.4	44.5 (-21%)	45.1 (-2.8%)	37.5	54.8 (-2.1%)	46.4 (-0%)	131
SC2	55	47.5	41.1 (-25%)	45.1 (-5.1%)	55.9	55 (0%)	47 (-1.1%)	158.5
SC3	41.5(*)	42.6	44.2 (+6.5%)	46.6 (+9.4%)	24	44.6 (+7.5%)	37 (-13%)	201.9

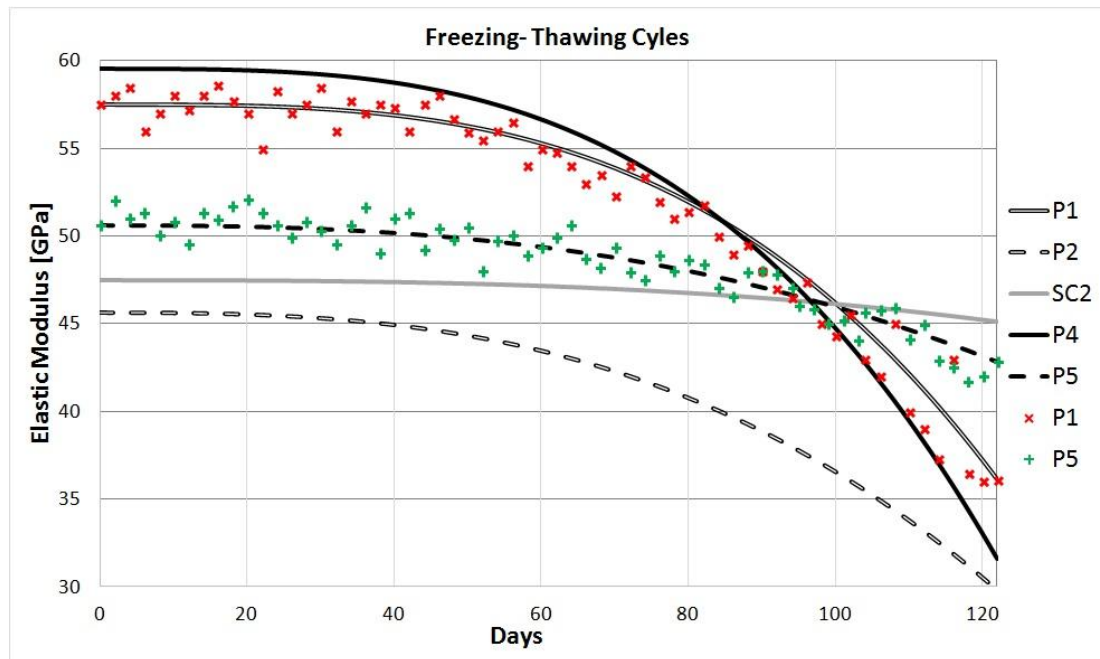
**Table 6:** Stiffness, Strength and mass variations after freezing thawing and wetting-drying test.

Figure 8 shows the results of the ultrasonic stiffness evolution over time; mixes P1 and P4 showed a sharp fall. As shown in Figure 8 and in Table 6, only a few mixes passed this severe test with a tolerable loss of strength and stiffness, because a loss of more than 20% of the initial value implies that the concrete is damaged. However, the set of compressive strength values of our mixes after the test, contained in the interval 37 to 48 MPa, implied no dramatic detriment face to their structural use. Also, the loss of mass was in the same order of magnitude in all of the mixes.

Considering both strength and stiffness together, better behavior is shown by mixes P5, SC1, SC2 and SC3, which all share the common characteristic of their high proportion of limestone fines. In particular, mix SC3 also has a notable proportion of occluded air, contains fly ash, and shows low capillary absorption-permeability. Additionally, the presence of delayed pozzolanic reactions of the fly ash is reconstructive; in absolute terms, the compressive strength of the SC3 concrete after the test is a good value.

Moreover, the type of porosity in SC1 explains its slight loss of stiffness that differs from the stiffness loss of the mixes containing EAF slag, which have two pore-types, pores in the matrix and pores in the slag. The additional porosity provided by EAF slag

to global concrete is not a positive factor. It may be recalled that the presence of EAF slag in the concrete will not favor this kind of durability, as previously observed [29]. Finally, the presence of LFS appears to have no clear influence on the results.



**Figure 8:** Stiffness variations during the freezing-thawing test

Wetting-drying tests

The wetting-drying test was performed by following the guidelines of the ASTM D 559 standard [47], although the standardized procedure was not rigorously followed, but was adapted to these mixes and samples. Once again, two cubic samples sized 100 mm for each mix were tested after a curing time of 90 days immersed in water. The study comprised 148 cycles each lasting one day, with the end of the test defined by the point at which the material loss at the edges of the samples was considered excessive (the loss appeared from cycle 118). A full 24-hour cycle consisted of the immersion of the samples in water at room temperature for 16 hours, followed by forced oven-drying at 60 °C for 6 hours, and then by air cooling for 2 hours to avoid thermal shock. As in the former case, the structural state of the samples was periodically controlled, verifying their external appearance, and also measuring the ultrasonic pulse velocity, as an estimation of the stiffness of the concrete, the variation of the stiffness during the test it is shown in Figure 9. Finally, a compressive test on the samples was performed when evident deterioration was detected and the final mass was measured. Table 6 shows the average results of the compressive tests, stiffness and mass

variation on samples subjected to the wetting-drying cycles and their percentile variations.

As shown in Table 6, almost all the mixes passed this test with a tolerable loss of strength and stiffness, having the same order of magnitude for loss of mass in all mixes. It may therefore be stated that the behavior of the mixes with EAF slag aggregate in the wetting-drying was acceptable. The better behavior, mainly in terms of stiffness, is again showed by mixtures whose singularity is the higher content of fines. As in the former case, the LFS presence had no influence on the results. Also, the long-term structural reconstruction of the pozzolanic reaction is effective in mix SC3.

Mix P1 showed the worst behavior, which has normal porosity, normal capillary absorption and good strength; hence this result was unexpected and slightly surprising. There appears to be no clear reasons that can explain its detrimental behavior in this kind of test; mix P1 supported the thermal shock in this test worst of all. The co-existence of two types of aggregates (natural and slag aggregate), which have quite different physical properties, in sizes larger than 1-2 mm (we must remember that this aggregate size value is the diffuse border between whether or not it forms part of the concrete cementitious matrix) could be identified as a cause of deterioration in a test characterized by severe thermal shocks.

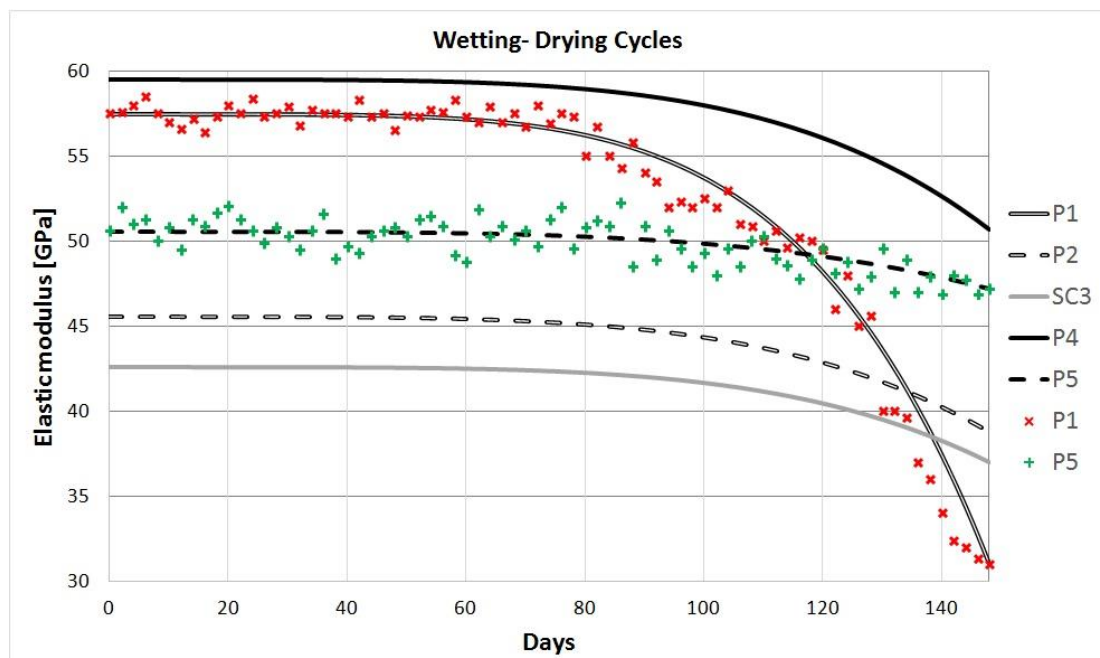


**Figure 9:** Stiffness variations and external aspect of several samples after the wetting-drying test



*Marine environment tests. Penetration of chlorine and sulfate ions.*

One application of concrete made with EAF slag as aggregate over the past few years (and nowadays in the port of Bilbao) is the construction of coastal defenses (dykes) against storms, in the breakwater structures of a marine environment. There is no reason why the same kind of concrete may not be used in other on-shore structures such as docks, wharfs, and quays. In view of these applications, further studies of the durability behavior of these reinforced concretes against saline water are very relevant.

The first part of this study is centered on ionic penetration into the concrete mass. Chlorine and sulfate ions permeate marine environments, are of potential danger and have to be monitored. The exposure of the samples to marine environments was done by suspending them in cages, at level zero of the Pasaia Donibane port. Hence, the samples suspended at “elevation zero” or at the “central level” of the intertidal zone, were exposed to tidal movements twice a day. They were soaked, as a result, for 12 hours every day and were exposed to the atmosphere over the remaining time, undergoing two wetting-drying cycles every day. The duration of the tests was classified into two groups, short-term tests during one year and long-term tests, over five years.

The concrete mixes used in these tests were chosen as follows. In the short-term test, all the concrete mixes described in section 3 of this article were tested. In the long-term test, mix P4 was used as an EAF slag concrete; additionally, another mix identical in volume to P4 but containing limestone aggregates, named P4CA, was used as a conventional aggregate concrete. These two long-term mixes were also used in the next section, to analyze the corrosion problems of the concrete reinforcement bars (rebars).

In general, 100x100x100 mm cubic samples were used in the short-term test. Following exposure to the marine environment, suitable pieces of the samples were cut to evaluate the presence of ions from the external surface to the center of samples, along a 50 mm fracture surface of the sample. The samples were placed in a nitrogen scanned camera of a low-vacuum pressure scanning electron microscope to obtain backscattered electron images; the dispersive energy of X-ray micro-analysis technique was used to obtain the chemical composition.

Figure 10 shows the evolution of the chlorine and sulfate ion concentrations in the short-term test, from the periphery to the center of the samples, in those samples exposed to the marine environment. The evaluation of these elements was performed on sites chosen in a recent fracture surface of the sample, increasing the distance from the periphery towards the center of the cubes, at all times performing the micro-analysis on a small area of the cementitious matrix; the visible aggregates (slag or limestone) were avoided. Exponential equations were successfully used to adjust the numerical results, instead of the more complicated error functions. In several cases the whole set of numerical results was represented (chlorine concentrations in mixes P1 and P2, sulfur in P1), in other cases only the adjusted curve was drawn to avoid an excessive number of points on the graph.

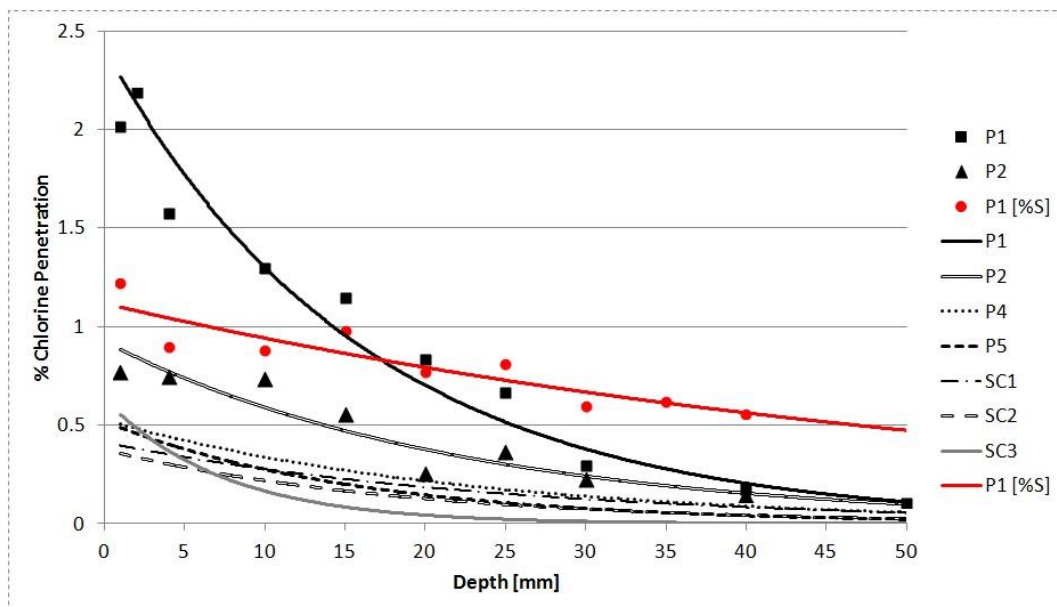


**Figure 10:** Penetration of chlorine and sulfur in mixtures.

Considering an amount of 0.1% as a “threshold value” in the chlorine content of a concrete matrix, it can be stated that some “pumpable” mixes showed a deeper penetration of chlorine (P1 and P2 in the order of 50 mm); penetration rates of almost 35 mm and 25 mm were observed in mixes P4 and SC1 and in mixes P5 and SC2, respectively. Mix SC3 is the most resistant against this penetration (estimated at about 15 mm), in coherence with its air-void structure and its low rate of capillary water uptake. Taking into account that the covering thickness of 40 to 60 mm prescribed for concrete marine structures is reached by any of the mixtures after one year of exposure, the results are not reassuring. Considering the higher volumetric proportion of slag aggregate in most mixes (except SC1), it can be stated that the presence of EAF slag has little effect on the penetration of chlorine ions in the concrete mass. In

comparison with the sample of conventional concrete, the improvement in the durability of EAF slag structural concrete under marine conditions was only very slight.

The proportion of chlorine in the cementitious matrix of the periphery of the pieces was especially high in mix P1, with values close to 2%; they were also higher in mix P2 than in the rest of mixes, which showed values in the order of 0.3-0.5%. Concerning the penetration of sulfur, mix P1 was the only mix that showed values higher than “normal” concrete values (close to 1% versus “normal” values of 0.6-0.7%) a few millimeters deep; hence, the dangerous risk of the appearance of secondary ettringite or thaumasite in the peripheral zone of the pieces is, in general, very low.

It has to be reiterated that the poor behavior of mix P1 in the marine environment does not respond to a clear reason, although it is coherent with the results of the wetting-drying test. It should also be remembered that marine exposure in the intertidal zone means that a wetting-drying cycle is repeated twice a day. The results of mix P2, containing a small proportion of ladle furnace slag, were less detrimental than P1. In general, self-compacting mixes performs better in these short-term tests in the marine environment.

In the long-term test, 150x300 mm cylindrical samples were exposed to a marine environment for over five years. The analyses were performed on concrete mixes P4 (with EAF slag) and P4CA (with limestone aggregate), using 200 mm portions in length of the aforementioned  $\phi 150$  cylindrical samples, obtained after an initial transversal cut that shortened the overall length by 100 mm, and subsequent breakage of the longer piece in a Brazilian test. Figure 11 shows the test result on mix P4 (EAF slag aggregate), where there is a macroscopic change of color in the presence or absence of ions.

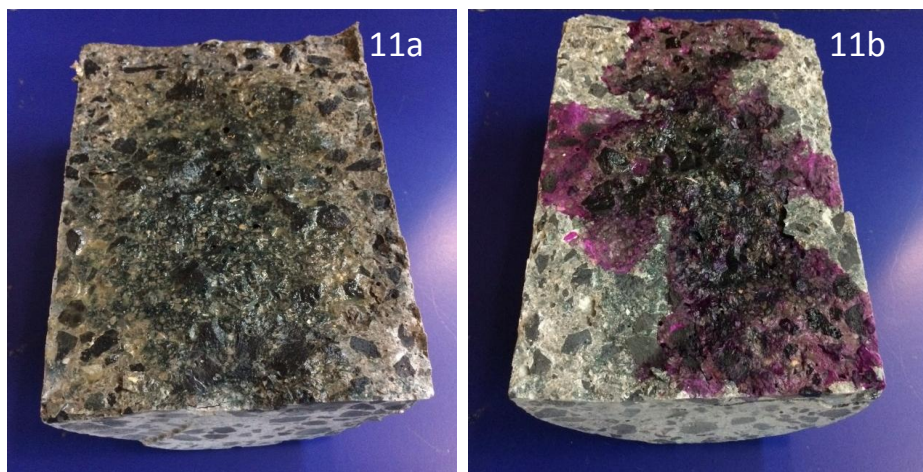


**Figure 11a and 11b:** Sample P4 after chloride (a) and after carbonation (b) penetration analysis.

A recently broken surface, Figure 11a, was sprayed with a silver nitrate solution, in order to detect ionic chloride penetration. If chloride ions are present in a proportion higher than a certain threshold, the natural surface color will remain unchanged; on the contrary, if the proportion of chloride is lower than the threshold, the surface becomes slightly darker. Obviously, this test yields broad results (all standardized tests of this sort show low accuracy), but it is nevertheless useful to ascertain a general state of the samples; the most significant variable is the value of the threshold, which must be near the maximum content of chlorine allowed by usual standards. In Spain, this value is fixed at 0.4% of cement content, a value equivalent to 0.06-0.08% in our mixes. The active chemical reagent used in our test was prepared to change the light shading at the aforementioned threshold.

The results of chloride penetration revealed total penetration after five years in the natural (limestone) aggregate mix, P4CA, i.e. 75 mm of the radius. However, in the case of mix P4, see Figure 11a, the average penetration was not at the middle of the radius, and was fixed at 30 mm; obviously, on the cut face (front) the dark zone is emergent. It may be concluded that the presence of the slag in these concrete mixes is positive.

The evaluation of carbonation performed on the aforementioned mixes, P4 and P4CA, was done with a similar test, by spraying a phenolphthalein solution on the recently broken surface of the samples. As is well known in chemical analysis, a  $\text{pH} > 9.5$  corresponds to an intense pinkish color in the solution that extends across the visible surface. Unlike the spraying method for the detection of chlorides, in this case only one significant region is sprayed, shown in Figure 11b, so that the ordinary tone of the concrete remained as a reference in the not-sprayed region. The dark pink color appeared very quickly, indicating a high value of pH.

The results of this latest test showed that carbonation does not exist in both concrete mixes after five years of exposure to tidal zones. The pH was higher than 9.5 units in the breaking surface of mixes P4 and P4CA, revealing the abundant presence of Portlandite in the concrete mass as a factor that determines a high pH, collaborating in the protection of the reinforcing steel bars.

### Corrosion of reinforcement bars

Structural concrete is a composite material consisting of concrete and steel reinforcing bars; the tensility of the steel withstands the external tensile stresses and the compressive forces are supported by the concrete mass. Several aspects of this composite (steel-concrete) coupling are decisive in achieving this effect; among which, the role of the concrete mass in the protection of the reinforcing steel bars against electrochemical corrosion in aqueous environments containing chlorine ions may be mentioned.

The concrete protects the steel from environmental corrosion at two levels; firstly, as a physical barrier of low permeability (covering concrete layer), and secondly as an electro-chemical protector granting a basic pH in the vicinity of the steel bars. Further study of the durable properties of EAF slag concretes in contact with steel rebars is reported in this section, in an attempt to analyze the protection against corrosion of this kind of slag concrete, in comparison with the protection given by ordinary aggregate concrete or “conventional concrete” (in this case, concrete made with crushed limestone aggregate).

EAF slag concrete and conventional concrete, both including reinforcing bars, were tested in the following way:

- Durability tests (wetting-drying with seawater, saline fog chamber submission) were performed on samples of reinforced concrete.
- Electrochemical corrosion variables (current density and electrochemical potential) were periodically controlled on the steel reinforcement.

The samples consisted of 150 mm x 150 mm cubes, into which a small steel structure formed of 10 mm diameter bars was embedded. Figure 12 shows the internal layout and the external appearance of these specimens. The emergent central steel bar was used as an electric contact to perform the measurements, which reflect the electrochemical evolution of the internal steel structure.

The concrete mixes used in these tests were chosen as in the former section. Mix P4 was used as an EAF slag concrete; and mix P4CA, identical in volumetric proportions to P4 with limestone aggregates in substitution of EAF slag, was used as a conventional aggregate concrete.

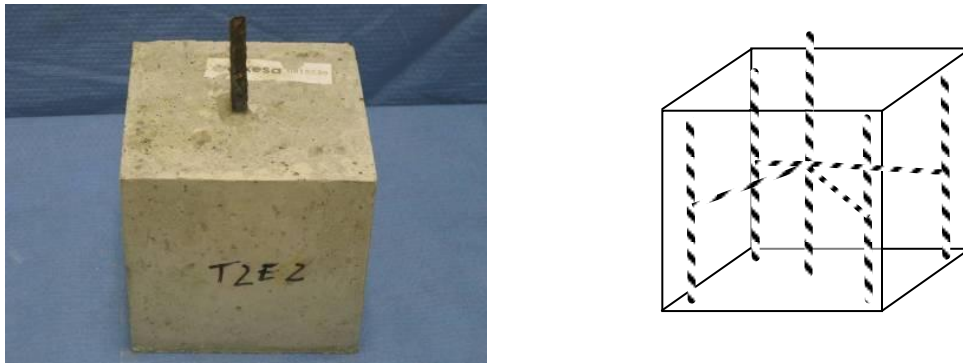


**Figure 12:** External appearance of samples and internal rebar layout

The corrosion risk of rebars embedded in a cementitious material depends on the electrical potential that is measured; in general, the specifications of the ASTM C-876 [47] standard are used, which indicates that an electrical potential lower than -400 mV corresponds to a very high risk. In our testing, the values were always in this risk zone except in the first moments of the durability tests.

The measure of electrical intensity (current density or electrical intensity divided by area) is a measure of the corrosion rate of the steel rebars. Hence, the main results of these tests center on the measurement of the current density over time in the corresponding wetting-drying and saline fog chamber tests. The limit between active and passive corrosion is placed at 0.1-0.2  $\mu\text{A}/\text{cm}^2$ , which in terms of generalized corrosion implies around 1-2  $\mu\text{m}/\text{year}$ . Table 7 indicates these effects.

$i_{\text{corr}}$ ( $\mu\text{A}/\text{cm}^2$ )	Corrosion
< 0.1	Low
0.1-0.5	Moderate
0.5-1	High
>1	Severe

**Table 7:** Steel reinforcement corrosion current density

The wetting-drying test using artificial marine water, in which the samples of this test were placed, has previously been described in the earlier section; in this case the thermal shock was in fact mitigated and significant results in terms of corrosion variables were obtained, while avoiding disintegration of the concrete mass. The samples were electrochemically controlled every 10 cycles, and the results are represented in the graphs in Figure 13, alongside an image of the EAF slag samples at the end of the test. It is relevant to point out that the results are highly scattered in

these tests and that very many measures are required before the tendency may be deduced as an average of the data cloud.

The obtained results showed a clear step in the results, probably associated to the moment in which the chloride ions arrive to steel bars in a steady state; the initial transient state corresponds to a “first phase” or “first stage”. Throughout this first phase of the test (around the initial 150 to 200 cycles), the corrosion rate can be considered almost constant and with a low average in both types of concrete. In the case of the EAF slag concrete the value was  $0.11 \mu\text{A}/\text{cm}^2$ , while the value in CA concrete was about  $0.17 \mu\text{A}/\text{cm}^2$ , with a moderate risk of corrosion risk according to the measure of the corrosion potential. In the last phase of the test, from 200 to 330 cycles of the test extension, the corrosion rates are higher, so the behavior of the concrete containing natural aggregates ( $0.77$  versus  $0.40 \mu\text{A}/\text{cm}^2$ ) was clearly worse than the results of the EAF slag concrete, with a notable risk of corrosion in both cases. There is little difference between the two types of concrete in terms of standard electrochemical evaluations of corrosion, in which variations lower than one order of magnitude (multiplying by ten) are of little importance, but the protection of the steel rebars in a marine environment is undoubtedly more effective in the concrete made with electric arc furnace slag as aggregate than in the conventional concrete aggregate.

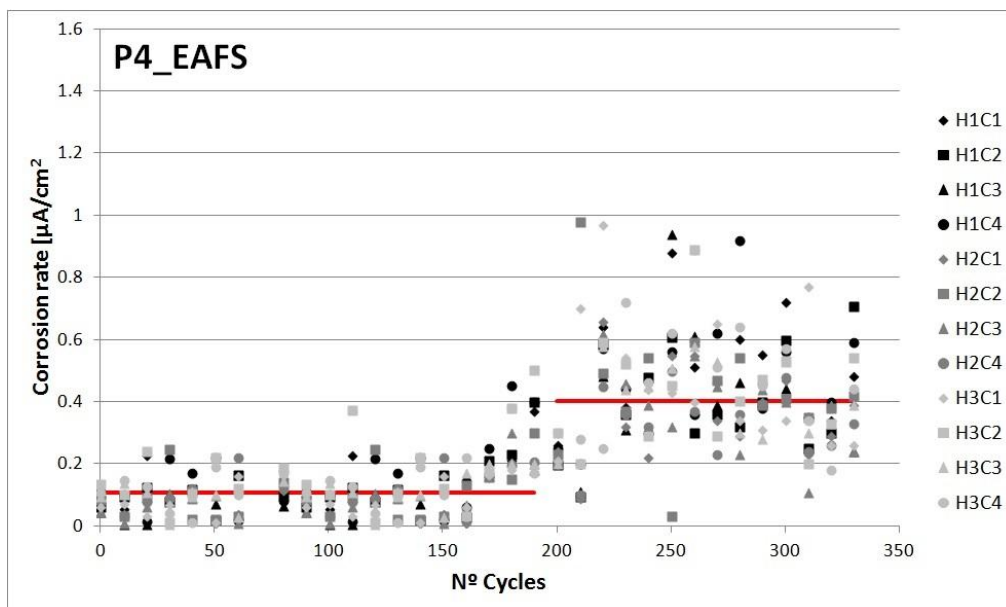
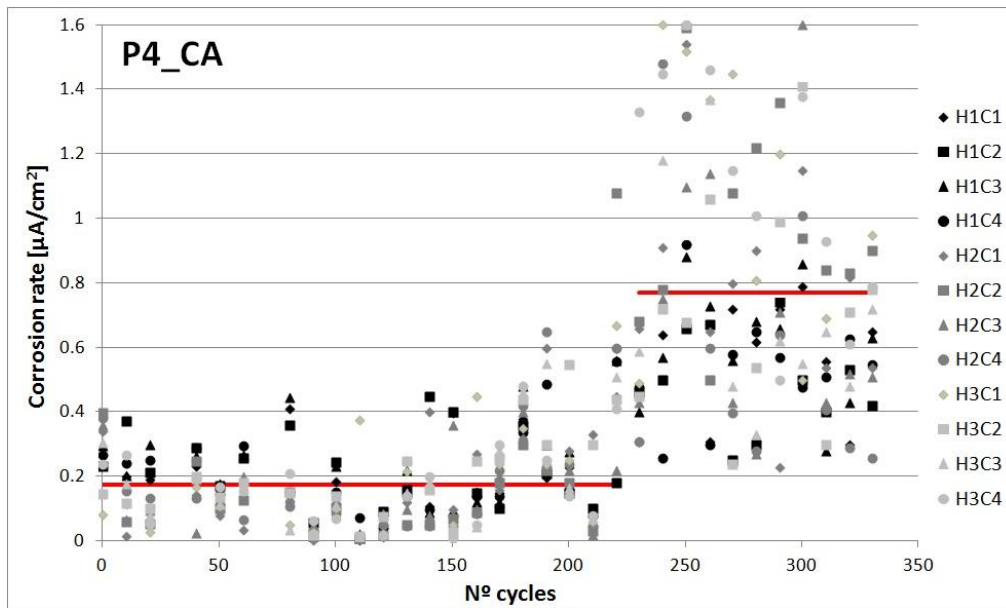


**Figure 13:** Corrosion rate in the two types of concrete after wetting-drying test. Image of EAF slag samples after the test



The saline fog chamber test was performed following the specifications in standard EN ISO 9227 [44]. An aqueous solution of NaCl is sprayed in the environment in a closed chamber, in which the samples are immersed. This test is extended over 3000 hours, with electrochemical measurements every 200 hours. After the test, the surface appearance of the samples was normal, see Figure 14; and the corrosion rate is shown in the graphs over time for the two mixes.

After around 1500 hours of exposure, in a similar way to the former tests, both mixes increased the corrosion rate from low values to higher values. The first stage values were  $0.1 \mu\text{A}/\text{cm}^2$  in the EAF slag concrete, and  $0.3 \mu\text{A}/\text{cm}^2$  in the conventional concrete. In the second stage (from 1500 to 3000 hours), the values rose respectively to  $0.28 \mu\text{A}/\text{cm}^2$  and  $1.5 \mu\text{A}/\text{cm}^2$  remaining almost constant until the end of the test. In this test, the long-term values reached by the conventional concrete were really severe; this situation denotes a worrying corrosion rate. The corrosion potential measurements indicate a high risk in both cases.

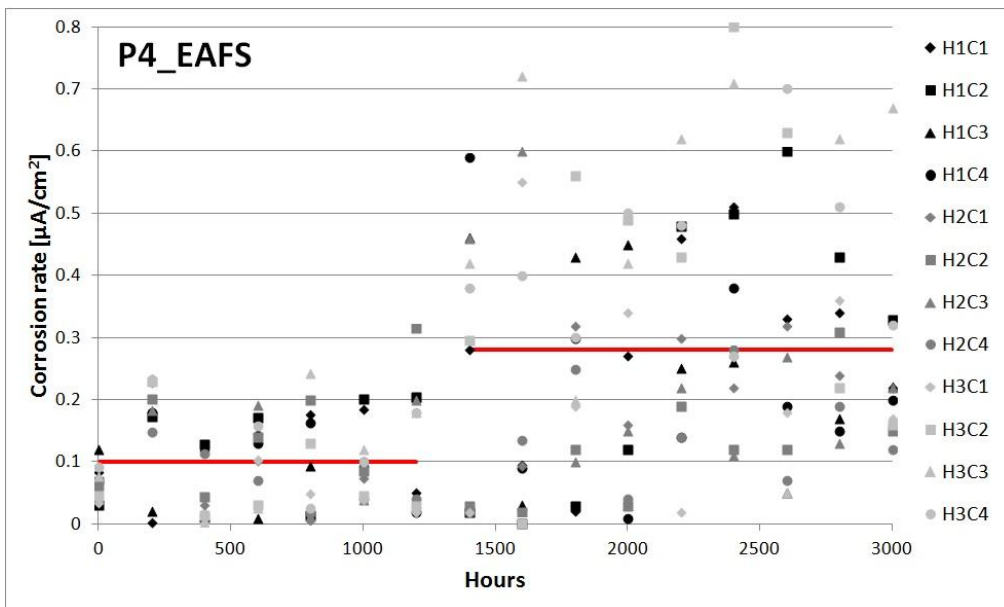
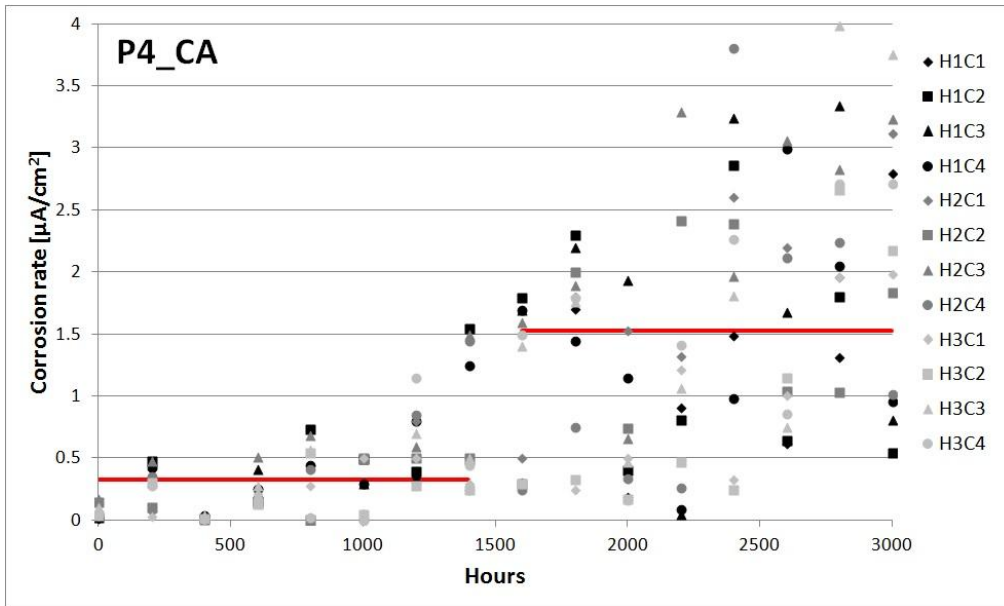


**Figure 14:** Corrosion rate in both types of concrete after a saline fog test. Image of samples after the test

In summary, it appears clear that the electrochemical corrosion rates of the steel rebars embedded in the conventional concrete (P4CA) shows a gradual evolution that is more detrimental than that of P-4 mix made with steelmaking aggregates. In the opinion of the authors, the EAF slag concrete is able over time to maintain higher pH values in the mass than the conventional concrete, these mixes showing slower steel corrosion rates in comparison with conventional concrete. This result can probably be associated with the slow but real lixiviation of (free) lime by the slag aggregate in the presence of external soaking in water, in a process that is clearly time bound.

Additionally, the hypothesis that the scarce presence of small metallic particles of iron (sized 0.5 to 2 mm) and the abundant presence of iron oxides in the slag can favorably influence (in a slight form) the global behavior of the mixes against rebar corrosion should not be discarded. This hypothesis should be confirmed in the future through long-term marine tests.

## **Conclusions**

Concerning the results obtained in this study, the following conclusions can be drawn:

The reuse of electric arc-furnace slag in the manufacturing of concrete has been shown to produce good quality mixes in terms of workability and mechanical strength. Self-compacting concrete mixes have been performed successfully, and the structure and several physical properties of these EAF slag concretes are similar to those of good conventional mixes.

The durability of concrete mixes that incorporate electric arc furnace slag as aggregate is, in general, fairly good, and similar to conventional mixes. In terms of their durability in aqueous environments, the comparison between these mixes and the mixes of conventional aggregate have neither shown clear benefits nor shown detrimental effects in either mix.

The advantageous resistance of the concretes incorporating electric arc furnace aggregates against steel rebar corrosion was only apparent in the electrochemical corrosion tests.

## References

- [1] Akinmusuru JO. Potential beneficial uses of steel slag wastes for civil engineering purposes. *Resources, Conservation and Recycling* 1991;5:73-80.
- [2] Morino K, Iwatsuki E. Utilization of electric arc furnace oxidizing slag. *Proc TMS Fall Extract Process Conf* 1999;1:521-30.
- [3] Rubio AR. La aplicación de las escorias de ACERIA en carreteras. , 1991.
- [4] San José J, Uría A. Escorias de horno de arco eléctrico en mezclas bituminosas. *Arte y Cemento* 2001:122-5.
- [5] San José J. Reutilización y valorización en obra civil de escorias de horno de arco eléctrico producidas en la CAPV. *Arte y Cemento* 2000:124-6.
- [6] European comision. Action Plan for a competitive and sustainable steel industry in Europe. Communication from the commission to the Parliament, the Council, the European Economic and Social Committee and the Committee of Regions. 2013.
- [7] European Comision E. Circular economy strategy. 2016.
- [8] Yearbook SS. World steel association. 2015.
- [9] Abu-Eishah SI, El-Dieb AS, Bedir MS. Performance of concrete mixtures made with electric arc furnace (EAF) steel slag aggregate produced in the Arabian Gulf region. *Constr Build Mater* 2012;34:249-56.
- [10] Bignozzi MC, Sandrolini F, Andreola F, Barbieri L, Lancellotti I. Recycling electric arc furnace slag as unconventional component for building materials. 2010:28-30.
- [11] Bosela P, Delatte N, Obratil R, Patel A. Fresh and hardened properties of paving concrete with steel slag aggregate. 2008.
- [12] Faraone N, Tonello G, Furlani E, Maschio S. Steelmaking slag as aggregate for mortars: Effects of particle dimension on compression strength. *Chemosphere* 2009;77:1152-6.
- [13] Autelitano F, Giuliani F. Electric arc furnace slags in cement-treated materials for road construction: Mechanical and durability properties. *Constr Build Mater* 2016;113:280-9.
- [14] Fronck BA. Feasibility of Expanding the use of Steel Slag as a Concrete Pavement Aggregate. 2012.

- [15] Yildirim IZ, Prezzi M. Use of steel slag in subgrade applications. 2009.
- [16] Adegoloye G, Beaucour A-, Ortola S, Noumowe A. Mineralogical composition of EAF slag and stabilised AOD slag aggregates and dimensional stability of slag aggregate concretes. *Constr Build Mater* 2016;115:171-8.
- [17] Faleschini F, Brunelli K, Zanini MA, DabalÃ M, Pellegrino C. Electric Arc Furnace Slag as Coarse Recycled Aggregate for Concrete Production. *Journal of Sustainable Metallurgy* 2016;2:44-50.
- [18] Faleschini F, Hofer L, Zanini MA, dalla Benetta M, Pellegrino C. Experimental behavior of beam-column joints made with EAF concrete under cyclic loading. *Eng Struct* 2017;139:81-95.
- [19] Pellegrino C, Faleschini F. Experimental behavior of reinforced concrete beams with electric arc furnace slag as recycled aggregate. *ACI Mater J* 2013;110:197-205.
- [20] Pellegrino C, Faleschini F. Experimental investigation on RC beams containing slag as recycled aggregate. *fib Symp : Concr Struct Sustainable Community - Proc* 2012:451-4.
- [21] Faleschini F, Alejandro Fernández-Ruíz M, Zanini MA, Brunelli K, Pellegrino C, Hernández-Montes E. High performance concrete with electric arc furnace slag as aggregate: Mechanical and durability properties. *Constr Build Mater* 2015;101:113-21.
- [22] Pellegrino C, Gaddo V. Mechanical and durability characteristics of concrete containing EAF slag as aggregate. *Cement and Concrete Composites* 2009;31:663-71.
- [23] Pellegrino C, Cavagnis P, Faleschini F, Brunelli K. Properties of concretes with Black/Oxidizing Electric Arc Furnace slag aggregate. *Cement and Concrete Composites* 2013;37:232-40.
- [24] Liapis I, Papayianni I. Advances in chemical and physical properties of electric arc furnace carbon steel slag by hot stage processing and mineral mixing. *J Hazard Mater* 2015;283:89-97.
- [25] Anastasiou EK, Papayianni I, Papachristoforou M. Behavior of self compacting concrete containing ladle furnace slag and steel fiber reinforcement. *Mater Des* 2014;59:454-60.
- [26] Papayianni I, Anastasiou E. Concrete incorporating high-calcium fly ash and EAF slag aggregates. *Magazine of Concrete Research* 2011;63:597-604.
- [27] Papayianni I, Anastasiou E. Production of high-strength concrete using high volume of industrial by-products. *Constr Build Mater* 2010;24:1412-7.

- [28] Juan Manuel Manso, David Hernandez, Maria Milagros Losanez, and Javier,Jesus Gonzalez. Design and Elaboration of Concrete Mixtures Using Steelmaking Slags. *Materials Journal* 2011;108.
- [29] Manso JM, Polanco JA, Losañez M, González JJ. Durability of concrete made with EAF slag as aggregate. *Cem Concr Compos* 2006;28:528-34.
- [30] Skaf M, Manso JM, Aragón Á, Fuente-Alonso JA, Ortega-López V. EAF slag in asphalt mixes: A brief review of its possible re-use. *Resour Conserv Recycl* 2017;120:176-85.
- [31] Arribas I, Santamaría A, Ruiz E, Ortega-López V, Manso JM. Electric arc furnace slag and its use in hydraulic concrete. *Constr Build Mater* 2015;90:68-79.
- [32] Manso JM, Gonzalez JJ, Polanco JA. Electric arc furnace slag in concrete. *J Mater Civ Eng* 2004;16:639-45.
- [33] Polanco JA, Gonzalez JJ, Manso JM. Electric Arc Furnace Slag in Concrete. *J Mater Civ Eng* 2004;16:639-45.
- [34] Polanco JA, Manso JM, Setién J, González JJ. Strength and durability of concrete made with electric steelmaking slag. *ACI Mater J* 2011;108:196-203.
- [35] Pasetto M, Baldo N. Cement bound mixtures with metallurgical slags for road constructions: mix design and mechanical characterization. *Inżynieria Mineralna* 2013;14.
- [36] Pasetto M, Baldo N. Experimental evaluation of high performance base course and road base asphalt concrete with electric arc furnace steel slags. *J Hazard Mater* 2010;181:938-48.
- [37] Pasetto M, Baldo N. Mix design and performance analysis of asphalt concretes with electric arc furnace slag. *Constr Build Mater* 2011;25:3458-68.
- [38] Santamaría A, Orbe A, Losañez MM, Skaf M, Ortega-Lopez V, González JJ. Self-compacting concrete incorporating electric arc-furnace steelmaking slag as aggregate. *Mater Des* 2017;115:179-93.
- [39] Santamaría A, Rojí E, Skaf M, Marcos I, González JJ. The use of steelmaking slags and fly ash in structural mortars. *Constr Build Mater* 2016;106:364-73.
- [40] Sheen Yn, Huang LJ, Sun TH, Le DH. Engineering Properties of Self-compacting Concrete Containing Stainless Steel Slags. *Procedia Engineering* 2016;142:79-86.
- [41] Sheen Yn, Le DH, Sun TH. Greener self-compacting concrete using stainless steel reducing slag. *Construction and Building Materials* 2015;82:341-50.

- [42] Sheen Y, Le D, Sun T. Innovative usages of stainless steel slags in developing self-compacting concrete. *Constr Build Mater* 2015;101, Part 1:268-76.
- [43] Arribas I, Vegas I, San-José JT, Manso JM. Durability studies on steelmaking slag concretes. *Mater Des* 2014;63:168-76.
- [44] CEN European Committee for standarization. Rue de Stassart, 36. Brussels B-1050.
- [45] Manso JM, Losañez M, Polanco JA, Gonzalez JJ. Ladle furnace slag in construction. *J Mater Civ Eng* 2005;17:513-8.
- [46] San-José JT, Vegas I, Arribas I, Marcos I. The performance of steel-making slag concretes in the hardened state. *Mater Des* 2014;60:612-9.
- [47] ASTM International.,. Annual book of ASTM standards. Annual book of ASTM standards. 2002.





Chapter 6:  
*Manufacture and  
Performance of Real Scale Beams*

---



# 6

## *Manufacture and performance of real-scale beams*

### **1. Introduction**

One of the main objectives of this thesis is to manufacture self-compacting concretes with Electric Arc Furnace (EAF) slag as aggregate. It is not enough to manufacture concrete at the laboratory scale to be able to say that this goal has been achieved. The laboratory is useful for testing different designs and evaluating the properties of different mixes. However, once good results are achieved in the laboratory, it is mandatory to evaluate the properties of the concrete in larger mixtures, simulating mixes at real construction sites. In this chapter, mixes of pumpable and self-compacting concretes with volumes of 600 liters have been developed for casting real-scale Reinforced Concrete (RC) beams, demonstrating that manufacturing self-compacting concretes with steel slag as aggregate is feasible.

The mechanical behavior of concretes manufactured with EAF slag as aggregate is widely reported in the literature with abundant research developed in the laboratory. In this chapter, the mechanical behavior of real-scale reinforced concrete beams is analyzed. A four-point bending test is carried out to evaluate the flexural behavior of EAF slag RC concrete beams; the experimental results are compared with the theoretical values of the existing formulations. The long-term deflection of the beams is also analyzed and, in this case, a three-point bending test is performed.



## **6.2. The performance of pumpable and self-compacting concrete beams incorporating electric arc furnace slag.**



## **Abstract**

Social concern over sustainability has motivated many researchers to study the use of steelmaking slag in the construction industry. One of the recognized uses of Electric Arc Furnace (EAF) slag is as a coarse aggregate in hydraulic mixes. The poor workability of hydraulic mixes manufactured with this type of aggregate has been one of the main drawbacks to its commercial use in real structural components. In addition, the bulk of the research to date has examined mass concrete, but there has been little research into Reinforced Concretes (RC) manufactured with EAF slag as aggregate. In this study, real-scale beams are manufactured with pumpable and self-compacting concrete using electric arc furnace slag as aggregate. Its performance under flexural loads is studied. It is demonstrate that real-scale RC elements manufactured with self-compacting mixes that are of the required workability and that the behavior of EAF slag RC elements can be predicted using the existing formulations.

## Introduction

We live in a consumer society that for many years has been manufacturing throw-away products with a short life, the manufacture and the disposal of which continues to generate vast amounts of waste. Fortunately, the concept of sustainability has been introduced and many sectors of society have started to express concern over the practical application of sustainable practice that is linked to the future of the planet. One of the main issues in global sustainability concerns the methods of reducing the volume of waste and the achievement of this aim, by finding uses for the waste materials that are produced as industrial by-products.

Both the building sector and the civil engineering industry have become central consumers of industrial by-products, using waste materials produced in their own industry (construction and demolition waste) [1-3], from the agricultural industry (palm oil fuel ash, bagasse ash, wood waste ash, bamboo leaf ash, corn cob ash, ice husk ash...), and from industrial processes (silica fume, fly ash steel slags...)[4-6].

The use of steelmaking slag in the construction industry was first advanced in the seminal papers of Motz, Geiseler and Koros [7-9]. Many researchers have since followed their advances, focusing their studies on the reuse of steel slags. With the objective of its inclusion in standards, the main topic of research for many years has centered on Ground Granulated Blast Furnace slag [10-13]. It is now specified in the EN 197-1 [14] standard for use as a mineral addition with Portland cement.

Studies regarding the use of Electric Arc Furnace (EAF) slag were initiated in Japan [15,16], following by many research groups around the world which have continued to advance new uses for this particular by-product. In Europe, groups from Spain, Italy and Greece stand out among others. Some of the uses that have been proposed for EAF slag are as bedding materials for roads and railways, water depuration, and energy storage [17]. However, the main research topic for the use of electric arc furnace slag has been as aggregate in bituminous mixes [18-25] and in hydraulic mixes [26-36].

The physical and chemical properties of EAF slag make it a suitable material for use as aggregate in concrete mixes, resulting in concretes with improved mechanical behavior [37-40] and similar durability when compared with ordinary concretes manufactured with natural aggregates [41-44].



Some of the disadvantages encountered when using EAF slag concrete have been its higher density, advantageous for some uses, but detrimental in suspended elements, and the poorer workability of the mixes manufactured with this type of aggregate.

In recent research [45,46], the manufacture of self-compacting concrete with EAF slag as aggregate has been achieved using a mix design that differs from the conventional one. Its higher density has also been studied [35] and is not seen as a very significant problem, taking into account its increase in material strength, if the strength-to-density ratio is kept within similar ranges to those of conventional concrete.

The good behavior of EAF slag concrete at a laboratory scale has encouraged some organizations to use it in real construction works. At Tecnalia (formerly Labein), the foundation slab and basement walls of the KUBIK research building [47] (shown in Figure 6.1) were manufactured with EAF slag concrete, in 2008. In 2015, the Port of Bilbao used this material to manufacture blocks to protect the “Punta Lucero” dock and to build the new “Punta Sollana” dock (see Figure 6.1)[48]. As previously stated, in these applications, where the structural elements depend on their mass to resist the pressure, the use of steel slag is very advantageous, due to its higher density.



**Figure 6.1:** Kubik foundation and basement walls (left), a concrete block from the Punta Lucero dock (center) and the new Punta Sollana dock wall (right).

Copious research results have been published on mass concrete, leaving far fewer studies on structural applications. Pellegrino and Faleschini [49] studied the flexural and shear failure of 2 m long EAF slag Reinforcement Concrete (RC) beams and a cross section of 185x300mm, showing that the ultimate flexural and shear capacity was higher in beams manufactured with slag concrete compared with beams manufactured with Natural Aggregate (NA) concrete. They also reported initial cracking at higher loads.

Sang-Woo, Yong-Jun and Kil-Hee studied the behavior of RC beams manufactured with EAF slag as aggregate [50,51]. They studied the flexural behavior of 3.4m long beams

with a cross section of 200x350mm, showing that the behavior of EAF concrete and NA concrete beams was similar and that it is possible to predict the behavior of EAF slag RC beams with the current code of equations.

These investigations also examined bonding behavior in RC beams manufactured with EAF slag concrete [52], concluding that bond behavior is enhanced with the use of this type of concrete. Faleschini et al. found similar results when studying the local bond strength between reinforcement bars and EAF slag concrete using the pull-out test.

In this research the flexural strength and long-term deflections of EAF slag RC beams are studied. Four-point bending tests were used to study the flexural behavior of 4 beams, each of a length of 4400mm, a cross section of 200x300mm and with a clear span of 4000mm, two of which were cast with a pumpable concrete and the other two with a self-compacting concrete. Different types of cement were used in each beam (Cement type I, Cement type IV) for each class of workability. The same concrete beams were studied under long-term loading (creep) test. Comparisons are shown between the experimental and the analytical results in accordance with European model codes.

## **Materials**

### *Water cement and natural aggregates*

Mix water containing no compounds that could adversely affect the hydraulic mixes was taken from the urban mains supply of the city of Burgos.

Two types of cement were used in the present research: first, a Portland cement type I 52.5 R; second, a Portland cement type IV/B-V 32.5-N; both in accordance with the UNE-EN 197-1 standard [14]. The cement type I included 90% Portland clinker, 5% calcium carbonate powder fines and 5% gypsum. The composition by weight of the cement type IV included 5% calcium carbonate powder fines, 40% fly ash, 50% Portland clinker, and 4% gypsum.

Fines of a commercial natural limestone were used with a maximum size aggregate of 1.18mm, a fineness modulus of 1.5 units and a gradation that is shown in Figure 6.2. Particles smaller than 1 mm have an important role in the workability of the concrete. In this research, these fines are added to improve concrete workability, to prevent the segregation of coarse aggregates and to compensate for the lack of fine particles in EAF slag.

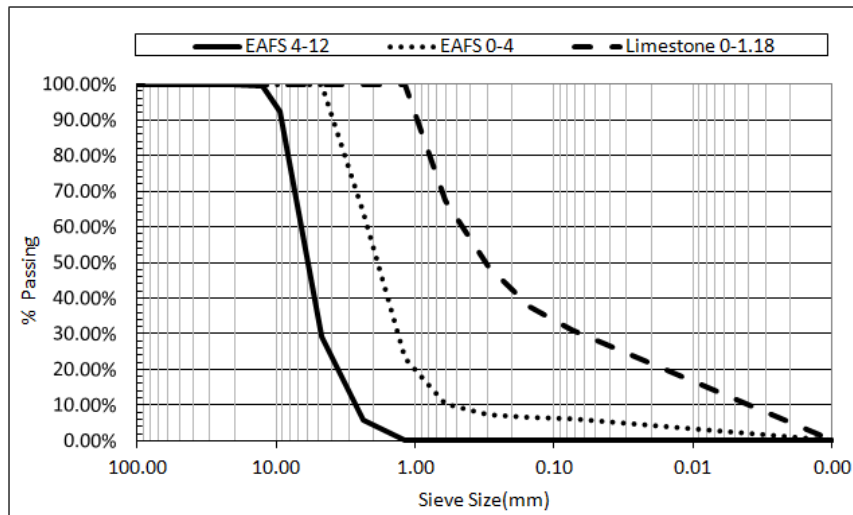


Figure 6.2: Grading of natural aggregates.

EAF slag

Crushed Electric Arc Furnace (EAF) slag in two size fractions (fine <4.75 mm and medium <12.5 mm), supplied by the company Hormor-Zestoa, was used in this research. The chemical composition and some physical properties are detailed in Table 6.1. Their grading is included in Figure 6.2.

Compounds	EAFS (0-5 mm)
Fe <sub>2</sub> O <sub>3</sub> (%)	22.3
CaO (%)	32.9
SiO <sub>2</sub> (%)	20.3
Al <sub>2</sub> O <sub>3</sub> (%)	12.2
MgO (%)	3.0
MnO (%)	5.1
SO <sub>3</sub> (%)	0.42
Cr <sub>2</sub> O <sub>3</sub> (%)	2.0
P <sub>2</sub> O <sub>5</sub> (%)	0.5
TiO <sub>2</sub> (%)	0.8
Loss on ignition (%)	gain
Water absorption (%)	1.12
Specific gravity (Mg/m <sup>3</sup> )	3.42
X-Diffraction main compounds	Wustite-Ghelenite Kirsteinite

Table 6.1: Chemical composition and physical characteristics of slags

A detailed description of these materials may be found in a recently published work [35] and only the main characteristics are included in this work, essential for a clear understanding of the arguments that are presented.

### Mix design

Four different concrete mixes were designed for the analysis of their structural behavior. All of the concrete mixes contained EAF slag as aggregate in various proportions. Two variables were introduced: first, the workability of the mixes, pumpable concretes and self-compacting concretes and second, the different types of cement used in their manufacture. A range of consistencies was selected to study the manufacture of concretes with the desired workability, varying the mix design. The beams were manufactured with Cement type I and Cement type IV. This variable was introduced, to show the influence of the cement types in the workability of the concretes, and to study the influence of the interaction between the mineral additions of the cement and the EAF slag in the structural response of the reinforced concrete.

The target of obtaining self-compacting mixes presented various problems and the steps taken in that direction may be found in a previously published paper by the authors of this research group [45]. After several attempts, some of which reported in the aforementioned paper, two different mix designs were selected for manufacturing the concrete of the RC beams. Their granulometry is shown in Figure 6.3 and the proportions of the materials in Table 6.2.

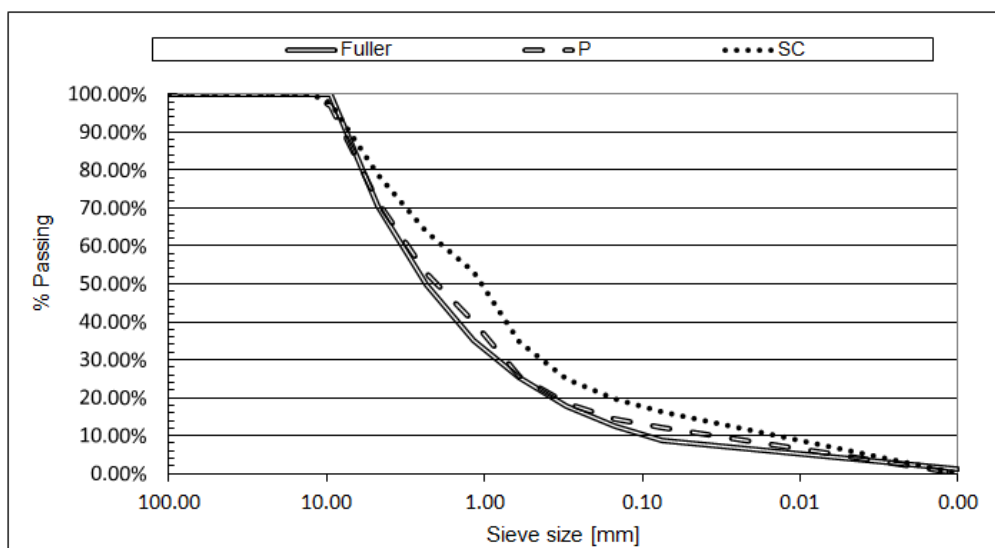


**Figure 6.3:** Gradation of the mixes

	IP	IVP	ISC	IVSC
<b>Cement I</b>	330		330	
<b>Cement IV</b>		330		330
<b>Water</b>	160	160	165	165
<b>EAFS coarse</b>	950	950	760	760
<b>EAFS sand</b>	690	690	550	550
<b>Lime sand</b>	650	950	900	900
<b>Plasticizer (%cement weight)</b>	1.5%	1.5%	2%	2%

**Table 6.2:** Mix proportions

### Rebars

Ribbed steel bars of  $\varnothing 25\text{mm}$  were used as tensile reinforcements, and  $\varnothing 8\text{mm}$  deformed steel bars were used as compression and shear reinforcement in the beams designed for the flexural strength test.

Ribbed steel bars of  $\varnothing 25\text{mm}$ ,  $\varnothing 8\text{mm}$  and  $\varnothing 6\text{mm}$  were used as tensile, compressive and shear reinforcements, respectively, in the beams designed for the flexural creep test.

All the deformed steel bars used as reinforcement were of the class AP 500 S, manufactured with B 500 SD steel, as per the specifications in UNE 36068.

### **Specimen details and test setup**

Two Reinforcement Concrete (RC) beams were manufactured for each mix design, with a total of 8 RC beams. All the beams had a cross-section of 300x200mm and a length of 4400mm.

One of the beams for each mix type was designed for flexural failure and the other one for shear failure. The beam designed for shear failure was first used to evaluate long-term deflection. This test is performing over one year, after which the beams in this test is going to be used to evaluate the structural response under shear loads. The reinforcement details of both beams are detailed in Table 6.3 and their geometrical characteristics are shown in Figures 6.4 and 6.6.

Beams	Reinforcement		
	Top	Bottom	Stirrups
<b>Flexural failure</b>	2 $\varnothing 8$	3 $\varnothing 25$	$\varnothing 8/100$ mm
<b>Shear failure</b>	2 $\varnothing 8$	2 $\varnothing 25$	$\varnothing 6 /200$ mm

**Table 6.3:** Reinforcement details

Twelve cubic concrete specimens of 100mm side were manufactured to evaluate the development of their compressive strength at 7, 28, 90 and 180 days. Their compressive strengths were lowered using the values shown in Table 6.4, taken from the fib model code for Concrete Structures 2010 [53]. Additionally, 3 specimens  $\varnothing 100 \times 200$ mm were used to obtain the Young's modulus of the concrete at 28 days.

Concrete grade	C12	C16	C20	C25	C30	C35	C40	C45	C50
$f_{ck}$ [MPa]	12	16	20	25	30	35	40	45	50
$f_{ck,cube}$ [MPa]	15	20	25	30	37	45	50	55	60
Concrete grade	C55	C60	C70	C80	C90	C100	C110	C120	
$f_{ck}$ [MPa]	55	60	70	80	90	100	110	120	
$f_{ck,cube}$ [MPa]	67	75	85	95	105	115	130	140	

**Table 6.4:** Characteristic strength values

Measurement of the fresh properties of the pumpable concretes was done with the slump flow test described in the ASTM C143 [54]. The workability of the self-compacting concretes was evaluated with the slump flow test described in the ASTM C1611 [54] and the L-box test described in the EFNARC [55]. Mechanical properties were evaluated using the European standard. The compressive strength test was performed in accordance with the instructions in EN 12390-3 [14] and the secant elastic modulus of the concrete was determined in accordance with the instructions in EN 12390-13 [14].

Four-point bending tests were performed to evaluate the flexural behavior of the beams. The details and test setup of the flexural beams are shown in Figures 6.4 and 6.5. The clear span of the beams was designed to be 4000mm. The distance between the two loading points of the specimen was 1000mm. As shown in Figure 6.4, strain gauges were attached to the longitudinal reinforcement in the mid-span, concretely 3 strain gauges were fixed, one in each  $\varnothing 25$  bar. 7 (IVP, IVSC) and 9 (IP, ISC) strain gauges were used to track the neutral axis at the mid-span of beams, as shown in Figure 6.5. Two located at the bottom of the beam, another two located in the top of the beam and at points at distances of 100mm (IP, ISC), 140mm (IP, ISC), 180mm, 220mm and 260mm from the bottom of the beam. The deflection of the beams was measured using six LVDTs and six dial gauges, as shown in Figure 6.5.



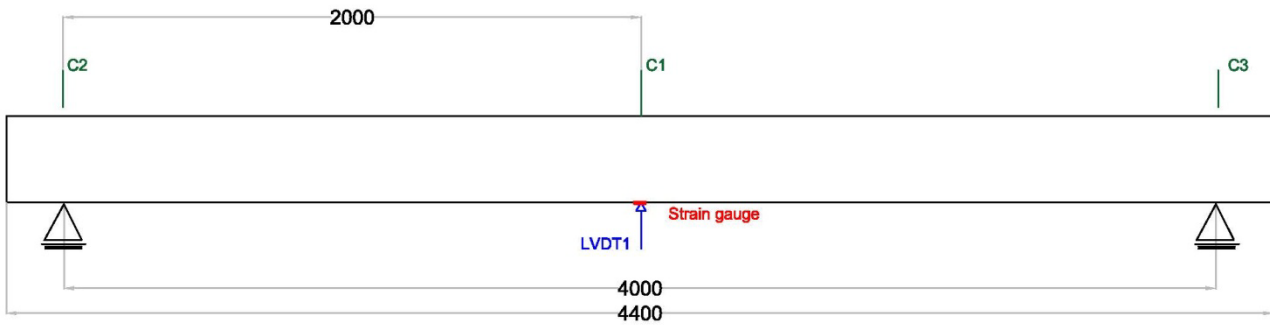


Figure 6.7: Delayed strain test setup

## Experimental results

### Fresh properties

An S3 consistency slump class was achieved for the pumpable concretes IP and IVP, and the values obtained in the Abrams cone are presented in Table 6.5. The same value was obtained for both types of cement. In this case, the mineral addition in the cement had no influence on concrete workability. In the casting processes of the beams, the concrete showed acceptable flowability and was easily poured, followed by the obligatory standard vibration.

	Slump	L-box	Density [Mg/m <sup>3</sup> ]	E [GPa]	fc 28 days [MPa]
IP	115 mm	-	2,75	38,58	49.5
IVP	115 mm	-	2,63	30,78	28.3
ISC	680 mm	1	2,69	39,90	50.2
IVSC	700 mm	1	2,55	31,35	31.5

Table 6.5: Fresh and hardened properties of the concretes.

The results of the slump test and the L-box test for self-compacting concretes are shown in Table 6.5. Both concretes achieved a SF2 slump class in the slump flow test and a PA2 class in the L-box test, in accordance with the EFNARC[55]. The concrete manufactured with cement type IV was slightly more flowable at first, although the workability of the concrete rapidly worsened during the casting of the beams. This reduced workability can be explained by the interaction of the cement mineral addition to the superplasticizer. Nevertheless, vibration of the concrete forming the beams was unnecessary and good results were achieved for both types of concretes.



Mechanical properties

The main mechanical characteristics of the concretes used in the beams are presented in Table 6.5, in which the concrete densities are shown to vary from 2.55 Mg/m<sup>3</sup> to 2.75Mg/m<sup>3</sup>. The pumpable concretes were heavier than the self-compacting concrete due to the higher content of EAF slag in the former. The mixes manufactured with Cement type I were also heavier than the same mix manufactured with Cement type IV, due to the higher density of the Cement type I. This variable will not influence the structural behavior of the beams, taking into account the magnitude of the load, due to the weight of the beam in comparison with the expected ultimate load.

The evolution of concrete strength up until the flexural test is shown in Figure 6.8. At early ages the concrete can be divided in two strength classes. Concretes manufactured with cement type IV that reached around 30 MPa and concretes manufactured with cement type I that reached around 50 MPa, at 28 days. These are the expected values taking into account that the cement type I is 52.5R and the cement type IV is 32.5. At 180 days, the self-compacting concretes reached higher values than the pumpable concretes, with both types of cement. These strengths can be explained by the higher content of limestone fines in the self-compacting concrete, which in some studies has been shown to improve long-term concrete strength.

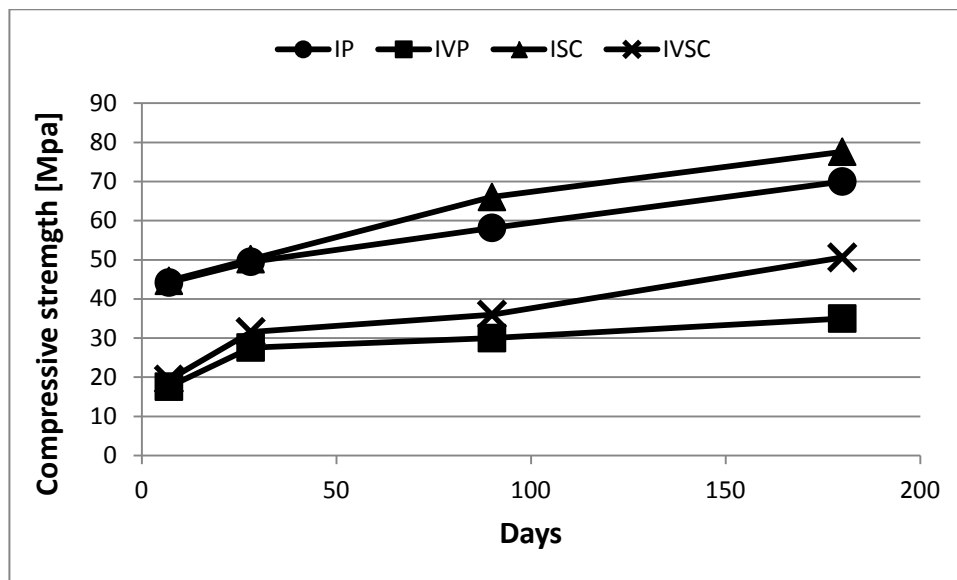


Figure 6.8: Development of compressive strength

Concerning the elastic properties, the concretes manufactured with cement type I had an elastic modulus of approximately 39 GPa and the concretes manufactured with cement type IV had a modulus of approximately 31 GPa, as shown in Table 6.5.

Flexural behavior

The flexural test in real-scale reinforced concrete beams was performed to evaluate the structural response of the electric arc furnace slag concrete. All the beams were designed to succumb to flexural failure when the concrete reached its maximum compression strength and the steel reinforcement bars yielded, in an evaluation of the behavior of the concrete and its influence on failure.

In Table 6.6, the main experimental values for the test and the expected theoretical results are shown. The average mechanical properties at 28 days and unit safety coefficients were assumed to obtain the theoretical results. The theoretical values were obtained using the equilibrium equations for sectional design at ultimate loading values, as proposed in EHE-08[56]. The theoretical values were based on the design of the beams and the predicted failure in the 3<sup>rd</sup> domain.

In the beams manufactured with the Cement type I, the theoretical and experimental values of the position of the neutral axis ( $X_u$ ) in the mid-span section of the beams is very similar and an increase of the ultimate load ( $P_u$ ) was observed.

	$P_u$ Theo. [KN]	$X_u$ Theo. [mm]	$P_u$ Exp. [KN]	$X_u$ Exp. [mm]	Deflection Exp. [mm]
<b>IP</b>	212	99	231	97	44.99
<b>ISC</b>	212	100	233	100	45.36
<b>IVP</b>	178	176	175	168	42.28
<b>IVSC</b>	186	158	195	147	44.38

**Table 6.6:** Experimental and theoretical results

The beams manufactured with Cement type IV showed higher theoretical values for the neutral axis at the mid-span section than the experimental values. The IVSC beam showed an increase in its ultimate flexural capacity, while the IVP beam showed a small decrease in the same value.

The poor evolution of the strength of these concrete specimens might explain the different behavior of the ultimate loading capacity of the IVP beams. A high scatter of the results has been noted in these specimens, with poor behavior shown in the beams manufactured with this type of concrete. It is evident that there might have been some problems during the manufacturing process.

As regards the difference between the analytical and the experimental values in beams manufactured with cement type IV could be due to the presumption in the analytical calculations of failure in the 3<sup>rd</sup> domain. In the following paragraphs, it is shown that the experimental failure of the beams manufactured with cement type IV actually occurred in the 4<sup>th</sup> domain.

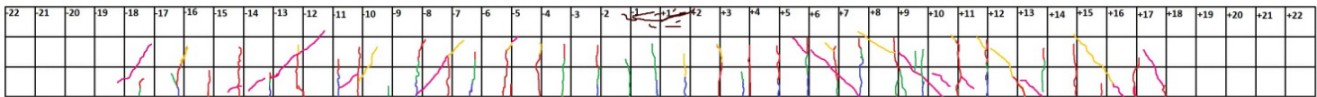
Figure 6.9 shows the crack pattern of the tested beams, in which the failure of the concrete in the upper area of the mid-span section of the beam may be appreciated, which, in accordance with the design specifications, demonstrates that the maximum compressive strength of the concrete has been exceeded.

The crack pattern is color coded to illustrate the formation of the cracks under different loads:

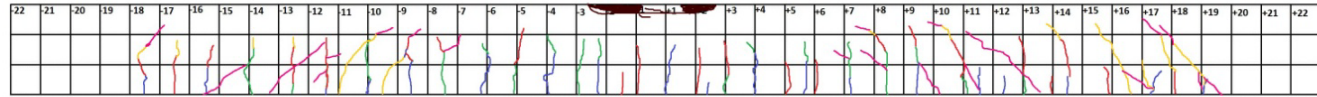
- Blue for 15KN
- Green for 26KN
- Red for 95KN
- Pink for 138KN
- Yellow for 170KN for cement IV and 200 for cement I

The crack pattern reflects the normal behavior of ordinary reinforced concretes. Cracks appeared every 100mm, reflecting the distance between the stirrups. First flexural cracking appeared at the center of the beams and the additional cracks spread upwards towards the supports.

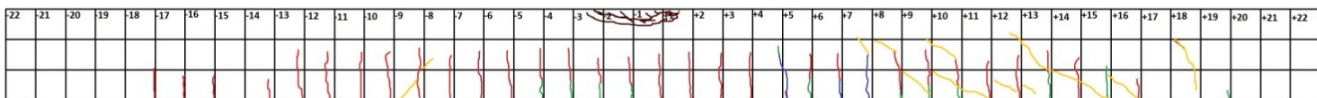
IP



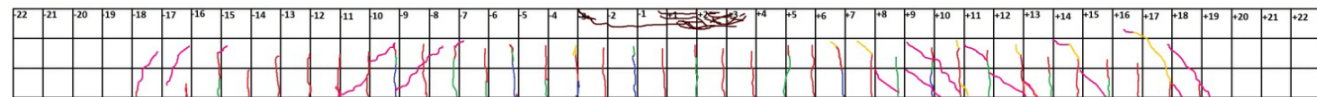
ISC



IVP

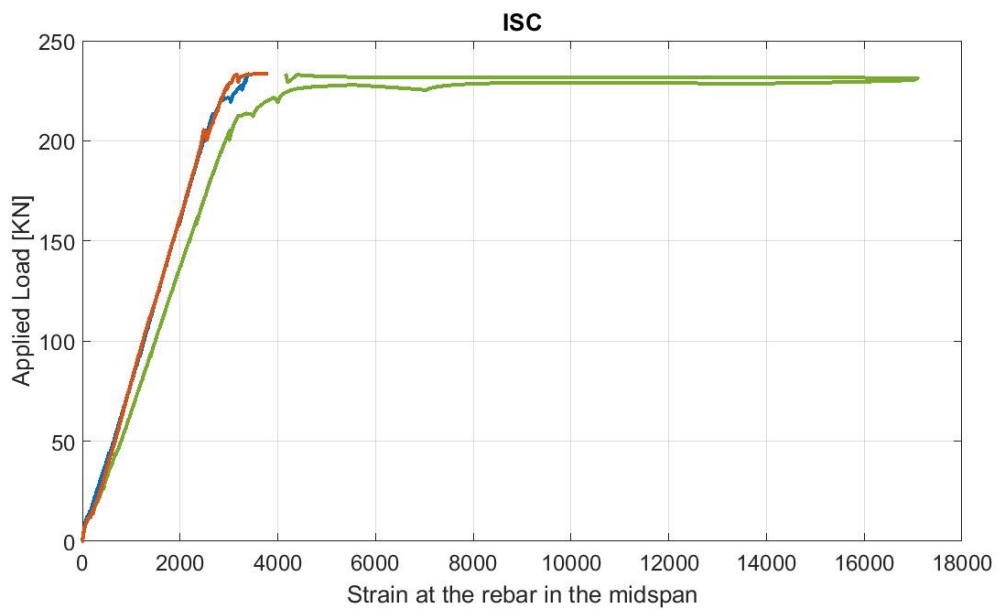
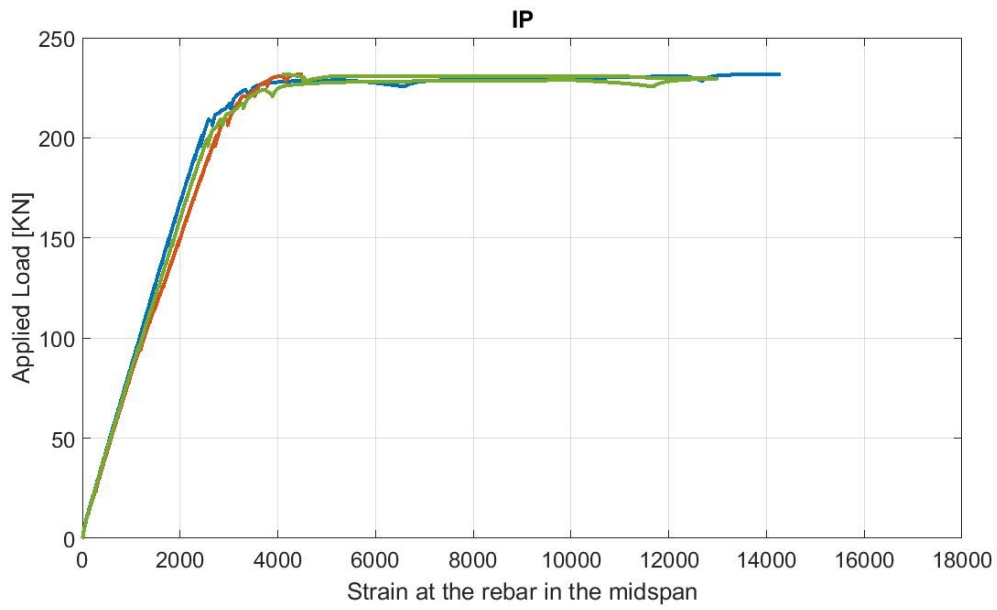


IVSC



**Figure 6.9:** Crack pattern of the beams

The concretes manufactured with cement type I achieved higher strengths. The consequence is that the beams manufactured with these concretes withstood higher loads, and at the ultimate stage the yield stress of the steel was exceeded, leaving it to work in the plastic area in the last stage of the test, as it is designed to do (see Figure 6.10). In the beams manufactured with cement type IV, this elastic limit of the steel was not reached, leaving it to work within the elastic range throughout the entire test (Figure 6.10). It is notable that the reinforcement bars of the IVSC beam had almost reached their ultimate yield strain, working in the last stage of the test at the limit between the elastic and plastic range.



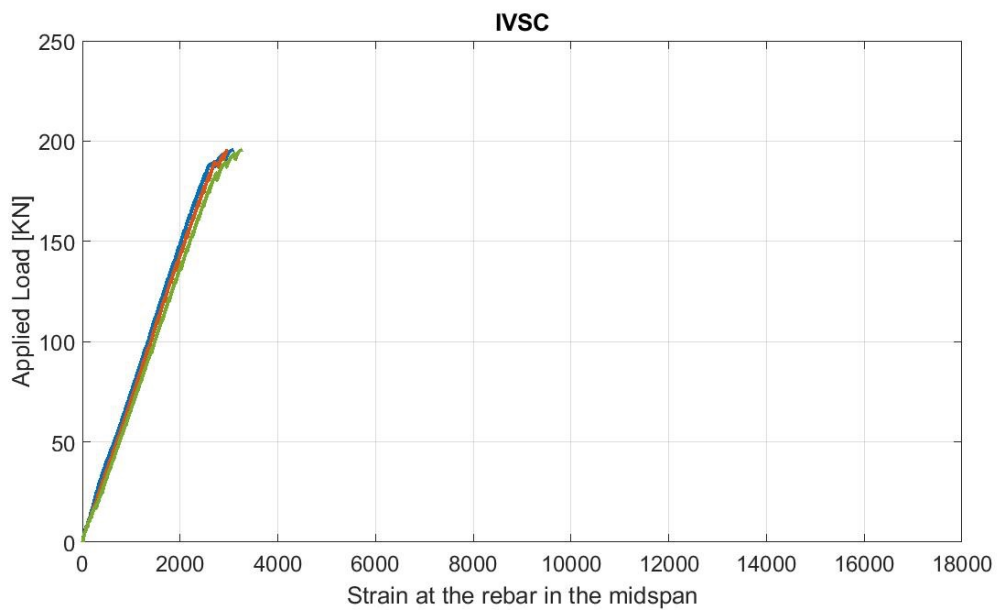
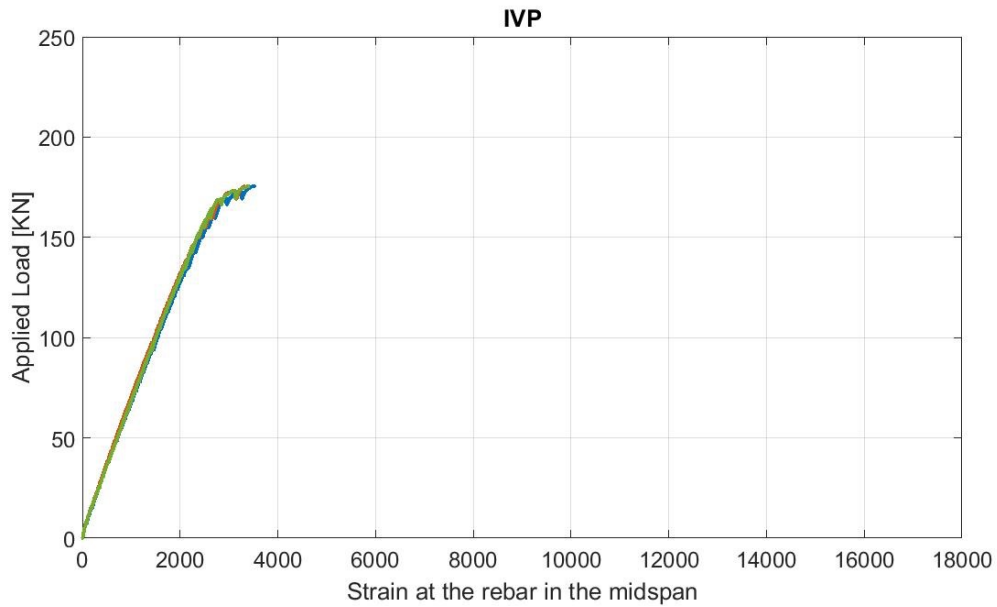


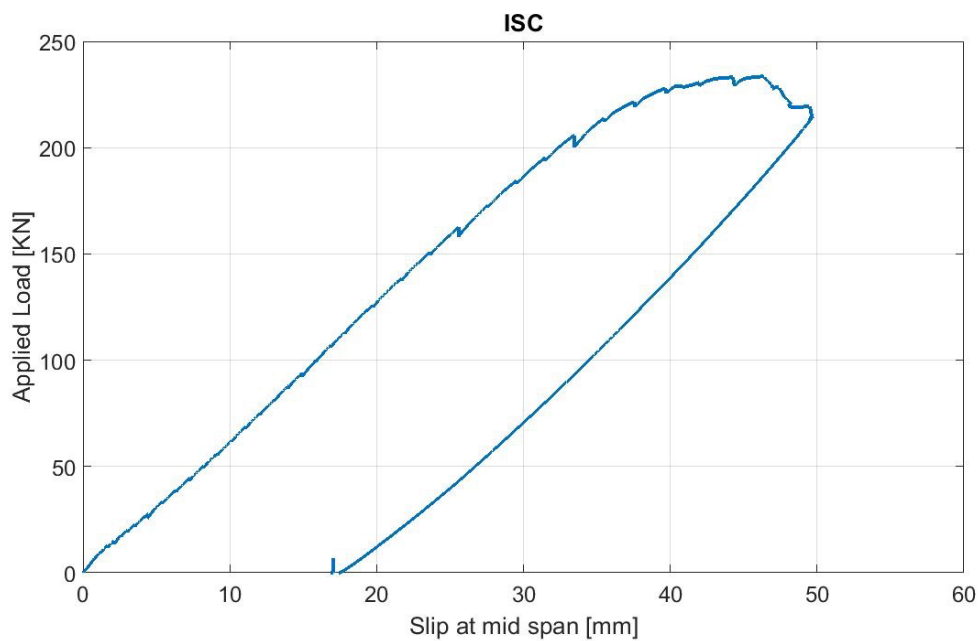
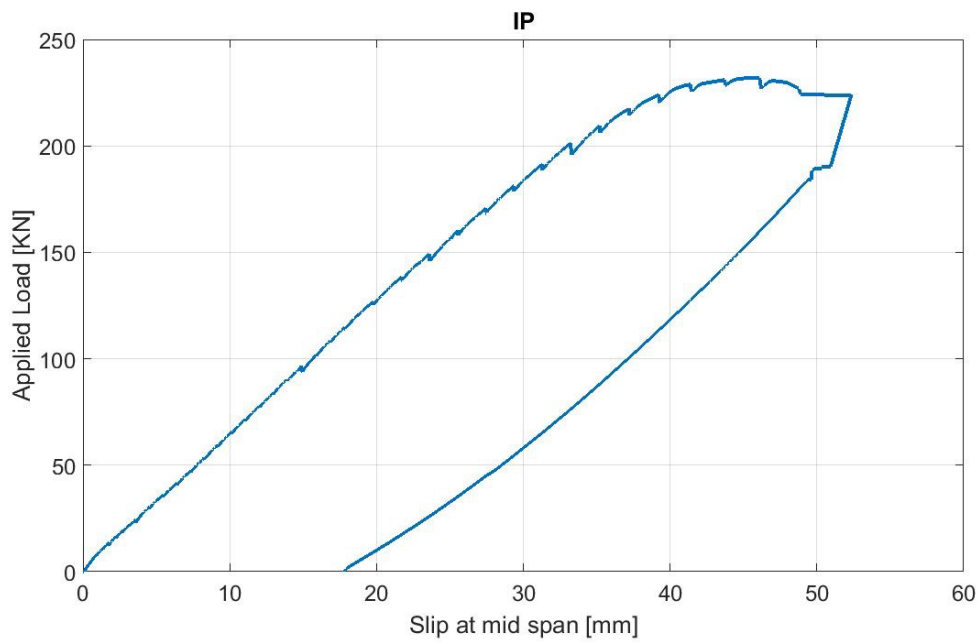
**Figure 6.10: Steel bar strain**

The load versus deflection relationships of the beams are shown in Figure 6.11. In both the IP and the ISC specimens, the instrumentation was maintained during the unloading stage, so the recovery of the displacement of the beams was recorded.

The behavior of the IP and ISC specimens is really quite similar. A first linear behavior is shown while the reinforced concrete is working in the elastic range, followed by a ductile flexural behavior after the reinforcement steel began to yield, followed by the

yielding of the concrete. During the unloading process the beams recover the elastic deformation, showing a perfect line almost parallel to the loading line.

Specimens IVSC and IVP also showed a linear elastic behavior, which in this case the ductile flexural behavior was after reaching the maximum load, when the concrete began to yield.



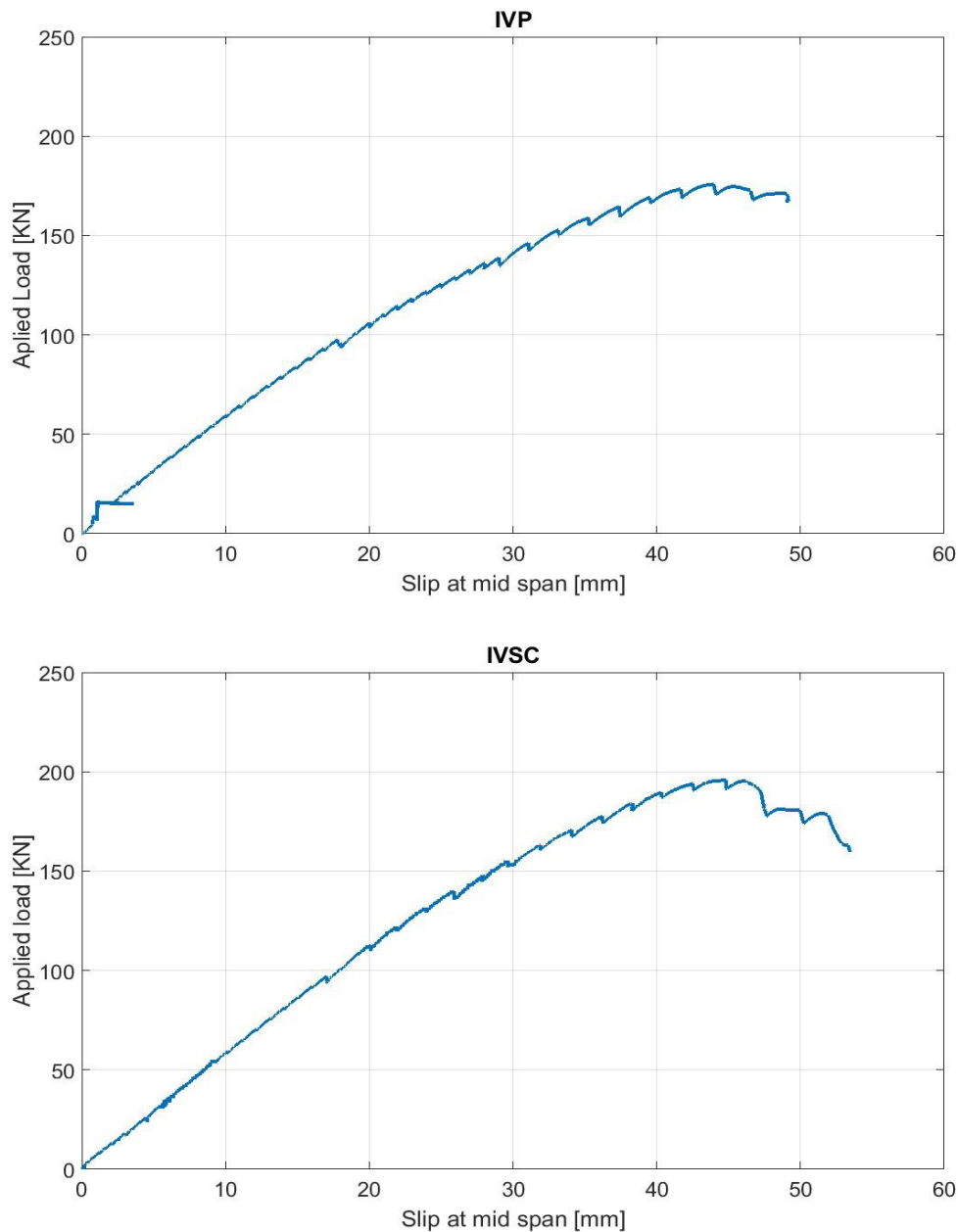


**Figure 6.11:** Load versus displacement relationship

The differences between the elastic modulus of the concrete used to manufacture the beams may be appreciated in Figure 6.12. This figure shows the gradual change in displacement on the beams at different loads.

Taking the displacement of the beam at 150kN as a reference, the IVP beams underwent the highest deformation, reaching a value of 30mm; knowing that many other parameters could influence this behavior, it can be considered a sign to confirm that these were the concrete beams with the lowest elastic modulus. The displacement of almost 30mm of the IVSC, without reaching this value, suggested that the concrete elastic modulus should be quite higher than IVP. Beams IP and ISC share



similar behavior, showing a displacement at 150 kN of around 23 mm, confirming that the two highest values, both very similar, were obtained for the two concrete elastic moduli.

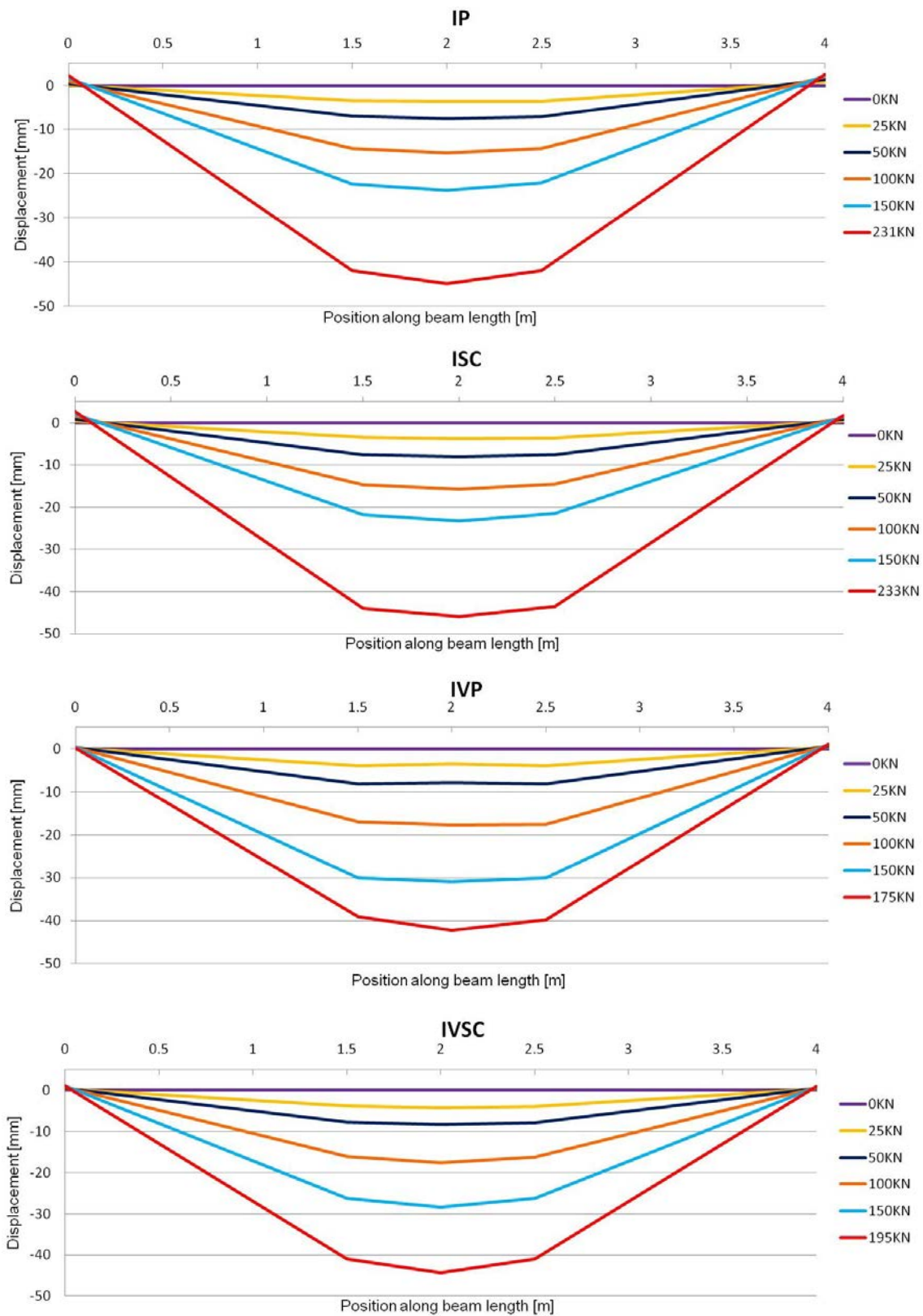


**Figure 6.12:** Measured displacement (LVDTs) along the length at different load levels.

In Figure 6.13, the evolution of the strain distribution in the mid-span section may be seen at different loads in all the beams, which also shows the position of the neutral axis at each load.

Two different structural responses of the neutral axis may be appreciated. In beams manufactured with Cement type I, it is almost constant during the test, remaining so up until the ultimate load is applied. In contrast, the neutral axis went down very slightly during the test in the beams manufactured with Cement type IV.

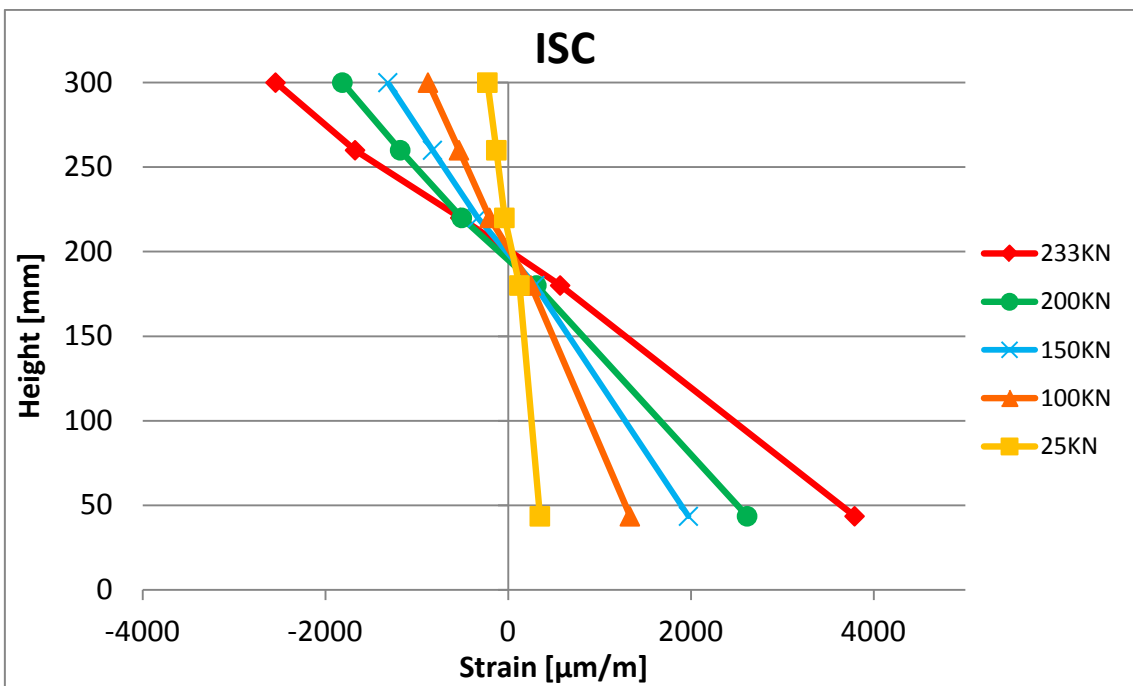
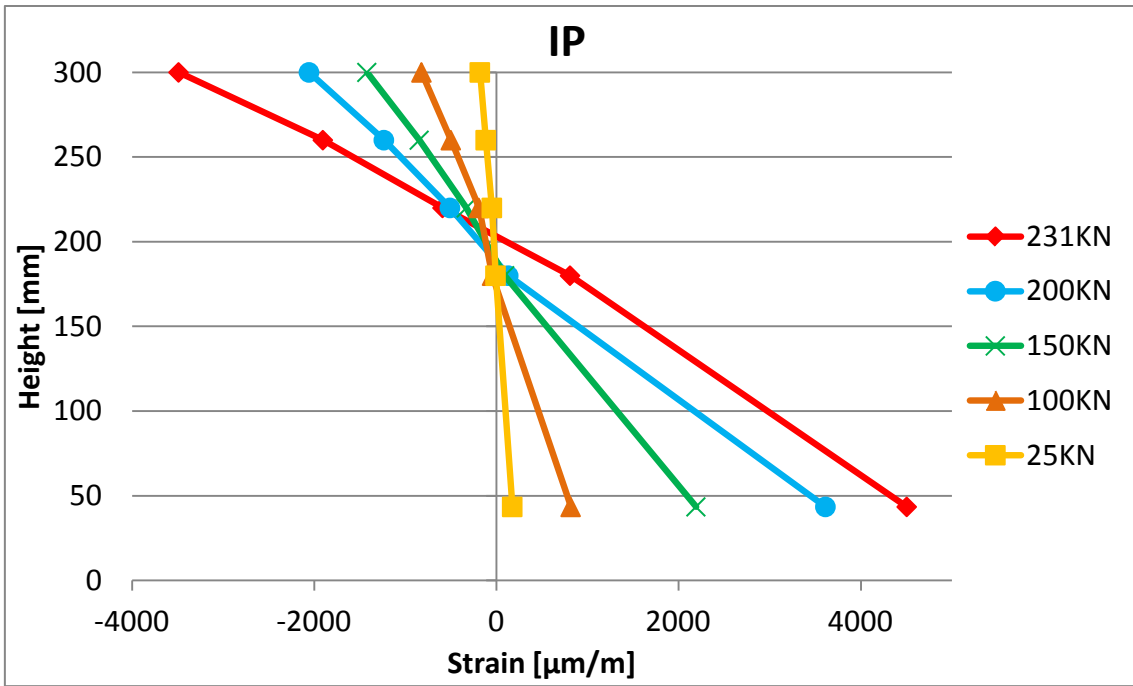
These are the expected behaviors in the ordinary reinforcement concrete, taking into account that the steel only exceeded its yield strain and showed plastic deformation in the beams manufactured with Cement type I, as shown in Figure 6.10.

According to the strain domains of each section [57], in the ultimate load state, based on the pivot diagram shown in Figure 6.14, and in the case of the beams manufactured with Cement type I, the reinforcement concrete reached the ultimate load working in the 3<sup>rd</sup> domain. This means that the neutral axis should be between  $x=0.259d$  (66,5mm) and  $x=x_{lim}$  (149mm). The experimental value of the neutral axis at the ultimate load for beam IP was 99mm and for beam ISC was 100mm.

In the case of the beams manufactured with cement type IV, it was working in the 4<sup>th</sup> domain in the ultimate load state, in which the reinforced steel has not reached its elastic limit. In this case, the neutral axis should be between  $x=x_{lim}$  (149mm) and  $x=d$  (256.5mm). The experimental value of the neutral axis at the ultimate load for beam IVP was 168mm and for beam IVSC was 147mm.

Even though the neutral axis of beam IVSC implies it will be working in domain 3, the  $x_{lim}$  was calculated with theoretical values, which means that this beam reached its maximum load, working in the limit between both domains. The same situation is also shown in Figure 6.10 in the curve stress-strain of the steel, where it may be appreciated that the steel had almost reached its yield strain, but had not begun to work in the plastic zone.

These data results confirmed that it is possible to use the ordinary calculus methods to predict the behavior of reinforcement concrete manufactured with electric arc furnace slag as aggregate.



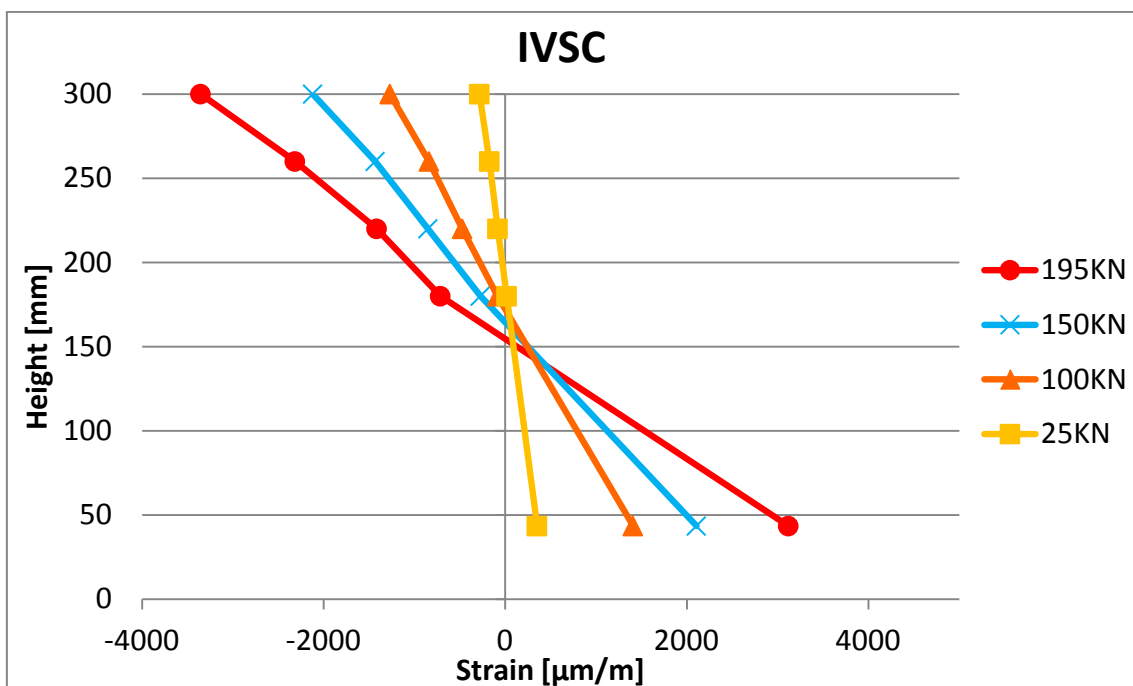
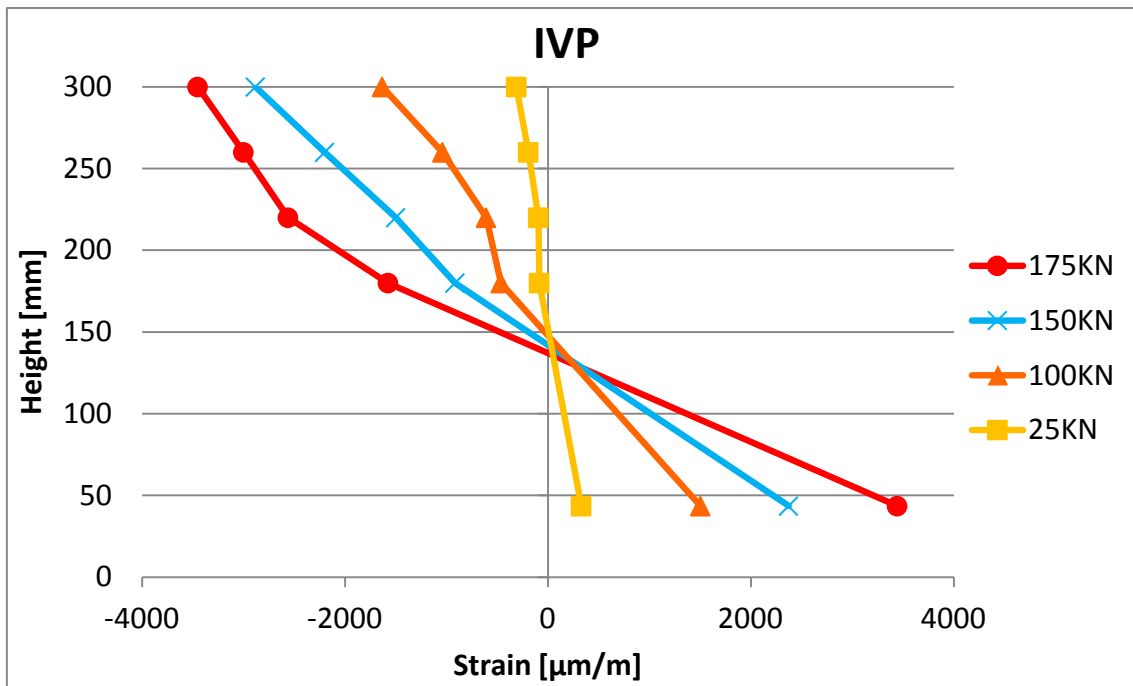


Figure 6.13: Strain distribution at different loads

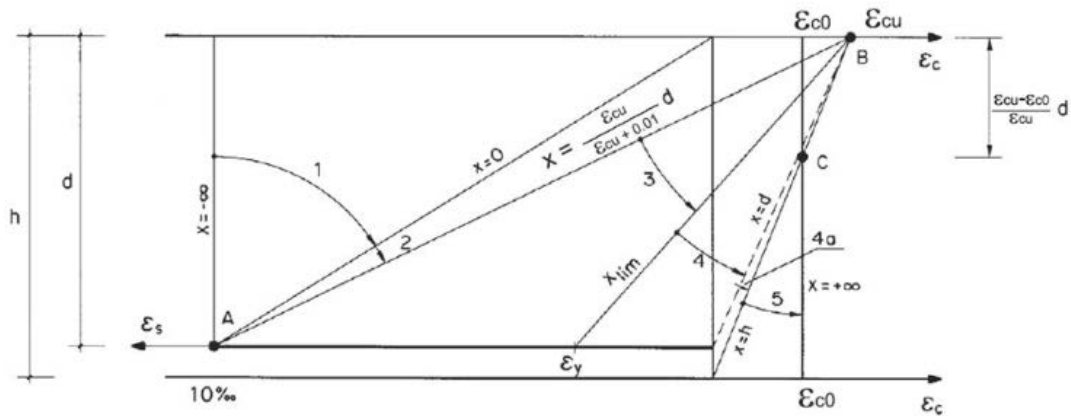
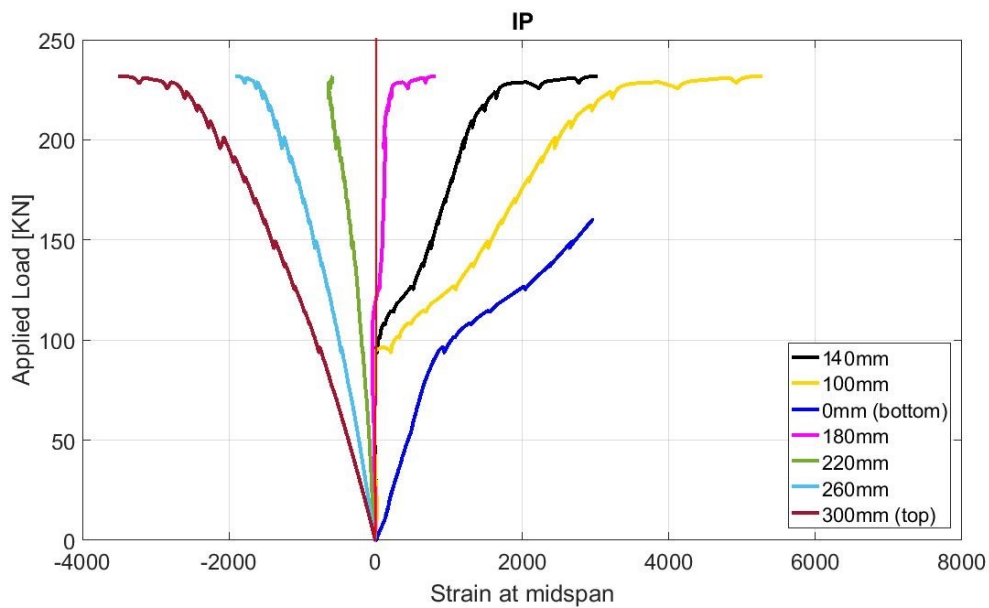
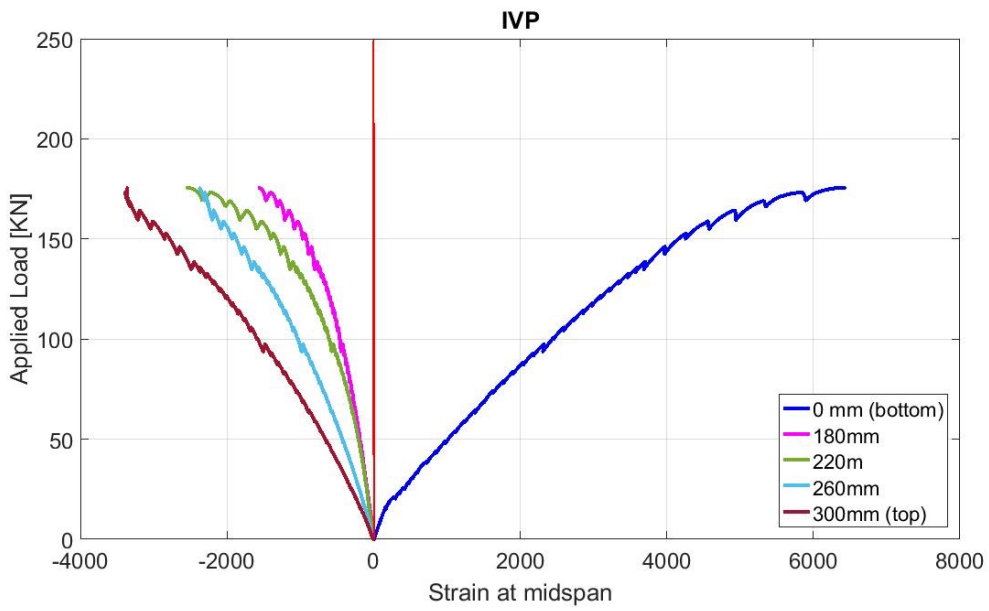
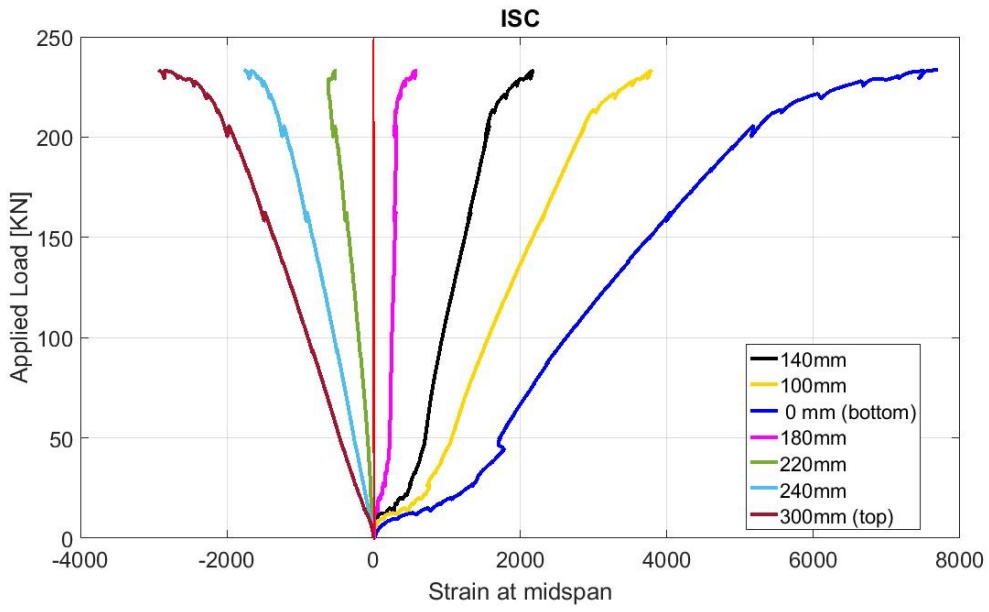
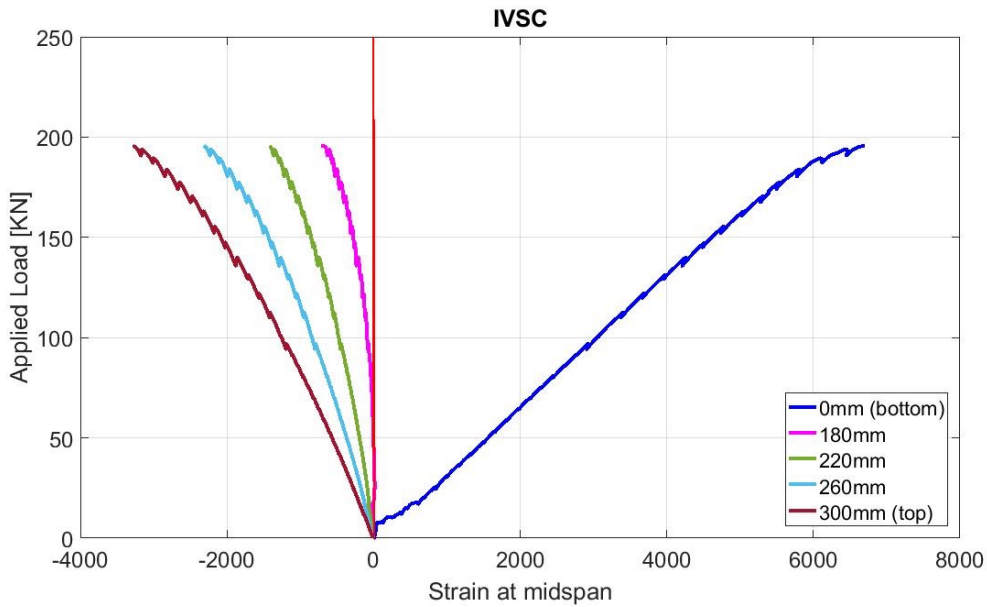


Figure 6.14: Pivot diagram

The measured load-strain relationship of each beam is shown in Figure 6.15. It may be observed that, as stated, the neutral axis of the beams manufactured with cement type I is located higher during the entire test than the neutral axis of the beams manufactured with cement type IV. The values of the gauges located at 0, 100 and 140mm were distorted due to the possible presence of cracks.







**Figure 6.15:** Load versus strain relationship

Long-term deflection

In Figure 6.16, the evolution of the deflection of each beam over time is shown. Within six months, beam IP had reached 13.52mm, beam ISC had reached 12.23 mm, beam IVP 16.902mm, and beam IVSC 12.53mm.

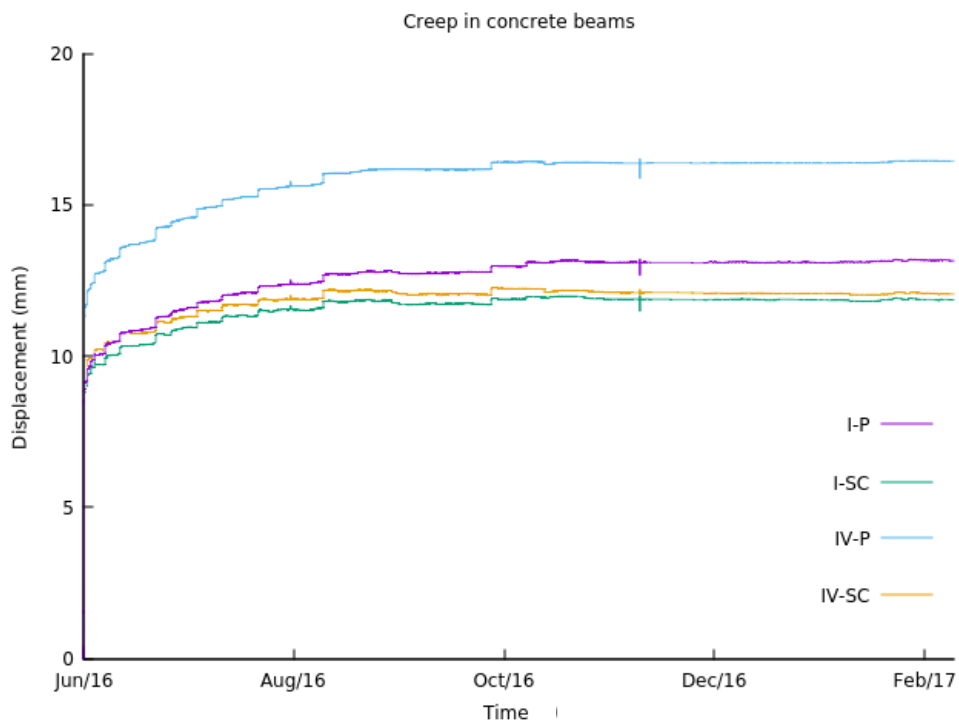


**Figure 6.16:** Displacement over time

Table 6.7 and 6.8 show estimates of the deflection of the beams which were done before the test, assuming an elastic modulus of 39GPa and 31 GPa respectively. At six months, the expected values were of 12.9mm and 16.2mm for beams manufactured with cement type I and cement type IV respectively. In beams IP, ISC and IVP, the theoretical and experimental creep values are very similar. Showing again the possibility of use the existing formulations for the prediction of the behavior of structural elements manufactured with EAF slag as aggregate. Even though beam IVSC show surprisingly less deformation than expected.

Days	0	1	3	7	14	30	60	90	120	180	210	240	270	360
<b>Instantaneous Deflection</b>	<b>5.8</b>													
$\xi$	0.0	0.0	0.0	0.2	0.5	0.7	0.9	1.0	1.1	1.2	1.3	1.3	1.4	1.4
<b>Total Deflection</b>	5.8	5.8	5.8	7.2	8.4	9.7	10.9	11.6	12.1	12.9	13.1	13.4	13.6	14.1

**Table 6.7:** Theoretical results of the deflection of the beams with  $E_c=39\text{GPa}$

Days	0	1	3	7	14	30	60	90	120	180	210	240	270	360
<b>Instantaneous Deflection</b>	<b>7.2</b>													
$\xi$	0.0	0.0	0.0	0.2	0.5	0.7	0.9	1.0	1.1	1.2	1.3	1.3	1.4	1.4
<b>Total Deflection</b>	7.2	7.2	7.2	9.0	10.6	12.2	13.8	14.7	15.3	16.2	16.5	16.8	17.1	17.7

**Table 6.8:** Theoretical results of the deflection of the beams with  $E_c=31\text{GPa}$

## Conclusions

The manufacture and performance of pumpable and self-compacting RC beams with EAF slag as aggregate have been examined to evaluate the casting process in real-scale elements and the suitability of EAF slag to RC members. The following conclusions may be drawn from the results obtained in this study:

- Real-scale mixtures of pumpable concretes have been successfully manufactured.
- The manufacture of real-scale self-compacting mixes with EAF slag as aggregate has been demonstrated and is therefore feasible. No problems were noted during the casting of the real-scale RC of aggregate segregation or passability through the reinforcement.



- The experimental flexural behavior of the RC beams made with EAF slag concrete has been tested and, as predicted by the existing formulation, was reasonably good.
- The flexural behavior of the EAF slag concrete RC beams has been analyzed in depth, to show in all cases that present the standard behavior of the ordinary RC elements.
- The long-term deflection test performed on the real-scale beams has shown a great correlation between the analytical and experimental results.

Nevertheless, further research should be conducted, to ensure that the behavior of the RC beams incorporating EAF slag could be predicted by the existing formulations.

## References

- [1] Thomas C, Cimentada A, Polanco JA, Setién J, Méndez D, Rico J. Influence of recycled aggregates containing sulphur on properties of recycled aggregate mortar and concrete. *Compos Part B: Eng* 2013;45:474-85.
- [2] Thomas C, Setién J, Polanco JA. Structural recycled aggregate concrete made with precast wastes. *Constr Build Mater* 2016;114:536-46.
- [3] Medina C, Sánchez De Rojas MI, Thomas C, Polanco JA, Frías M. Durability of recycled concrete made with recycled ceramic sanitary ware aggregate. Inter-indicator relationships. *Constr Build Mater* 2016;105:480-6.
- [4] Felekoglu B, Tosun K, Baradan B+, Altun A, Uyulgan B. The effect of fly ash and limestone fillers on the viscosity and compressive strength of self-compacting repair mortars. *Cement and Concrete Research* 2006;36:1719-26.
- [5] Jalal M, Pouladkhan A, Harandi OF, Jafari D. Comparative study on effects of Class F fly ash, nano silica and silica fume on properties of high performance self compacting concrete. *Construction and Building Materials* 2015;94:90-104.
- [6] Güneyisi E, Gesoğlu M, Altan İ, Öz HÖ. Utilization of cold bonded fly ash lightweight fine aggregates as a partial substitution of natural fine aggregate in self-compacting mortars. *Constr Build Mater* 2015;74:9-16.

- [7] Motz H, Geiseler J. Products of steel slags an opportunity to save natural resources. *Waste Manage* 2001;21:285-93.
- [8] Geiseler J. Use of steelworks slag in Europe. *Waste Management* 1996;16:59-63.
- [9] Koros PJ. Dusts, scale, slags, sludges... Not wastes, but sources of profits. *Metallurgical and Materials Transactions B* 2003;34:769-79.
- [10] Neupane K. Fly ash and GGBFS based powder-activated geopolymer binders: A viable sustainable alternative of portland cement in concrete industry. *Mechanics of Materials* 2016;103:110-22.
- [11] Kuo WT, Chen SH, Wang HY, Lin JC. A study on the mechanical and electricity properties of cement mortar added with GGBFS and piezoelectric powder. *Construction and Building Materials* 2013;49:251-6.
- [12] Nath SK, Kumar S. Evaluation of the suitability of ground granulated silico-manganese slag in Portland slag cement. *Construction and Building Materials* 2016;125:127-34.
- [13] Kuo WT, Wang HY, Shu CY. Engineering properties of cementless concrete produced from GGBFS and recycled desulfurization slag. *Construction and Building Materials* 2014;63:189-96.
- [14] CEN European Committee for standardization. Rue de Stassart, 36. Brussels B-1050.
- [15] Morino K, Iwatsuki E. Utilization of electric arc furnace oxidizing slag. *Proc TMS Fall Extract Process Conf* 1999;1:521-30.
- [16] Morino K, Iwatsuki E. Durability of concrete using electric arc furnace oxidizing slag aggregates. *Infrastructure regeneration and rehabilitation improving the quality of life through better construction International conference* 1999:213-22.
- [17] Ortega-Fernandez I, Gil A, Faik A, Rodriguez-Aseguinolaza J, D'Aguanno B. Parametric and thermal management optimization of a steel slag based packed bed heat storage. 2015;1.
- [18] Ameri M, Hesami S, Goli H. Laboratory evaluation of warm mix asphalt mixtures containing electric arc furnace (EAF) steel slag. *Construction and Building Materials* 2013;49:611-7.

- [19] Skaf M, Manso JM, Aragón Á, Fuente-Alonso JA, Ortega-López V. EAF slag in asphalt mixes: A brief review of its possible re-use. *Resour Conserv Recycl* 2017;120:176-85.
- [20] Pasetto M, Baldo N. Experimental evaluation of high performance base course and road base asphalt concrete with electric arc furnace steel slags. *J Hazard Mater* 2010;181:938-48.
- [21] Pasetto M, Baldo N. Fatigue Behavior Characterization of Bituminous Mixtures Made with Reclaimed Asphalt Pavement and Steel Slag. *Procedia - Social and Behavioral Sciences* 2012;53:297-306.
- [22] Pasetto M, Baldo N. Mix design and performance analysis of asphalt concretes with electric arc furnace slag. *Constr Build Mater* 2011;25:3458-68.
- [23] Oluwasola EA, Hainin MR, Aziz MMA. Evaluation of asphalt mixtures incorporating electric arc furnace steel slag and copper mine tailings for road construction. *Transportation Geotechnics* 2015;2:47-55.
- [24] Kavussi A, Qazizadeh MJ. Fatigue characterization of asphalt mixes containing electric arc furnace (EAF) steel slag subjected to long term aging. *Construction and Building Materials* 2014;72:158-66.
- [25] Bosela P, Delatte N, Obratil R, Patel A. Fresh and hardened properties of paving concrete with steel slag aggregate. 2008.
- [26] Bäverman C, Aran Aran F. A study of the potential of utilising electric arc furnace slag as filling material in concrete. *Studies in Environmental Science* 1997;71:373-6.
- [27] Manso JM, Gonzalez JJ, Polanco JA. Electric arc furnace slag in concrete. *J Mater Civ Eng* 2004;16:639-45.
- [28] Papayianni I, Anastasiou E. Production of high-strength concrete using high volume of industrial by-products. *Constr Build Mater* 2010;24:1412-7.
- [29] Etxeberria M, Pacheco C, Meneses JM, Berridi I. Properties of concrete using metallurgical industrial by-products as aggregates. *Construction and Building Materials* 2010;24:1594-600.

- [30] Qasrawi H, Shalabi F, Asi I. Use of low CaO unprocessed steel slag in concrete as fine aggregate. *Constr Build Mater* 2009;23:1118-25.
- [31] Polanco JA, Manso JM, Setián J, González JJ. Strength and durability of concrete made with electric steelmaking slag. *ACI Mater J* 2011;108:196-203.
- [32] Coppola L, Lorenzi S, Buoso A. Electric arc furnace granulated slag as a partial replacement of natural aggregates for concrete production. *Int Conf Sustainable Constr Materials Technol* 2010.
- [33] Brand AS, Roesler JR. Steel furnace slag aggregate expansion and hardened concrete properties. *Cement and Concrete Composites* 2015;60:1-9.
- [34] Faleschini F, Brunelli K, Zanini MA, Dabalã M, Pellegrino C. Electric Arc Furnace Slag as Coarse Recycled Aggregate for Concrete Production. *Journal of Sustainable Metallurgy* 2016;2:44-50.
- [35] Arribas I, Santamaría A, Ruiz E, Ortega-López V, Manso JM. Electric arc furnace slag and its use in hydraulic concrete. *Constr Build Mater* 2015;90:68-79.
- [36] Adegoloye G, Beaucour A-, Ortola S, Noumowe A. Mineralogical composition of EAF slag and stabilised AOD slag aggregates and dimensional stability of slag aggregate concretes. *Constr Build Mater* 2016;115:171-8.
- [37] Pellegrino C, Cavagnis P, Faleschini F, Brunelli K. Properties of concretes with Black/Oxidizing Electric Arc Furnace slag aggregate. *Cement and Concrete Composites* 2013;37:232-40.
- [38] Juan Manuel Manso, David Hernandez, Maria Milagros Losanez, and Javier, Jesus Gonzalez. Design and Elaboration of Concrete Mixtures Using Steelmaking Slags. *Materials Journal* 2011;108.
- [39] San-José JT, Vegas I, Arribas I, Marcos I. The performance of steel-making slag concretes in the hardened state. *Mater Des* 2014;60:612-9.
- [40] Abu-Eishah SI, El-Dieb AS, Bedir MS. Performance of concrete mixtures made with electric arc furnace (EAF) steel slag aggregate produced in the Arabian Gulf region. *Constr Build Mater* 2012;34:249-56.
- [41] Manso JM, Polanco JA, Losañez M, González JJ. Durability of concrete made with EAF slag as aggregate. *Cem Concr Compos* 2006;28:528-34.

- [42] Arribas I, Vegas I, San-José JT, Manso JM. Durability studies on steelmaking slag concretes. *Mater Des* 2014;63:168-76.
- [43] Monosi S, Ruello ML, Sani D. Electric arc furnace slag as natural aggregate replacement in concrete production. *Cement and Concrete Composites* 2016;66:66-72.
- [44] Pellegrino C, Gaddo V. Mechanical and durability characteristics of concrete containing EAF slag as aggregate. *Cement and Concrete Composites* 2009;31:663-71.
- [45] Santamaría A, Orbe A, Losañez MM, Skaf M, Ortega-Lopez V, González JJ. Self-compacting concrete incorporating electric arc-furnace steelmaking slag as aggregate. *Mater Des* 2017;115:179-93.
- [46] Sheen Yn, Le DH, Sun TH. Greener self-compacting concrete using stainless steel reducing slag. *Construction and Building Materials* 2015;82:341-50.
- [47] Arribas I, San-José JT, Vegas IJ, Hurtado JA, Chica JA. Application of steel slag concrete in the foundation slab and basement wall of the Labein-Tecnalia Kubik building. 6th European Slag Conference, EUROSLAG pub 2010.
- [48] José, Luis García Mochales. Utilización de Áridos siderúrgicos en obras por la autoridad portuaria de Bilbao. 2016.
- [49] Pellegrino C, Faleschini F. Experimental investigation on RC beams containing slag as recycled aggregate. *fib Symp : Concr Struct Sustainable Community - Proc* 2012:451-4.
- [50] Kim SW, Lee YJ, Kim KH. Flexural Behavior of Reinforced Concrete Beams with Electric Arc Furnace Slag Aggregates. *Journal of Asian Architecture and Building Engineering* 2012;11:133-8.
- [51] Kim SW, Lee YJ, Lee YH, Kim KH. Flexural Performance of Reinforced High-Strength Concrete Beams with EAF Oxidizing Slag Aggregates. *Journal of Asian Architecture and Building Engineering* 2016;15:589-96.
- [52] Kim SW, Lee YJ, Kim KH. Bond Behavior of RC Beams with Electric Arc Furnace Oxidizing Slag Aggregates. *Journal of Asian Architecture and Building Engineering* 2012;11:359-66.

- [53] du Béton FI. fib model code for concrete structures 2010. Berlin, Germany 2013.
- [54] ASTM International.,. Annual book of ASTM standards. Annual book of ASTM standards. 2002.
- [55] EFNARC S. Guidelines for self-compacting concrete. London, UK: Association House 2002:32-4.
- [56] Fomento M. Instrucción de Hormigón Estructural EHE-08. Fomento, Madrid, España 2008.
- [57] Jiménez Montoya P, García Meseguer A, Morán Cabré F, Arroyo Portero JC. Hormigón armado. 15th ed. : Editorial Gustavo Gili, S.L, 2010.

*Chapter 7:*  
*General Conclusions*

---





# 7

## *General Conclusions*

An exhaustive study on different scales of hydraulic mixes manufactured with Electric Arc Furnace Slag as aggregate has been completed in this PhD thesis. Although some conclusions are presented at the end of each chapter, in order to gather together the main ideas of the research and to present the main lessons that can be learnt, the general and the most important conclusions that can be derived from the results of the research are listed below.

1. With regard to the interaction of Electric Arc Furnace (EAF) slag and Ladle Furnace (LF) slag with different types of EU standardized Portland cements:
  - The use of electric arc furnace slag as aggregate mixed with Portland cement has shown good results in terms of the fresh and hardened properties of the resulting concrete. No detrimental reactions in the concrete during the course of the research have been noted.
  - The use of Portland cement containing notable amounts of fly ash with electric arc furnace slag has proven itself to be positive in the different mixes manufactured during this research: their workability is similar to mixes manufactured with Ordinary Portland Cement, producing more flowable mixtures with the same dosage, and the mechanical properties have demonstrated an excellent mechanical strength to clinker content ratio, while any problems in terms of durability have been noted. The structural behavior of beams manufactured with Ordinary Portland Cement, fly ash and EAF slag has shown encouraging results.

- The interaction of LF slag with Portland cement and fly ash has shown good results. Its presence slightly delays the increase in the mechanical strength of mixes, but with no notable detriment in the final value. A 20% proportion of the total binder can be recommended, while proportions of 30% are acceptable. Higher proportions could be problematic in relation to durability, due to the presence of expansive compounds.
  - The simultaneous use of fly ash, as an addition along with the LF slag, and EAF slag aggregate has in general yielded acceptable results, showing good compatibility, while economizing on the total consumption of Portland clinker.
2. With regard to the manufacture of concrete with the desired workability using Electric Arc Furnace slag as aggregate:
- It has been demonstrated that manufacturing pumpable structural concrete with EAF slag as aggregate is beneficial, affordable and a viable solution, both at the laboratory scale and in real scale.
  - Self-compacting structural mixes have been successfully designed and produced using EAF slag as heavy aggregate; designing appropriate dosages by careful control of the fine fraction. Better workability results have been achieved by manufacturing concretes in large volumes than at the laboratory scale.
  - Traditionally, it is assumed that the superplasticizer only interacts with the cement particles, so special attention must not be paid to its interaction with the EAF slag. Nevertheless, it has been shown that, while some superplasticizer works very well with natural aggregates, it does not produce the same effects in concretes manufactured with steel slags.
  - The numerical simulation of the viscous flux of these self-compacting mixes, using a suitable model, has produced very acceptable results.

3. With regard to the mechanical behavior of EAF slag hydraulic mixes:

- The compressive strength of hydraulic mixes manufactured with EAF slag as aggregate has shown promising results; a consequence of a cohesive internal structure, as is evident from the MIP and CAT analyses.
- The mixes containing slag demonstrate, in general, less stiffness than the natural aggregate mixes of similar strengths.
- The density of hydraulic mixes with EAF slag is higher than mixes manufactured with natural aggregate. However, the increase in strength in many cases, due to the use of steel slag, could compensate for this higher density.
- Air-entrainment admixtures have demonstrated little or no relevant consequences in the EAF slag mixes, because the strength loss was not compensated by gains in density.
- SEM observation of the fracture surfaces in the SCC-EAF slag concrete has revealed significant features that shed light on their structure and mechanical behavior.

4. With regard to the durability of EAF slag hydraulic mixes:

- The results of the potential expansion tests performed on the mixes with EAF and LF slags, have shown no adverse effects when using EAF slag, and even when using appropriate proportions of LF slag the effects were within safe margins.
- In general, concretes that incorporate EAF slag as aggregate shows fairly good durability, and similar to conventional concretes.
- It has been shown in the electromechanical corrosion tests advantageous resistance of the concretes incorporating EAF slag aggregates against steel rebar corrosion.

5. With regard to the structural behavior of EAF slag Reinforced Concrete (RC) elements:

- The analysis of the flexural behavior of EAF slag RC beams has shown the typical behavior expected in ordinary RC beams, which can be predicted with the existing formulations.
- The long-term deflection test performed on real-scale beams has shown creeps value similar to analytically predicted values.

After analyzing the general conclusions, it can be stated that the main objective of this thesis has been achieved. This work represents a step towards the standardization of the re-use of Electric Arc Furnace slag as raw materials for manufacturing hydraulic mixes to be used in the construction industry and in civil engineering. It has been demonstrated that the manufacture of real-scale structural elements with the desired workability is a feasible option.

*Chapter 8:*  
*Future Research Lines*

---



# 8

## *Future Research Lines*

Moving forward, future lines of research into EAF slag concrete will have to work towards its standardization. Now that the problem of workability has been solved, and having demonstrated that its higher density will not involve a major detrimental influence on the structural behavior of these concretes, it is time to encourage producers to use this material in various applications and to look for applications where the use of steel slag concrete can deliver better value. To achieve this goal, the following lines of research are proposed:

1. Study the behavior of EAF slag concrete in extreme atmospheric conditions. It would be interesting study its behavior when subjected to high temperatures, cryogenic conditions, radiological radiations and gypsum soils.
2. Analyze the possibility of using EAF slag concrete in façades, developing a study related to its thermal, acoustic and vibration conductivity.
3. Go deeper into the study of the rheological characteristics of EAF slag concrete. An improvement in the numerical model proposed in this work could be interesting to develop.
4. Further analysis of the structural behavior of EAF slag RC elements is necessary. It could be interesting to develop a finite element analysis of the structural behavior of EAF slag RC elements and to manufacture other structural elements to study their behavior and compare it with theoretical results.

5. Develop investigations on the use of EAF slag concrete in prestressed elements. Manufacturing real-scale beams, testing them in the laboratory and developing a numerical analysis of their behavior.
6. Design fiber-reinforced self-compacting mixes with EAF slag as aggregate, evaluating its behavior at the laboratory scale, as well as testing real scale elements.



*Appendix:*  
*Publications and Congresses*

---



## Publications and Congresses derived from the Doctoral thesis

---

### *SCIENTIFIC JOURNAL PAPERS*

---

Autores: SANTAMARIA LEON, AMAIA; ORBE MATEO, AIMAR; LOSÁÑEZ, MILAGROS; SKAF, MARTA; ORTEGA LÓPEZ, VANESA; GONZALEZ MARTINEZ, JAVIER JESUS

Título: Self-compacting concrete incorporating electric arc-furnace steelmaking slag as aggregate

ISSN: 0261-3069

Nombre revista: MATERIALS & DESIGN

Volumen: 115

Número:

Página inicial: 179

Página final: 193

Año de publicación: 2017

---

Autores: SANTAMARIA LEON, AMAIA; ROJI CHANDRO, EDUARDO; SKAF, MARTA; MARCOS RODRIGUEZ, IGNACIO; GONZALEZ MARTINEZ, JAVIER JESUS

Título: The use of steelmaking slags and fly ash in structural mortars

ISSN: 0950-0618

Nombre revista: CONSTRUCTION AND BUILDING MATERIALS

Volumen: 106

Número:

Página inicial: 364

Página final: 373

Año de publicación: 2016

---

Autores: SANTAMARIA LEON, AMAIA; GONZALEZ MARTINEZ, JAVIER JESUS; LOSÁÑEZ, MILAGROS; ORTEGA LÓPEZ, VANESA; SKAF, MARTA

Título: The design of self-compacting structural mortar containing heavy steelmaking slags as aggregates

Nombre revista: CEMENT AND CONCRETE COMPOSITES

Cargado febrero 2016

---

Autores: SANTAMARIA LEON, AMAIA; GONZALEZ MARTINEZ, JAVIER JESUS; SAN-JOSÉ LOMBERA, JOSÉ-TOMÁS; ORBE MATEO, AIMAR

Título: A study on the durability of structural concrete incorporating electric steelmaking slag as aggregate

Nombre revista: MATERIALS & DESIGN

Cargado Mayo 2017

---

CONGRESSES

---

Autores: SANTAMARIA LEON, AMAIA; ORTEGA LOPEZ, VANESA; SKAF, MARTA; MARCOS RODRIGUEZ, IGNACIO; SAN JOSE LOMBERA, JOSE TOMAS; GONZALEZ MARTINEZ, JAVIER J.

Título: Performance of Hydraulic Mixes Manufactured with Electric Arc Furnace Slag Aggregates

Tipo de participación: Comunicación Oral

Congreso: 3rd Pan American Material Congress

Publicación: Proceedings of the 3rd Pan American Materials Congress. The Minerals, Metals & Materials Series

Lugar celebración: San Diego País: Estados Unidos de América

Fecha inicio: 26/02/2017 Fecha Fin: 02/03/2017

---

Autores: SANTAMARIA LEON, AMAIA; GONZALEZ MARTINEZ, JAVIER JESUS; LOSAÑEZ, MARIA MILAGROS; VEGAS, IÑIGO ; ARRIBAS, IDOIA; ROJI CHANDRO, EDUARDO

Título: SELF-COMPACTING CONCRETE CONTAINING EAF SLAG AS AGGREGATE

Tipo de participación: Ponencia

Congreso: 8th European Slag Conference

Publicación: SELF-COMPACTING CONCRETE CONTAINING EAF SLAG AS AGGREGATE

Lugar celebración: Linz País: Austria

Fecha inicio: 21/10/2015 Fecha Fin: 23/10/2015

---

Autores: SANTAMARIA LEON, AMAIA; GONZALEZ MARTINEZ, JAVIER JESUS; SAN JOSE LOMBERA, JOSE TOMAS; IÑIGO VEGAS ; IDOIA ARRIBAS; ROJI CHANDRO, EDUARDO

Título: Performance of self-compacting mortars containing EAF slag as aggregate

Tipo de participación: Ponencia

Congreso: WASCON 2015 &#8211; Resource Efficiency in Construction. 9th International Conference on the Environmental and Technical Implications of Construction with Alternative Materials

Publicación: WASCON 2015 &#8211; Resource Efficiency in Construction. 9th International Conference on the Environmental and Technical Implications of Construction with Alternative Materials

Lugar celebración: Santander País: España

Fecha inicio: 10/06/2015 Fecha Fin: 12/06/2015

---

*EVENTS*

---

Título del Evento: Baskrete Open Days 2016  
Tipo de evento: Jornada Científica  
Tipo de participación: Ponente  
Entidad organizadora: Dipc, UPV/EHU, Tecnalía, Euskampus  
Fecha: 10/11/2016 - 11/11/2016  
Localidad: Donostia  
Pais: España

---

Título del Evento: Reuse of Waste in Building and Civil Engineering  
Tipo de evento: Jornada Científica  
Tipo de participación: Ponente  
Entidad organizadora: University of Burgos  
Fecha: 19/09/2016 - 19/09/2016  
Localidad: Burgos  
Pais: España

---

Título del Evento: I Jornadas doctorales de la UPV/EHU  
Tipo de evento: Jornada Científica  
Tipo de participación: Ponente (Premio Mejor Ponencia)  
Entidad organizadora: UPV/EHU  
Fecha: 11/06/2016 - 12/06/2016  
Localidad: Bilbao  
Pais: España

---

